



January 2019

Corn, Wheat, And Switchgrass Biomass Production In The Northern Plains: Evaluating Opportunities And Tradeoffs

Rob Alan Proulx

Follow this and additional works at: <https://commons.und.edu/theses>

Recommended Citation

Proulx, Rob Alan, "Corn, Wheat, And Switchgrass Biomass Production In The Northern Plains: Evaluating Opportunities And Tradeoffs" (2019). *Theses and Dissertations*. 2481.
<https://commons.und.edu/theses/2481>

This Dissertation is brought to you for free and open access by the Theses, Dissertations, and Senior Projects at UND Scholarly Commons. It has been accepted for inclusion in Theses and Dissertations by an authorized administrator of UND Scholarly Commons. For more information, please contact zeinebyousif@library.und.edu.

CORN, WHEAT, AND SWITCHGRASS BIOMASS PRODUCTION IN THE NORTHERN
PLAINS: EVALUATING OPPORTUNITIES AND TRADEOFFS

by

Rob Alan Proulx

Bachelor of Science, University of Minnesota Crookston, 2006

Master of Science, University of Minnesota Twin Cities, 2008

A Dissertation

Submitted to the Graduate Faculty

of the

University of North Dakota

in partial fulfillment of the requirements

for the degree of

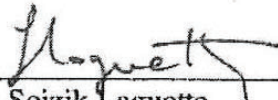
Doctor of Philosophy

Grand Forks, North Dakota


May
2019

Copyright 2019 Rob Alan Proulx


This dissertation, submitted by Rob Alan Proulx in partial fulfillment of the requirements for the Degree of Doctor of Philosophy from the University of North Dakota, has been read by the Faculty Advisory Committee under whom the work has been done and is hereby approved.



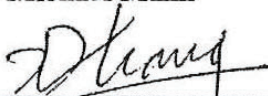
Dr. Soizik Laguette



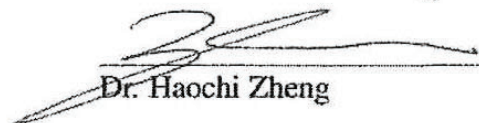
Dr. Michael Hill



Dr. Michael Mann



Dr. Xiaodong Zhang



Dr. Haochi Zheng

This dissertation is being submitted by the appointed advisory committee as having met all of the requirements of the School of Graduate Studies at the University of North Dakota and is hereby approved.



Chris Nelson
Associate Dean of the School of Graduate Studies

4/24/19

Date

PERMISSION

Title

Corn, Wheat, and Switchgrass Biomass Production in the Northern Plains:
Evaluating Opportunities and Tradeoffs

Department

Earth System Science and Policy

Degree

Doctor of Philosophy

In presenting this dissertation in partial fulfillment of the requirements for a graduate degree from the University of North Dakota, I agree that the library of this University shall make it freely available for inspection. I further agree that permission for extensive copying for scholarly purposes may be granted by the professor who supervised my dissertation work or, in her absence, by the Chairperson of the department or the dean of the School of Graduate Studies. It is understood that any copying or publication or other use of this dissertation or part thereof for financial gain shall not be allowed without my written permission. It is also understood that due recognition shall be given to me and to the University of North Dakota in any scholarly use which may be made of any material in my dissertation.

Rob Alan Proulx
April 24, 2019

TABLE OF CONTENTS

LIST OF FIGURES	ix
LIST OF TABLES	xxi
ACKNOWLEDGEMENTS	xxiii
ABSTRACT	xxv
CHAPTER	
I. INTRODUCTION	1
II. AN IMPROVED METHOD FOR ALMANAC SIMULATION OF UPLAND SWITCHGRASS ECOTYPES IN THE NORTHERN US	8
2.1. Abstract	8
2.2. Introduction	8
2.3. Materials and Methods	13
2.3.1. ALMANAC overview	13
2.3.2. Switchgrass parameterization	14
2.3.3. ALMANAC validation	18
2.3.4. Statistical analysis	25
2.3.5. Sensitivity analyses	28
2.4. Results	30
2.4.1. Annual yield outcomes	30
2.4.2. Multiyear-average yield outcomes	32
2.4.3. Within-season outcomes	32
2.4.4. Sensitivity analyses	37

2.5. Discussion	44
2.6. Conclusions	46
III. CORN AND WHEAT ALMANAC SIMULATIONS FOR MODERATE-RESOLUTION REGIONAL ASSESSMENTS	48
3.1. Abstract	48
3.2. Introduction	49
3.3. Materials and Methods	53
3.3.1. ALMANAC description	55
3.3.2. Final parameterizations – environmental variables	57
3.3.3. Final parameterizations – crop growth and management	61
3.3.4. ALMANAC validation	73
3.3.5. ALMANAC calibration and sensitivity analyses	76
3.4. Results and Discussion	78
3.4.1. Validation of county-average yields	78
3.4.2. Evaluation of within-county productivity	84
3.4.3. Moisture stress and yield estimation biases	91
3.4.4. Sensitivity analyses	96
3.4.5. Improving ALMANAC estimates	108
3.5. Conclusions	112
IV. BIOMASS AVAILABILITY IN THE EASTERN DAKOTAS AND WESTERN MINNESOTA: FEASIBILITY AND BENEFITS OF SUBSTITUTING SWITCHGRASS FOR EXISTING CORN AND WHEAT RESOURCES	115
4.1. Abstract	115
4.2. Introduction	116
4.3. Materials and Methods	123
4.3.1. ALMANAC simulations	127

4.3.2.	Potential biorefinery locations	131
4.3.3.	Corn and wheat expenses and revenue	132
4.3.4.	Switchgrass expenses	141
4.3.5.	Switchgrass parity price	148
4.3.6.	Environmental outcomes	152
4.3.7.	Supplanting corn or wheat with switchgrass	154
4.3.8.	Embedded assumptions	157
4.4.	Results and Discussion	158
4.4.1.	Technical availability of corn and wheat biomass	158
4.4.2.	Economic availability of corn and wheat biomass	165
4.4.3.	Switchgrass economic competitiveness	169
4.4.4.	Switchgrass environmental benefits	176
4.4.5.	Scenarios for subsidizing switchgrass production	180
4.4.6.	Land-use changes with subsidized switchgrass	189
4.4.7.	Improving switchgrass competitiveness through increased yield	201
4.5.	Conclusions	204
V.	GENERAL DISCUSSION	207
5.1.	Methods for estimation of regional-scale biophysical outcomes at low-to-moderate resolution	208
5.1.1.	Modeling overview	208
5.1.2.	Estimating biomass cropping outcomes	209
5.1.3.	Calibration and validation of yield outcomes	211
5.1.4.	Calibration and validation of environmental outcomes	214
5.1.5.	Tradeoffs	215
5.2.	Estimating and incentivizing land-use outcomes: Moving from regional to local scale	216

5.2.1. Existing ethanol infrastructure	216
5.2.2. Farmers' willingness to supply biomass	217
5.2.3. Subfield allocation of cellulosic biomass cropping	218
5.3. Conclusions	220
APPENDICES	223
REFERENCES	252

LIST OF FIGURES

Figure	Page
<p>1. (a) The approximate North American adaptation ranges of upland and lowland ecotypes of switchgrass (adapted from Casler et al., 2011), the sites of the switchgrass field evaluations used to develop and validate the ALMANAC parameters for upland switchgrass presented herein, and the TX field sites used by Kiniry et al. (1996) to parameterize ALMANAC for ‘Alamo’ switchgrass. (b) Site numbers (see Table 2) and average precipitation (mm; in parenthesis) of the 13 validation sites from (a).</p>	10
<p>2. Comparisons of default ALMANAC parameters (DFLT), the modified parameters (MOD) presented herein, and regression models fit to field observations of switchgrass growth (FLD) as reported by Madakadze et al. (1998a,b). (a) By the fraction of the growing season that has passed (SYP), effect of modified DMLA, DLAI, DLAP1, DLAP2, and RLAD on simulated leaf area index (LAI). (b) Effect of modified RUE and EXTINC on biomass accumulation, assuming LAI development from (a). (c) Effect of modified FRST1 and FRST2 on the fraction of aboveground biomass lost to frost damage at a given temperature.</p>	19
<p>3. Comparisons of measured annual switchgrass yields to ALMANAC (ALNC) simulations using the (a) default parameters, (c) default parameterization with CNY adjusted from 0.016 to 0.005, and (e) modified parameters presented herein. (b, d, f) ALMANAC model residuals for the simulations described in (a, c, e). . . .</p>	31
<p>4. Comparisons of measured multiyear average switchgrass yields to ALMANAC (ALNC) simulations using the (a) default parameters, (c) default parameterization with CNY adjusted from 0.016 to 0.005, and (e) modified parameters presented herein. (b, d, f) ALMANAC model residuals for the simulations described in (a, c, e).</p>	33
<p>5. For Site 11 with no nitrogen fertilizer (Table 2), comparison of daily simulated leaf area index (LAI), aboveground plant mass (AGPM), and dominant plant growth stress for the default ALMANAC parameters and the modified parameters presented herein. Water, nitrogen, and temperature stress values represent the average over all simulation years. Superimposed on the daily outputs are annual and multiyear average (MYA) simulated and field-measured yields.</p>	35

6.	For Site 3 (Table 2), comparison of daily simulated leaf area index (LAI), aboveground plant mass (AGPM), and dominant plant growth stress for the default ALMANAC parameters and the modified parameters presented herein. Water, nitrogen, and temperature stress values represent the average over all simulation years. Superimposed on the daily outputs are annual and multiyear average (MYA) simulated and field-measured yields.	36
7.	Distribution of simulated switchgrass maturity date under the default ALMANAC parameterization and the modified parameterization presented herein.	37
8.	Distribution of the normalized sensitivity parameter for simulated yield sensitivity analyses under the parameterization changes outlined in Table 1.	39
9.	Relationships between simulated switchgrass yield under the modified parameterization presented herein (x-axis) and under each sensitivity analysis outlined in Table 1 (y-axis). The dotted line is the 1:1 line and the fitted curve and its shaded region are the fit and 95% confidence interval of a local polynomial regression included as a visual aid (Section 2.3.4). Statistics represent sensitivity analysis values relative to the modified parameterization: MBE = mean bias error, PBAIS = percent mean bias, PMC = parameter mean change.	41
10.	Cropping frequency and ALMANAC calibration counties for (a) corn and (b) wheat. Cropping frequencies are derived from 2006 to 2015 Cropland Data Layers.	50
11.	Examples of ALMANAC simulation and aggregation units. (a) The 99-county study area. (b) County inset (Polk, MN) with overlying 4 km resolution climate cells. (c) Climate cell inset with geographic identifiers for the six soil mapunit polygons enclosed within and overlying estimates of 2007 corn planting-harvest date pairs (see Figure 15, Section 3.3.3). Each soil polygon represents a simulation unit, assigned the most prevalent planting-harvest date pair. (d) Same as (c), but with overlying 800 m resolution cells used to aggregate simulation yields for mapping.	54
12.	(a) Geographic identifiers for corn management zones. (b) Potential Heat Units (PHU) for soybean.	56
13.	Estimated fertilizer rates for (a) corn nitrogen (N), (b) corn phosphorus (P), (c) wheat N, and (d) wheat P.	67
14.	(a) Ratio of evapotranspiration (ET) to potential evapotranspiration (PET) for corn simulations. (b) Parcels identified as water-limited, based on visual examination of (a). (c) Corn planting density (CPD), calculated using Equation [22].	69

15.	Example of spatially-explicit estimation of planting and harvest progression, for corn in 2007. Progression of (a) corn emergence as a function of leaf greenness estimated by (b) normalized difference vegetative index (NDVI). (c) Estimated corn planting progresses in accordance with (a). Numbers in (a) and (c) are statewide planting and harvest progress according to USDA Crop Progress reports.	71
16.	For 20 calibration counties (see Figure 10), corn (a) ALMANAC yield and (b) ALMANAC yield residuals vs. USDA NASS yield. For 79 validation counties, (c) and (d) are same as (a) and (b). Each point represents a mean county-average yield for 2006 to 2015.	79
17.	For corn (CRN), maps of (a) USDA NASS yield, (b) ALMANAC (ALNC) yield, and (c) percent bias (PBIAS) of ALMANAC yield. For wheat (WHT), (d – f) same as (a – c). Counties outlined in red are considered potential outliers due to their high yield bias. Variables are averaged across 2006 though 2015 values.	80
18.	For 18 calibration counties (see Figure 10), wheat (a) ALMANAC yield and (b) ALMANAC yield residuals vs. USDA NASS yield. For 72 validation counties, (c) and (d) are same as (a) and (b). Each point represents a mean county-average yield for 2006 to 2015. Outliers correspond to counties outlined in Figure 17.	82
19.	For 79 validation counties, corn (a) ALMANAC yield and (b) ALMANAC yield residuals vs. USDA NASS yield. For 72 validation counties, wheat (c) ALMANAC yield and (d) ALMANAC yield residuals vs. USDA NASS yield. Each point represents an annual county-average yield for 2006 to 2015. Outliers correspond to counties outlined in Figure 17.	83
20.	For parcels with CDL-indicated corn or wheat production from 2006 to 2015 (see Figure 10), county-specific standard deviations of (a) crop productivity index (CPI), (b) ALMANAC-derived corn productivity index (CNPI), and (c) ALMANAC-derived wheat productivity index (WTPI). (d – f) Corresponding parcel-specific values of CPI, CNPI, and WTPI.	86
21.	For parcels without CDL-indicated corn or wheat production from 2006 to 2015 (see Figure 10), county-specific standard deviations of (a) crop productivity index (CPI), (b) ALMANAC-derived corn productivity index (CNPI), and (c) ALMANAC-derived wheat productivity index (WTPI). (d – f) Corresponding parcel-specific values of CPI, CNPI, and WTPI.	87
22.	(a) Land capability classes for all study area parcels. (b) Distributions of crop productivity index (CPI) and ALMANAC-derived corn productivity (CNPI) and wheat productivity (WTPI) indexes, grouped by land capability class.	89
23.	For (a) corn and (b) wheat, ALMANAC yield bias vs. mean growing season drought severity and coverage index (DSCI). Each point represents a county-average value for a single year.	92

24.	For corn, crop available water (CAW), water stress (WS), and harvest index (HI) anomalies vs. ALMANAC yield bias, grouped by drought severity and coverage index (DSCI; see Figure 23). Each point represents a county-average value for a single year.	94
25.	For wheat, crop available water (CAW), water stress (WS), and harvest index (HI) anomalies vs. ALMANAC yield bias, grouped by drought severity and coverage index (DSCI; see Figure 23). Each point represents a county-average value for a single year.	95
26.	Distributions of the normalized sensitivity parameter for sensitivity analyses (Table 6) across (a) 80,207 corn simulation units and (b) 60,433 wheat simulation units. For clarity, outliers (points extending beyond the whiskers) were omitted. HI = harvest index, CN = runoff curve number, EXTINC = light extinction coefficient, PAW = plant-available water.	99
27.	For corn, (a) Yield bias and (b) water stress bias of ALMANAC sensitivity analysis (ALNC SA) comparison parameterization (COMP) minus baseline parameterization (BL) (see Table 6) vs. yield bias of ALMANAC sensitivity analysis baseline parameterization minus USDA NASS. Each point represents a county-average value. HI = harvest index, CN = runoff curve number, EXTINC = light extinction coefficient, PAW = plant-available water, CROP SEQ = crop sequencing, PLTHRV MED NASS = median NASS planting and harvest dates, PLTHRV ALL EST = all estimated planting and harvest dates. PMC = parameter mean change, PBIAS = percent mean bias.	100
28.	For 80,207 corn simulation units, yield bias distributions for ALMANAC sensitivity analysis (ALNC SA) comparison parameterization (COMP) minus baseline parameterization (BL; see Table 6), grouped by land suitability for cropping (G = good, F = fair, P = poor) and calibration area (see Figure 10). In these box and whisker plots, a dot represents the median, vertical lines represent the whiskers, and the gap between lines represents the interquartile range. For clarity, outliers (points extending beyond the whiskers) were omitted. HI = harvest index, CN = runoff curve number, EXTINC = light extinction coefficient, PAW = plant-available water, CROP SEQ = crop sequencing, PLTHRV MED NASS = median NASS planting and harvest dates, PLTHRV ALL EST = all estimated planting and harvest dates.	102

29.	For wheat, (a) Yield bias and (b) water stress bias of ALMANAC sensitivity analysis (ALNC SA) comparison parameterization (COMP) minus baseline parameterization (BL; see Table 6) vs. yield bias of ALMANAC sensitivity analysis baseline parameterization minus USDA NASS. Each point represents a county-average value. CN = runoff curve number, PAW = plant-available water, CROP SEQ = crop sequencing, PLTHRV MED NASS = median NASS planting and harvest dates, PLTHRV ALL EST = all estimated planting and harvest dates. PMC = parameter mean change, PBIAS = percent mean bias.	107
30.	For 60,433 wheat simulation units, yield bias distributions for ALMANAC sensitivity analysis (ALNC SA) comparison parameterization (COMP) minus baseline parameterization (BL; see Table 6), grouped by land suitability for cropping (G = good, F = fair, P = poor) and calibration area (see Figure 10). In these box and whisker plots, a dot represents the median, vertical lines represent the whiskers, and the gap between lines represents the interquartile range. For clarity, outliers (points extending beyond the whiskers) were omitted. CN = runoff curve number, PAW = plant-available water, CROP SEQ = crop sequencing, PLTHRV MED NASS = median NASS planting and harvest dates, PLTHRV ALL EST = all estimated planting and harvest dates.	109
31.	Characterizing study region land-use/land-cover (LULC). (a) Generalized LULC from 2011 National Land Cover Database. (b) Land capability classification (LCC). (c) Parcels considered eligible for biomass cropping. Frequency of (d) corn and (e) wheat production from 2006 to 2015, as indicated by USDA Cropland Data Layers. (f) Existing corn and wheat parcels considered eligible for substitution with switchgrass.	122
32.	Estimated fertilizer rates for switchgrass (a) nitrogen (N), (b) phosphorus (P), and (c) potassium (K).	130
33.	Illustrations for generalized calculations of corn (a) grain revenue, (b) grain expense, (c) biomass harvest expense, and (d) biomass transport expense. Wheat calculations were similar, but with a constant seed cost.	135
34.	Comparison of FINBIN and model-derived grain production expenses (GE) for (a) corn and (b) wheat, aggregated by USDA Agricultural District. Expenses are averaged across tillage systems.	138
35.	Illustrations for generalized calculations of switchgrass (a) biomass production expense and (b) biomass transport expense.	143

36.	Consolidation of switchgrass parity price (SPP) estimates across (a) its competing cropping systems in a reduced tillage (RT) system and (b) management systems with (+F) or without (–F) fertilizer applications. In (a), SPP estimates for all combinations of establishment scenario (low-cost [LC] or high-cost [HC]) and fertilizer application are consolidated by keeping the competing cropping system requiring the greatest SPP (corn-soybean [CRN-SOY] or wheat-soybean [WHT-SOY]). In (b), the LC and HC outputs from (a) are consolidated to keep the lowest SPP across the +F and –F options.	153
37.	For (a) corn (CRN) and (b) wheat (WHT), the predominant harvest system (see Table 11) within each parcel and the percent of parcels within each classification under conventional tillage (CT), reduced tillage (RT), and no-till (NT) systems. For (c) CRN and (d) WHT, the percent biomass removal within each parcel and the percent of parcels within each classification under the CT, RT, and NT systems. Percent biomass removal is a continuous variable due to the mixing of biomass harvest systems within parcels.	159
38.	Collection areas for potential biorefineries under (a) conventional tillage (CT), (b) reduced tillage (RT), and (c) no-till (NT) systems. As an example of biomass harvest extent for a single year, corn or wheat biomass removal (from Figure 39) is displayed for each parcel with corn and wheat production according to the 2015 Cropland Data Layer. (d – f) Under each tillage system, the relative fractions of corn and wheat biomass supplying each potential biorefinery location.	162
39.	Simulated (a) corn and (b) wheat grain yield under conventional tillage (CT), reduced tillage (RT), and no-till (NT) systems. Simulated (c) corn and (d) wheat biomass removal under the CT, RT, and NT systems. Biomass removal reflects the harvest systems in Figure 37.	163
40.	Estimated revenue, expense, and profit for corn grain production under (a) conventional tillage (CT), (b) reduced tillage (RT), and (c) no-till (NT) systems. Estimated harvest expense, transport expense, and breakeven price for corn biomass production under (d) CT, (e) RT, and (f) NT systems. Overlain on transport expense and breakeven price are the biorefinery collection areas from Figure 38. . .	166
41.	Estimated revenue, expense, and profit for wheat grain production under (a) conventional tillage (CT), (b) reduced tillage (RT), and (c) no-till (NT) systems. Estimated harvest expense, transport expense, and breakeven price for wheat biomass production under (d) CT, (e) RT, and (f) NT systems. Overlain on transport expense and breakeven price are the biorefinery collection areas from Figure 38. . .	167

42.	Under the low-cost (LC) and high-cost (HC) establishment scenarios, with (+F) and without (–F) fertilizer applications, the estimated (a) yield, (b) production expense, and (c) transport expense associated with switchgrass (SWG) biomass production. Overlain on transport expense are the biorefinery collection areas from Figure 38. All values represent the annualized net present value of 10-year returns with a discount rate of 5%.	171
43.	For the low-cost (LC) establishment scenario, the biomass price necessary for switchgrass to generate the same net return as a competing corn or wheat system (SPP, switchgrass parity price) under (a) conventional tillage (CT), (b) reduced tillage (RT) or (c) no-till (NT). (d – f) The net return of switchgrass production at the SPP.	173
44.	For the high-cost (HC) establishment scenario, the biomass price necessary for switchgrass to generate the same net return as a competing corn or wheat system (SPP, switchgrass parity price) under (a) conventional tillage (CT), (b) reduced tillage (RT) or (c) no-till (NT). (d – f) The net return of switchgrass production at the SPP.	174
45.	Environmental benefits of switchgrass production relative to corn or wheat and under the most profitable fertilization option (e.g. Figure 36) for the low-cost (LC) establishment scenario: (a) mitigation of soil erosion, (b) mitigation of nitrogen (N) runoff into surface water, and (c) carbon (C) sequestration. Maps of (d) slope and (e) initial soil C from SSURGO are provided to provide context to the spatial patterns of a – c.	177
46.	(a) For switchgrass with low-cost (LC) establishment; subsidized environmental services; and competing with corn or wheat in a conventional tillage (CT), reduced tillage (RT), or no-till (NT) system; required annual subsidy and environmental services payments to achieve 1 to 5% conversion of eligible corn and wheat parcels to switchgrass production. (b) The required annual subsidy and biomass price with subsidized biomass production. (c – d) Corresponding values for high-cost (HC) establishment.	182
47.	For switchgrass with low-cost (LC) establishment, subsidized (a) environmental services payments or (b) biomass production, and competing with corn or wheat in a conventional tillage (CT), reduced tillage (RT), or no-till (NT) system, the changes in biomass production within or outside a biorefinery collection area (BCA; Figure 38) when converting 1 to 5% of eligible corn or wheat parcels to switchgrass production. (c – d) Corresponding values for HC establishment.	185

48.	For switchgrass with low-cost (LC) establishment, subsidized (a) environmental services payments or (b) biomass production, and competing with corn or wheat in a conventional tillage (CT), reduced tillage (RT), or no-till (NT) system, the resulting soil retention, nitrogen (N) retention, and carbon (C) sequestration within or outside a biorefinery collection area (BCA; Figure 38) provided by converting 1 to 5% of eligible corn or wheat parcels to switchgrass production. (c – d) Corresponding values for HC establishment.	187
49.	For switchgrass substitution on 5% of eligible corn or wheat parcels under conventional tillage (CT), reduced tillage (RT), or no-till (NT), the percent difference in annual subsidy (subs), biomass production (prod), soil retention (S ret), nitrogen retention (N ret), and carbon sequestration (C seq) between the subsidized environmental services (SES) and subsidized biomass production (SBP) approaches. (a) low-cost (LC) switchgrass establishment, parcels within biorefinery collection areas (BCA); (b) LC establishment, all parcels; (c) high-cost (HC) establishment, parcels within BCA; (d) HC establishment, all parcels.	190
50.	For switchgrass with low-cost (LC) establishment, subsidized (a) environmental services payments or (b) biomass production, and competing with corn or wheat in a conventional tillage (CT), reduced tillage (RT), or no-till (NT) system, the distribution of land capability classifications (LCC) among converted parcels when converting 1 to 5% of corn and wheat parcels considered eligible for switchgrass production. The reference (ref) column refers to the distribution of LCC among all corn and wheat production parcels eligible for conversion to switchgrass. (c – d) Corresponding values for HC establishment.	192
51.	Distances from biomass-producing corn and wheat parcels to the nearest potential biorefinery under (a) conventional tillage (CT), (b) reduced tillage (RT), and (c) no-till (NT) systems (biorefineries from Figure 38). Distances from biomass-producing corn and wheat parcels to the nearest potential biorefinery and the proportions of corn, wheat, and switchgrass (swg.) biomass collected by each biorefinery where switchgrass with low-cost establishment and subsidized environmental services payments (SES) replaced 5% of eligible corn or wheat parcels under (d) CT, (e) RT, and (f) NT. (g – i) Same as (d – f), except for switchgrass with subsidized biomass production (SBP).	195
52.	Distances from biomass-producing corn and wheat parcels to the nearest potential biorefinery under (a) conventional tillage (CT), (b) reduced tillage (RT), and (c) no-till (NT) systems (biorefineries from Figure 38). Distances from biomass-producing corn and wheat parcels to the nearest potential biorefinery and the proportions of corn, wheat, and switchgrass (swg.) biomass collected by each biorefinery where switchgrass with high-cost establishment and subsidized environmental services payments (SES) replaced 5% of eligible corn or wheat parcels under (d) CT, (e) RT, and (f) NT. (g – i) Same as (d – f), except for switchgrass with subsidized biomass production (SBP).	196

53. Under the biomass prices necessary to convert 1 to 5% of eligible corn or wheat parcels in a reduced tillage system to switchgrass production, (a) switchgrass progression across existing corn or wheat parcels assuming low-cost establishment and subsidized biomass production and (b) existing perennial grassland parcels where switchgrass would be profitable and economically competitive with corn or wheat production. 199

54. (a – c) For a biomass price (BP) of \$60 Mg⁻¹ and switchgrass production with low-cost (LC) establishment, the biomass yield increase necessary for switchgrass to generate the same net return as a competing corn or wheat system (SPYI, switchgrass parity yield increase) under conventional tillage (CT), reduced tillage (RT) or no-till (NT). (d – f) Corresponding values for high-cost (HC) establishment. 203

55. For Site 1 (Table 2), comparison of daily simulated leaf area index (LAI), aboveground plant mass (AGPM), and dominant plant growth stress for the default ALMANAC parameters and the modified parameters presented herein. Water, nitrogen, and temperature stress values represent the average over all simulation years. Superimposed on the daily outputs are annual and multiyear average (MYA) simulated and field-measured yields. 225

56. For Site 2 (Table 2), comparison of daily simulated leaf area index (LAI), aboveground plant mass (AGPM), and dominant plant growth stress for the default ALMANAC parameters and the modified parameters presented herein. Water, nitrogen, and temperature stress values represent the average over all simulation years. Superimposed on the daily outputs are annual and multiyear average (MYA) simulated and field-measured yields. 226

57. For Site 3 (Table 2), comparison of daily simulated leaf area index (LAI), aboveground plant mass (AGPM), and dominant plant growth stress for the default ALMANAC parameters and the modified parameters presented herein. Water, nitrogen, and temperature stress values represent the average over all simulation years. Superimposed on the daily outputs are annual and multiyear average (MYA) simulated and field-measured yields. 227

58. For Site 4 (Table 2), comparison of daily simulated leaf area index (LAI), aboveground plant mass (AGPM), and dominant plant growth stress for the default ALMANAC parameters and the modified parameters presented herein. Water, nitrogen, and temperature stress values represent the average over all simulation years. Superimposed on the daily outputs are annual and multiyear average (MYA) simulated and field-measured yields. 228

59. For Site 5 (Table 2), comparison of daily simulated leaf area index (LAI), aboveground plant mass (AGPM), and dominant plant growth stress for the default ALMANAC parameters and the modified parameters presented herein. Water, nitrogen, and temperature stress values represent the average over all simulation years. Superimposed on the daily outputs are annual and multiyear average (MYA) simulated and field-measured yields. 229

60. For Site 6 (Table 2), comparison of daily simulated leaf area index (LAI), aboveground plant mass (AGPM), and dominant plant growth stress for the default ALMANAC parameters and the modified parameters presented herein. Water, nitrogen, and temperature stress values represent the average over all simulation years. Superimposed on the daily outputs are annual and multiyear average (MYA) simulated and field-measured yields. 230

61. For Site 7 (Table 2), comparison of daily simulated leaf area index (LAI), aboveground plant mass (AGPM), and dominant plant growth stress for the default ALMANAC parameters and the modified parameters presented herein. Water, nitrogen, and temperature stress values represent the average over all simulation years. Superimposed on the daily outputs are annual and multiyear average (MYA) simulated and field-measured yields. 231

62. For Site 8 (Table 2), comparison of daily simulated leaf area index (LAI), aboveground plant mass (AGPM), and dominant plant growth stress for the default ALMANAC parameters and the modified parameters presented herein. Water, nitrogen, and temperature stress values represent the average over all simulation years. Superimposed on the daily outputs are annual and multiyear average (MYA) simulated and field-measured yields. 232

63. For Site 9 (Table 2), comparison of daily simulated leaf area index (LAI), aboveground plant mass (AGPM), and dominant plant growth stress for the default ALMANAC parameters and the modified parameters presented herein. Water, nitrogen, and temperature stress values represent the average over all simulation years. Superimposed on the daily outputs are annual and multiyear average (MYA) simulated and field-measured yields. 233

64. For Site 10 (Table 2), comparison of daily simulated leaf area index (LAI), aboveground plant mass (AGPM), and dominant plant growth stress for the default ALMANAC parameters and the modified parameters presented herein. Water, nitrogen, and temperature stress values represent the average over all simulation years. Superimposed on the daily outputs are annual and multiyear average (MYA) simulated and field-measured yields. 234

65.	For Site 11 with no nitrogen fertilizer (Table 2), comparison of daily simulated leaf area index (LAI), aboveground plant mass (AGPM), and dominant plant growth stress for the default ALMANAC parameters and the modified parameters presented herein. Water, nitrogen, and temperature stress values represent the average over all simulation years. Superimposed on the daily outputs are annual and multiyear average (MYA) simulated and field-measured yields.	235
66.	For Site 11 with 112 kgN ha ⁻¹ fertilizer application (Table 2), comparison of daily simulated leaf area index (LAI), aboveground plant mass (AGPM), and dominant plant growth stress for the default ALMANAC parameters and the modified parameters presented herein. Water, nitrogen, and temperature stress values represent the average over all simulation years. Superimposed on the daily outputs are annual and multiyear average (MYA) simulated and field-measured yields.	236
67.	For Site 11 with 224 kgN ha ⁻¹ fertilizer application (Table 2), comparison of daily simulated leaf area index (LAI), aboveground plant mass (AGPM), and dominant plant growth stress for the default ALMANAC parameters and the modified parameters presented herein. Water, nitrogen, and temperature stress values represent the average over all simulation years. Superimposed on the daily outputs are annual and multiyear average (MYA) simulated and field-measured yields.	237
68.	For Site 12 (Table 2), comparison of daily simulated leaf area index (LAI), aboveground plant mass (AGPM), and dominant plant growth stress for the default ALMANAC parameters and the modified parameters presented herein. Water, nitrogen, and temperature stress values represent the average over all simulation years. Superimposed on the daily outputs are annual and multiyear average (MYA) simulated and field-measured yields.	238
69.	For Site 13 (Table 2), comparison of daily simulated leaf area index (LAI), aboveground plant mass (AGPM), and dominant plant growth stress for the default ALMANAC parameters and the modified parameters presented herein. Water, nitrogen, and temperature stress values represent the average over all simulation years. Superimposed on the daily outputs are annual and multiyear average (MYA) simulated and field-measured yields.	239
70.	Relationship between slope and the length-slope (LS) factor of the Universal Soil Loss Equation, for 3471 SSURGO soil components within the study region.	244
71.	Using annual FINBIN data for 2010 to 2015, aggregated by USDA Agricultural District, the estimation of soybean revenue as a function of (a) corn revenue and (b) wheat revenue, and the estimation of soybean expense as a function of (c) corn expense and (d) wheat expense.	247

72. Consolidation of switchgrass parity price (SPP) estimates across (a) its competing cropping systems in a conventional tillage (CT) system and (b) management systems with (+F) or without (-F) fertilizer applications. In (a), SPP estimates for all combinations of establishment scenario (low-cost [LC] or high-cost [HC]) and fertilizer application are consolidated by keeping the competing cropping system requiring the greatest SPP (corn-soybean [CRN-SOY] or wheat-soybean [WHT-SOY]). In (b), the LC and HC outputs from (a) are consolidated to keep the lowest SPP across the +F and -F options. 248
73. Consolidation of switchgrass parity price (SPP) estimates across (a) its competing cropping systems in a no-till (NT) system and (b) management systems with (+F) or without (-F) fertilizer applications. In (a), SPP estimates for all combinations of establishment scenario (low-cost [LC] or high-cost [HC]) and fertilizer application are consolidated by keeping the competing cropping system requiring the greatest SPP (corn-soybean [CRN-SOY] or wheat-soybean [WHT-SOY]). In (b), the LC and HC outputs from (a) are consolidated to keep the lowest SPP across the +F and -F options. 249
74. For the low-cost (LC) establishment scenario, the biomass price necessary for switchgrass to generate the same annualized net return as a single year of corn or wheat (SPP, switchgrass parity price) under (a) conventional tillage (CT), (b) reduced tillage (RT) or (c) no-till (NT). For the high-cost (HC) establishment scenario, (d - f) same as (a - c). 250
75. Environmental benefits of switchgrass production relative to corn or wheat and under the most profitable fertilization option (e.g. Figure 36) for the high-cost (HC) establishment scenario: (a) mitigation of soil erosion, (b) mitigation of nitrogen (N) runoff into surface water, and (c) carbon (C) sequestration. Maps of (d) slope and (e) initial soil C from SSURGO are provided to provide context to the spatial patterns of a - c. 251

LIST OF TABLES

Table	Page
1. Comparison of modified northern upland switchgrass parameters presented herein to default ALMANAC values from Kiniry et al. (2008b) and to values used in parameter sensitivity analyses.	15
2. Details for ALMANAC validation sites presented in Figure 1.	21
3. Averaged across 66 location-years, relative proportion of growing season plant growth stress due to nitrogen (NS), water (WS), and temperature (TS) stresses under the modified parameterization presented herein and each sensitivity analysis outlined in Table 1.	40
4. Summary of findings from Chapter II results (Section 2.4).	47
5. Out of 16,466 components and 60,242 component horizons, the number of missing values for ALMANAC soil parameters provided by SSURGO.	58
6. Comparison of final ALMANAC corn and wheat parameterizations presented herein to the default ALMANAC parameterization and to the baseline and comparison parameterizations used in parameter sensitivity analyses.	62
7. Rates for the first and second applications of nitrogen fertilizer within the corn and wheat management systems.	65
8. Tabulation of study area parcels by land capability class (LCC) for all parcels, parcels with corn or wheat (C/W) production, and parcels without C/W production.	90
9. Summary of findings from Chapter III results (Section 3.4).	113
10. Comparison of assumptions for the low-cost (LC) and high-cost (HC) switchgrass establishment scenarios.	124
11. Description, approximate residue removal rates, areal harvest costs (AHC), and yield-based harvest costs (YHC) for the five residue harvest systems used in this study. Systems adapted from (Muth et al., 2013).	126

12.	For those equations within Sections 4.3.3 to 4.3.5 describing calculations of economic variables, summary of relevant crop(s), output variables, input variables, reference figures, and prerequisite equations. Output variables from prerequisite equations are used as input variables for Equations [38] to [41] and [43].	133
13.	Study-region average input costs for corn and wheat grain production, biomass harvest, and biomass transport within conventional tillage (CT), reduced tillage (RT), and no-till (NT) systems.	137
14.	Detailed crop chemicals and machinery cost estimates for the low-cost (LC) and high-cost (HC) establishment scenarios in year 1 (YR1), year 2 (YR2), and subsequent years (YR3+) of switchgrass production.	146
15.	Study-region average input costs for combinations of establishment scenario (low-cost [LC], high-cost [HC]) and fertilizer option (–F, +F) in year 1 (YR1), year 2 (YR2), and subsequent years (YR3+) of switchgrass production. Transport costs are to the nearest biorefinery, with biorefinery locations determined by available corn and wheat biomass under conventional tillage (CT), reduced tillage (RT), and no-till (NT) systems.	147
16.	Summary of findings from Chapter IV results (Section 4.4).	205
17.	Required ALMANAC soil parameters.	241
18.	Presence (+) or absence (–) of tillage, planting, harvest, and fertilizing operations for corn grown in conventional tillage (CT), reduced tillage (RT), and no-till (NT) management systems.	245
19.	Presence (+) or absence (–) of tillage, planting, harvest, and fertilizing operations for wheat grown in conventional tillage (CT), reduced tillage (RT), and no-till (NT) management systems.	246

ACKNOWLEDGEMENTS

I offer my profound thanks to my adviser, Dr. Soizik Laguette, for her highly detailed reviews of my dissertation drafts and her advice, support, and encouragement throughout the duration of my studies. I also thank my advisory committee members, Dr. Michael Hill, Dr. Michael Mann, Dr. Xiaodong Zhang, and Dr. Haochi Zheng, for their time, input, and guidance throughout my studies. I offer particular thanks to Dr. Hill, who especially challenged areas of my work in need of improvement and clarification. This final product is greatly improved as a result. I thank Dr. Dave Muth and Dr. Ian Bonner for providing the spatially-explicit crop residue removal rates that were integral to my work. Lastly, I thank the entire faculty, staff, and students of the Earth System Science and Policy department, both past and present. Although my work commitments limited my time spent on campus, I am proud to have belonged to a learning community built upon systems-based science and the representation of diverse backgrounds, disciplines, and expertise.

To Jen, for your love, support, patience, and encouragement.

ABSTRACT

The US government has mandated the annual usage of 61 GL of cellulosic biofuel by 2022. Cellulosic residues from annual crops, such as corn (*Zea mays* L.) and wheat (*Triticum aestivum* L. ssp. *aestivum*) represent a potential source of cellulosic biomass. Another source is the production of cellulosic bioenergy crops. Switchgrass (*Panicum virgatum* L.) was identified as a model biomass crop by the US Department of Energy in 1992, features the most advanced agronomic development among herbaceous perennial bioenergy feedstock candidates, and is widely adapted across North America. In three interconnected studies considering a 99-county area of the eastern Dakotas and western Minnesota, this dissertation characterizes the existing resource base of corn and wheat cellulosic biomass, estimates the biomass prices necessary for switchgrass to be competitive with collection of existing corn and wheat biomass, and estimates the necessary incentives for switchgrass to supplant sufficient corn or wheat area to offset recent grassland-to-cropland conversions observed within the study region. An improved parameterization of upland switchgrass ecotypes for the ALMANAC (Agricultural Land Management Alternative with Numerical Assessment Criteria) model was shown to predict multiyear-average yields with an RMSE of 1.95 Mg ha⁻¹ and PBIAS of 7.2%. Using moderate-resolution regional inputs, ALMANAC estimated county-scale multiyear-average corn yields with an RMSE of 0.71 Mg ha⁻¹ and PBIAS of 1.9%, and corresponding wheat yields with an RMSE of 0.28 Mg ha⁻¹ and PBIAS of 2.8%. Corn and wheat can supply up to 16.48 Tg of biomass annually within estimated biorefinery collection areas, at a biomass price of \$60 Mg⁻¹ or less. Switchgrass would require biomass prices of \$60 to \$180 Mg⁻¹ to supplant corn or wheat production, dependent on establishment and production cost assumptions. Annual payments of \$120 to \$290 million would encourage sufficient switchgrass production to offset recent grassland-to-cropland conversions in the study region, and can be strategically directed

to maximize the environmental benefits of switchgrass production.

CHAPTER I

INTRODUCTION

Through the second Renewable Fuel Standard (RFS2), the US government has mandated the annual usage of 61 GL of cellulosic biofuel by 2022 (Bracmort, 2019a). However, a commercialized cellulosic biofuel industry has been slow to develop. Actual cellulosic ethanol usage has fallen well short of the mandates specified in RFS2, as production volumes in 2017 met just 1% of the original mandate of 21 GL (Bracmort, 2019b; US EPA, 2019). Nonetheless, cellulosic biofuels remain critically important for a projected future where biofuels will account for a considerable portion of transportation fuels (Robertson et al., 2017).

The Billion Ton Report provides official US government estimates of nationwide agricultural biomass available for bioenergy production. The first edition (Perlack et al., 2005) characterized nationwide technical biomass availability, with no considerations for biomass harvest costs and generalized assumptions regarding the amount of biomass that could be harvested without causing excessive soil erosion. The second edition (U.S. Department of Energy, 2011) introduced economic modeling of feedstock farmgate prices by county, introduced spatially-explicit modeling of residue removal rates that prevent the depletion of soil organic matter and limit soil erosion to less than the tolerable limit defined by the USDA Natural Resources Conservation Service (Muth et al., 2013), and presented all outcomes at county scale. The latest edition (U.S. Department of Energy, 2016, 2017) introduces empirical modeling of dedicated bioenergy crops (switchgrass, miscanthus, energy cane, biomass sorghum), uses the Supply Characterization Model (Webb et al., 2014) to provide an economic analysis of biomass delivery to potential utilization facilities, and presents a comprehensive technical, economic, and environmental assessment at county scale for the entire US. The combined technical and economic assessment (U.S. Department of Energy, 2016) considers

biomass availability from the four dedicated bioenergy crops and residue removal from five grain crops (corn, wheat, oat, barley, sorghum), under scenarios encompassing four annual rates of bioenergy crop yield increase (1 to 4%) and three biomass prices (\$44, \$66, \$88 Mg⁻¹). The environmental assessment (U.S. Department of Energy, 2017) estimates nitrogen (N), phosphorus (P), and sediment loadings in two tributary basins of the Mississippi River, the corn stover-dominated Iowa River Basin and the switchgrass-dominated Arkansas White and Red River Basin, and county-scale outcomes of six variables across the entire US: land-use change between annual and perennial cover, greenhouse gas (GHG) intensity, water and irrigation requirements, air pollution, avian species richness, and projected yields in response to climate change.

While the Billion Ton Report offers an integrated technical, environmental, and economic assessment that considers harvest of grain crop residues and production of dedicated bioenergy crops, examinations at sub-county scale may reveal tradeoffs among technical, environmental, and economic outcomes that cannot be detected at county scale. There are several such investigations presenting an integrated assessment of technical and environmental outcomes. In an early example, Brown et al. (2000) examined switchgrass yield, N runoff, and soil erosion at 50 km resolution across a region spanning Minnesota, Iowa, Nebraska, and Kansas. Qin et al. (2015) examined yields and GHG emissions of switchgrass and miscanthus at a resolution of 0.25 degrees across US lands considered physically marginal for crop production, while Gelfand et al. (2013) estimated yield and GHG emissions at 60 m resolution for prairie grown on physically marginal lands across 10 states in the US upper Midwest. Jones et al. (2017a) estimated yields and soil organic carbon changes associated with corn stover harvest at 56 m resolution across 12 states in the US upper Midwest, while Zhang et al. (2010) estimated yield, GHG emissions, soil erosion, N loss, and P loss at 60 m resolution across nine Michigan counties for each of 54 scenarios containing one of six bioenergy crops (corn, grass mix, miscanthus, native prairie, hybrid poplar, switchgrass). However, no comparable investigations were found that simultaneously considered technical,

economic, and environmental outcomes at sub-county resolution. Thus, the goal of this dissertation is to present an integrated technical, economic, and environmental assessment of bioenergy cropping outcomes at a moderate spatial resolution (800 m).

The geographical focus of this investigation is a 99-county area of eastern North Dakota, eastern South Dakota, and western Minnesota. Influenced by declining precipitation from east to west and increasing temperature from north to south (PRISM Climate Group, 2019), this region features gradients in land use and native vegetative cover. Cultivated cropland dominates the study region, which also represents a transitional area between major corn and wheat production regions. Native vegetative cover ranges from mixed prairie in the west to tallgrass prairie in the east, with forested areas bordering the northeastern portion of the study region. Very little native prairie remains, but widespread areas of the western study region and isolated portions of the eastern study region feature cultivated cropland intermixed with various forms of perennial grasslands, primarily remnant prairie, rangeland (i.e. pasture and hay), and retired cropland enrolled in the USDA Conservation Reserve Program. Although this region has experienced increased grassland cover and decreased agricultural use between 1973 and 2000 (Sleeter et al., 2013), land-use changes from the mid-2000s to early 2010s have been characterized by an increase in cultivated cropland at the expense of grassland cover (Faber et al., 2012; Johnston, 2014; Lark et al., 2015, 2018; Wright and Wimberly, 2013).

This investigation considers corn stover, wheat straw, and switchgrass as potential cellulosic bioenergy crops within the study region. Corn (*Zea mays* L.) stover is the most abundant crop residue in the US (Muth et al., 2013), and all commercial-scale cellulosic ethanol plants to date have used corn stover as a feedstock (DuPont, 2015; POET-DSM, 2014; US DOE, 2014). Wheat (*Triticum aestivum* L. ssp. *aestivum*) straw is the second most abundant crop residue nationwide and is more abundant than corn stover in northern Montana, North Dakota, and Minnesota (Muth et al., 2013). Switchgrass (*Panicum virgatum* L.) was identified as a model biomass crop by the US Department of Energy in 1992 (Wright and Turhollow, 2010) and is the most advanced herbaceous perennial bioenergy feedstock in terms of its agronomic

development (Mitchell et al., 2012). Switchgrass is widely adapted to areas of North America east of the 100th meridian ranging from southern Canada to northern Mexico (Casler, 2012; Mitchell et al., 2014), with upland ecotype cultivars adapted to the northern US and lowland ecotype cultivars adapted to the southern US (Casler et al., 2011). Furthermore, switchgrass is reported to offer ecological benefits through carbon sequestration, provision of biodiversity and wildlife habitat, reduction in soil erosion and nutrient loss, and water retention and purification (e.g. Follett et al., 2012; Hartman et al., 2011; Jungers et al., 2015; Robertson et al., 2011a,b,c; Smith et al., 2013; Werling et al., 2014; Wiens et al., 2011).

Given its existing resource base of corn and wheat production, its suitability for upland ecotypes of switchgrass, and the dynamic nature of its land-use conversions between grasslands and agriculture, this region is well-suited for an integrated technical, economic, and environmental analysis of corn, wheat, and switchgrass biomass production. This investigation features six objectives in support of this overarching goal: (i) present an improved parameterization for simulation of upland switchgrass ecotypes in the ALMANAC (Agricultural Land Management Alternative with Numerical Assessment Criteria) model, (ii) characterize the accuracy and precision of the ALMANAC model for moderate-resolution estimation of corn and wheat yields, (iii) estimate the existing resource of corn and wheat biomass, (iv) estimate the biomass prices necessary for switchgrass to be economically competitive with biomass harvest in corn or wheat, (v) estimate the necessary incentives for switchgrass to supplant sufficient corn or wheat area to offset recent grassland-to-cropland conversions, and (vi) evaluate possible land use and environmental implications of switchgrass production. The first objective is addressed in Chapter II, the second objective is addressed in Chapter III, and the remaining four objectives are addressed in Chapter IV.

In Chapter II, I present an improved parameterization for simulation of upland switchgrass ecotypes using the ALMANAC model. ALMANAC is widely used for simulation of switchgrass growth, with parameterization of ‘Alamo’ switchgrass growth in Texas representing the seminal investigation of switchgrass simulation using ALMANAC (Kiniry

et al., 1996). Parameters for ‘Alamo’, a lowland ecotype cultivar released in 1978 and originally collected along the Frio River in Live Oak County, TX (USDA NRCS, 2012), have subsequently been modified for simulation of upland ecotype growth in the northern US (Kiniry et al., 2008a,b). However, I demonstrate that the seasonal growth patterns of upland ecotypes in northern locations do not resemble the seasonal growth patterns of ‘Alamo’ in Texas. For simulating the growth of upland switchgrass ecotypes in the northern US, I illustrate the improvements offered by a new set of ALMANAC parameters developed from field observations of switchgrass growth in southern Quebec, Canada. For example, as compared against a set of 66 field observations across Minnesota, North Dakota, and South Dakota, the improved ALMANAC parameterization reduces the RMSE of predicted single-year yields from 3.74 Mg ha⁻¹ to 2.52 Mg ha⁻¹, and reduces the mean bias from -18.3% to 7.2%. The improved ALMANAC parameterization presented in this chapter provides the basis for the simulated switchgrass yields used in the comparative analyses of Chapter IV.

In Chapter III, I present a protocol for using ALMANAC to simulate corn and wheat yields using moderate-resolution regional inputs. ALMANAC has successfully simulated corn yields across the US when utilizing field-scale input parameters, such as observed management practices (e.g. planting and harvest dates), measured weather conditions, and characterization of soil layers and physical properties through soil sampling (Kiniry and Bockholt, 1998; Kiniry et al., 1997, 2004; Xie et al., 2001). The EPIC (Erosion Productivity Impact Calculator) model, from which ALMANAC is derived, has similarly been used to estimate wheat yields in the northern US and southern Canada (Kiniry et al., 1995; Moulin and Beckie, 1993; Touré et al., 1995). However, few investigations have illustrated the use of regional-scale input parameters in ALMANAC modeling. I demonstrate accurate ALMANAC estimations of multiyear corn and wheat yields with weather inputs from a gridded climate dataset, soil properties from a soil survey dataset, and generalized management practices. As compared to multiyear county-average corn and wheat yields reported by the USDA, corresponding ALMANAC estimates feature mean biases of less than 5% and coefficients of variation of

less than 10%. ALMANAC estimates of single-year corn and wheat yields are less accurate, however, as ALMANAC tends to overestimate yields in years with abundant soil moisture and underestimate yields in years with limited soil moisture. Furthermore, I demonstrate that ALMANAC yield estimates are most sensitive to parameterization changes that increase water stress or are affected by increased water stress. The corn and wheat parameterizations developed in Chapter III provide the basis for the simulated corn and wheat yields used in the comparative analyses of Chapter IV.

Finally, Chapter IV investigates the feasibility of switchgrass biomass production relative to the collection of corn and wheat cellulosic residues. Sustainable residue removal rates for corn and wheat under conservation tillage, reduced tillage, and no-till systems (Muth et al., 2013) were combined with ALMANAC yield estimates to characterize the quantity of corn and wheat biomass potentially available for biofuel production. When combined with remotely-sensed locations of corn and wheat production, a subsequent moving-filter analysis characterized the areas of the study region with sufficient biomass to support a cellulosic refinery matching the nameplate capacity and annual biomass demand of a commercial-scale cellulosic ethanol plant in Emmetsburg, IA. Biomass prices from \$30 to \$60 Mg⁻¹ would be sufficient to cover the expenses of corn and wheat biomass collection within these biorefinery collection areas, while switchgrass would require biomass prices of \$100 to \$180 Mg⁻¹ to generate economic returns similar to those from corn and wheat produced for grain and biomass. To convert 410,000 ha of existing corn or wheat land to switchgrass, which would offset recent grassland-to-cropland conversions within the study region (Lark et al., 2015; Wright and Wimberly, 2013), would require annual payments of \$120 to \$230 million. Directing these payments towards parcels where switchgrass would provide the greatest soil erosion mitigation, N loss mitigation, and soil carbon sequestration relative to corn or wheat, rather than to parcels where switchgrass provides the greatest biomass yield increase, would result in one- to four-fold increases in these environmental outcomes.

In summary, Chapter II focuses on an improved method for simulating yields of upland

switchgrass ecotypes adapted to the northern US, and validates this improved parameterization against field observations. Chapter III focuses on simulating corn and wheat yields at a moderate resolution over a regional scale, and demonstrates accuracy in estimating multiyear average yields for the study region. Chapter IV combines switchgrass, corn, and wheat outcomes derived from the parameterizations presented in Chapters II and III and finds that market-based pricing would be insufficient to make switchgrass production as profitable as corn or wheat grown for grain and biomass. If subsidizing switchgrass production on existing corn or wheat land, prioritizing the conversion of parcels where switchgrass provides the greatest environmental benefit would increase the resulting amount of soil retention, N retention, and soil C sequestration by up to 420%, 210%, and 120%, respectively, as compared to the environmental outcomes from prioritizing switchgrass production on the parcels where it provides the greatest increase in biomass yield.

CHAPTER II

AN IMPROVED METHOD FOR ALMANAC SIMULATION OF UPLAND SWITCHGRASS ECOTYPES IN THE NORTHERN US

2.1. Abstract

Switchgrass (*Panicum virgatum* L.) is a perennial warm-season grass that has attracted recent attention as a potential bioenergy crop. Relative to the default parameterization utilizing switchgrass growth characterizations from Texas, this investigation improves the simulation of upland switchgrass ecotypes in northern US locations with the ALMANAC (Agricultural Land Management Alternative with Numerical Assessment Criteria) model. Growth of upland ecotypes was parameterized by field evaluations from Montreal, QC, Canada and sites throughout the northern US Great Plains. Resulting ALMANAC simulations were validated against measured yields from 66 location-years of switchgrass production across 13 sites in Minnesota, North Dakota, and South Dakota. As contrasted to the model defaults, the modified parameterization reduced residual mean square error of annual simulated yields from 3.74 to 2.52 Mg ha⁻¹ and improved percent bias from -18% to 7.2%. Similar improvements were observed for multiyear average yields. The modified parameterization also extended the median simulated maturity date from August 1 to August 28, consistent with field observations of switchgrass phenology within the study region. Of the 13 parameters modified in this study, simulated switchgrass yield was most sensitive to modifications of radiation use efficiency, light extinction coefficient, and potential heat units. The modified parameterization offers improved simulation of upland switchgrass ecotypes in the northern US.

2.2. Introduction

Switchgrass (*Panicum virgatum* L.) is a perennial warm-season grass well-suited for conservation, livestock forage production, and bioenergy production. Switchgrass is native to

areas of North America east of the 100th meridian ranging from southern Canada to northern Mexico and was once the dominant vegetation of the US tallgrass prairie and its associated ecosystems (Casler, 2012; Mitchell et al., 2014). Switchgrass is widely adaptable due to its considerable morphological and physiological variability within existing genetic populations. Such variation is characterized by ecotype, the primary taxonomic classification of phenotypic variation, which is based upon differences in habitat and morphology (Casler, 2012; Casler et al., 2011; Mitchell et al., 2014; Parrish and Fike, 2005). Upland ecotypes were first discovered in higher landscape positions characterized by well-drained, droughty soils, while lowland types were first associated with riverine habitats, floodplains, and other depressional landscape positions characterized by hydric soils exhibiting seasonally waterlogged conditions (Casler et al., 2011; Parrish and Fike, 2005). Morphologically, lowland switchgrass is taller and possesses longer and wider leaf blades, fewer tillers per plant, larger stem diameter, and later maturity when contrasted with upland switchgrass (Casler, 2012; Casler et al., 2011). In the US, upland ecotypes are widely adapted to northern regions and lowland ecotypes are broadly adapted to southern regions, with a large transitional area between (Figure 1; Casler et al., 2011). Specifically, upland ecotypes are widely adapted to areas north of 34° N latitude but are extremely rare in areas southward, while lowland ecotypes are widely adapted up to approximately 42° N latitude in the western portion of its range and 45° N latitude in the eastern part of its range (Casler, 2012).

Switchgrass has attracted recent attention due to its potential as a cellulosic bioenergy crop. The US Department of Energy first identified switchgrass as a candidate bioenergy crop in 1992 (Sanderson et al., 1996). Further supporting switchgrass as a cellulosic feedstock, the Renewable Fuel Standard in the US Energy Independence and Security Act of 2007 required 42 GL annual consumption of cellulosic biofuels by 2022, with a projected 12 to 30 GL of ethanol being produced from 3 to 5 Mha of perennial grasses (Keeler et al., 2013). Subsequently, in response to production shortfalls and substantial year-to-year variability in production, the mandates for cellulosic fuel production have been repeatedly scaled back (Lade et al., 2018;

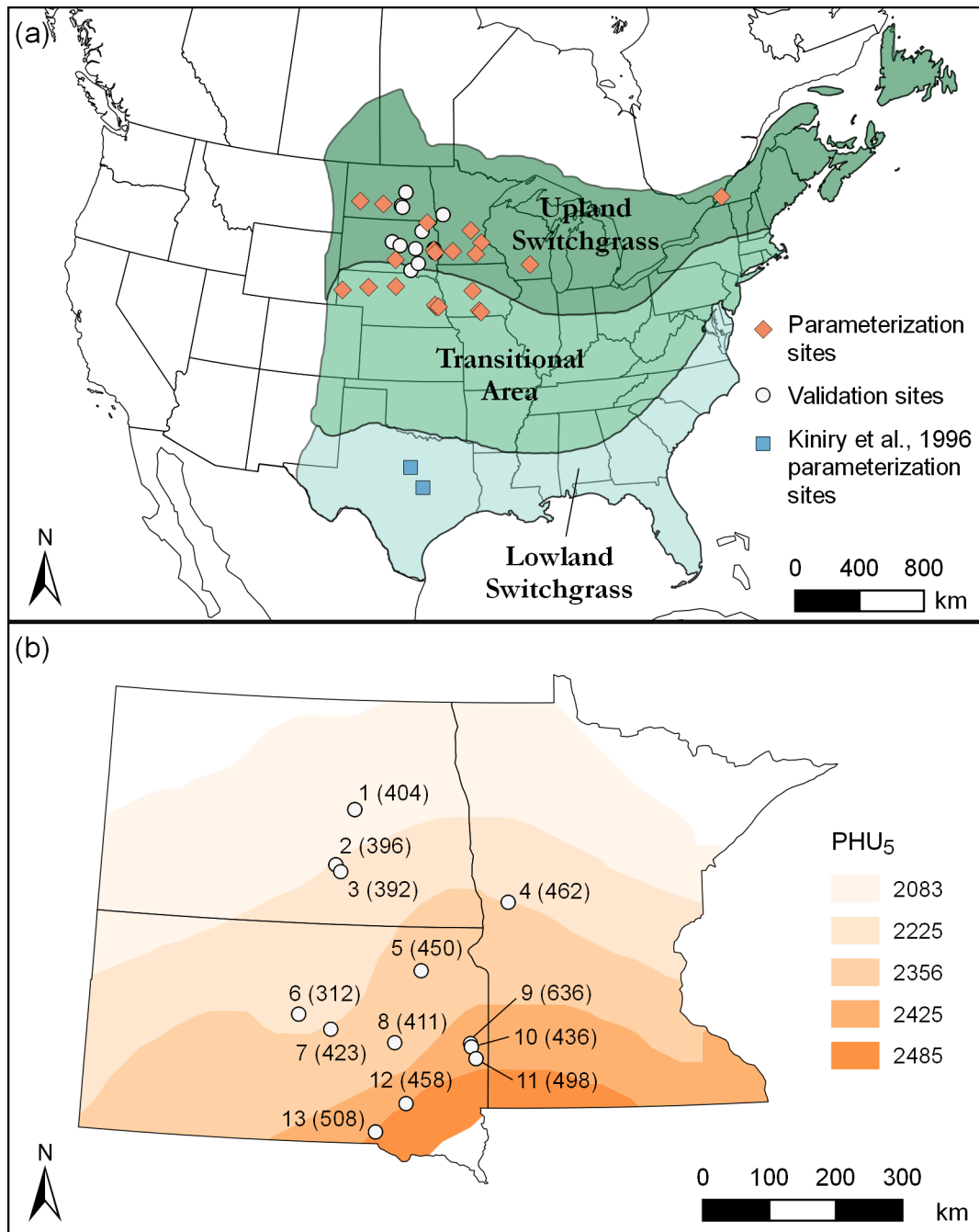


Figure 1. (a) The approximate North American adaptation ranges of upland and lowland ecotypes of switchgrass (adapted from Casler et al., 2011), the sites of the switchgrass field evaluations used to develop and validate the ALMANAC parameters for upland switchgrass presented herein, and the TX field sites used by Kiniry et al. (1996) to parameterize ALMANAC for ‘Alamo’ switchgrass. (b) Site numbers (see Table 2) and average precipitation (mm; in parenthesis) of the 13 validation sites from (a).

Stokes and Breetz, 2018). Nonetheless, switchgrass remains a promising candidate for future biomass cropping systems. First, switchgrass is reported to offer ecological benefits through provision of biodiversity and wildlife habitat, reduction in soil erosion and nutrient loss, carbon sequestration, and water retention and purification (e.g. Follett et al., 2012; Hartman et al., 2011; Jungers et al., 2015; Robertson et al., 2011a,b,c; Smith et al., 2013; Werling et al., 2014; Wiens et al., 2011). Second, switchgrass is the most advanced herbaceous perennial bioenergy feedstock in terms of its agronomic development. The US Department of Agriculture has had an active switchgrass research program since 1936 (Mitchell et al., 2012). Early uses for switchgrass included pasture, wildlife habitat, and conservation plantings (Mitchell et al., 2012; Parrish and Fike, 2005), with intensive research on improvement of forage yield and quality beginning in the 1970s (Parrish and Fike, 2005). More recently, management of switchgrass for bioenergy has been investigated throughout much of the central and eastern US (e.g. Adler et al., 2006; Anderson et al., 2013; Berdahl et al., 2005; Casler et al., 2007; Gamble et al., 2015; Heggenstaller et al., 2009; Ma et al., 2001; Miesel et al., 2017; Mulkey et al., 2006; Sanderson et al., 1999; Vogel et al., 2002) and specific cultural practices for switchgrass planting, maintenance, and harvest have been developed to assist growers in most switchgrass-producing regions of the US (Bughrara et al., 2007; Drinnon et al., 2015; Garland, 2008; Hancock, 2017; Holman et al., 2011; McGuire and Rupp, 2013; Mitchell et al., 2015; Newman et al., 2014; Reitsma et al., 2011; Shankle and Garrett, 2014; Teel et al., 2003). Breeding of improved switchgrass cultivars remains an area of active research (Moore et al., 2014), including a successful effort to develop a high-yielding lowland switchgrass ecotype broadly adapted to northern areas more typically suitable for upland ecotypes (Vogel et al., 2014). Nonetheless, most published accounts of successful switchgrass production in the northern Plains feature upland ecotypes (Arundale, 2012; Casler and Boe, 2003; Lee et al., 2007; Perrin et al., 2008; Schmer et al., 2006; Tober et al., 2007; Wang et al., 2013).

Numerous assessments have quantified switchgrass potential productivity across wide regions of the US. Several investigations have utilized an empirical approach, where switch-

grass yields were predicted based upon statistical relationships with variables such as temperature, precipitation, nitrogen (N) fertility, soil depth to bedrock, harvest frequency, stand age, soil water capacity, and latitude (Barney and DiTomaso, 2010; Evans et al., 2010; Grassini et al., 2009; Jager et al., 2010; Wullschleger et al., 2010). In other investigations, dynamic system simulation models (see Jones et al., 2016) have provided insight into switchgrass productivity and its variability across cultivars, management practices, environmental conditions, and projected climate change scenarios (Behrman et al., 2013, 2014; Brown et al., 2000; McLaughlin et al., 2006; Thomson et al., 2009). One such model widely used for switchgrass simulation is the ALMANAC (Agricultural Land Management Alternative with Numerical Assessment Criteria) model. Parameterization of ‘Alamo’ switchgrass growth in Texas represents the seminal investigation of switchgrass simulation using ALMANAC (Kiniry et al., 1996). Parameters for ‘Alamo’, a lowland ecotype cultivar released in 1978 and originally collected along the Frio River in Live Oak County, TX (USDA NRCS, 2012), have subsequently been adapted and extensively tested for switchgrass productivity estimation across the central and southern Great Plains and the southeastern US (Kiniry et al., 2005, 2008a; McLaughlin et al., 2006; Woli et al., 2012). By modifying two of the parameters developed by Kiniry et al. (1996), degree days to maturity and potential leaf area index, ALMANAC has also been adapted for simulation of upland ecotype growth across several locations of the northern US (Kiniry et al., 2008a,b). Subsequent uses of ALMANAC for regional and national assessments of switchgrass productivity have utilized a similar approach for simulation of upland ecotypes in northern locations (Behrman et al., 2013; Krohn, 2015).

Although ALMANAC has been tested for simulation of switchgrass growth in northern locations (Kiniry et al., 2008a,b), the approach utilized in these investigations relies primarily on characterizations of switchgrass growth for a lowland ecotype grown in TX. Considering that switchgrass cultivars and accessions are known to be adapted to a relatively narrow latitudinal range (Casler et al., 2004, 2007) and that lowland and upland ecotypes demonstrate clear differences in vegetative morphology (Casler, 2012; Casler et al., 2011), reliance on

these parameters is problematic for characterizing growth of upland ecotypes in northern locations. Using characterizations of switchgrass growth from within the range of adaptation for upland ecotypes (Figure 1), this investigation presents an improved parameterization of the ALMANAC model for simulation of upland ecotypes in northern locations of the US. The improved parameters are validated against field-measured yields from Minnesota, North Dakota, and South Dakota and contrasted to the default ALMANAC parameters for northern upland switchgrass previously reported by Kiniry et al. (2008b). The development of these parameters is necessary for the comparative technical, economic, and environmental analysis presented in Chapter IV, which requires accurate spatially-explicit estimates of switchgrass yield across the eastern Dakotas and western Minnesota.

2.3. Materials and Methods

2.3.1. ALMANAC overview

ALMANAC is a process-oriented model that simulates, on a daily time step, the processes of nutrient balance, soil water balance, and crop growth as a function of light interception by leaves, production of dry matter, and partitioning of biomass into grain (Kiniry et al., 1992, 2002). Soil water and nutrient subroutines are taken from the Erosion Productivity Impact Calculator (EPIC) model (Sharpley and Williams, 1990). Crop biomass accumulation is simulated as the product of intercepted photosynthetically active radiation (IPAR) and the efficiency of the crop species in converting IPAR into biomass (i.e. radiation use efficiency [RUE]). Beer's law (Monsi and Saeki, 1953), with light extinction coefficient (EXTINC; Kiniry et al., 1999, 2011) and leaf area index (LAI) as inputs, is used to estimate IPAR. Daily increases in LAI and biomass accumulation are constrained by the biomass growth stress factor, which ranges from 0 to 1 and is taken as the maximum of separate stress factors for water, temperature, N, phosphorus, and aeration (Williams et al., 1989). Separate from stress calculations, ALMANAC simulates the loss of standing live biomass due to frost damage through the user-defined FRST1 and FRST2 parameters. The progression of LAI development is temperature-driven through the parameter SYP, which represents the accumulated heat units

(HU) as a fraction of potential heat units (PHU). The shape of the LAI development curve is determined by maximum potential LAI (DMLA) and two parameters defining the shape of the nonstress leaf development s-curve function (DLAP1, DLAP2). LAI and RUE simultaneously decline in the latter stages of the growing season, as specified by the LAI decline factor (RLAD) and the rate of biomass decline factor (RBMD), after a user-specified SYP (denoted as DLAI) has accumulated. HU are calculated as the average of daily maximum and minimum temperatures minus the base temperature for growth (TG), with the maximum changed to the optimum temperature (TB) if it exceeds the optimum, and HU accumulate daily until reaching a user-specified PHU. Thus, all heat unit calculations are dependent upon user-specified values of TG and TB for growth of the simulated species. Hereafter, PHU calculated with TG = 5°C is referred to as PHU₅ while PHU with TG = 12°C is referred to as PHU₁₂.

2.3.2. Switchgrass parameterization

Switchgrass parameterization changes outlined herein were made in accordance with characterizations of switchgrass growth and physiology found in the existing literature. A suite of investigations conducted in Montreal, QC, Canada (45°28' N 73°45' W), examining established stands of two (Madakadze et al., 1998a, 1999a,b) or seven (Madakadze et al., 1998b) upland ecotype switchgrass cultivars over 2 to 3 years, serves as the primary source of switchgrass growth characterizations for this investigation. The seven cultivars, with place of origin in parenthesis, were Blackwell (northern Oklahoma and developed at Manhattan, KS), Dacotah (North Dakota and developed at Bismarck, ND), Forestburg (South Dakota and developed at Bismarck, ND), ND3743 (experimental line from Bismarck, ND), Pathfinder (South Dakota and developed at Lincoln, NE), Sunburst (South Dakota and developed at Brookings, SD), and Shelter (West Virginia and developed at Corning, NY). All other switchgrass growth characterizations were drawn from upland ecotypes grown under controlled conditions (Awada et al., 2002; Madakadze et al., 2003) or in the northern Great Plains states of Iowa, Minnesota, Nebraska, North Dakota, and South Dakota (Berdahl et al., 2005; Casler and Boe, 2003; Follett et al., 2012; Gamble et al., 2015; Lemus et al., 2008; Mulkey et al.,

Table 1. Comparison of modified northern upland switchgrass parameters presented herein to default ALMANAC values from Kiniry et al. (2008b) and to values used in parameter sensitivity analyses.

ALMANAC Parameter					
Notation	Description	Default Value	Modified Value(s)	Sens. Analy. Value(s)	Modified Value Reference(s)
DMLA	maximum potential leaf area index	3.3	6.5	3.3	Madakadze et al. (1998a)
DLAI	fraction of growing season after which leaf area index and radiation-use efficiency decline	0.7	0.55	0.7	Madakadze et al. (1998a)
DLAP1	parameter determining the first point on the optimal leaf area index development curve	10.2	15.31	10.2	Madakadze et al. (1998a)
DLAP2	parameter determining the second point on the optimal leaf area index development curve	20.95	55.99	20.95	same as DLAP1
RLAD	parameter governing the rate of leaf area index decline	1	0.2	1	Madakadze et al. (1998a)
RUE	radiation-use efficiency under nonstress conditions (kg ha ⁻¹ MJ ⁻¹ m ⁻²)	49	19.8	49	Madakadze et al. (1998b); Madakadze et al. (1999b)

Table 1. cont.

ALMANAC Parameter					
Notation	Description	Default Value	Modified Value(s)	Sens. Analy. Value(s)	Modified Value Reference(s)
EXTINC	extinction coefficient for calculating light interception	0.33	0.52	0.33	Madakadze et al. (1998b) ; Madakadze et al. (1999b)
GSI	maximum stomatal conductance for water vapor (mm s^{-1})	0.0074	0.0042	0.0074	Awada et al. (2002)
CNY	nitrogen fraction of harvested biomass	0.016	0.005	0.016	Gamble et al. (2015); Lemus et al. (2008); Madakadze et al. (1999a); Vogel et al. (2002); Wayman, Bowden, and Mitchell (2014)
FRST1	parameter determining the first point on the frost damage curve	1.01	98.001	1.01	Berdahl et al. (2005); Casler and Boe (2003); Follett et al. (2012); Mulkey et al. (2006)
FRST2	parameter determining the second point on the frost damage curve	3.95	99.002	3.95	same as FRST1
CN _A	runoff curve number for soil hydrologic group A	31	30	24, 36 [†]	USDA NRCS (1986)
CN _B	runoff curve number for soil hydrologic group B	59	58	46, 70 [†]	same as CN _A

Table 1. cont.

ALMANAC Parameter					
Notation	Description	Default Value	Modified Value(s)	Sens. Analy. Value(s)	Modified Value Reference(s)
CN _C	runoff curve number for soil hydrologic group C	72	71	57, 85 [†]	same as CN _A
CN _D	runoff curve number for soil hydrologic group D	79	78	62, 94 [†]	same as CN _A
TG	minimum temperature for plant growth (°C)	12	5	12	Madakadze et al. (2003)
PHU ₅	potential heat units for plant growth, TG = 5 °C	—	2083–2485 [‡]	1250–1491 [§]	Abatzoglou, 2013
PHU ₁₂	potential heat units for plant growth, TG = 12 °C	600 (ND), 700 (MN) [¶] , 800 (SD)	—	—	—

[†] Modified value $\pm 20\%$

[‡] Values from Figure 1b

[§] Values from Figure 1 –40%

[¶] Not specified in Kiniry et al. (2008b); average of ND and SD values

2006; Vogel et al., 2002; Wayman et al., 2014).

Table 1 outlines all switchgrass parameterization changes relative to those published by Kiniry et al. (2008b). The progression of leaf area index (LAI) throughout the growing season (Figure 2a) was modified by adjusting DMLA, DLAI, DLAP1, DLAP2, and RLAD in accordance with experimental data from Madakadze et al. (1998a,b). The resultant pattern of LAI progression was verified against regression models of LAI over HU presented in Madakadze et al. (1998a). Biomass accumulation (Figure 2b) was modified by adjusting RUE and EXTINC to match values published in Madakadze et al. (1998a); the resultant pattern of biomass accumulation was verified against regression models of biomass accumulation over time presented in Madakadze et al. (1999a). Runoff curve number (CN) for hydrologic soil groups A–D were set to match published values for meadow, which is defined as continuous grass protected from grazing and generally mowed for hay (Cronshey et al., 1986). Water vapor stomatal conductance (GSI) was set to 0.0042 mm s^{-1} (Awada et al., 2002), the N fraction of harvested biomass (CNY) was set to 0.005 (5 g kg^{-1} ; Gamble et al., 2015; Lemus et al., 2008; Madakadze et al., 1999b; Vogel et al., 2002; Wayman et al., 2014), and the minimum temperature for plant growth (TG) was set to 5°C (Madakadze et al., 2003). Lastly, FRST1 and FRST2 were set to 98.001 and 99.002, respectively, effectively negating the ALMANAC frost damage subroutine (Figure 2c). This adjustment is not directly supported by the literature, as a detailed description of switchgrass frost damage in northern locations could not be found. However, this adjustment is consistent with observations of switchgrass yield maximization in northern regions when harvesting after a killing frost, especially under long-term management (Berdahl et al., 2005; Casler and Boe, 2003; Follett et al., 2012; Mulkey et al., 2006).

2.3.3. ALMANAC validation

Simulations utilizing the modified ALMANAC parameters were validated against 66 location-years of switchgrass production across 13 sites in the eastern Dakotas and western Minnesota (Table 2, Figure 1b). Consistent with the methods of Kiniry et al. (2008b), two additional years were included at the beginning of each simulation to allow soil N and soil

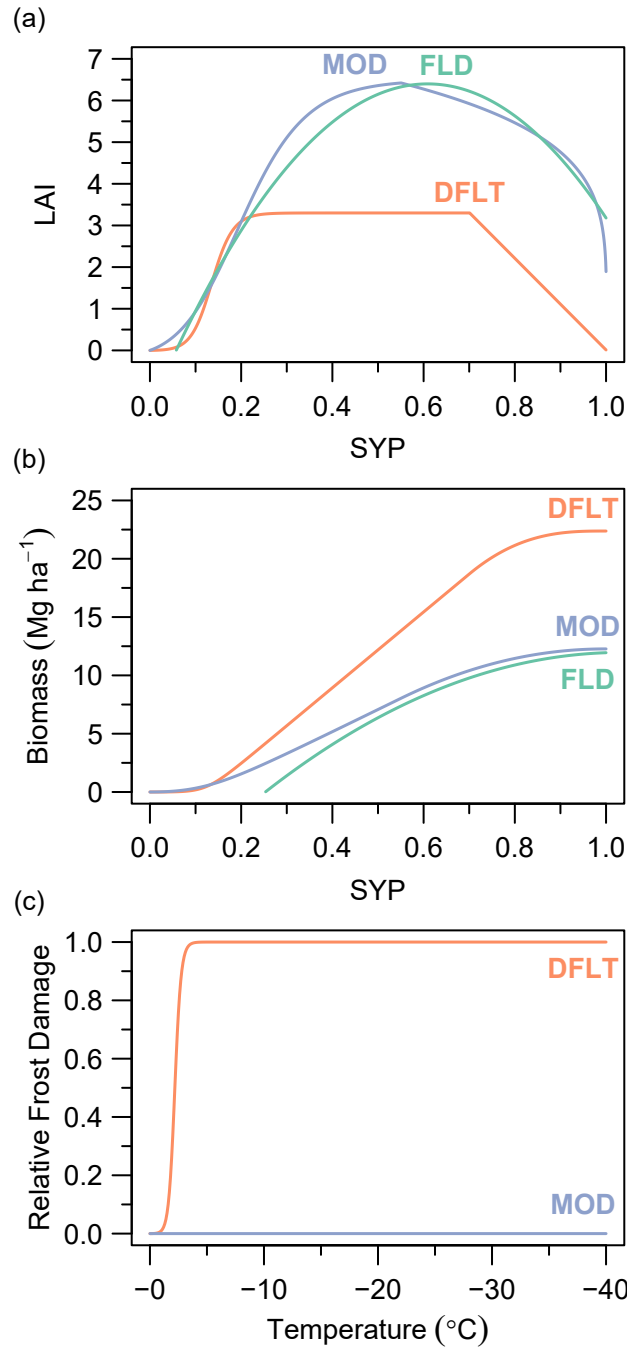


Figure 2. Comparisons of default ALMANAC parameters (DFLT), the modified parameters (MOD) presented herein, and regression models fit to field observations of switchgrass growth (FLD) as reported by Madakadze et al. (1998a,b). (a) By the fraction of the growing season that has passed (SYP), effect of modified DMLA, DLAI, DLAP1, DLAP2, and RLAD on simulated leaf area index (LAI). (b) Effect of modified RUE and EXTINC on biomass accumulation, assuming LAI development from (a). (c) Effect of modified FRST1 and FRST2 on the fraction of aboveground biomass lost to frost damage at a given temperature.

water to stabilize at values typical of established switchgrass fields. The validation sites featured average seasonal (April–September) precipitation from 265 to 840 mm, PHU₅ from 2083 to 2485, and PHU₁₂ from 1017 to 1289, as well as a range of years, N fertilizer rates, and harvest dates (Table 2). PHU for each site represents the average across 1980 to 2015 temperatures and within local adaptation ranges identified for corn (Stine Seed Company, 2015). While narrower than necessary to represent differing switchgrass maturities across latitudes, these adaptation ranges are consistent with the observation that switchgrass maturity is responsive to latitude (Casler et al., 2004, 2007). Required daily weather inputs (minimum and maximum temperatures [°C], precipitation [mm], relative humidity [%], wind velocity [m s^{-1} at 10 m height], and solar radiation [$\text{MJ m}^{-2} \text{d}^{-1}$]) were provided by gridMET (University of Idaho Climatology Lab, 2018), a moderate-resolution (4 km) gridded dataset of surface meteorological variables derived from a combination of the PRISM and NLDAS-2 climate datasets (Abatzoglou, 2013). Concomitantly, ALMANAC was configured to simulate evapotranspiration by the Penman-Monteith method (Allen et al., 1998).

The SSURGO soil survey database, with several modifications, provided the soil parameters required by ALMANAC. First, due to characteristics of the EPIC soil water routines incorporated into ALMANAC, a shallow (0.01 m) layer was added to the top of each soil. Because EPIC calculates soil water evaporation for the top 0.2 m of soil (see Sharpley and Williams, 1990, Equation 2.59), a surface soil layer depth of greater than 0.2 m results in error values for soil water evaporation and all other hydrologic variables. Adding a 0.01 m layer to the top of the soil profile alleviates this issue and is standard practice when using ALMANAC. Second, all soils with a representative slope of 0% were set to 0.0001%. In ALMANAC, each simulation unit is considered to be a small watershed. An EPIC routine incorporated into ALMANAC calculates the time of concentration, which is defined as the time period needed for water to flow from the most remote point in the watershed to the watershed outlet (Haan et al., 1994). Because the equation for time of concentration features slope in the denominator (see Sharpley and Williams, 1990, Equation 2.24), ALMANAC calculates infinite

Table 2. Details for ALMANAC validation sites presented in Figure 1.

Site	Reference(s)	City	State	Years	Soil	N [†]	Harvest Dates [‡]	Precip [§]
1	Wang et al. (2013)	Carrington	ND	2007–2013	Heimdal-Emrick loams (coarse-loamy, mixed, superactive, frigid Calcic Hapludolls; coarse-loamy, mixed, superactive, frigid Pachic Hapludolls)	56	12 Sep 2007; 17 Sep 2008; 23 Sep 2009; 18 Sep 2010; 17 Sep 2011; 16 Sep 2012; 14 Sep 2013	435; 439; 301; 428; 589; 309; 326
2	Wang et al. (2013)	Streeter	ND	2007–2013	Williams-Bowbells loams (fine-loamy, mixed, superactive, frigid Typic Argiustolls; fine-loamy, mixed, superactive, frigid Pachic Argiustolls)	56	same as Site 1	445; 356; 291; 543; 469; 311; 357
3	Perrin et al. (2008); Schmer et al. (2006)	Streeter	ND	2002–2005	Barnes-Svea loams (fine-loamy, mixed, superactive, frigid Calcic Hapludolls; fine-loamy, mixed, superactive, frigid Pachic Hapludolls)	69 [¶]	10 Aug	325; 372; 429; 444
4	Tober et al. (2007)	Fergus Falls	MN	1983–1987	Barnes-Langhei loam (fine-loamy, mixed, superactive, frigid Calcic Hapludolls; fine-loamy, mixed, superactive, frigid Typic Eutrudepts)	0	16 Oct	390; 384; 506; 700; 331

Table 2. cont.

Site	Reference(s)	City	State	Years	Soil	N [†]	Harvest Dates [‡]	Precip [§]	
5	Perrin et al. (2008); Schmer et al. (2006)	Bristol	SD	2002– 2005	Forman-Buse-Aastad loams (fine-loamy, mixed, frigid Udic Argiborolls; fine-loamy, mixed, frigid Udic Calciborolls; fine-loamy, mixed, frigid Pachic Udic Haploborolls)	99 [¶]	10 Aug	370; 415; 489; 525	
6	Tober et al. (2007)	Onida	SD	1985– 1989	Lowry silt loam (coarse-silty, mixed, mesic Typic Haplustolls)	0	16 Oct	266; 489; 265; 265; 275	
22	7	Perrin et al. (2008); Schmer et al. (2006)	Highmore	SD	2003– 2005	Glenham-Prosper loams (fine-loamy, mixed, mesic Typic Argiustolls; fine-loamy, mixed, mesic Pachic Argiustolls)	31 [¶]	10 Aug	343; 492; 434
8	Perrin et al. (2008); Schmer et al. (2006)	Huron	SD	2002– 2005	Dudley-Tetonka silt loams (fine, montmorillonitic, mesic Typic Natrustolls; fine, montmorillonitic, mesic Argiaquic Argialbolls)	39 [¶]	10 Aug	275; 342; 538; 488	
9	Arundale (2012)	Brookings	SD	2010– 2011	McIntosh-Badger silty clay loam (fine-silty, frigid Aeric Calciaquolls; fine, montmorillonitic, frigid Typic Argiaquolls); Vienna-Brookings silt loam complex (fine-loamy, mixed, frigid Udic Haploborolls; fine-silty, mixed, frigid Pachic Udic Haploborolls)	0	10 Aug	840; 431	

Table 2. cont.

Site	Reference(s)	City	State	Years	Soil	N [†]	Harvest Dates [‡]	Precip [§]
10	Casler and Boe (2003)	Brookings	SD	1998–2001	Vienna silt loam (fine-loamy, mixed, frigid Calcic Hapludoll)	112	14 Oct 1998; 14 Oct 1999; 14 Oct 2000; 4 Oct 2001	368; 477; 421; 479
11	Lee et al. (2007)	Brookings	SD	2001–2004	Houdek clay loam (fine-loamy, mixed, mesic Typic Argiustolls)	0; 112; 224	14 Aug 2001; 5 Aug 2002; 13 Aug 2003; 6 Aug 2004	522; 425; 431; 613
12	Perrin et al. (2008); Schmer et al. (2006)	Ethan	SD	2002–2005	Houdek-Prosper loams (fine-loamy, mixed, mesic Typic Argiustolls; fine-loamy, mixed, mesic Pachic Argiustolls)	104 [¶]	10 Aug	360; 431; 528; 513
13	Tober et al. (2007)	Lake Andes	SD	1984–1988	Agar silt loam (Fine-silty, mixed, mesic Typic Argiustolls)	0	23 Oct	588; 492; 638; 358; 464

[†] Nitrogen fertilizer rate(s), kg ha⁻¹

[‡] Harvest dates for locations 1–9 and 12–13 were estimated from generalized descriptions provided in reference text

[¶] Average of (variable) yearly rates

[§] Apr–Sep precipitation (mm) for each year

time of concentration when slope gradient is zero, resulting in error values for all hydrologic variables. Third, Gijsman et al. (2002) reported that laboratory-measured values of wilting point and field capacity, such as those available within SSURGO, are unsuitable to predict plant-available water under field conditions and may therefore result in major errors when modeling crop growth and yield. Among alternative approaches that estimate plant-available water as a function of basic soil data, the methods of Saxton et al. (1986) performed best out of the eight methods tested by Gijsman et al. (2002). In this investigation, wilting point and field capacity were estimated as a function of sand, clay, and organic matter using the updated equations of Saxton and Rawls (2006):

$$\begin{aligned}
 \theta_{1500} &= \theta_{1500t} + (0.14 \times \theta_{1500t} - 0.02); R^2 = 0.86 \\
 \theta_{1500t} &= -0.024S + 0.487C + 0.006OM + 0.005(S \times OM) \\
 &\quad - 0.013(C \times OM) + 0.068(S \times C) + 0.031 \\
 \theta_{33} &= \theta_{33t} + \left[1.283(\theta_{33t})^2 - 0.374(\theta_{33t}) - 0.015 \right]; R^2 = 0.63 \\
 \theta_{33t} &= -0.251S + 0.195C + 0.011OM + 0.006(S \times OM) \\
 &\quad - 0.027(C \times OM) + 0.452(S \times C) + 0.299
 \end{aligned} \tag{1}$$

where θ_{1500} and θ_{33} are the percent soil water content at wilting point (1500 kPa soil water tension) and field capacity (33 kPa tension); θ_{1500t} and θ_{33t} are the first solutions of θ_{1500} and θ_{33} ; and S , C , and OM are the percent sand, clay, and organic matter content of the soil, respectively. Fourth, coarse fragment content was calculated, as a weight percentage of the horizon, as the sum of rock fragments greater than 10 inches in size, rock fragments 3 to 10 inches in size, and the soil fraction remaining on top of a no. 10 sieve (Wentworth, 1922). Coarse fragment values were subsequently converted to a volume percentage using the method of Saxton and Rawls (2006):

$$R_v = (\alpha R_w) / [1 - R_w(1 - \alpha)] \tag{2}$$

where R_v is the volume fraction of coarse fragments (in g cm^{-3}), R_w is the weight fraction of gravel (in g g^{-1}), and α is the soil bulk density from SSURGO (in g cm^{-3}) divided by an assumed coarse fragments density of 2.65 g cm^{-3} . Fifth, soil organic carbon was estimated by multiplying the soil organic matter values from SSURGO by 0.58, as soil organic matter contains approximately 58% carbon (USDA NRCS, 2009). Finally, those required soil parameters not available within SSURGO were set to default ALMANAC values (Appendix B, Table 17).

2.3.4. Statistical analysis

Simulations were conducted with the ALMANAC command line interface. R (R Core Team, 2018) was used to store the necessary input tables, provide system calls to ALMANAC, extract results from ALMANAC output files, and prepare the graphs presented herein. Maps were created using QGIS (QGIS Development Team, 2018) and are projected using the ‘USA Contiguous Albers Equal Area Conic USGS Version’ projection (Spatial Reference, 2018). ALMANAC performance was evaluated by visual examination of yield outputs and through a set of statistics outlined in the extensive reviews of Bennett et al. (2013) and Moriasi et al. (2007). The chosen metrics can be divided into two broad categories, those for concurrent evaluation of real and modeled values and those for evaluation of model residuals, and were estimated using the ‘robustbase’ (Maechler et al., 2018) and ‘hydroGOF’ (Zambrano-Bigiarini, 2017) R packages.

Consistent with numerous other ALMANAC investigations (Kiniry et al., 2005; Kiniry and Bockholt, 1998; Kiniry et al., 1996, 1997, 2004; Xie et al., 2001), concurrent evaluation of field-measured and ALMANAC-simulated biomass yields was performed using a linear regression and its coefficient of determination (R^2). Due to the presence of high-leverage points identified in an ordinary least squares (OLS) regression, an iterated reweighted least squares (IRLS) regression with an MM-type regression estimator (Koller and Stahel, 2011; Yohai, 1987) was used. Nonetheless, there are well-documented problems inherent to using linear regression of simulated outcomes against measured values for the evaluation of biophysical

models. For instance, although the analyst can conduct significance tests of the regression model slope and intercept against the zero intercept and unit slope of a perfect regression model, with increasing scatter in the data points these hypothesis tests will increasingly fail to reject the null hypotheses of zero intercept and unit slope (Analla, 1998; Bellocchi et al., 2010; Bennett et al., 2013; Harrison, 1990; Kleijnen et al., 1998). Thus, this analysis will often reject a valid simulation model. In addition, regression of observed versus simulated values may violate the regression model assumptions that the X-axis values are known without error; the Y-axis values are independent, random, and with equal variance; and that residuals are independent and identically distributed (Bellocchi et al., 2010; Moriasi et al., 2007). Considering these limitations, a novel linear regression (Kleijnen et al., 1998) was also used to concurrently evaluate measured and simulated yields. This approach considers a simulation model to be valid if and only if the real and simulated systems have identical means, identical variances, and positively correlated real and simulated responses:

$$\mu_x = \mu_y = \mu \text{ and } \sigma_x^2 = \sigma_y^2 = \sigma^2 \text{ and } \rho_{xy} > 0. \quad [3]$$

This approach is implemented by performing an OLS regression on derived variables d and u :

$$\begin{aligned} d_i &= y_i - \hat{y}_i \\ u_i &= y_i + \hat{y}_i \\ d_i &= \gamma_0 + \gamma_1 u_i \end{aligned} \quad [4]$$

where \hat{y} represents simulated values and y represents measured values. The null hypothesis of identical means and variances for the real and simulated responses is as follows:

$$H_0: \gamma_0 = 0 \text{ and } \gamma_1 = 0. \quad [5]$$

An F -statistic with $n - 2$ and 2 degrees of freedom is used to test this joint hypothesis

simultaneously:

$$\begin{aligned} \text{SSE}_{\text{reduced}} &= \sum_{i=1}^n d_i^2 \\ \text{SSE}_{\text{full}} &= \sum_{i=1}^n (d_i - \hat{d}_i)^2 \end{aligned} \quad [6]$$

$$F_{2,n-2} = [(n-2)/2] [\text{SSE}_{\text{reduced}} - \text{SSE}_{\text{full}}] / \text{SSE}_{\text{full}}$$

where \hat{d}_i is the OLS estimate of d_i . If F is sufficiently high, and its p -value thus sufficiently low, the analyst rejects the null hypothesis and concludes that the simulation model does not meet the stringent validation requirement. This analysis is hereafter referred to as the unequal distribution test (UDT). Finally, the index of agreement (IOA; Willmott, 1981) provides an additional measure for concurrent evaluation of measured and simulated values. The IOA compares the sum of squared error to the potential error (Willmott, 1984), which is the sum of squared absolute differences between the simulated values and the mean measured value and between the measured values and the mean measured value:

$$\text{IOA} = 1 - \frac{\sum_{i=1}^n (y_i - \hat{y}_i)^2}{\sum_{i=1}^n (|\hat{y}_i - \bar{y}| + |y_i - \bar{y}|)^2}. \quad [7]$$

Similar to R^2 , the IOA is expressed on a 0 to 1 scale with 0 representing no agreement between simulated and measured values and 1 representing perfect agreement. However, unlike R^2 , the IOA is designed to effectively handle differences in means and variances between modeled and measured values (Willmott, 1981).

Evaluation of ALMANAC model residuals against measured values were evaluated by the root mean square error (RMSE), mean absolute error (MAE), and percent bias (PBIAS):

$$\begin{aligned} \text{RMSE} &= \sqrt{\frac{1}{n} \sum_{i=1}^n (y_i - \hat{y}_i)^2} \\ \text{MAE} &= \frac{1}{n} \sum_{i=1}^n |y_i - \hat{y}_i| \\ \text{PBIAS} &= \left[\frac{\sum_{i=1}^n (y_i - \hat{y}_i) \times 100}{\sum_{i=1}^n y_i} \right]. \end{aligned} \quad [8]$$

Although RMSE and MAE provide similar information on model error, RMSE penalizes greater errors more heavily while MAE reduces this bias towards large events. To aid in visualizing scatter plots of model residuals against measured yields, the fANCOVA R package (Wang, 2010) was used to fit local polynomial regressions. The second-degree polynomial equations were fit by least-squares and with automatic selection of the smoothing parameter according to the bias-corrected Akaike Information Criterion (Hurvich et al., 1998).

2.3.5. Sensitivity analyses

To examine the relative influence of each modified parameter in obtaining the simulation outcomes presented herein, sensitivity analyses were conducted for each of the parameters outlined in Table 1. Local sensitivity analyses were conducted utilizing one-factor-at-a-time perturbations (Norton, 2015; Pianosi et al., 2016). Following this method, each input parameter from the modified parameterization was perturbed individually while holding all other values constant. However, parameters considered to belong to a functional group were analyzed together within a single sensitivity analysis. For example, since DMLA, DLAI, DLAP1, DLAP2, and RLAD collectively modify the leaf area development curve (Figure 2a), changes to these parameters were evaluated within a single sensitivity analysis (hereafter, LAI). Similarly, FRST1 and FRST2 were grouped within a single sensitivity analysis (FRST), as were CN2A, CN2B, CN2C, and CN2D (CN). Since calculations of PHU are dependent on TG, PHU₁₂ values were calculated for the sensitivity analysis where TG = 12. Each sensitivity analysis was conducted over all years and validation sites.

The normalized sensitivity parameter (Norton, 2015) was used to rank the ALMANAC input parameters according to their relative contributions to simulated yield variability. For each sensitivity analysis j in year k and location l , the normalized sensitivity parameter (NSP) expresses changes in simulated yield as a function of changes to input parameters:

$$\text{NSP}_{jkl} = \frac{(\hat{y}_{jkl} - y_{kl}) / y_{kl}}{(\hat{p}_{jl} - p_l) / p_l} \quad [9]$$

where \hat{y} and \hat{p} are yields and parameters from the sensitivity analysis while y and p are yields and parameters from the modified ALMANAC parameterization. Changes in yields and parameters were normalized due to the differing units among the input parameters and simulated yield outputs. For the LAI sensitivity analysis, the denominator of Equation [9] was the normalized difference in area underneath the ‘DFLT’ and ‘MOD’ leaf development curves of Figure 2a. A differing approach was used for the FRST sensitivity analysis, as frost damage values (Figure 2c) are only implemented on those days when the minimum temperature is less than 0 °C. Thus, normalized frost damage (FD) was calculated as the amount of biomass lost during days where damage is allowed to occur, summed within years k and locations l :

$$\frac{\{\hat{B}_{kl1}, \hat{B}_{kl2}, \dots, \hat{B}_{kln}\}}{\{B_{kl1}, B_{kl2}, \dots, B_{kln}\}} = \sum_{m=1}^M (B_{klm}, B_{klm}) \text{ where } T_m < 0 \quad [10]$$

$$\{FD_{kl1}, FD_{kl2}, \dots, FD_{kln}\} = (B_{kl} - \hat{B}_{kl}) / B_{kl}$$

where m is one day within a growing season (M) days long, B is biomass produced under the modified ALMANAC parameterization, \hat{B} is biomass produced under the FRST sensitivity analysis, and T is minimum daily temperature.

Scatter plots of sensitivity analysis yields against those from the modified ALMANAC parameterization were used to further evaluate yield responses to parameterization changes. Accompanying the scatter plots are measurements of percent bias and mean bias error (MBE):

$$MBE = \frac{1}{n} \sum_{i=1}^n (\hat{y}_i - y_i) \quad [11]$$

where \hat{y} represents simulated values and y represents measured values. Sensitivity analyses scatter plots were created using the ‘ggplot2’ (Wickham, 2009) R package. Finally, to evaluate changes in ALMANAC model functioning associated with sensitivity analysis yield responses, daily simulated water, N, and temperature stresses were summed to an annual basis and

normalized as follows:

$$PGS_{jklm} = \max(\{WS_{jklm}, NS_{jklm}, TS_{jklm}\})$$

$$\{RWS_{jkl}, RNS_{jkl}, RTS_{jkl}\} = \frac{\sum_{m=1}^M (\{WS_{jklm}, NS_{jklm}, TS_{jklm}\} \subset PGS_{jklm})}{\sum_{m=1}^M (PGS_{jklm})} \quad [12]$$

where sensitivity analysis is j , year is k , location is l , and m is one day within a growing season M days long; PGS is the plant growth stress, taken as the maximum of separate stresses for water (WS), N (NS), and temperature (TS); and RWS , RNS and RTS are relative stresses for water, N, and temperature, respectively.

2.4. Results

2.4.1. Annual yield outcomes

The ability of ALMANAC to accurately estimate year-to-year yields is the primary test of its suitability in simulating switchgrass growth. Comparisons of annual field-measured and simulated switchgrass biomass yields under default and modified ALMANAC parameters are presented in Figure 3. Evaluation of annual outputs under the default parameterization revealed eight location-years where simulated biomass yields were less than 2 Mg ha⁻¹ while measured yields ranged from approximately 5 to 9 Mg ha⁻¹ (Figure 3a). Investigation of daily simulation outputs for these instances revealed that the simulated yield outcomes were due to the default ALMANAC parameterization for CNY (Table 1) in locations with no fertilizer N, which was causing ALMANAC to simulate nearly absolute N stress following removal of aboveground N with biomass harvest. Modification of CNY corrected this issue (Figure 3c), improved the bias in mean simulated yield over mean measured yield from -18% (Figure 3b) to 11% (Figure 3d), and reduced RMSE and MAE by 0.83 and 0.82 Mg ha⁻¹, respectively. Nonetheless, the inclusion of all other modifications outlined in Table 1 further improved the simulation outcomes (Figure 3e,f), resulting in an IOA of 0.65 and 13%, 5%, and 32% reductions in RMSE, MAE, and PBIAS when compared to the default parameters with corrected CNY (Figure 3c,d). In addition, unlike the other two parameterizations (Figure 3a,c),

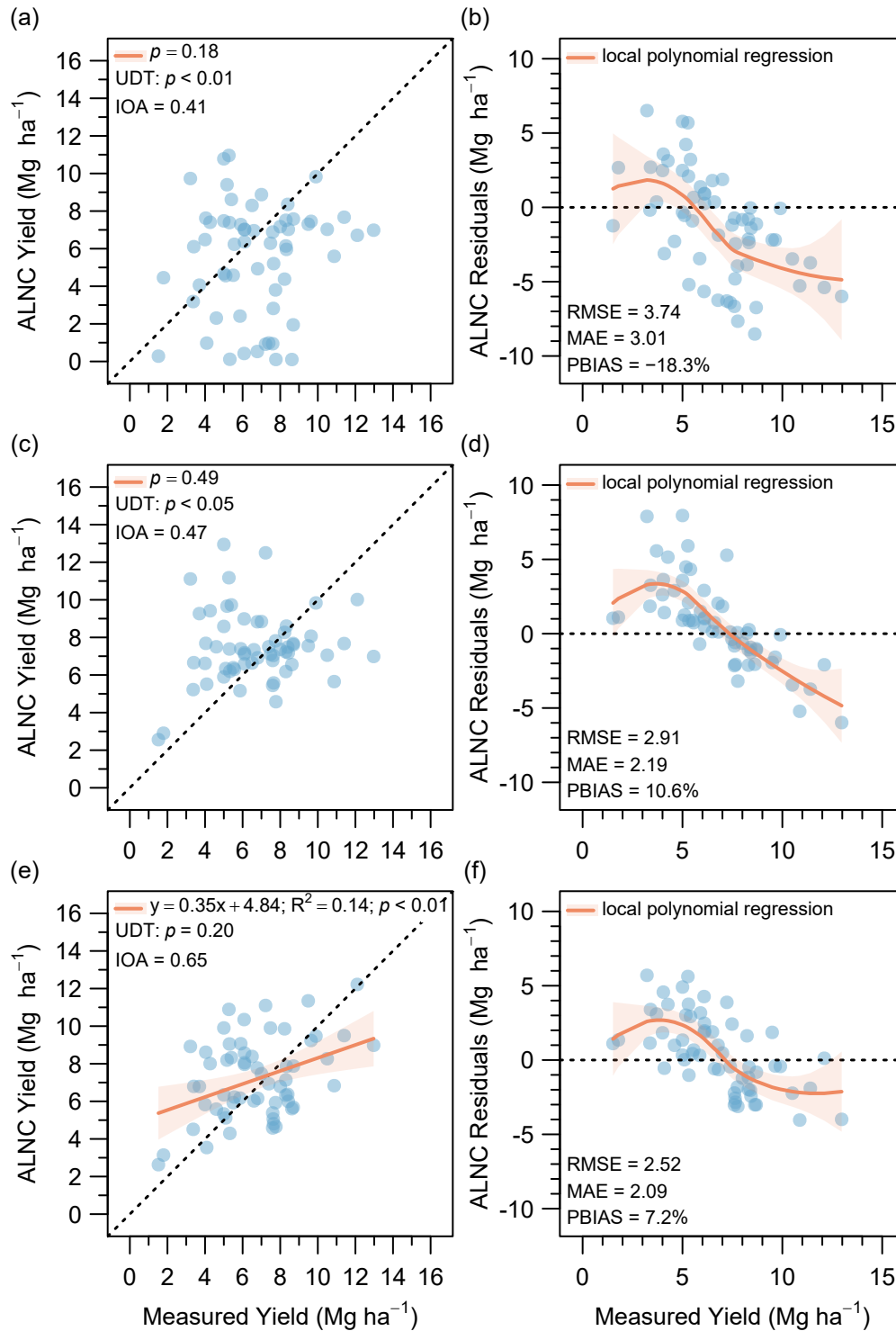


Figure 3. Comparisons of measured annual switchgrass yields to ALMANAC (ALNC) simulations using the (a) default parameters, (c) default parameterization with CNY adjusted from 0.016 to 0.005, and (e) modified parameters presented herein. (b, d, f) ALMANAC model residuals for the simulations described in (a, c, e).

the UDT ($p = 20$) in Figure 3e indicates that the measured and simulated yields are drawn from populations with equal means and variances, providing further evidence of an acceptable model parameterization.

2.4.2. Multiyear-average yield outcomes

Comparisons of multiyear average yields provide further evidence in support of the modified parameters. The IOA (0.68) is largest for the modified parameterization (Figure 4e), indicating an improved model fit compared to the other parameterizations (Figure 4a,c), and the RMSE (1.95 Mg ha^{-1}), MAE (1.44 Mg ha^{-1}), and PBIAS (11.7%) are lowest (Figure 4f). Nonetheless, the UDT suggests acceptable model performance under any of the three parameterizations (Figure 4a,c,e), and the default parameterization with corrected CNY resulted in a slightly better fit in the robust linear regression of simulated versus measured yields (Figure 4c). These outcomes highlight the importance of examining annual simulation outcomes in evaluations of ALMANAC performance, as multiyear average results may conceal parameterization issues otherwise revealed by annual results.

2.4.3. Within-season outcomes

While accurate estimation of annual and multiyear average yields is an important indicator of ALMANAC model performance, simulated patterns of within-season growth must also match observed patterns from field investigations. Examining within-season LAI development, accumulation of aboveground plant mass (AGPM), and N stress values for switchgrass growth in Site 11 (Figure 5) provides further insight into the impact of the elevated CNY value in the default parameterization. Switchgrass in the 0 N treatment of Site 11 was harvested in 2001 to 2004 (Table 2). Relative to measured yield, the 2001 simulated yield demonstrates a bias of -5 Mg ha^{-1} due to severe N deficiency following switchgrass N removal during the two model spin-up years (Figure 5, top panel). Simulated yields in 2002 are within 0.5 Mg ha^{-1} of measured yields, as there is minimal simulated N stress following the limited crop N removal in 2001. In 2003 and 2004, the pattern repeats, with low yield in 2003 and a reasonable yield estimate in 2004. This outcome demonstrates the inability of the default

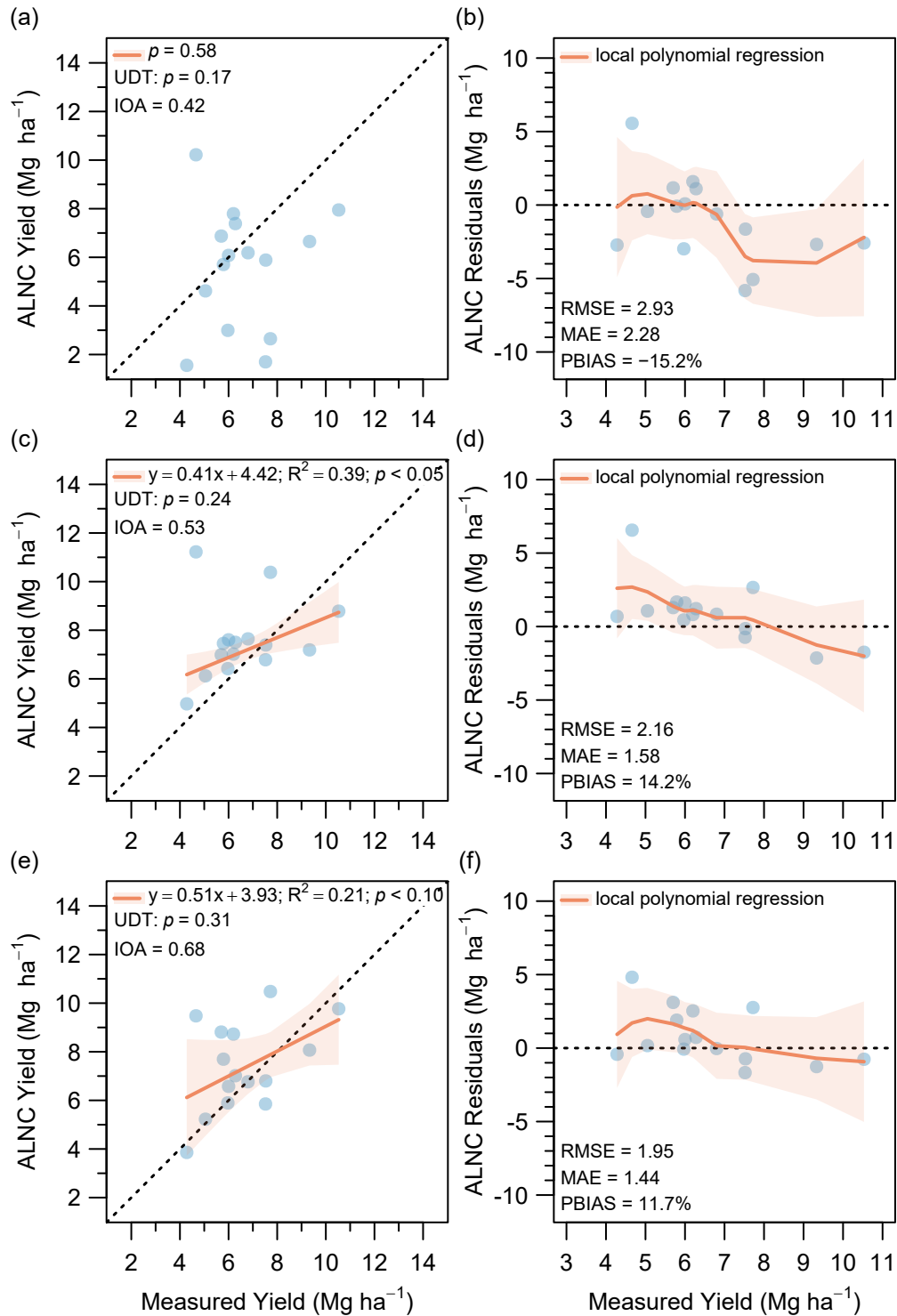


Figure 4. Comparisons of measured multiyear average switchgrass yields to ALMANAC (ALNC) simulations using the (a) default parameters, (c) default parameterization with CNY adjusted from 0.016 to 0.005, and (e) modified parameters presented herein. (b, d, f) ALMANAC model residuals for the simulations described in (a, c, e).

ALMANAC parameterization to accurately simulate yield in low N environments, and the modified parameterization does not feature this issue (Figure 5, bottom panel). In addition to highlighting the inaccuracy of simulated N stress in the default parameterization, these example within-season traces further illustrate the pitfalls of evaluating simulation outcomes solely on the basis of multiyear average yields. Within-season outcomes for all years and locations are presented in Appendix A.

The default and modified parameterizations also result in drastic differences in simulated switchgrass phenology, even in instances where simulated yields are similar. In Site 3 (Figure 6), both the default and modified parameterizations are effective in estimating the multiyear average yield. Nonetheless, only the modified parameterization (Figure 6, bottom panel) results in switchgrass growth characteristics consistent with the literature for upland ecotypes in northern locations (e.g. Figure 2a). The modified parameterization demonstrates seasonal LAI development gradually increasing over the first half of the growing season before reaching its maximum and declining shortly thereafter, with maximum LAI ranging from 3.5 to 5.5 across years. In contrast, the default parameters (Figure 6, top panel) result in a maximum LAI no greater than 2, with maximum LAI occurring after just 20% of the growing season has elapsed and remaining steady thereafter until declining once 70% of the growing season has elapsed. Final AGPM is similar across the two parameterizations due to differences in RUE and growing season length. In the default parameterization (Figure 6, top panel), final yield is a result of high RUE (Table 1) compensating for low LAI and a short growing season (590 HU₁₂). In the modified parameterization (Figure 6, bottom panel), final yield is a function of lower RUE combining with higher LAI and a longer growing season (1508 HU₅).

Distributions of switchgrass maturity dates further demonstrate the difference in simulated switchgrass phenology between the default and modified parameterizations. While the default parameterization results in switchgrass maturity dates with a distribution symmetrical around a median maturity date of August 1 (Figure 7), the distribution of maturity dates under the modified parameterization has a median of August 28 and a skew towards maturity dates in

ALMANAC stresses: ■ Water ■ Nitrogen ■ Temperature
 ALMANAC outputs: — LAI — AGPM
 ALMANAC yields: - - - MYA ■ 2001 ● 2002 ▲ 2003 ◆ 2004
 Field yields: - - - - MYA ■ 2001 ● 2002 ▲ 2003 ◆ 2004
 MYA Weather (Apr – Sep): 498 mm precipitation, 758 HU₁₂, 1622 HU₅

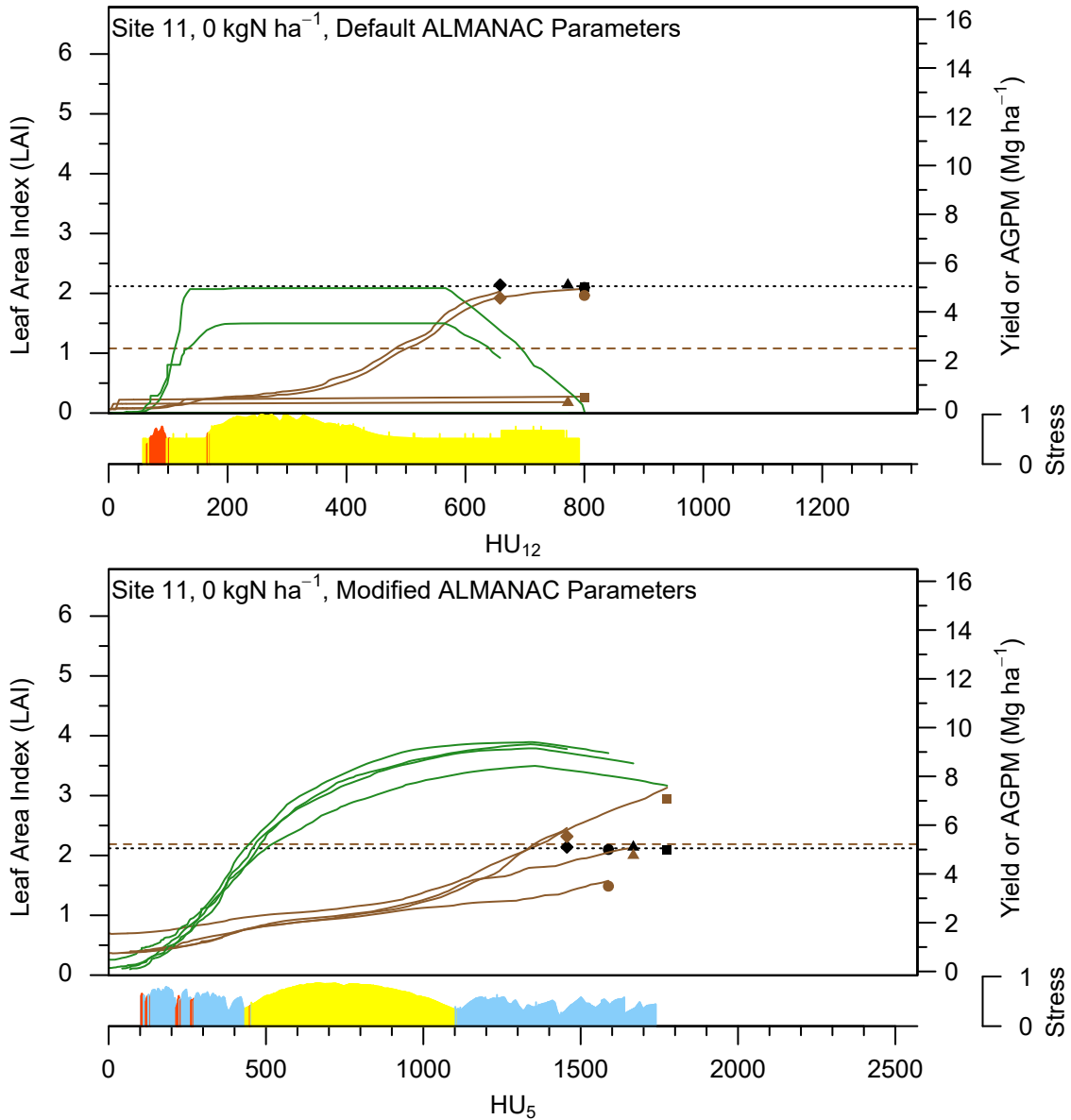


Figure 5. For Site 11 with no nitrogen fertilizer (Table 2), comparison of daily simulated leaf area index (LAI), aboveground plant mass (AGPM), and dominant plant growth stress for the default ALMANAC parameters and the modified parameters presented herein. Water, nitrogen, and temperature stress values represent the average over all simulation years. Superimposed on the daily outputs are annual and multiyear average (MYA) simulated and field-measured yields.

ALMANAC stresses: Water Nitrogen Temperature
 ALMANAC outputs: LAI AGPM
 ALMANAC yields: MYA 2002 2003 2004 2005
 Field yields: MYA 2002 2003 2004 2005
 MYA Weather (Apr – Sep): 392 mm precipitation, 590 HU₁₂, 1508 HU₅

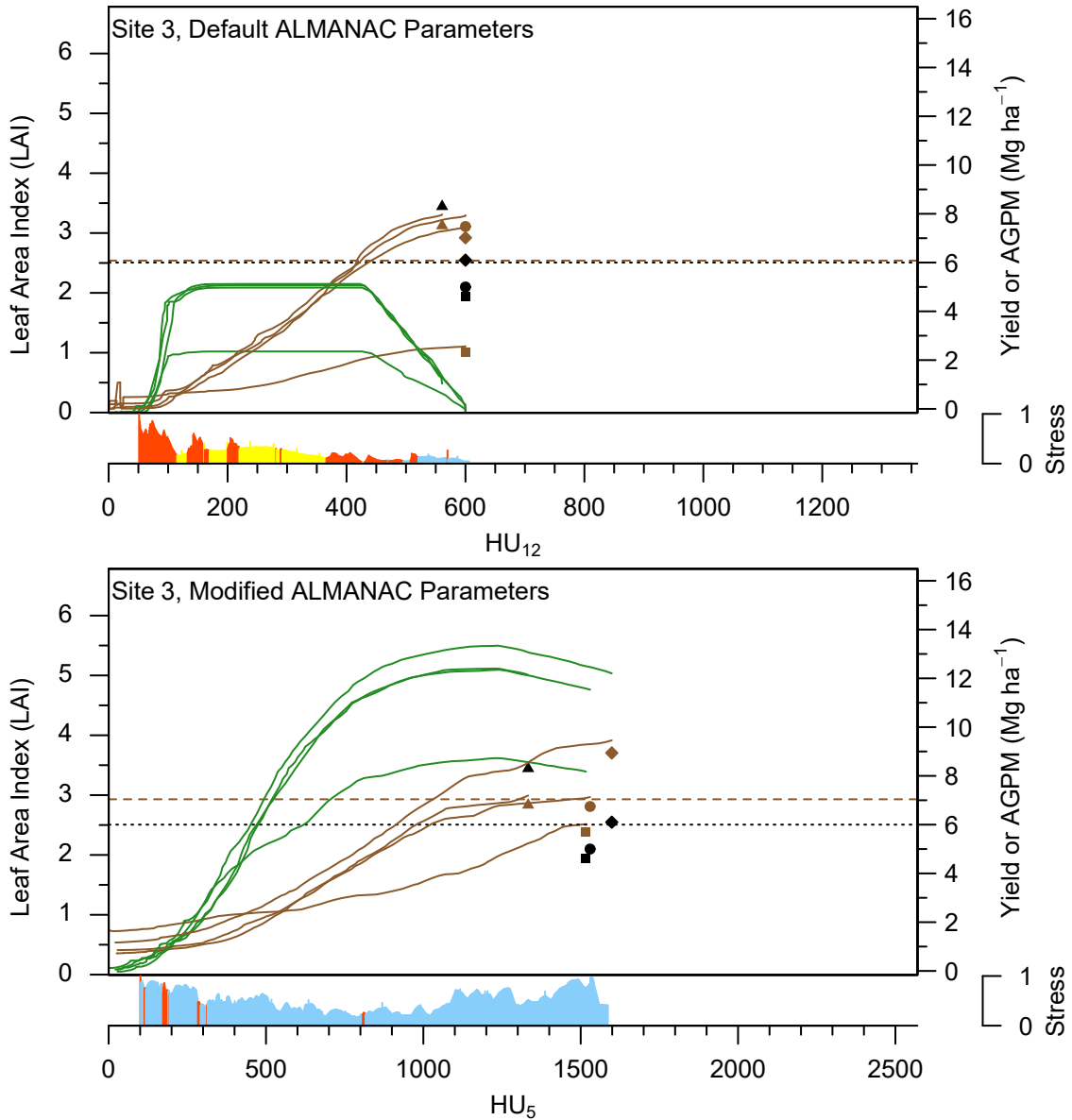


Figure 6. For Site 3 (Table 2), comparison of daily simulated leaf area index (LAI), aboveground plant mass (AGPM), and dominant plant growth stress for the default ALMANAC parameters and the modified parameters presented herein. Water, nitrogen, and temperature stress values represent the average over all simulation years. Superimposed on the daily outputs are annual and multiyear average (MYA) simulated and field-measured yields.

mid- to late-September.

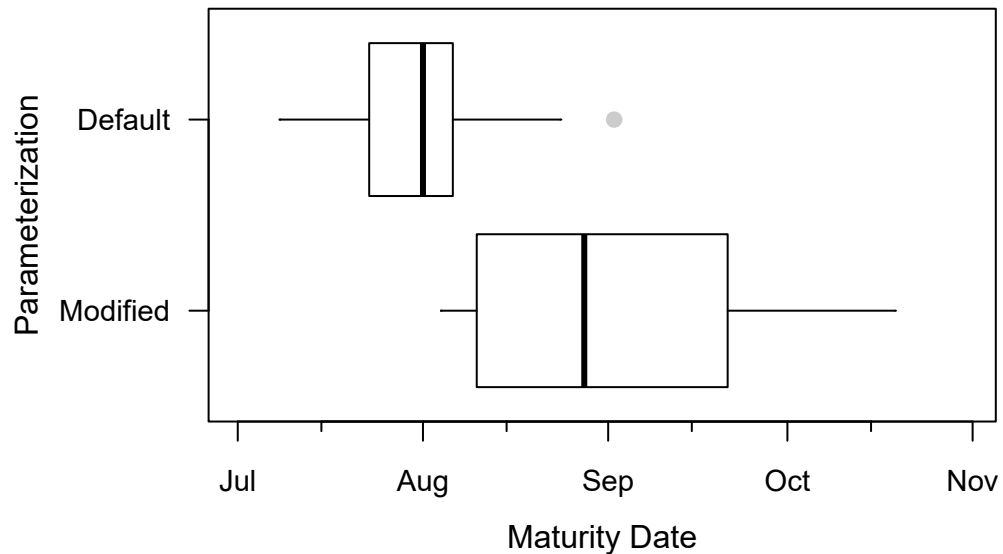


Figure 7. Distribution of simulated switchgrass maturity date under the default ALMANAC parameterization and the modified parameterization presented herein.

2.4.4. Sensitivity analyses

In simulation modeling, sensitivity analyses indicate how uncertainty in model inputs affects uncertainty in model outputs, and indicates which parameters require the greatest attention when parameterizing the model for future investigations. Sensitivity analyses outlined in Table 1 were used to demonstrate the relative impacts of ALMANAC parameterization changes on simulated yields.

Distributions of the normalized sensitivity parameter across all years and locations of the validation dataset are shown in Figure 8. The normalized sensitivity parameter expresses the magnitude change in simulated yield response as a proportion of the magnitude change of a given parameter within its sensitivity analysis. Positive values indicate positive correlation between parameterization changes and subsequent yield responses, while negative values indicate negative correlation. The relative influence of each parameter on simulated yield outcomes can be obtained by sorting on the absolute value of the normalized sensitivity

parameter. For the 66 location-years included in the sensitivity analyses, the scatter plots in Figure 9 compare the simulated yield outcomes of the modified parameterization to each of the sensitivity analyses. Averaged across 66 location-years, Table 3 displays the relative proportion of season-long growth stress attributable to the individual temperature, water, and N stresses. Together, Figure 9 and Table 3 provide further insight into the impact of sensitivity analysis parameterization changes on ALMANAC model function.

2.4.4. 1. Parameters defining maximum productivity

In ALMANAC, the maximum productivity of the simulated crop is determined by its LAI development curve, the efficiency in which leaf area intercepts photosynthetically active radiation as defined by EXTINC, and the efficiency in converting intercepted light into biomass as defined by RUE. As measured by the normalized sensitivity parameter, ALMANAC was most sensitive to adjustments of RUE and EXTINC in this investigation, with median values of 0.48 and 0.45, respectively (Figure 8). Adjustments of the LAI development curve resulted in a relative sensitivity of -0.16 , which ranks 5th out of the 10 parameter adjustments investigated. The sensitivity analysis for RUE increased its value from 19.8 to 49 kg ha⁻¹ MJ⁻¹ m⁻², resulting in the largest absolute changes in simulated yield and the balance between simulated stresses of any sensitivity analysis. Yield increased by an average of 5.58 Mg ha⁻¹ (74%) and by as much as 15 Mg ha⁻¹ (Figure 9, 'RUE'). Yields were primarily limited by N availability under high RUE, with the proportion of plant growth stress due to N increasing from 20% to 45% (Table 3). The sensitivity analysis for EXTINC decreased its value from 0.52 to 0.33, resulting in an average yield decrease of 0.97 Mg ha⁻¹ (12.9%; Figure 9, 'EXTINC'). However, changes to EXTINC resulted in negligible change in the balance of stress factors (Table 3). Compared to RUE and EXTINC, modifying the LAI development curve had modest effects on simulated yield. Decreasing the area under the LAI curve (Figure 2a) increased yield by an average of 0.55 Mg ha⁻¹ (7.3%; Figure 9, 'LAI'). However, modifying the LAI curve decreased water stress from 40% to 30% of total seasonal stress (Table 3). Collectively, these results indicate that accurately defining RUE is

relatively more important than defining EXTINC and LAI when parameterizing maximum crop productivity in ALMANAC. Nonetheless, LAI and EXTINC adjustments had a meaningful impact on simulated yields, and adjusting LAI altered the balance between simulated stresses.

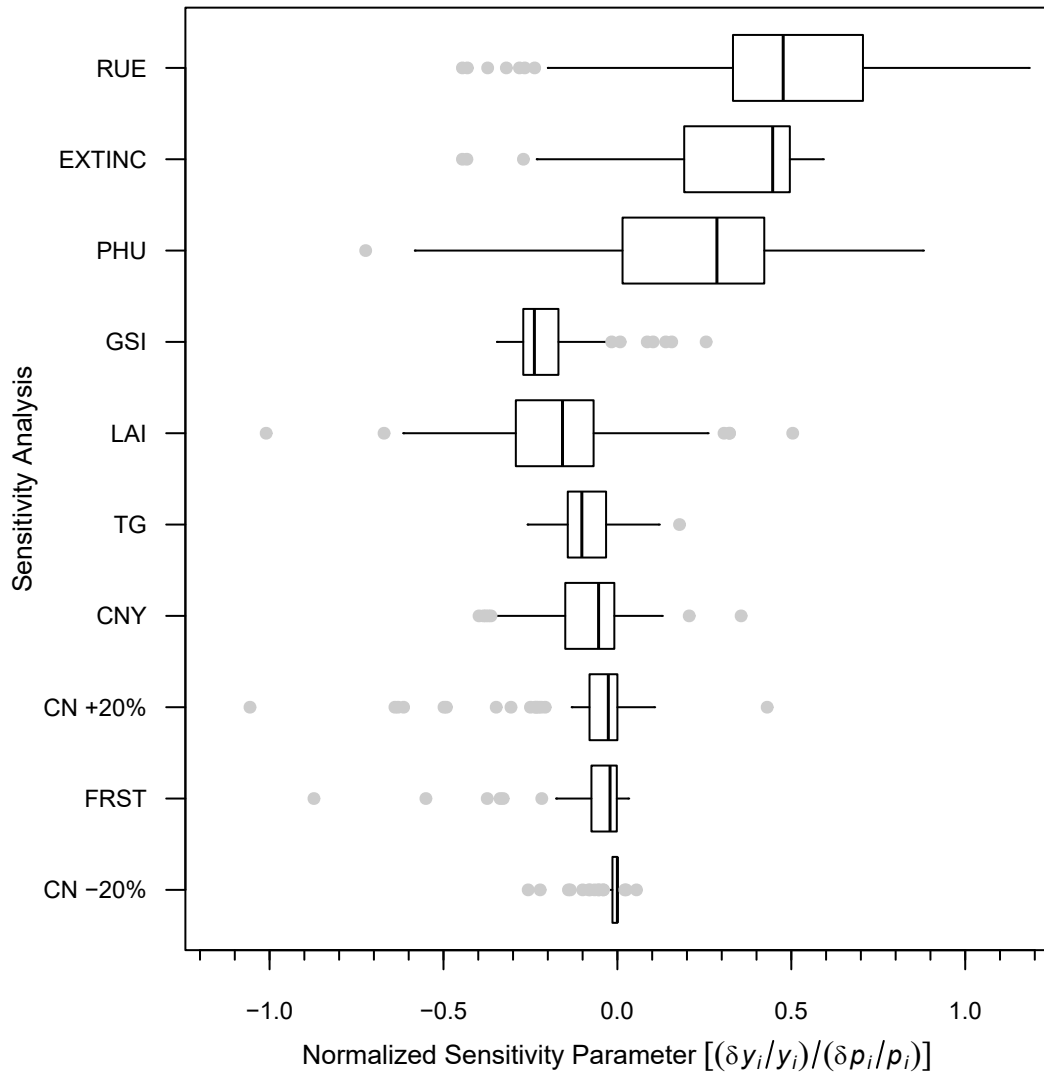


Figure 8. Distribution of the normalized sensitivity parameter for simulated yield sensitivity analyses under the parameterization changes outlined in Table 1.

2.4.4. 2. Parameters defining phenology

Section 2.4.3 described the effect of the modified parameterization on switchgrass phenology. In ALMANAC, crop phenology is determined by its maximum potential heat units

Table 3. Averaged across 66 location-years, relative proportion of growing season plant growth stress due to nitrogen (NS), water (WS), and temperature (TS) stresses under the modified parameterization presented herein and each sensitivity analysis outlined in Table 1.

ID	Relative Proportion of Growing Season Stress		
	NS	WS	TS
Modified parameterization	0.20	0.40	0.40
Sensitivity analysis			
RUE	0.45	0.25	0.30
EXTINC	0.15	0.45	0.40
PHU	0.20	0.35	0.45
GSI	0.15	0.50	0.35
LAI	0.25	0.30	0.50
TG	0.20	0.40	0.40
CNY	0.35	0.30	0.35
FRST	0.15	0.40	0.45
CN-20%	0.20	0.40	0.40
CN+20%	0.20	0.40	0.40

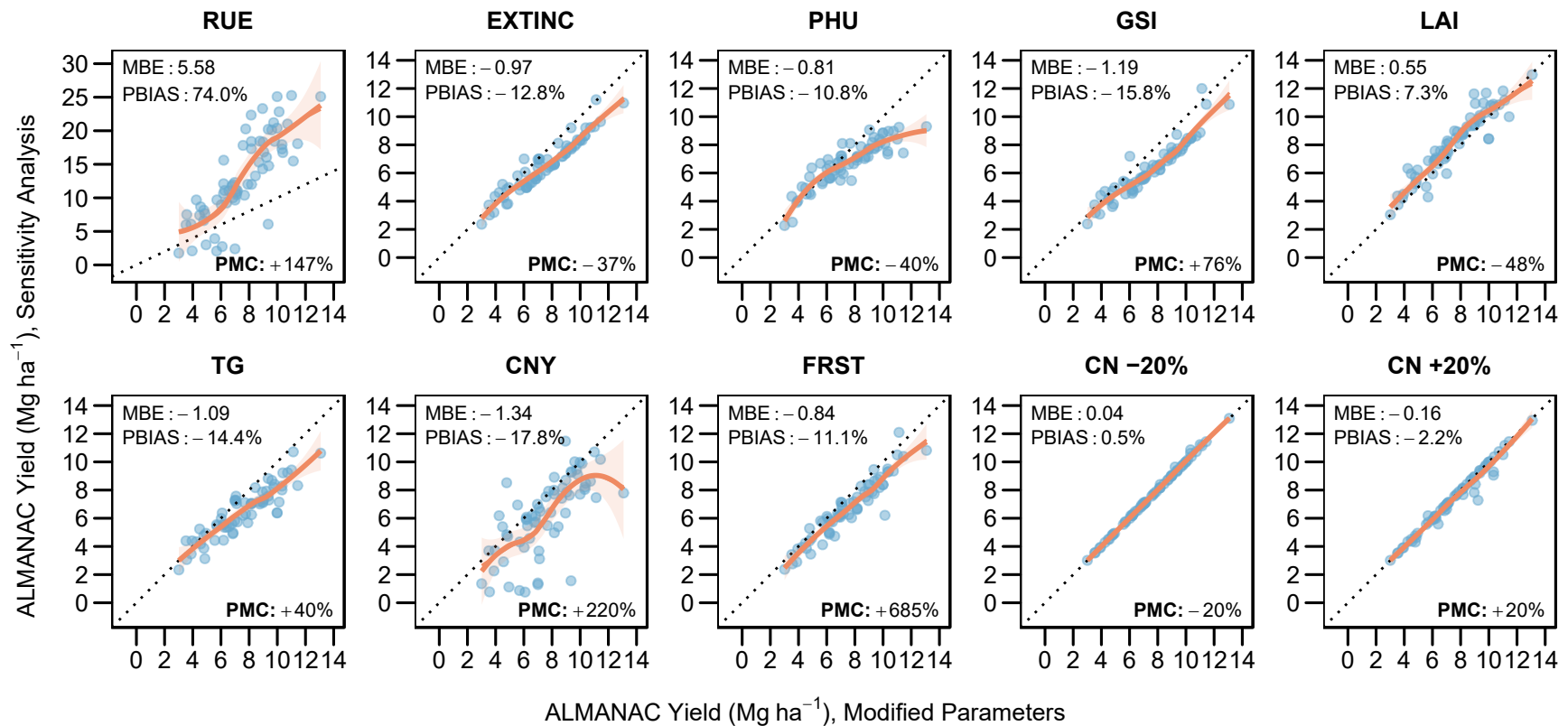


Figure 9. Relationships between simulated switchgrass yield under the modified parameterization presented herein (x-axis) and under each sensitivity analysis outlined in Table 1 (y-axis). The dotted line is the 1:1 line and the fitted curve and its shaded region are the fit and 95% confidence interval of a local polynomial regression included as a visual aid (Section 2.3.4). Statistics represent sensitivity analysis values relative to the modified parameterization: MBE = mean bias error, PBAIS = percent mean bias, PMC = parameter mean change.

(PHU) and its base temperature for growth (TG). In the modified parameterization presented herein, ALMANAC was adjusted so that TG equaled 5 °C rather than the default value of 12 °C (Table 1), while PHU₅ and PHU₁₂ values for each site were calculated from historical weather data (Section 2.3.3). The sensitivity analysis for TG tests the modified value against the default (Table 1) and uses the calculated PHU values for each site. The sensitivity analysis for PHU tests the calculated PHU₅ values for each site against values reduced by 40%, as the PHU values used by Kiniry et al. (2008b) were approximately 40% lower than those calculated from historical weather data.

In terms of relative sensitivity, adjustments to PHU and TG ranked 3rd and 6th among the 10 parameters modified in this investigation (Figure 8). Effects on simulated yield were similar for these two parameters, as the sensitivity analyses reverting to default values caused yield decreases of 0.81 Mg ha⁻¹ for PHU (10.8%; Figure 9, ‘PHU’) and 1.09 Mg ha⁻¹ for TG (14.4%; Figure 9, ‘TG’). In addition, yield impacts were primarily limited to those environments where simulated yields under the modified parameterization were greater than 6 Mg ha⁻¹, suggesting that accurately estimating switchgrass phenology is most critical in high-yielding environments. The impacts of modified PHU and TG are relevant primarily to yield, as the balance of stress responses was minimally affected in these sensitivity analyses (Table 3).

2.4.4. 3. Parameters defining environmental responses

All other sensitivity analyses examined parameter changes influencing crop response to environmental conditions (Table 1). Adjustments to CN and GSI (maximum stomatal conductance) influence water availability and crop water use. A unitless empirical parameter ranging from 0 to 100 (Cronshey et al., 1986), CN partitions water between infiltration and runoff following precipitation events. Increasing CN (CN+) results in increased runoff, while decreasing CN (CN-) results in increased infiltration. When GSI is increased, ALMANAC simulates greater plant water loss through transpiration. The amount of N in harvested biomass is defined by CNY; since switchgrass is a perennial, the increased value of CNY in the

sensitivity analysis impacted the N status of the crop in future growing seasons. Finally, the ‘FRST’ sensitivity analysis evaluated the impact of allowing frost damage, as the modified parameterization effectively negated the frost damage subroutine (Section 2.3.2).

As measured by relative sensitivity, adjusting frost damage (FRST), increasing CN (CN+), or decreasing CN (CN–) had negligible impact on the median yield response (Figure 8). The relative sensitivity for FRST is misleading, however, as relatively large changes in parameter values were necessary to negate the frost damage routine. If frost damage is allowed, simulated yield decreased by an average of 0.84 Mg ha^{-1} (11.1%; Figure 9, ‘FRST’). The low relative sensitivities for CN+ and CN– accurately describe the negligible impacts on yield (Figure 9, ‘CN –20%’ and ‘CN +20%’) and lack of impact on the balance between stress factors (Table 3) that were encountered when adjusting CN. ALMANAC simulations of switchgrass, a perennial crop with a deep root system, appear to be minimally affected by the balance between runoff and infiltration in these relatively low-rainfall northern environments.

Relative sensitivities of GSI and CNY were -0.24 and 0.05 , respectively, which ranked 4th and 7th among the 10 adjusted parameters (Figure 8). Similar to FRST, the relative sensitivity of CNY is misleading due to the large magnitude change in parameter values between the default and modified parameterizations (Table 1). The yield impacts of modifying CNY and GSI were similar; increasing CNY from 5 to 16 g kg^{-1} resulted in an average yield decrease of 1.34 Mg ha^{-1} (17.8%; Figure 9, ‘CNY’), while increasing GSI from 0.0042 to 0.0074 mm s^{-1} resulted in an average yield decrease of 1.19 Mg ha^{-1} (15.8%; Figure 9, ‘GSI’). Second only to the effects of changing RUE, increasing CNY resulted in the next largest change in a single stress factor, increasing the N stress fraction from 20% to 35% (Table 3). Increasing GSI, which increased simulated transpiration from leaf surfaces, caused water stress to increase from 40% to 50% of total stress (Table 3). Among all the parameters affecting simulated crop responses to environmental conditions (CN, FRST, GSI, CNY), only adjustments to CN were found to have minimal effect on simulated yields and stress responses.

2.5. Discussion

The modified parameterization presented herein featured adjustments to values consistent with observations from environments across the northern US and southern Canada. The modified parameterization improved the estimation of yield outcomes in the study region (Sections 2.4.1 and 2.4.2) and resulted in more accurate estimation of N stress within growing seasons (Section 2.4.3). Defining switchgrass maximum potential productivity through adjustments to RUE, EXTINC, and LAI had the greatest overall impact on improving the accuracy of yield estimation. Considering that published values of switchgrass EXTINC range from 0.23 to 1.11 across locations and cultivars (Kiniry et al., 1999, 2011), ALMANAC users should take great care in identifying an appropriate EXTINC value for simulating switchgrass growth. The N stress response was affected mostly by CNY. While the default value of CNY was found to be appropriate for N removal by switchgrass seed, it was nearly three times greater than the average N removal from switchgrass biomass harvest in northern locations (Gamble et al., 2015; Lemus et al., 2008; Madakadze et al., 1999b; Vogel et al., 2002; Wayman et al., 2014). Therefore, the nearly complete N stress realized in certain years of the default parameterization is in contrast with field observations of high switchgrass productivity in environments with limited fertilizer N inputs (Lee and Boe, 2005; Lee et al., 2007; Lemus et al., 2008; Mulkey et al., 2006; Tober et al., 2007).

The modified parameterization also resulted in a median maturity date nearly one month later than the default parameterization (Section 2.4.3). Phenology of the six cultivars used to develop the modified parameterization has been evaluated in several locations and years throughout the study region (Berdahl et al., 2005; Tober et al., 2007) and only one cultivar (Dacotah) has been documented to reach full maturity by early August (Tober et al., 2007). While others (ND3743, Sunburst, Forestburg) have been documented to reach the heading stage by early July to mid-August (Berdahl et al., 2005), or the early seed filling stages by early August (Tober et al., 2007), upland ecotypes adapted to this region are most often found in the flowering and seed filling stages in early September (Tober et al., 2007). These field

observations support the longer growing season of the modified ALMANAC parametrization, further validating its outcomes for the study region.

Other than modifications of PHU and LAI, the default ALMANAC parameters for upland ecotypes (Kiniry et al., 2008b) are identical to parameters developed for a lowland ecotype cultivar ('Alamo') grown in Temple, TX (Kiniry et al., 1996). Although this default parameterization was tested for 10 locations across North Dakota, South Dakota, and Nebraska (Kiniry et al., 2008b), the modified parameters presented herein result in a much improved simulation of upland switchgrass ecotypes for 13 locations across Minnesota, North Dakota, and South Dakota. It appears that the growth characteristics of a lowland switchgrass ecotype grown in Temple, TX (31°3' N 97°21' W) are comparatively ineffective in characterizing the growth of upland ecotypes grown in latitudes approximately 1600 km northward (43°10' N to 47°31' N). This is supported by observations that upland and lowland ecotypes are unadapted to areas more than approximately 2 degrees (≈ 220 km) north or south of their adapted range (Casler et al., 2004, 2007). In contrast, parameters approximating vegetative development and RUE from upland switchgrass ecotypes grown in Montreal, QC (45°28' N 73°45' W) are highly predictive in northern US locations of a similar latitude, even though these locations were approximately 1900 km westward (96°5' W to 100°4' W). This outcome is consistent with past evidence that switchgrass populations are broadly adaptable to areas east or west of their adaptive range (Casler et al., 2007), and supports the potential use of the modified parameterization across those areas of the northern US and southern Canada adapted to switchgrass production. Although the parameters developed by Kiniry et al. (2008b) for upland switchgrass ecotypes in northern locations have subsequently been used in several investigations (Behrman et al., 2013; Kang et al., 2014; Krohn, 2015; Timmons, 2012), future ALMANAC users should consider the issues raised within this investigation when defining accurate characterizations of switchgrass growth for their region of interest.

2.6. Conclusions

A summary of findings is presented in Table 4. When compared to the default parameters for upland switchgrass ecotypes in northern locations, the modified parameters presented herein improved annual and multiyear average yield estimates from ALMANAC (Sections 2.4.1 and 2.4.2). Effects of the modified parameterization were more pronounced for annual simulated yields, as multiyear average yields can mask anomalous simulation outputs identified in examinations of annual outputs. In addition to improved yield estimation, the modified parameterization corrected a condition in the default parameterization where annual outputs showed severe N stress and no biomass accumulation (Section 2.4.3). The modified parameterization also simulated a median switchgrass maturity date of August 28, compared to August 1 with the default, which is consistent with late-August to early-September maturity dates observed across Minnesota and the Dakotas. This investigation modified 13 parameters characterizing switchgrass growth. The combined effect of modifying RUE, EXTINC, and LAI resulted in the largest changes in simulated yields, as these parameters define maximum switchgrass productivity (Section 2.4.4). However, ALMANAC was clearly most sensitive to RUE. Modifications of the parameters influencing water loss through transpiration (GSI), N removed at harvest (CNY), and frost damage (FRST1, FRST2) caused average changes in estimated yields of over 10%. This work provides an improved characterization of upland switchgrass ecotypes in northern US locations for future ALMANAC users and for the comparative feasibility analysis presented in Chapter IV.

Table 4. Summary of findings from Chapter II results (Section 2.4).

Section	Finding
2.4.1	modified parameterization improved annual yield estimation for upland ecotype switchgrass (IOA from 0.41 to 0.65, RMSE from 3.74 to 2.52 Mg ha ⁻¹ , PBIAS from -18% to 7.2%)
2.4.2	modified parameterization improved multiyear average yield estimation for upland ecotype switchgrass (IOA from 0.42 to 0.68, RMSE from 2.93 to 1.95 Mg ha ⁻¹ , PBIAS from -15.2% to 11.7%) solely evaluating multiyear average yields may conceal parameterization issues revealed by evaluations of annual yields
2.4.3	default CNY (fraction of N in harvested biomass) resulted in absolute N stress (no biomass accumulation due to N stress), which is inconsistent with field observations modified parameterization simulates maturity nearly one month later than default, which is consistent with field observations
2.4.4	parameter modifications defining maximum switchgrass productivity (RUE, EXTINC, LAI) had the greatest impact on estimated yield as a deep-rooted perennial, switchgrass yield estimation is unaffected by the allocation of rainfall between runoff and infiltration (i.e. CN, runoff curve number) all other parameter modifications influencing switchgrass response to environmental conditions (GSI, CNY, FRST1, FRST2) altered final yield estimates by over 10%

CHAPTER III

CORN AND WHEAT ALMANAC SIMULATIONS FOR MODERATE-RESOLUTION REGIONAL ASSESSMENTS

3.1. Abstract

Dynamic system simulation models are widely used for cropping system decision management and policy analysis. This study investigates regional-scale yield estimation for corn (*Zea mays* L.) and spring wheat (*Triticum aestivum* L. ssp. *aestivum*) using the ALMANAC (Agricultural Land Management Alternative with Numerical Assessment Criteria) dynamic system simulation model, across a 99-county area of the eastern Dakotas and western Minnesota representing a transitional region between these two crops. Yields were simulated at approximately 800 m spatial resolution. Simulated yields from areas of corn and wheat production, as identified by USDA Cropland Data Layers, were aggregated to generate county-average yield estimates. Compared to USDA yield surveys, ALMANAC provided reasonable estimates of multiyear-average county yields. Corn yield was estimated with just 1.9% bias and 8.8% coefficient of variation (CV), while wheat yield was estimated with just 2.8% bias and 8.5% CV. Within counties, ALMANAC accurately represented corn and wheat yield variability across soil types considered suitable for cropping, but appeared to overestimate productivity in soil types generally considered unsuitable for cropping. In addition, ALMANAC did not accurately simulate annual variability in yield, as it generally overestimated yield in years with abundant soil moisture and underestimated yield in years with limited soil moisture. Yield estimation was most sensitive to adjustments in parameters that influence simulated water stress or are responsive to simulated water stress. Improved estimation of crop available water should improve ALMANAC estimation of corn and wheat yields.

3.2. Introduction

With a 2017 harvest of 371 million Mg (14.6 billion bu) valued at US\$48 billion, corn (*Zea mays* L.) is currently the number one field crop in the US in production and production value (USDA NASS, 2018). With 2017 production of 47.4 billion Mg (1.74 billion bu) and \$8.1 billion, wheat (*Triticum aestivum* L. ssp. *aestivum*) ranks third among US field crops in production and fourth in production value. Corn is also ranked first in production and production value across the northern Great Plains states of Minnesota, North Dakota, and South Dakota, with respective values of 67.7 million Mg (2.67 billion bu) and \$8.0 billion, while wheat is ranked third in both production (9.68 million Mg, 356 million bu) and production value (\$2.1 billion). This region represents the primary spring wheat production area of the US, with spring wheat constituting 86% of wheat production and production value within these three states. While corn and spring wheat (hereafter wheat) are highly important within the agricultural economy of the northern Great Plains, the eastern Dakotas and western Minnesota also represents a transitional area between corn and wheat production regions (Figure 10; USDA ERS, 2000). Requiring 355 to 430 mm precipitation for high yields and having optimum growth at 24 to 25 °C (Wiersma and Ransom, 2005; Wright et al., 2005), wheat is a cool-season grass well-adapted to the cooler and drier conditions found in the northern and western portions of this region. In contrast, corn is a warm-season grass requiring 510 to 635 mm precipitation for high yields (Cooperative Extension System, 2008) and temperatures of 29 to 32 °C for optimum growth (Lutt et al., 2016; Stoll and Saab, 2016). Thus, corn is better adapted to the warmer and wetter southern and eastern portions of this transitional region. Considering the economic importance of corn and wheat to this region, and this region's status as a boundary between agroecological regions well-adapted to these two crops, the eastern Dakotas and western Minnesota is well-suited for an evaluation of regional-scale corn and wheat simulations.

The development and use of crop simulation models has been an area of active research since the 1960s (Jones et al., 2016). In general, crop models are developed for three

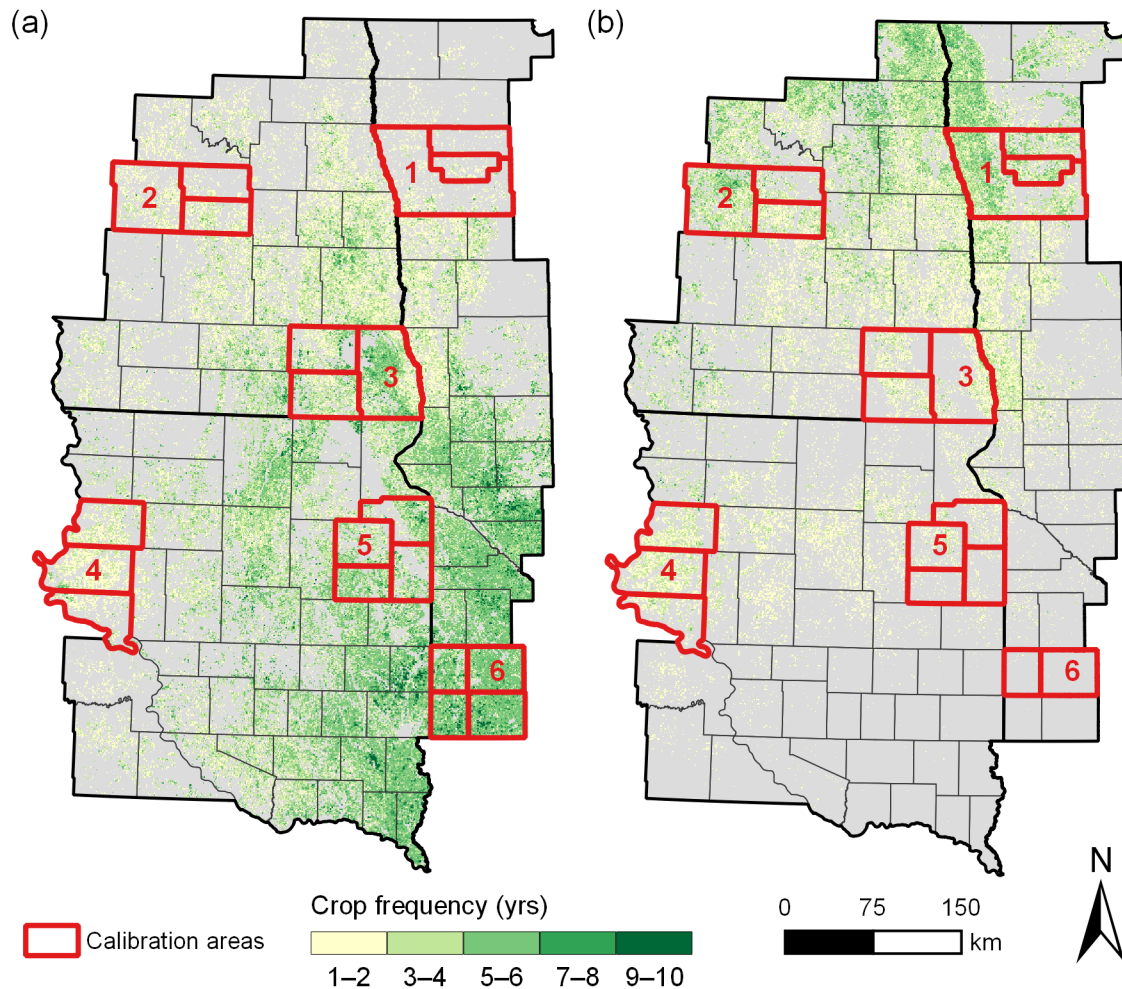


Figure 10. Cropping frequency and ALMANAC calibration counties for (a) corn and (b) wheat. Cropping frequencies are derived from 2006 to 2015 Cropland Data Layers.

broad purposes: synthesis of research understanding, cropping system decision management, and policy analysis (Boote et al., 1996; Jones et al., 2016). Models to increase scientific understanding are typically mechanistic models, designed to simulate known or hypothesized physical, chemical, or biological processes occurring in crop production systems (Boote et al., 1996; Di Paola et al., 2016; Jones et al., 2016). These models tend to operate on fine time scales (instantaneous to hourly), include a large number of parameters, and require input information that may not be readily available for general applications. In contrast, dynamic system simulation models are a widely used approach for cropping system decision management and policy analysis (Jones et al., 2016). Dynamic system simulation models

describe changes to cropping system states in response to external drivers such as weather conditions, management practices, and soil characteristics. These models typically integrate several mechanistic and functional routines, with functional routines defined as empirical functions that approximate complex physical, chemical, or biological processes (Boote et al., 1996; Jones et al., 2016). Examples of functional routines commonly used in dynamic system simulation models include approximation of crop productivity via leaf area index (LAI) and radiation use efficiency (Sinclair and Muchow, 1999b) and simulation of potential evapotranspiration using the Penman-Monteith or Priestley-Taylor equations (Allen et al., 1998). Dynamic system simulation models are used to inform decision-making across a range of spatial scales, from management and enterprise decisions at the field and farm scales to economic optimization, environmental management, land use planning, and food security analysis at district, regional, national, and global scales (Boote et al., 2010; Jones et al., 2016). Reflecting the multitude of objectives and approaches utilized by crop model developers, numerous mechanistic and dynamic system models are available for use by crop modeling practitioners. For example, a recent review categorizes over 70 models applicable to a broad spectrum of crops and cropping systems (Di Paola et al., 2016).

Presented herein are regional simulations of corn and wheat using the ALMANAC (Agricultural Land Management Alternative with Numerical Assessment Criteria) model. Derived from the EPIC (Erosion Productivity Impact Calculator) model, which provides soil nutrient and water balance subroutines, ALMANAC is a dynamic cropping system model that simulates crop growth as a function of light interception by leaves, conversion of intercepted light energy into biomass, and partitioning of biomass into grain (Kiniry et al., 1992, 2002). ALMANAC simulates field-scale plant growth in a general manner, allowing for ease of application to new environments and different crop species. In the US, ALMANAC successfully simulated corn yield for 70 location-year combinations in Texas, encompassing a range of water-limiting and high-yielding irrigated conditions (Kiniry and Bockholt, 1998; Kiniry et al., 2004; Xie et al., 2001). These investigations benefited from field-scale input

parameters, specifically measured weather conditions (Kiniry and Bockholt, 1998; Kiniry et al., 2004; Xie et al., 2001) and characterization of soil layers and physical properties through soil sampling (Xie et al., 2001). Investigations of ALMANAC wheat simulation within US sites could not be found in the literature. However, EPIC has successfully simulated long-term average wheat yields in Montana and the Canadian provinces of Saskatchewan and Alberta (Kiniry et al., 1995; Moulin and Beckie, 1993; Touré et al., 1995). Similar to corn, these investigations utilized field-scale soil characterizations and weather conditions.

ALMANAC, like most other field-scale models (Jones et al., 2016), parameterizes soil properties as varying vertically with depth but assumes homogeneity of soil, weather, and management variables horizontally across the simulated area. Thus, unlike agricultural system models designed to operate on regional to global scales (see Di Paola et al., 2016), field-scale models such as ALMANAC must be upscaled or generalized when used in regional assessments. An example of generalized yield estimation using ALMANAC is presented by Kiniry et al. (2004), who for each of four Texas counties compared county-average corn yields from the USDA National Agricultural Statistics Service (NASS) database (USDA NASS, 2018) to ALMANAC simulations for a single soil deemed to be representative of the county. Kiniry et al. (1997) utilized a similar approach for a single county in each of nine states: Minnesota, New York, Iowa, Illinois, Nebraska, Missouri, Kansas, Louisiana, and Texas. To increase the spatial resolution of such regional-scale assessments, multiple homogeneous fields can be simulated using spatially-varying soil, weather, and/or management inputs. Simulations from these individual fields subsequently serve as building blocks for the regional scale (Jones et al., 2016), and interfacing with geographic information systems (GIS) facilitates aggregate analysis of simulation outputs (Hartkamp et al., 1999). Hartkamp et al. (1999) propose the terms linking, combining, and integrating to describe the various possible levels of interfacing between a crop model and GIS. Briefly, linkage strategies use GIS to display model outputs without integrating the GIS into the crop model's software system or user interface, combination automates information exchange between the GIS and crop model using

a shared user interface (e.g. AgroMetShell; Mukhala and Hoefsloot, 2004), and integration fully incorporates one system into the other (e.g. IMPACT; IMPACT Model Team, 2015).

Building on past corn investigations conducted at the county scale (Kiniry et al., 1997, 2004), and demonstrating linkage of ALMANAC with GIS (Hartkamp et al., 1999), the objective of this investigation is to evaluate the use of ALMANAC for corn and wheat regional yield assessments at moderate spatial resolution. Using gridded climate data and soil characterizations from the USDA SSURGO database (Soil Survey Staff, 2013), corn and wheat yields are simulated over 10 years for all soil types considered suitable for cropping within a 99-county area of the eastern Dakotas and western Minnesota. The procedures and parameterizations described within are necessary for the comparative technical, economic, and environmental analysis presented in Chapter IV, which requires accurate spatially-explicit estimates of corn and wheat grain and biomass yields across the eastern Dakotas and western Minnesota.

3.3. Materials and Methods

Corn and wheat grain yields were simulated using the ALMANAC model, utilizing soil inputs from the USDA-NRCS SSURGO soil survey database (Soil Survey Staff, 2013) and 2006 to 2015 weather inputs from gridMET (University of Idaho Climatology Lab, 2018), a moderate-resolution (4 km) gridded dataset of surface meteorological variables derived from a combination of the PRISM and NLDAS-2 climate datasets (Abatzoglou, 2013). Soil classification within SSURGO features mapunit as the unit of spatial delineation (Figure 11c), mapunits consisting of one or more soil components, and components divided into soil horizons. For a given mapunit, simulation outputs represent an area-weighted average across all soil components featuring horizon information. Following Gelfand et al. (2013), simulations were conducted on soils with SSURGO land capability classifications (LCC) of 1 to 4 and soils having LCC of 5 to 7 along with a slope gradient of less than 20%. Land capability classification shows, in a general way, the suitability of soils for most types of field crops (Soil Survey Staff, 2018). Soils in classes 1 through 4 are generally considered suitable for cultivated

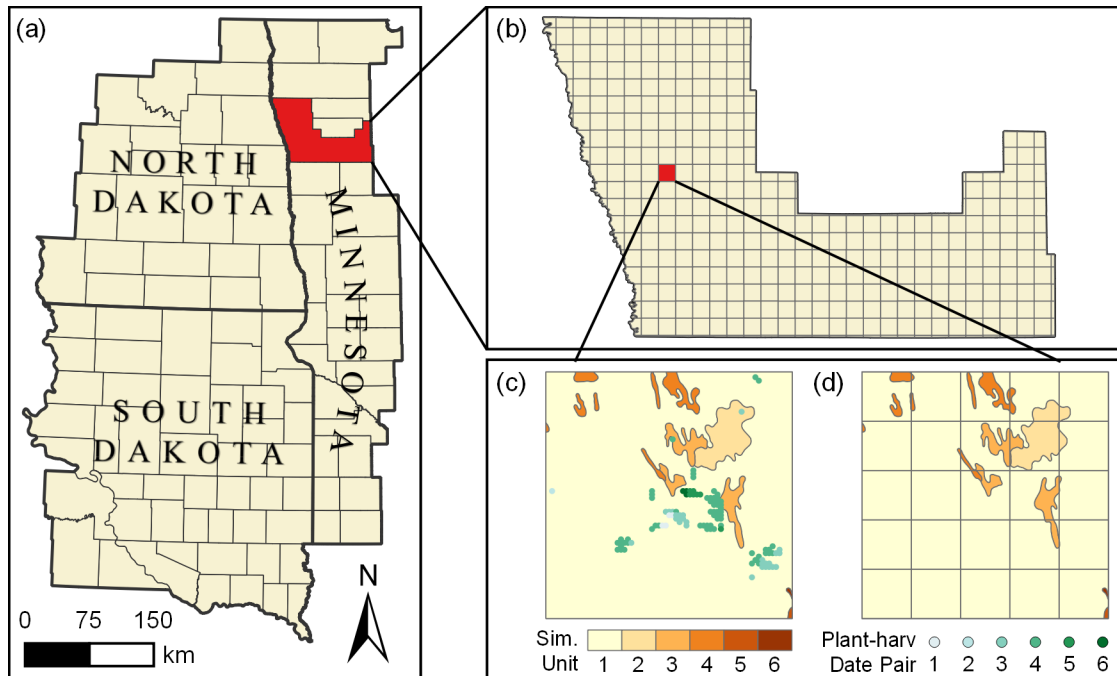


Figure 11. Examples of ALMANAC simulation and aggregation units. (a) The 99-county study area. (b) County inset (Polk, MN) with overlying 4 km resolution climate cells. (c) Climate cell inset with geographic identifiers for the six soil mapunit polygons enclosed within and overlying estimates of 2007 corn planting-harvest date pairs (see Figure 15, Section 3.3.3). Each soil polygon represents a simulation unit, assigned the most prevalent planting-harvest date pair. (d) Same as (c), but with overlying 800 m resolution cells used to aggregate simulation yields for mapping.

cropping, with class 1 soils having few limitations, class 2 soils having moderate limitations requiring moderate conservation practices, and class 3 and 4 soils having severe or very severe limitations requiring careful management. Soils in classes 5 through 7 are generally considered unsuitable for cultivated cropping, as they have severe or very severe limitations that restrict their use mainly to pasture, rangeland, grazing, forestland, or wildlife habitat. Class 8 soils have limitations that preclude commercial plant production, and are thus excluded from this investigation. In total, yields were simulated for 15,353 unique soil components within 10,215 mapunits. There were 561,166 simulation units, which were defined by the intersection of SSURGO mapunit polygons and gridMET cells (Figure 11).

Corn and wheat simulations were conducted under reduced tillage systems and within

a two-year rotation with soybean. Corn management zones (Figure 12a) were defined using a corn hybrid relative maturity map from Stine Seed Company (Stine Seed Company, 2015); this was necessary because corn hybrids are developed and marketed as having adaptability to a narrow geographical range. The boundaries defined by the corn management zones were subsequently used to delineate boundaries among four other parameters affected by corn hybrid characteristics (maximum root depth, light extinction coefficient, planting date, harvest date). Full details of corn, wheat, and soybean management parameterizations are presented in Section 3.3.3.

All statistical analyses were performed in R (R Core Team, 2018). Maps were created using QGIS (QGIS Development Team, 2018) and are projected using the ‘USA Contiguous Albers Equal Area Conic USGS Version’ projection (Spatial Reference, 2018). With the exception of county-level choropleth maps, mapped variables were first aggregated to an approximately 800 m grid, as illustrated in Figure 11d. Continuous variables were aggregated by an area-weighted average, while categorical variables (e.g. LCC) were aggregated by assigning the value occupying the greatest area within the aggregation grid.

3.3.1. ALMANAC description

ALMANAC is a process-oriented model that simulates, on a daily time step, the processes of nutrient balance, soil water balance, and crop growth as a function of light interception by leaves, production of dry matter, and partitioning of biomass into grain (Kiniry et al., 1992, 2002). Soil water and nutrient subroutines are taken from the EPIC model (Sharpley and Williams, 1990). Crop biomass accumulation is simulated as the product of intercepted photosynthetically active radiation (IPAR) and the efficiency of the crop species in converting IPAR into biomass (i.e. radiation use efficiency). Beer’s law (Monsi and Saeki, 1953), with light extinction coefficient (Flénet et al., 1996) and leaf area index (LAI) as inputs, is used to estimate IPAR. LAI accumulation is simulated as a function of plant population density and cumulative heat units. Daily increases in LAI and biomass accumulation are constrained by the biomass growth stress factor, which ranges from 0 to 1 and is taken as

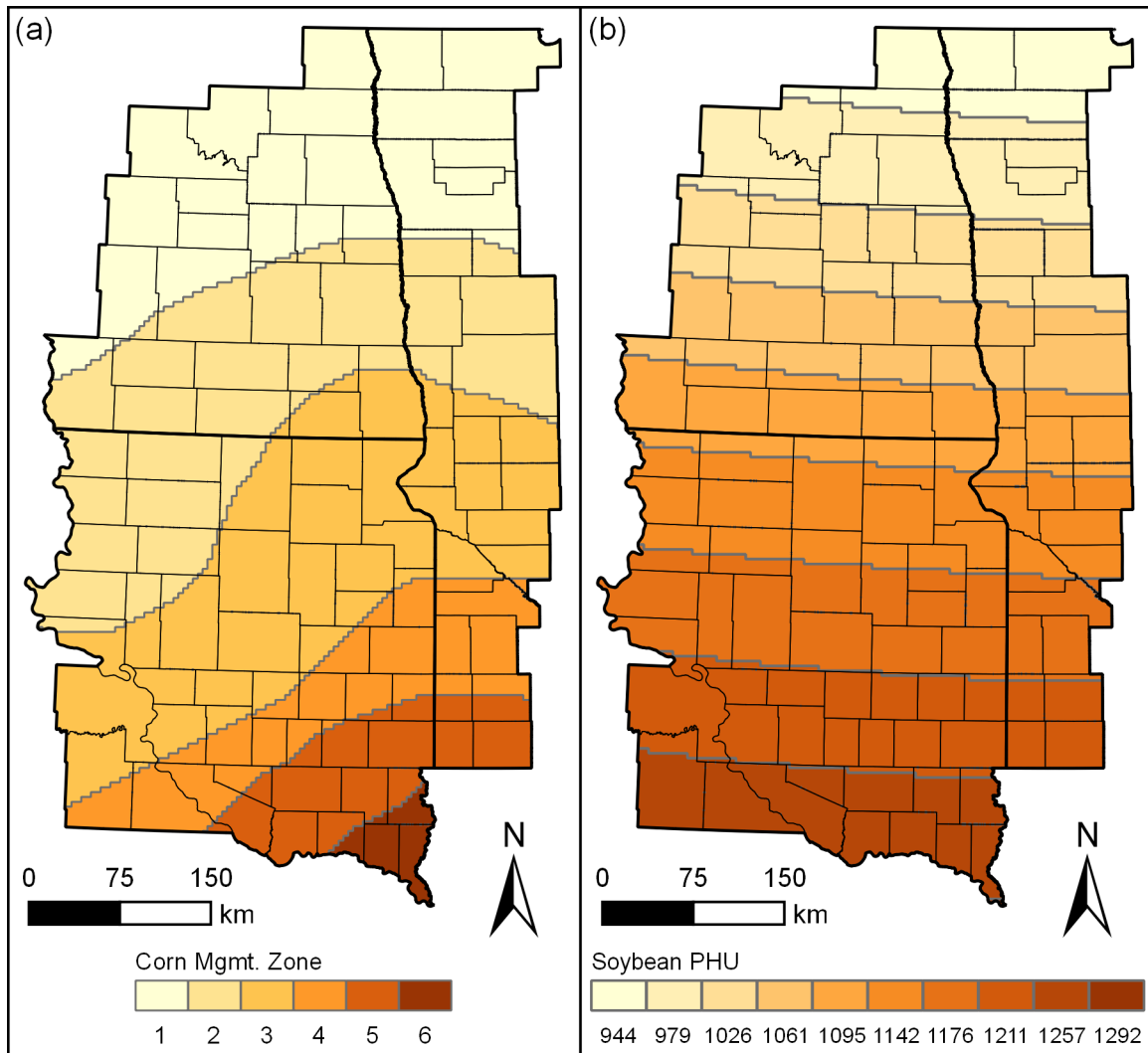


Figure 12. (a) Geographic identifiers for corn management zones. (b) Potential Heat Units (PHU) for soybean.

the maximum of separate stress factors for water, temperature, nitrogen (N), phosphorus (P), and aeration (Williams et al., 1989). Grain yield at the end of the growing season is simulated using the harvest index (HI), which represents grain yield as a crop-specific fraction of total aboveground biomass at maturity. ALMANAC will reduce HI if drought stress occurs near anthesis (from 45 to 60% of the seasonal heat units), restrained by a user-specified minimum limit of HI (Xie et al., 2001). This time frame corresponds to the heading and flowering stages of wheat growth (Bauer et al., 1992) and the tasseling, silking, pollination, and fertilization

stages of corn growth (Neild and Newman, 1990). In these growth stages, kernel development in wheat (Wiersma and Ransom, 2005) and corn (Ransom et al., 2004) is extremely sensitive to drought stress.

3.3.2. Final parameterizations – environmental variables

All weather inputs required by ALMANAC (minimum and maximum temperatures [°C], precipitation [mm], relative humidity [%], wind velocity [m s^{-1} at 10 m height], and solar radiation [$\text{MJ m}^{-2} \text{d}^{-1}$]) were provided by gridMET. Concomitantly, ALMANAC was configured to simulate evapotranspiration by the Penman-Monteith method (Allen et al., 1998).

The SSURGO soil survey database provides many of the soil parameters required by ALMANAC (Appendix B, Table 17). However, several deviations from SSURGO were necessary. First, as required to avoid calculation errors for hydrologic variables, all soils with a representative slope of 0% were set to 0.0001% and a shallow (0.01 m) layer was added to the top of all soils (see Section 2.3.3). Second, due to inaccuracies inherent to laboratory-measured values of wilting point and field capacity (Gijssman et al., 2002), such as those available within SSURGO, wilting point and field capacity of each soil were estimated as a function of sand, clay, and organic matter contents (Saxton and Rawls, 2006; Section 2.3.3; Equation [1]). Third, excluding those soils identified by SSURGO as having ‘BR’ (bedrock), ‘WB’ (weathered bedrock), or ‘UWB’ (unweathered bedrock) at the base of their profile, for corn simulations the bottom soil layer was extended to a depth of 2.0 m in management zone 1 and 2.7 m in management zones 2 to 6 (Figure 12a). This is consistent with observations of increased deep-soil water extraction by corn hybrids with increasing relative maturity (Norwood, 2001), field observations (DeJong, 2017; Fawcett, 2013; Weaver, 1926) and simulations (Hammer et al., 2009) suggesting that corn roots can explore soil depths beyond 2 m, and the deep soils of the study area characterized by glacial till parent material reaching a depth of 30 to 120 m throughout much of the region (Whitehead, 1996). Fourth, coarse fragment content was calculated, as a weight percentage of the horizon, as the sum of rock fragments greater than 10 inches in size, rock fragments 3 to 10 inches in size, and the soil fraction remaining on top of

a no. 10 sieve (Wentworth, 1922). Coarse fragment values were subsequently converted to a volume percentage (Saxton and Rawls, 2006; Section 2.3.3; Equation [2]). Fifth, soil organic carbon was estimated by multiplying the soil organic matter values from SSURGO by 0.58, as soil organic matter contains approximately 58% carbon (USDA NRCS, 2009). Finally, those required soil parameters not available within SSURGO were set to default ALMANAC values (Appendix B, Table 17).

Table 5. Out of 16,466 components and 60,242 component horizons, the number of missing values for ALMANAC soil parameters provided by SSURGO.

SSURGO			
Table	Notation	Description	Missing Values
component	hydgrp	hydrologic soil group	38
component	albedodry_r	soil albedo	37
component	elev_r	elevation, representative	149
component	slopelenusle_r	slope length, representative	12,995
horizon	sandtotal_r	sand content	10
horizon	silttotal_r	silt content	16
horizon	dbthirdbar_r	bulk density of the soil layer	2240
horizon	cec7_r	cation exchange capacity	75
horizon	fraggt10_r	rock fragments greater than 10 inches, representative	142
horizon	frag3to10_r	rock fragments 3 to 10 inches, representative	61
horizon	dbovendry_r	bulk density (oven dry)	60

In addition to the aforementioned modifications, procedures were developed to estimate missing values of four soil component variables and seven soil horizon variables required by ALMANAC (Table 5). Among the 11 variables, slope length was most often missing from SSURGO. Along with slope, slope length is used by ALMANAC in the calculation of water erosion. Considering this, and that all soil components had complete slope information,

missing slope length values were assigned as a function of slope. First, utilizing information from 3471 soil components containing complete slope and slope length information, their combined effects on soil erosion were quantified by calculating the slope-length gradient factor (LS) of the Universal Soil Loss Equation (USLE; Stone and Hilborn, 2012). The USLE predicts the long-term average rate of erosion on a field slope based on rainfall pattern, soil type, topography, crop system, and management practices and is calculated as follows:

$$A = R \times K \times LS \times C \times P \quad [13]$$

where A is the potential long-term average annual soil loss ($\text{Mg ha}^{-1} \text{ yr}^{-1}$), R is the rainfall and runoff factor, K is the soil erodibility factor, LS is the slope-length gradient factor, C is the crop/vegetation and management factor, and P is the support practice factor. LS represents a ratio of soil loss under given conditions relative to a site with a “standard” slope gradient of 9% and slope length of 22.1 m, with higher values representing steeper and higher slopes and a greater risk for erosion. The equation for calculation of LS (LS) is as follows:

$$LS = (0.065 + 0.0456S + 0.006541S^2) \times (SL/22.1)^{NN} \quad [14]$$

$$\text{where } NN = \begin{cases} 0.2 & \text{for } S < 1 \\ 0.3 & \text{for } 1 \leq S < 3 \\ 0.4 & \text{for } 3 \leq S < 5 \\ 0.5 & \text{for } S \geq 5 \end{cases},$$

S is slope, and SL is slope length. For the aforementioned 3471 soil components, the relationship between slope and slope length was modeled as a second order polynomial regression (Appendix B, Figure 70):

$$LS = 0.0635 + 0.0702S + 0.00686S^2; p < 0.001; R^2 = 0.99. \quad [15]$$

For soils with missing slope length, Equation [15] was used to predict LS as a function of

slope. Subsequently, slope length was calculated using a reorganization of the equation for calculating LS:

$$SL = [LS / (0.065 + 0.0456S + 0.006541S^2)]^{1/NW} \times 22.1$$

$$\text{where } NW = \begin{cases} 0.2 & \text{for } S < 1 \\ 0.3 & \text{for } 1 \leq S < 3 \\ 0.4 & \text{for } 3 \leq S < 5 \\ 0.5 & \text{for } S \geq 5 \end{cases} \quad [16]$$

For missing values of other soil component variables, hydrologic soil group and soil albedo were assigned the most frequent values from soil components of the same name, while elevation was taken from the nearest weather station among the 975 provided within the ALMANAC weather and wind stations database.

For missing soil horizon variables, bulk density of oven dry soil was assigned the most frequent value from soil horizons with a similar texture, while rock fragments greater than 10 inches and rock fragments from 3 to 10 inches were assigned values from other soil horizons of the same soil component. Following the methods of St. Arnaud and Sephton (1972), who used a multiple linear regression to model the relationship between cation exchange capacity, clay content, and soil organic matter, missing values of cation exchange capacity were estimated as follows:

$$CEC = 0.859 + 0.581CLY + 1.56SOM + 0.00344(CL Y \times SOM); p < 0.001; R^2 = 0.82 \quad [17]$$

where *CEC* is cation exchange capacity, *CLY* is clay content, and *SOM* is soil organic matter. Equation [17] was derived from 59,607 study region soil horizons with complete information for all three variables. Finally, missing bulk density values were estimated using the method of Saxton and Rawls (2006):

$$\rho_N = (1 - \theta_S)2.65 \quad [18]$$

where ρ_N is normal soil density, θ_S is the percent soil water content at saturation (0 kPa soil water tension), and 2.65 is the assumed density of coarse fragments (in g cm^{-3}).

3.3.3. Final parameterizations – crop growth and management

Corn and wheat parameterizations generally followed examples presented in existing literature, with several modifications, and are presented in Table 6. For wheat simulations, runoff curve numbers (CN) were updated to reflect a small grain cover type, with straight rows and crop residue cover, in a good hydrologic condition (Cronshey et al., 1986). All other wheat parameters were taken from Kiniry et al. (1995).

For corn simulations, a HI of 0.56 and minimum limit of HI of 0.48 were used, as estimated across 13 growing seasons in east-central Minnesota (Linden et al., 2000). Runoff curve numbers reflected a row crops cover type, with straight rows and crop residue cover, in a good hydrologic condition (Cronshey et al., 1986). Maximum root depth was set to 2.0 m in management zone 1 and 2.7 m in management zones 2 to 6 (Figure 12a), reflecting greater deep-soil water extraction by corn hybrids with increasing relative maturity (Hammer et al., 2009; Norwood, 2001). Light extinction coefficients, which in corn are a function of row spacing (Flénet et al., 1996; Xie et al., 2001), were 0.57 for management zones 1 to 3 and 0.53 for management zones 4 to 6. These values correspond to row spacings of 56 cm in zones 1 to 3 and 76 cm for zones 4 to 6, reflecting a tendency for growers within the study area to utilize narrower row spacings at higher latitudes due to increased yield potential (Stahl et al., 2009). All other corn parameters were taken from the default parameters provided with the ALMANAC software.

Corn and wheat simulations were conducted under a reduced tillage (RT) system with soybean as a rotational crop. Reduced tillage systems (Appendix B, Tables 18 and 19) were defined using the standard management database (USDA NRCS, 2004) and tillage system definitions (USDA NRCS, 2014a,b) of the United States Department of Agriculture (USDA) Natural Resources Conservation Service (NRCS). To allow soil N and water values to stabilize, each year of simulated corn or wheat production was preceded by a spinup year of simulated

Table 6. Comparison of final ALMANAC corn and wheat parameterizations presented herein to the default ALMANAC parameterization and to the baseline and comparison parameterizations used in parameter sensitivity analyses.

Crop	ALMANAC Parameter			Sensitivity Analysis			
	Notation	Description	Default Param.	Final Param.	Baseline Param.	Comparison Param.	Notation [†]
corn	HI	harvest index; fraction of aboveground biomass allocated to grain	0.53	0.56	0.56	0.53	HI
corn	WSYF	minimum limit of harvest index	0.30	0.48	0.48	0.30	HI
corn	EXTINC	extinction coefficient for calculating light interception	—	0.57, 0.53 [‡]	0.53	0.57	EXTINC
corn	RDMX	maximum root depth (m)	2.0	2.0, 2.7 [§]	2.0, 2.7 [§]	2.0	SOIL DEPTH
corn	—	depth of the soil profile (m)	from SSURGO	2.0, 2.7 [§]	2.0, 2.7 [§]	from SSURGO	SOIL DEPTH
corn	CN _A	runoff curve number for soil hydrologic group A	67	64	64	58; 70 [¶]	CN +10%; CN -10%
corn	CN _B	runoff curve number for soil hydrologic group B	78	75	75	68; 83 [¶]	CN +10%; CN -10%

Table 6. cont.

Crop	ALMANAC Parameter			Sensitivity Analysis			
	Notation	Description	Default Param.	Final Param.	Baseline Param.	Comparison Param.	Notation [†]
corn	CN _C	runoff curve number for soil hydrologic group C	85	82	82	74; 90 ^{fl}	CN +10%; CN -10%
corn	CN _D	runoff curve number for soil hydrologic group D	89	85	85	77; 94 ^{fl}	CN +10%; CN -10%
wheat	CN _A	runoff curve number for soil hydrologic group A	67	60	60	54; 66 ^{fl}	CN +10%; CN -10%
wheat	CN _B	runoff curve number for soil hydrologic group B	78	72	72	65; 79 ^{fl}	CN +10%; CN -10%
wheat	CN _C	runoff curve number for soil hydrologic group C	85	80	80	72; 88 ^{fl}	CN +10%; CN -10%
wheat	CN _D	runoff curve number for soil hydrologic group D	89	84	84	76; 92 ^{fl}	CN +10%; CN -10%
corn, wheat	—	cropping sequence	—	one soybean spin-up year	one soybean spin-up year	10-year rotation with soybean	CROP SEQ

Table 6. cont.

		ALMANAC Parameter			Sensitivity Analysis		
Crop	Notation	Description	Default Param.	Final Param.	Baseline Param.	Comparison Param.	Notation [†]
corn, wheat	—	planting and harvest dates	—	mode of spatially-explicit estimates [#]	mode of spatially-explicit estimates [#]	median USDA NASS values; all spatially-explicit estimates [#]	PLTHRV MED NASS; PLTHRV ALL EST
corn, wheat	U	soil layer wilting point	from SSURGO	from Saxton-Rawls equation	from Saxton-Rawls equation	from SSURGO	PAW
corn, wheat	FC	soil layer field capacity	from SSURGO	from Saxton-Rawls equation	from Saxton-Rawls equation	from SSURGO	PAW

[†] Notation corresponds to labels in Figures 26 to 30

[‡] 0.57 for management zones 1 to 3, 0.53 for zones 4 to 6 (see Figure 12)

[§] 2.0 for management zone 1, 2.7 for zones 2 to 6 (see Figure 12)

[¶] Baseline value $\pm 10\%$

[#] See Figure 15

soybean production. Thus, for each unique combination of soil type and weather conditions, ten separate simulations were used to estimate yield outputs from 2006 to 2015.

Table 7. Rates for the first and second applications of nitrogen fertilizer within the corn and wheat management systems.

Crop	Soil Texture	Soil Productivity (Mg ha ⁻¹)	Nitrogen Rate (kgN ha ⁻¹)	
			Fall [†]	Spring [‡]
corn	High-clay [§]	≥ 10.05	212	0
corn	High-clay	< 10.05	123	89
corn	Medium-textured [¶]	≥ 10.05	194	0
corn	Medium-textured	< 10.05	123	71
wheat	—	> 4.04	200	—
wheat	—	2.76 – 4.04	117	—
wheat	—	< 2.76	76	—

[†] Applied in fall, after prior crop harvest

[‡] Applied in spring, prior to planting

[§] Includes clay loam, silty clay loam, sandy clay, silty clay, and clay

[¶] Includes sand, loamy sand, sandy loam, loam, silt loam, silt, sandy clay loam, and organic soils

Corn and wheat N fertilizer rates were taken from North Dakota State University recommendations (Franzen, 2014a,b), which were developed from N response trials in North Dakota, northwest Minnesota, and northern South Dakota. These recommendations are based on the “Maximum Return to N” approach (Sawyer et al., 2006), an economic production function that takes into account the economic value of the produced crop and its yield response to added N, less the cost of the N. Nitrogen rates used in this study assumed price-value ratios (N cost [$\$ \text{ lbN}^{-1}$] / crop price [$\$ \text{ bu}^{-1}$]) of 0.125 for corn and 0.075 for wheat, representing average price-value ratios for these commodities from 2001 to 2013 (USDA ERS, 2015a,b). Specific N rates and management practices for a given soil were also dependent on soil

productivity (i.e. historic crop yields) and, for corn, soil texture (Table 7). Soil productivity (SP ; Mg ha^{-1}) was estimated as

$$SP_{ijk} = (CPI_{ij}/\overline{CPIP}_j) \times YLD_{jk} \quad [19]$$

where i represents a soil in county j growing crop k , CPI is the Crop Productivity Index from SSURGO, \overline{CPIP} is the mean Crop Productivity Index for prime farmland, and YLD (Mg ha^{-1}) is the highest county-average yield in the USDA National Agricultural Statistics Service database (USDA NASS, 2018) for the period of record through 2015. This method assumes that YLD reasonably estimates the maximum yield potential for prime farmland of average productivity. SP estimates were also used to assign corn, wheat, and soybean phosphorus fertilization rates to each soil. University of Minnesota equations for P fertilization (Kaiser and Lamb, 2012; Kaiser et al., 2013; Rehm et al., 2006), which are a function of Olsen soil test P and yield goal, were used:

$$PR_{ijk} = \begin{cases} (5.455 - 0.3429 \times STP_{ijk}) \times SP_{ijk} & \text{for } k = \text{corn} \\ (7.790 - 0.4873 \times STP_{ijk}) \times SP_{ijk} & \text{for } k = \text{wheat} \\ (12.74 - 0.9608 \times STP_{ijk}) \times SP_{ijk} & \text{for } k = \text{soybean} \end{cases} \quad [20]$$

where PR is the P fertilizer rate (kgP ha^{-1}), SP is soil productivity (Mg ha^{-1}), and STP is the amount of plant-available soil P as defined by the Olsen soil test (mg kg^{-1}). STP was estimated according to a defined relationship with labile P (LBP) in calcareous soils (Sharpley et al., 1984):

$$STP_{ijk} = LBP_{ijk} \times 0.917 - 2.9; R^2 = 0.74. \quad [21]$$

ALMANAC was used to estimate labile P values (Sharpley and Williams, 1990). Maps of N and P fertilizer rates are shown in Figure 13. Consistent with farming practices of the region, where soybean P fertility is oftentimes met by residual P from its rotational crop, the soybean P fertilizer rate was added to the corn and wheat P rates.

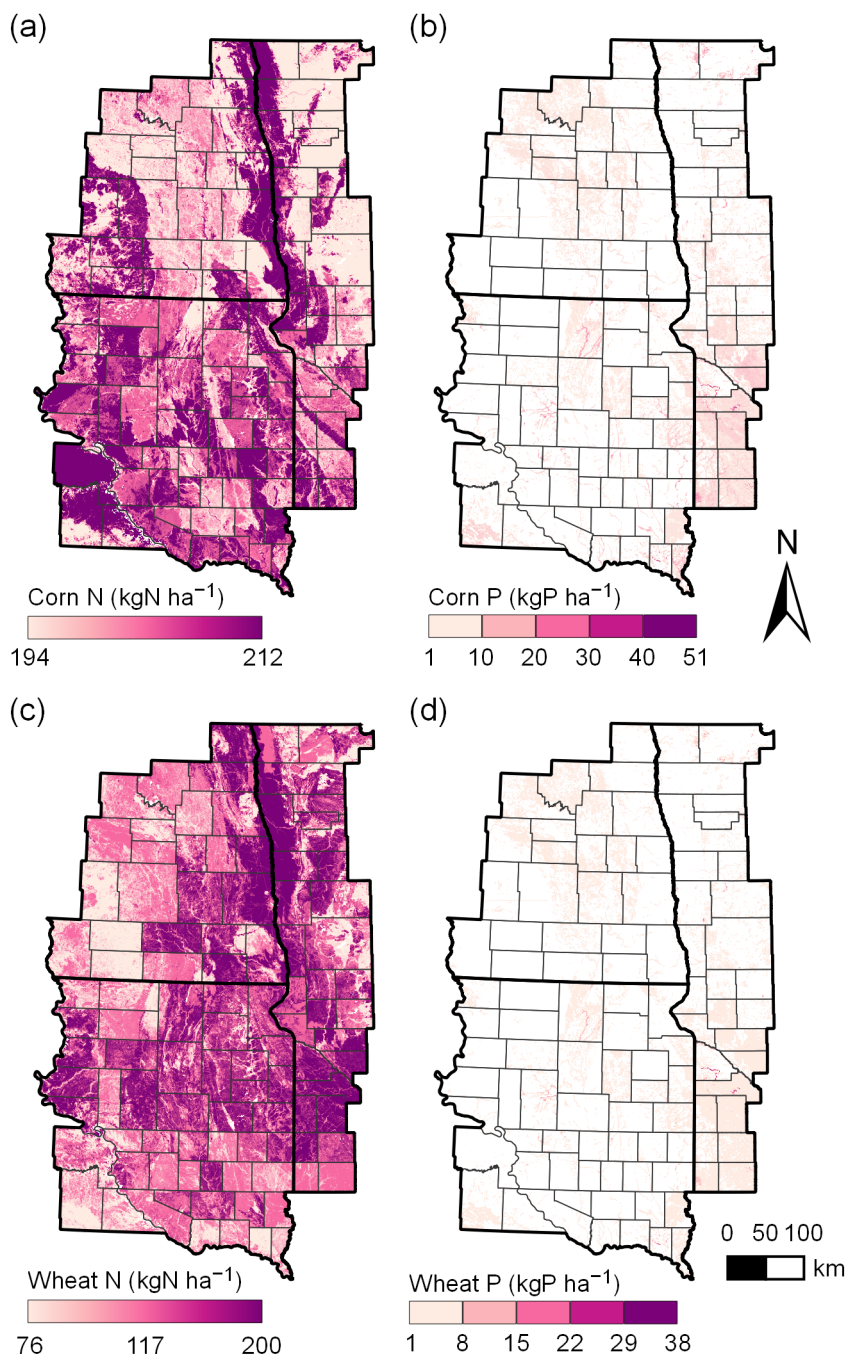


Figure 13. Estimated fertilizer rates for (a) corn nitrogen (N), (b) corn phosphorus (P), (c) wheat N, and (d) wheat P.

Consistent with recommendations from the university extension services of Minnesota and North Dakota, the entire study region was assigned a wheat plant population of 346 plants m^{-2} (Wiersma et al., 2005) and a soybean plant population of 37 plants m^{-2} (Kandel, 2014; Naeve, 2009). In contrast, University of Minnesota Extension recommends choosing an economically-optimum corn planting rate based upon the price of corn seed and value of corn grain (Coulter, 2009, 2015) while university extension services in North Dakota (Ransom et al., 2004) and South Dakota (Hall et al., 2009) recommend considering corn seed cost and soil productivity in planting rate decisions. Thus, corn planting density (PD ; plants m^{-2}) was estimated as a function of soil productivity (SP) and relationships between economically-optimum planting density and soil productivity defined by the DuPont Pioneer corn planting rate estimator (DuPont Pioneer, 2015):

$$PD_{ik} = \begin{cases} 0.407 \times SP_{ik} + 2.65; p < 0.0001, \text{marginal } R^2 = 0.50 & \text{for } ET_{ik}/PET_{ik} > 0.43 \\ 0.396 \times SP_{ik} + 1.98; p < 0.0001, \text{marginal } R^2 = 0.70 & \text{for } ET_{ik}/PET_{ik} \leq 0.43 \end{cases} \quad [22]$$

where i represents a soil growing $k = \text{corn}$ and ET and PET are ALMANAC-simulated values of evapotranspiration and potential evapotranspiration from a preliminary ALMANAC simulation under 1980 to 2013 weather conditions. Relationships between SP and PD were represented by mixed-model regressions fit by restricted maximum likelihood using the ‘lme4’ (Bates et al., 2015), ‘lmerTest’ (Kuznetsova et al., 2017), and ‘piecewiseSEM’ (Lefcheck, 2016) R packages, with fixed terms defining a slope and intercept across all hybrids and random terms defining a separate slope and intercept for each hybrid. The coefficients within Equation [22] represent the fixed effect model terms, while the reported marginal R^2 values describe the proportion of variance explained by the fixed factors alone.

The planting rate estimator returns economically-optimum planting density under normal or water-limited conditions, utilizing yield response data of DuPont Pioneer corn hybrids and user-specified values of seed cost (\$ 1000-seed $^{-1}$) and grain price (\$ bu $^{-1}$). Water-

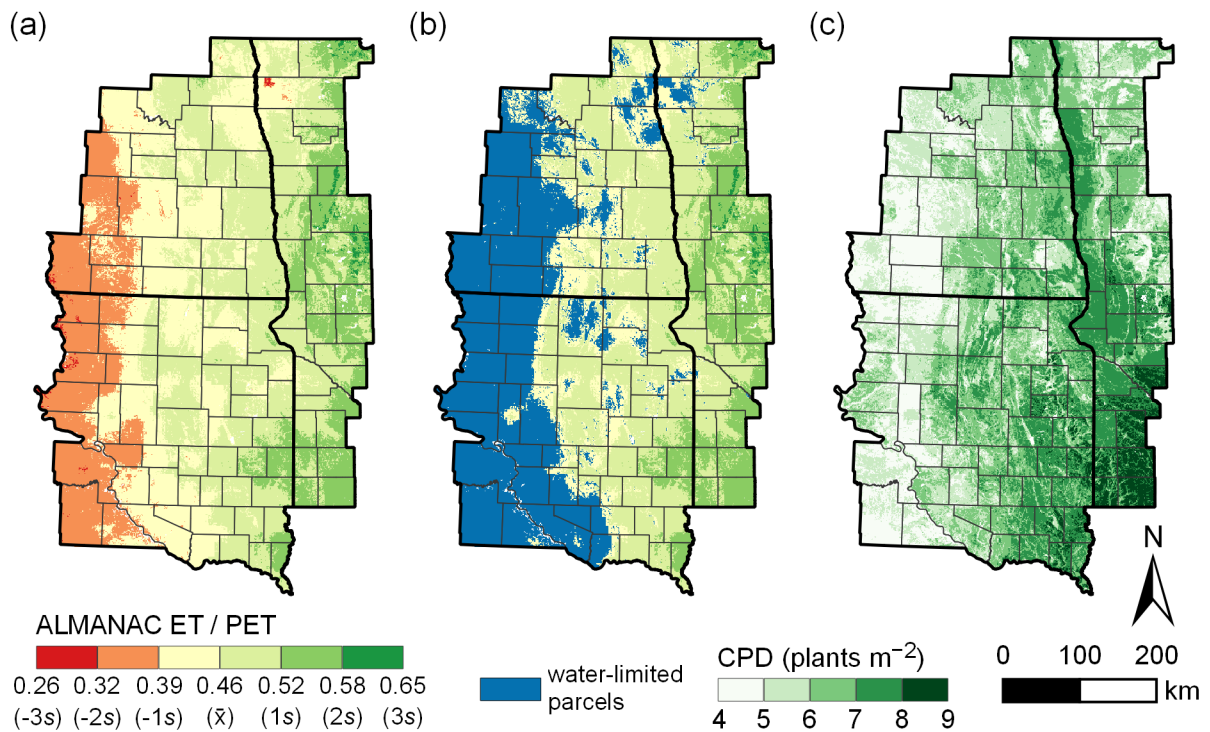


Figure 14. (a) Ratio of evapotranspiration (ET) to potential evapotranspiration (PET) for corn simulations. (b) Parcels identified as water-limited, based on visual examination of (a). (c) Corn planting density (CPD), calculated using Equation [22].

limited soils were defined as those with an ET/PET of 0.43 or lower, with this criterion determined by visual examination of an ET-to-PET ratio map (Figure 14). A seed cost of $\$3.275 \text{ 1000-seed}^{-1}$ was used, representing the average retail price across 100 corn hybrids from four seed companies for the 2013-14 and 2014-15 planting seasons (E.T. Proulx, personal communication, 2015). Assumed corn grain price was $\$3.52 \text{ bu}^{-1}$, calculated from the aforementioned price-value ratio for corn and a 2001 to 2013 average urea fertilizer price of $\$0.44 \text{ lbN}^{-1}$ (USDA ERS, 2015b). Estimated planting rates were calculated for all hybrids ranging in relative maturity from 72 to 110, which is the appropriate range of hybrid maturities across the study region. There were 80 hybrids tested under normal conditions and 21 hybrids tested under water-limited conditions.

Within each year, spatially-explicit planting dates were estimated for all areas of corn and wheat production (Figure 10). The estimation processes utilized three datasets. Corn and

wheat areas were estimated using the Cropland Data Layer (CDL; Han et al., 2012) of the USDA National Agricultural Statistics Service (NASS), which provides estimated cropland cover at 30 m resolution. USDA Crop Progress reports (USDA NASS, 2018) provided, in tabular format, statewide estimates of weekly planting and emergence for Minnesota, North Dakota, and South Dakota. Utilizing MODIS satellite imagery, USDA NASS VegScape (USDA NASS, 2015b) provided weekly vegetation indices at 250 m resolution across the study region. This investigation utilizes the Normalized Difference Vegetative Index (NDVI), which is derived from measurements of red and near-infrared reflectance and ranges from -1 to 1 . Water is indicated by NDVI values less than 0 , bare soil by NDVI of 0 to ≈ 0.2 , and vegetation by NDVI of ≈ 0.2 to near 1 (Sentinel Hub, 2019).

Planting date estimation was conducted using a custom script written in the R programming language (R Core Team, 2018). The script was run separately for corn and wheat and executed three primary steps. First, pixels representing corn or wheat production were extracted from the full CDL. Second, the weekly progression of statewide crop emergence (tabular, from USDA Crop Progress) was spatially distributed (Figure 15a) according to progression of weekly leaf greenness from NASS VegScape (Figure 15b). Specifically, weekly increases in percent emergence were assigned to a corresponding percentage of unassigned CDL pixels with the greatest NDVI. Due to differing spatial resolutions among datasets, 30 m for CDL and 250 m for VegScape, the NDVI values assigned to a corn or wheat pixel may actually represent an NDVI for mixed vegetation. Nonetheless, this process should provide a reasonable proxy of emergence across the region, as the weather conditions favorable for greening of vegetation surrounding a 30 m pixel of corn or wheat should also be favorable for germination and emergence of corn or wheat. Third, weekly progression of statewide crop planting (tabular, from USDA Crop Progress) was spatially distributed (Figure 15c) according to the crop emergence estimates, assuming that the earliest-emerging CDL pixels were also planted earliest. Among CDL pixels with the same estimated emergence date, planting dates were first assigned to those pixels with greatest NDVI.

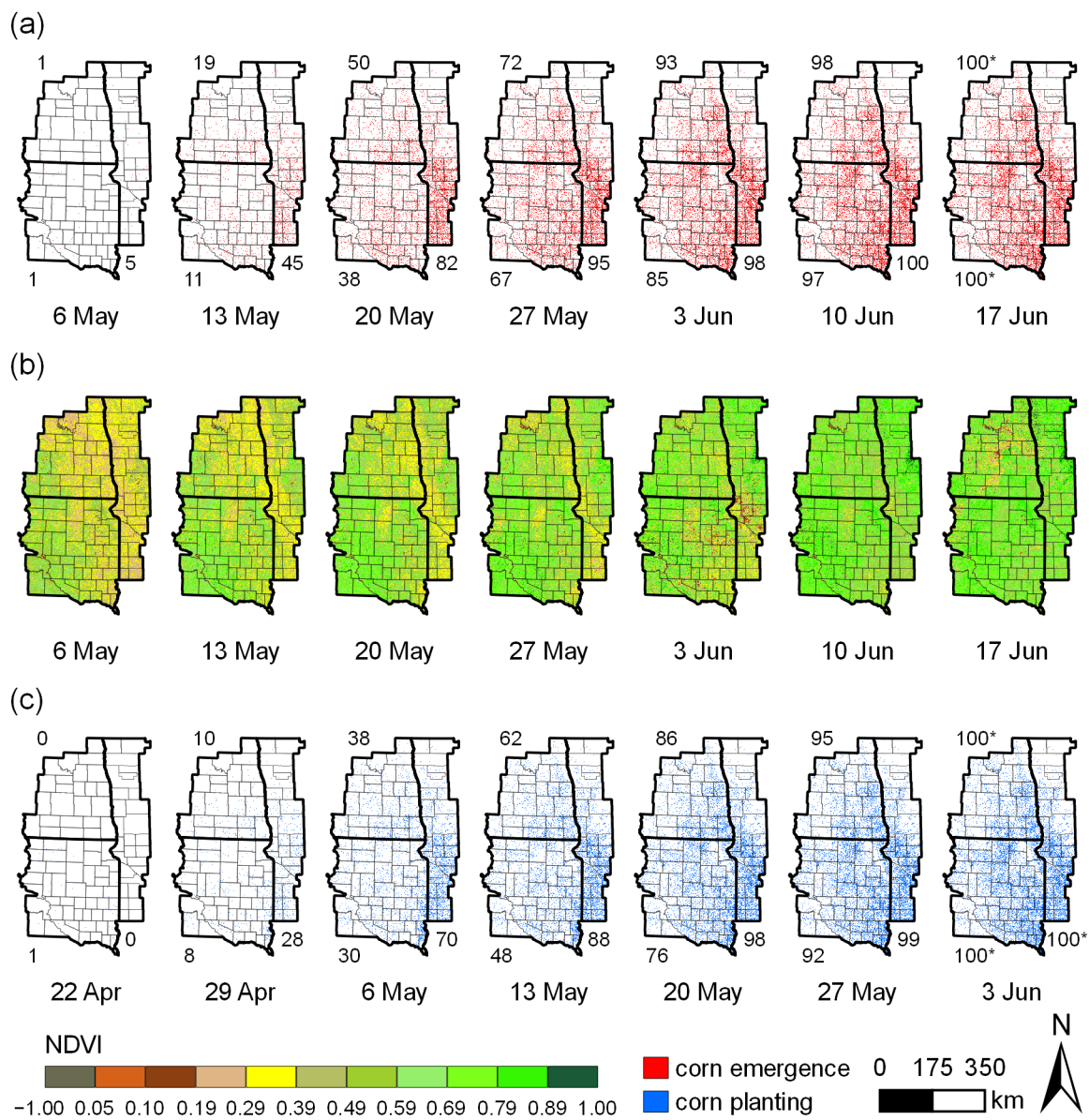


Figure 15. Example of spatially-explicit estimation of planting and harvest progression, for corn in 2007. Progression of (a) corn emergence as a function of leaf greenness estimated by (b) normalized difference vegetative index (NDVI). (c) Estimated corn planting progresses in accordance with (a). Numbers in (a) and (c) are statewide planting and harvest progress according to USDA Crop Progress reports.

Harvest date estimates were generated in a similar manner as planting date estimates. USDA Crop Progress reports (USDA NASS, 2018) provided, in tabular format, statewide estimates of weekly maturity and harvest for Minnesota, North Dakota, and South Dakota. Weekly progression of crop maturity was associated with the lowest NDVI values (i.e. leaf brownness), with maturity estimates subsequently associated with weekly harvest progression. Harvest date estimates were constrained by planting date, however, thus associating the earliest planting dates with the earliest harvest dates.

The planting date and harvest date estimation procedures resulted in multiple spatially-explicit estimates for each simulation unit (e.g. Figure 11c). For ALMANAC parameterization, each simulation unit was assigned the predominant planting-harvest date pair among its intersecting CDL pixels. The analyses presented in Section 3.4.2 required planting and harvest date estimates for simulation units without intersecting CDL pixels (i.e. without remotely-sensed corn or wheat production). Using the ‘RANN’ R package (Arya et al., 2017), these simulation units were assigned the planting and harvest dates of the nearest neighboring simulation unit that contained an estimated planting-harvest date pair.

All other corn, wheat, and soybean management factors were taken from university and industry references. Potential heat units (PHU) for corn were 1156, 1217, 1279, 1340, 1414, and 1476 for management zones 1 to 6 (Figure 12a), respectively, and were established using a corn relative maturity map from Stine Seed Company (Stine Seed Company, 2015) and a regression equation relating relative maturity to PHU (J.A. Coulter, personal communication, 2015):

$$PHU.C = 12.3RM + 145; p < 0.0001; R^2 = 0.98 \quad [23]$$

where *PHU.C* is potential heat units for corn (in °C) and *RM* is relative maturity. Similarly, soybean PHU (Figure 12b) were established using a soybean maturity group map from the University of Missouri (University of Missouri, 2015) and a regression equation relating

maturity group to PHU (Akyüz et al., 2017):

$$PHU.S = 15.569MG + 816.44; p < 0.0001; R^2 = 0.99 \quad [24]$$

where *PHU.S* is potential heat units for soybean (in °C) and *MG* is maturity group. Unlike corn hybrids and soybean cultivars, wheat cultivars are not marketed with maturity ratings that correspond to narrow geographical ranges of adaptation. Thus, wheat PHU was set to 1780 across the entire study region, in accordance with the crop calendar for the northern Great Plains of Bauer et al. (1992). Spatial delineations of soybean planting and harvest dates were set according to corn management zones (Figure 12a). Soybean planting dates were set to 10 days after corn planting dates recommended by the University of Minnesota, North Dakota State University, and South Dakota State University (Coulter, 2012, 2015; Hall et al., 2009; Ransom et al., 2004) and were May 15, 13, 11, 9, 7, and 5, respectively, for corn management zones 1 to 6. Soybean harvest dates were set as the fall freeze date (−2 °C, 90% probability) averaged across U.S. Climate Normals stations within each corn management zone (NCDC, 2005) and were October 15, 16, 19, 22, 23, and 22, respectively, for corn management zones 1 to 6.

3.3.4. ALMANAC validation

Simulated corn and wheat yields were validated against 2006 to 2015 USDA NASS county-average grain yields, with separate analyses performed for annual and multiyear average yield comparisons. For these analyses, county-average ALMANAC yields were calculated from the parcel-specific simulated yield outcomes. Since mapunit is the unit of spatial delineation in SSURGO (Figure 11c) but each mapunit contains one or more soil components, weighted average annual yields were first calculated across soil components within simulation units. Component percentages were used as the weighting variable. Then, weighted average annual yields were calculated by county, with CDL pixel counts within each simulation unit serving as the weighting variable (e.g. Figure 11c). As discussed in

Section 2.3, ALMANAC performance was evaluated by visual examination of yield outputs and through a set of statistics outlined in the extensive reviews of Bennett et al. (2013) and Moriasi et al. (2007). The chosen metrics can be divided into two broad categories, those for concurrent evaluation of real and modeled values and those for evaluation of model residuals, and were estimated using the ‘robustbase’ (Maechler et al., 2018) and ‘hydroGOF’ (Zambrano-Bigiarini, 2017) R packages. Concurrent evaluations of field-measured and ALMANAC-simulated biomass yields were performed using an iterated reweighted least squares (IRLS) regression with an MM-type regression estimator (Koller and Stahel, 2011; Yohai, 1987) and its coefficient of determination (R^2), an unequal distribution test (UDT) determined using a novel linear regression (Equations [3] to [6]; Kleijnen et al., 1998), and the index of agreement (IOA; Equation [7]; Willmott, 1981). The residuals of ALMANAC model estimates against measured values were evaluated by the root mean square error (RMSE), mean absolute error (MAE), and percent bias (PBIAS; Equation [8]). To aid in visualizing scatter plots of model residuals against measured yields, the fANCOVA R package (Wang, 2010) was used to fit second-degree polynomial local polynomial regressions with automatic selection of the smoothing parameter according to the bias-corrected Akaike Information Criterion (Hurvich et al., 1998). Spatial patterns of USDA NASS and ALMANAC county-average yields were evaluated through maps of multiyear average yields.

ALMANAC simulates growth stresses due to water, temperature, N, P, and aeration. Preliminary evaluation of ALMANAC outputs revealed that water stress was the predominant growth-limiting factor across the study region. To further evaluate the impact of soil water availability on simulated yields, the bias of ALMANAC county-average yield estimates compared to USDA NASS values was further evaluated through comparisons to county-level soil moisture conditions. Soil moisture conditions were characterized by the US Drought Monitor (USDM; <https://droughtmonitor.unl.edu>), a collaborative effort of the National Drought Mitigation Center at the University of Nebraska-Lincoln, the National Oceanic and Atmospheric Administration, and the USDA. The USDM characterizes drought through a

combination of climatological inputs, a fire risk index, satellite-based assessments of vegetation health, various indicators of soil moisture, and hydrologic data. Experts synthesize these numeric inputs and incorporate ground truthing from a network of 450 observers across the country, including state climatologists, National Weather Service staff, Extension agents, and hydrologists. The USDM is released weekly, consisting of maps that delineate five categories of drought conditions across the US: abnormally dry (D0), moderate drought (D1), severe drought (D2), extreme drought (D3), and exceptional drought (D4).

In this investigation, county-level soil moisture status for each year was represented by a mean growing season drought severity and coverage index (DSCI), calculated from weekly county-level USDM reports (University of Nebraska-Lincoln NDMC et al., 2018). Although an experimental method that has not yet been widely tested, the DSCI is presented by the authors of the USDM as a convenient way to convert USDM data from categorical to continuous, and to aggregate from spatially-specific to geopolitical boundaries. The DSCI was calculated as follows:

$$DSCI_{ij} = \sum_{i=1}^n \left\{ \frac{1}{n} [1 (D0_{ij}) + 2 (D1_{ij}) + 3 (D2_{ij}) + 4 (D3_{ij}) + 5 (D4_{ij})] \right\} \quad [25]$$

where i is one week during a growing season n weeks long; j is county; and $D0$, $D1$, $D2$, $D3$, and $D4$ are the percentages of the county that are in abnormally dry, moderate drought, severe drought, extreme drought, and exceptional drought conditions, respectively. For calculating DSCI, the corn growing season is defined as April 1 through September 30 while the wheat growing season is defined as April 1 through August 31. A linear-plateau regression model was fit to the relationship between ALMANAC yield bias and DSCI, using the ‘easynls’ R package (Arnhold, 2017). The confidence interval of the linear-plateau relationship was determined using the ‘propagate’ R package (Spiess, 2018).

To evaluate the suitability of within-county ALMANAC yield estimates, productivity indices calculated from simulated corn and wheat yield outcomes were compared to Crop

Productivity Index (CPI) values reported within SSURGO. A unitless rating ranging from 0 to 100 and calculated by soil survey area (i.e. county), CPI provides a relative ranking of soils based on their potential for intensive crop production (Soil Survey Staff, 2018). Productivity indices (*PI*) based on ALMANAC yield estimates were calculated by averaging ALMANAC yields (*AY*) for each crop (*l*) across years (*y*) and aggregating by SSURGO mapunit:

$$AY_{jkl} = \sum_{y=1}^n \left\{ \frac{1}{n} \left[\sum_{i=1}^n \left(\frac{1}{n} \times AY_{ijkly} \right) \right] \right\} \quad [26]$$

where *i* is a simulation unit (e.g. Figure 11c) within mapunit *j* and county *k*, and subsequently dividing the outputs of Equation [26] by the maximum *AY* value for the county:

$$AY_{kl} = \max \{AY_{jkl1}, \dots, AY_{jkl n}\} \quad [27]$$

$$PI_{jkl} = AY_{jkl} / AY_{kl}.$$

To evaluate the suitability of ALMANAC yield estimates across soils of varying land uses and suitability for cropping, Section 3.4.2 contrasts mapped CPI to mapped *PI* among parcels with CDL-indicated corn or wheat production between 2006 and 2015 (see Figure 10), among parcels without corn or wheat production during this time, and in boxplots showing the distribution of parcel values when grouped by LCC.

3.3.5. ALMANAC calibration and sensitivity analyses

ALMANAC was calibrated to approximate multiyear average corn and wheat grain yields for 2006 to 2015. Calibration was performed on contiguous multi-county areas spatially distributed across the study area, in regions with remotely-sensed corn and spring wheat production histories (Figure 10). Within each year, calibration simulations were limited to those simulation units (e.g. Figure 11c) having corn or spring wheat production as determined by the CDL (Figure 10). Planting and harvest dates were estimated as described in Section 3.3.3. However, unlike the final parameterization, annual yields for calibration runs were estimated for all unique planting-harvest date pairs within a simulation unit.

Subsequently, pixel counts for each date pair were used to calculate a weighted-average yield for the simulation unit. A unified scheme was used for all other management practices in the wheat calibration runs: N and P fertilizer rates were 280 and 90 kg ha⁻¹, respectively (Kaiser et al., 2013), PHU (base 0 °C) was 1780 (Bauer et al., 1992), and plant population was 346 plants m⁻² (Wiersma et al., 2005). For corn, the N rate was 303 kg ha⁻¹ (Franzen, 2014b); the P rate was 142 kg ha⁻¹ (Rehm et al., 2006); PHU (base 10 °C) values for calibration areas 1 to 6 (Figure 10) were 1156, 1156, 1248, 1248, 1310, and 1414, respectively (J.A. Coulter, personal communication, 2009; Stine Seed Company, 2015); and the respective plant populations for calibration areas 1 to 6 were 9.86, 9.86, 8.62, 8.62, 8.20, and 8.20 plants m⁻² (Coulter, 2015). All environmental variables were as described in Section 3.3.2.

To examine the relative influence of ALMANAC parameter modifications in obtaining the simulation outcomes presented herein, sensitivity analyses (SA) were conducted for each of the parameters outlined in Table 6. Local SA were conducted utilizing one-factor-at-a-time perturbations (Norton, 2015; Pianosi et al., 2016). Following this method, each input parameter from the final parameterization was perturbed individually while holding all other values constant. However, parameters considered to belong to a functional group were analyzed together within a single SA. Since HI and the minimum limit of HI (WSYF) collectively modify the final HI, changes to these parameters were evaluated within a single SA. Since field capacity and wilting point collectively determine the plant-available water within each soil, changes were evaluated within a single SA. Similarly, soil depth and corn root depth were grouped within a single SA, as were planting and harvest dates, and increases or decreases of CN2A, CN2B, CN2C, and CN2D. Each SA was conducted within the same multi-county areas used for model calibration. The normalized sensitivity parameter (NSP; Equation [9] Norton, 2015) was used to rank the ALMANAC input parameters according to their relative contributions to simulated yield variability. Changes in yields and parameters were normalized due to the differing units among the input parameters and simulated yield outputs. Since parameterization changes could not be quantified in the SA evaluating crop sequencing and

planting/harvest dates, these parameters were excluded from comparisons of the NSP.

3.4. Results and Discussion

3.4.1. Validation of county-average yields

To facilitate regional-scale estimation of corn and wheat yields across the study region, the ALMANAC model was calibrated on a subset of 20 study area counties for corn and 18 counties for wheat (Figure 10) to approximate USDA NASS multiyear average corn and wheat grain yields from 2006 to 2015. Following model calibration, NASS county-average grain yields were validated against ALMANAC outputs for the remaining study area counties (i.e. the validation counties).

3.4.1. 1. Multiyear-average outcomes

For corn, there is strong agreement between ALMANAC and NASS multiyear average yields. For the calibration and validation sets, a linear regression of ALMANAC versus NASS yields has an R^2 of approximately 0.80 and does not substantially differ from the zero intercept and unit slope of a perfect regression fit (Figure 16a,c). In addition, in each comparison IOA is 0.93, PBIAS is less than 5%, RMSE is less than 0.75 Mg ha^{-1} , and ALMANAC model residuals display an even spread across the range of NASS yields (Figure 16c,d). Within the validation counties, the RMSE of ALMANAC yield (0.71 Mg ha^{-1}) is just 8.8% of the NASS yield grand mean of 8.03 Mg ha^{-1} (Figure 16d).

Corn yield maps also reveal that ALMANAC accurately captured spatial variability in yield across the study area. NASS multiyear average corn yields display a clear gradient from northwest to southeast, with average corn yields of 5 to 8 Mg ha^{-1} in the western and northwestern portions of the study area, 9 to 11 Mg ha^{-1} in the southeast, and 8 to 9 Mg ha^{-1} in between (Figure 17a). ALMANAC yields displayed a similar west-to-east trend across the study area, although with higher yields extending slightly further northward in Minnesota (Figure 17b). Nonetheless, most counties had ALMANAC yield within 10% of NASS yield, with just 10 counties displaying a bias of -10 to -32% and 12 counties displaying a bias of 10 to 30% (Figure 17c).

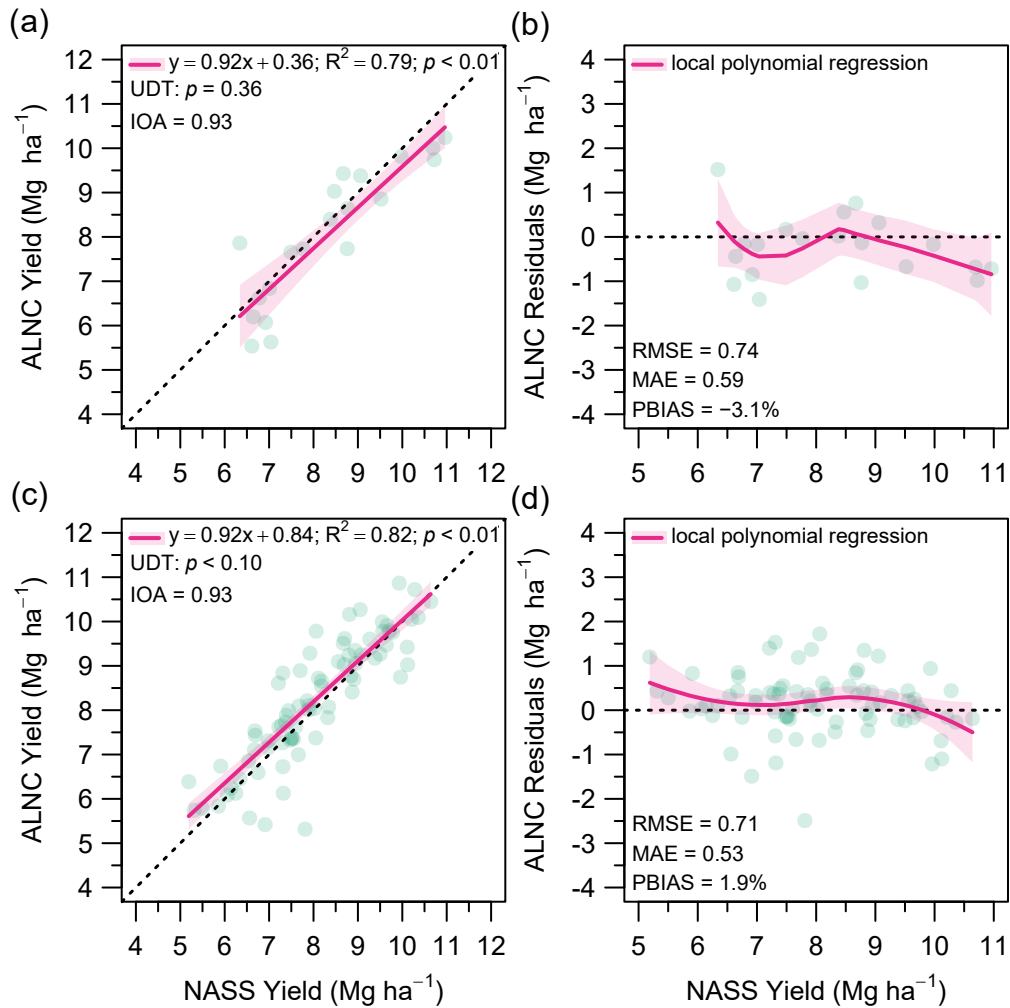


Figure 16. For 20 calibration counties (see Figure 10), corn (a) ALMANAC yield and (b) ALMANAC yield residuals vs. USDA NASS yield. For 79 validation counties, (c) and (d) are same as (a) and (b). Each point represents a mean county-average yield for 2006 to 2015.

ALMANAC estimates of multiyear average wheat yield also agreed with NASS values, although the relationships were not as strong as those observed for corn. When compared to NASS yields, ALMANAC yield estimates in the calibration counties have an IOA of 0.88, PBIAS of 0.4%, and RMSE of 0.25 Mg ha^{-1} (Figure 18a,b). Also, a linear regression of ALMANAC versus NASS yields has an R^2 of 0.62 and a slope and intercept not substantially different than zero intercept and unit slope. ALMANAC relationships to NASS yields were relatively poorer across validation counties, however, displaying a clear positive bias in lower-yielding counties, an overall PBIAS of 7.7%, an IOA of 0.70, and an RMSE of 0.49 Mg ha^{-1}

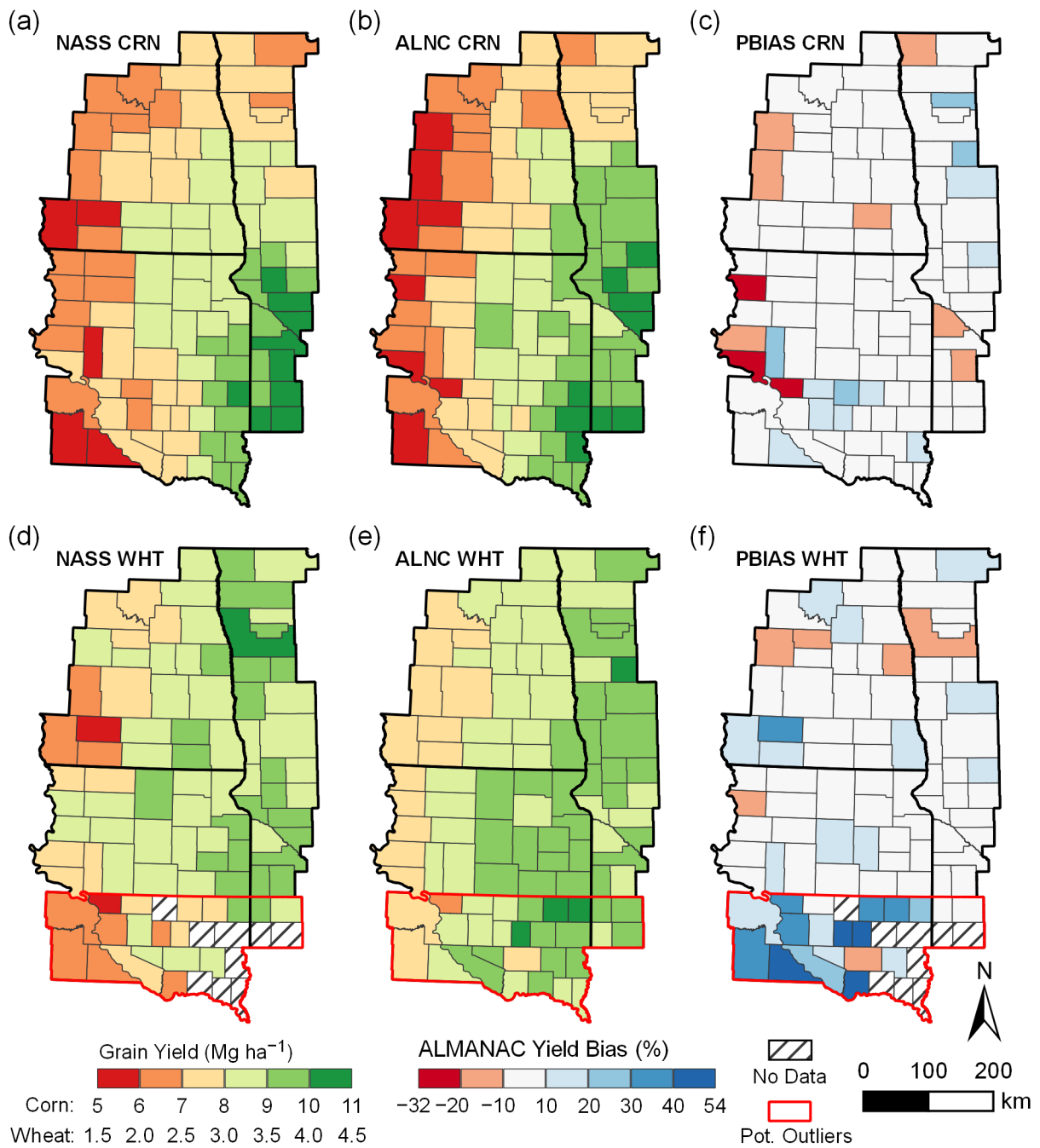


Figure 17. For corn (CRN), maps of (a) USDA NASS yield, (b) ALMANAC (ALNC) yield, and (c) percent bias (PBIAS) of ALMANAC yield. For wheat (WHT), (d – f) same as (a – c). Counties outlined in red are considered potential outliers due to their high yield bias. Variables are averaged across 2006 though 2015 values.

(Figure 18c,d).

Wheat yield maps reveal that the southernmost counties of the study area are primarily responsible for this poorer fit. Among the 17 southernmost South Dakota counties and 2 southernmost Minnesota counties where comparisons can be made to NASS yields, 5 display a yield bias of 10 to 30% and 9 display a yield bias of 30 to 54% (Figure 17c). Just 11 counties across the remaining study area display a positive yield bias, and only one of these counties has a bias greater than 20%. Accordingly, removing these southernmost counties (i.e. outliers) from the analyses presented in Figure 18c,d greatly improves agreement with NASS, reducing PBIAS from 7.7% to 2.8%, increasing IOA from 0.70 to 0.85, and decreasing RMSE from 0.49 to 0.28 Mg ha⁻¹ (just 8.5% of the grand mean of 3.28 Mg ha⁻¹). These results suggest that at least one aspect of wheat growth and development in the southern portions of the study area is significantly different than the rest of the region and is unaccounted for by the ALMANAC parameterization for wheat presented herein. Considering the lack of wheat production in these counties (Figure 10b), no effort was made to improve the presented wheat parameters for use in the southern portions of the study area. All further analyses omit wheat simulation results from these southernmost study area counties.

3.4.1. 2. Annual outcomes

While ALMANAC generates reasonable multiyear average yield estimates for corn and wheat, it is much less precise in estimating annual yield outcomes. Across validation counties, the RMSE of ALMANAC corn yield estimates increases from 0.71 Mg ha⁻¹ with multiyear average values (Figure 16d) to 2.13 Mg ha⁻¹ with annual values (Figure 19b). Therefore, even though the PBIAS of annual estimates is just 2.0% (Figure 19b) and the linear regression against NASS values indicates only slight deviation from the 1:1 line (Figure 19a), annual corn yield estimates from ALMANAC are clearly less reliable than multiyear average estimates. In wheat, the linear regression of annual ALMANAC wheat yields versus NASS values results in a poor fit ($R^2 = 0.03$; Figure 19c) and the RMSE of ALMANAC yield estimates increases from 0.49 Mg ha⁻¹ with multiyear average values (Figure 16d) to 1.00 Mg ha⁻¹ with annual

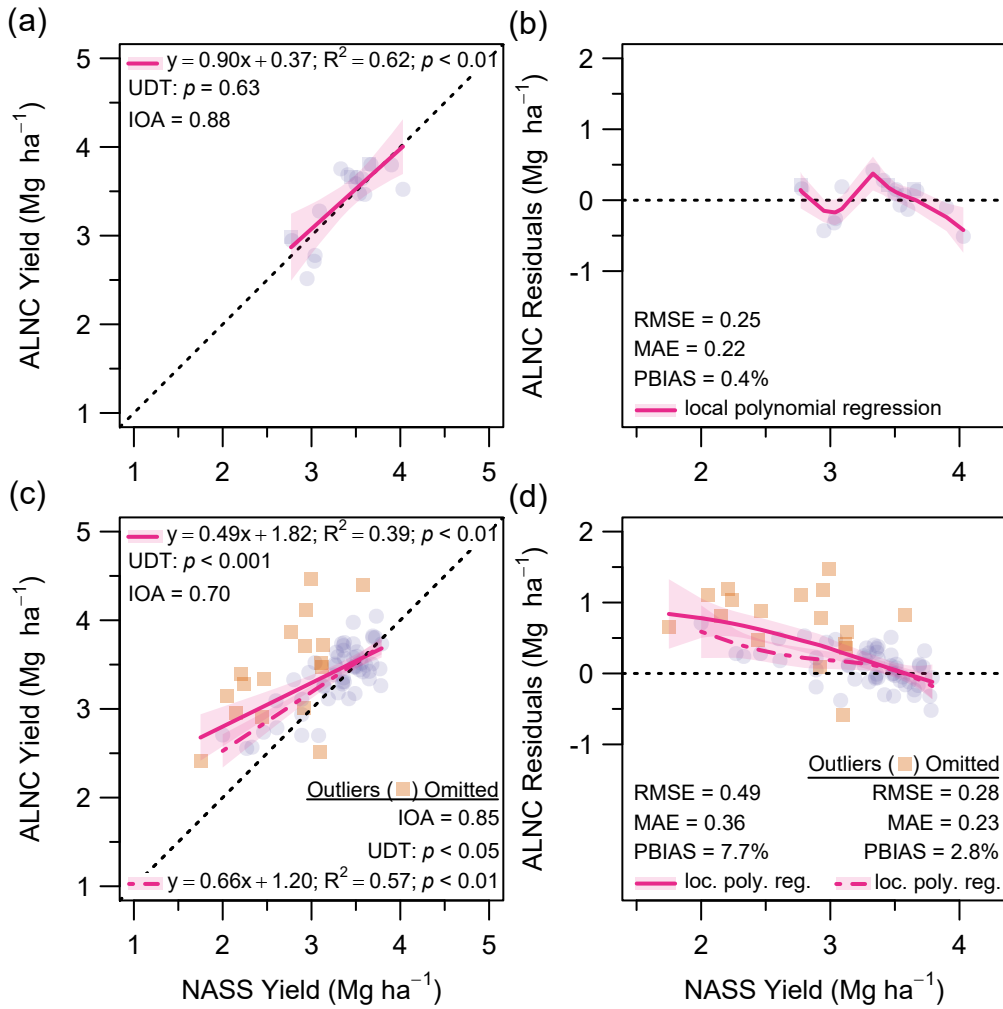


Figure 18. For 18 calibration counties (see Figure 10), wheat (a) ALMANAC yield and (b) ALMANAC yield residuals vs. USDA NASS yield. For 72 validation counties, (c) and (d) are same as (a) and (b). Each point represents a mean county-average yield for 2006 to 2015. Outliers correspond to counties outlined in Figure 17.

values (Figure 19d). Removing observations from the southernmost tier of study area counties does not improve the agreement of annual ALMANAC yield estimates with NASS values.

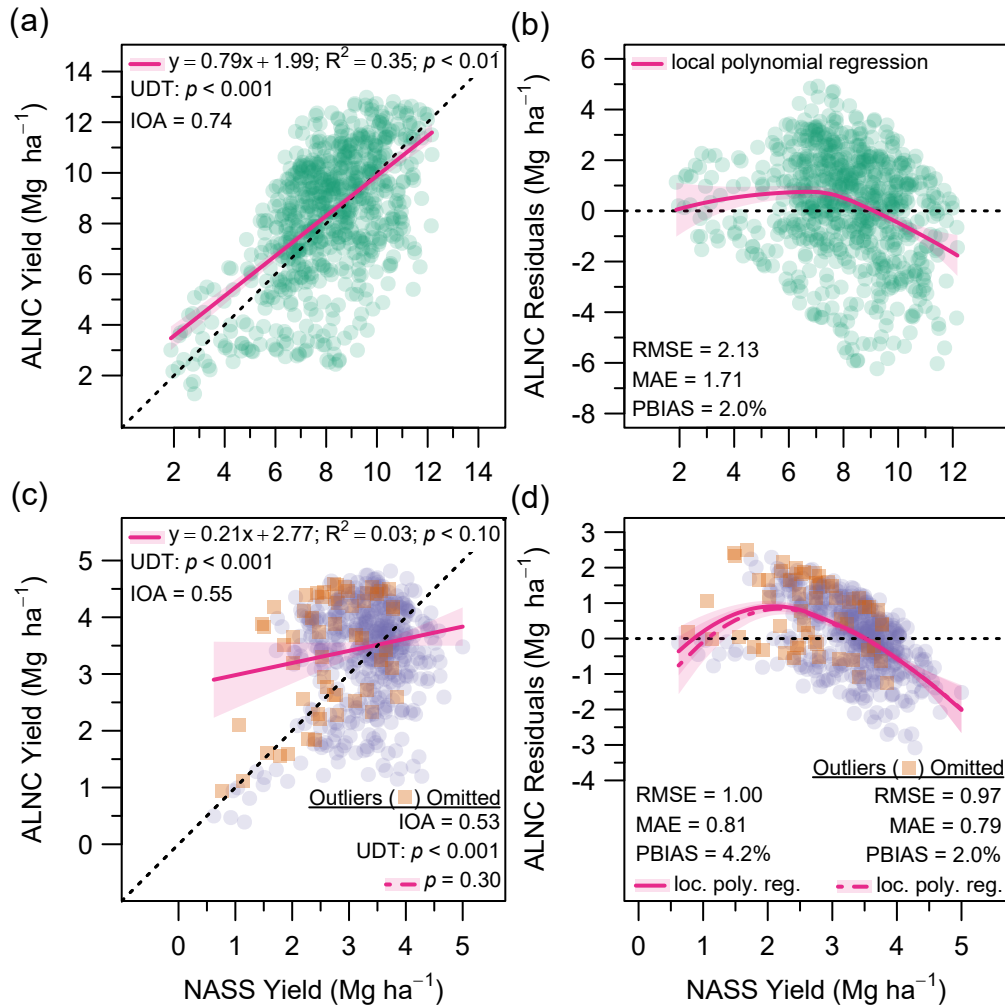


Figure 19. For 79 validation counties, corn (a) ALMANAC yield and (b) ALMANAC yield residuals vs. USDA NASS yield. For 72 validation counties, wheat (c) ALMANAC yield and (d) ALMANAC yield residuals vs. USDA NASS yield. Each point represents an annual county-average yield for 2006 to 2015. Outliers correspond to counties outlined in Figure 17.

The successful estimation of multiyear average yields but poor representation of year-to-year yield variability is consistent with past ALMANAC simulations of regional corn yield. Pooled across nine counties spanning the US Midwest, a regression of 10-year average simulated corn yields to USDA NASS featured y-intercept and slope not significantly different

from a 1:1 line, R^2 of 0.98, and mean simulated yields within 5% of mean measured yields (Kiniry et al., 1997). In contrast, when considering annual yields just four of nine US counties featured a regression relationship not significantly different from a 1:1 line. Kiniry et al. (2004) showed similar multiyear average results as Kiniry et al. (1997) for evaluations pooled across four counties in the Texas High Plains, with R^2 of 0.78 instead of 0.98, but observed that regression relationships of simulated and observed annual yields were not statistically significant within any of the four counties. Although unsuccessful in certain instances (Kiniry and Bockholt, 1998), field-scale simulations parameterized with local weather and soil parameters have demonstrated success in estimating year-to-year corn yield variability (Kiniry et al., 2004; Xie et al., 2001). Collectively, past and current results suggest that ALMANAC consistently provides accurate estimates of multiyear average yields for regional corn simulations, but may require field observations of management practices, soil characteristics, and weather conditions to accurately characterize year-to-year yield variability. Comparable ALMANAC simulations of regional wheat yield could not be found in the literature, but current results suggest outcomes similar to corn – success in estimating multiyear average yields and difficulties in estimating year-to-year yield variability.

3.4.2. Evaluation of within-county productivity

While ALMANAC provides multiyear average, county-level yield estimates in general agreement with corresponding NASS values, comparisons to NASS cannot evaluate the suitability of within-county ALMANAC yield estimates. Furthermore, no known data source provides parcel-specific measured yields that could be used for this purpose. To estimate the suitability of within-county yield estimates generated by ALMANAC, corn production index (CNPI) and wheat production index (WTPI) values were calculated from ALMANAC multiyear average yields (Equations [26] and [27]) and compared to CPI values reported within SSURGO. Crop productivity index provides a relative ranking of soils based on their potential for intensive crop production (Soil Survey Staff, 2018) but does not take into account climatic factors and thus is not comparable for soils across survey areas (i.e. across counties).

Nonetheless, CPI provides a standard against which to evaluate the within-county variability of simulated corn and wheat yields.

3.4.2. 1. *CPI, CNPI, and WTPI maps*

For parcels with CDL-indicated corn or wheat production between 2006 and 2015 (Figure 10), the standard deviation of CPI ranged from 8 to 11 across much of the study area; from 11 to 14 in southern North Dakota, northern South Dakota, and northwestern Minnesota; and from 14 to 20 within five counties (Figure 20a). In contrast, standard deviation of CNPI and WTPI was no greater than 11 to 14 in any one county and ranged from 2 to 5 or 5 to 8 across most of the study area (Figure 20b,c). When compared to CPI, CNPI and WTPI displayed less variability within all counties. This effect was most pronounced in South Dakota, however, where values of CNPI and WTPI were elevated when compared to CPI. For example, of the 74,005 parcels with corn or wheat production in South Dakota, the proportion of parcels with a value of 80 to 100 was 67% for CNPI (Figure 20e), 91% for WTPI (Figure 20f), and just 38% for CPI (Figure 20d). These outcomes indicate that, for parcels with estimated corn or wheat production from 2006 to 2015, ALMANAC did not simulate as much within-county variability in corn and wheat yield as would be expected from CPI values.

Relative differences in CPI, CNPI, and WTPI were even more pronounced for parcels without corn or wheat production from 2006 to 2015. The standard deviation of CPI ranged from 11 to 15 across one-third of counties, 15 to 19 across one-half of counties, and 19 to 23 across remaining counties (Figure 21a). In contrast, the standard deviation of CNPI and WTPI ranged from 3 to 11 across 90% of all study area counties (Figure 21b,c). Similar to corn and wheat production parcels, values of CNPI and WTPI between 80 and 100 were much more prevalent across non-production parcels than were similar values of CPI, especially throughout South Dakota (Figure 21d–f). Furthermore, while CPI values of 0 to 40 were found throughout the western Dakotas, northeast South Dakota, west-central Minnesota, and northwest Minnesota, similar values of CNPI and WTPI were only observed in a small region of western North Dakota.

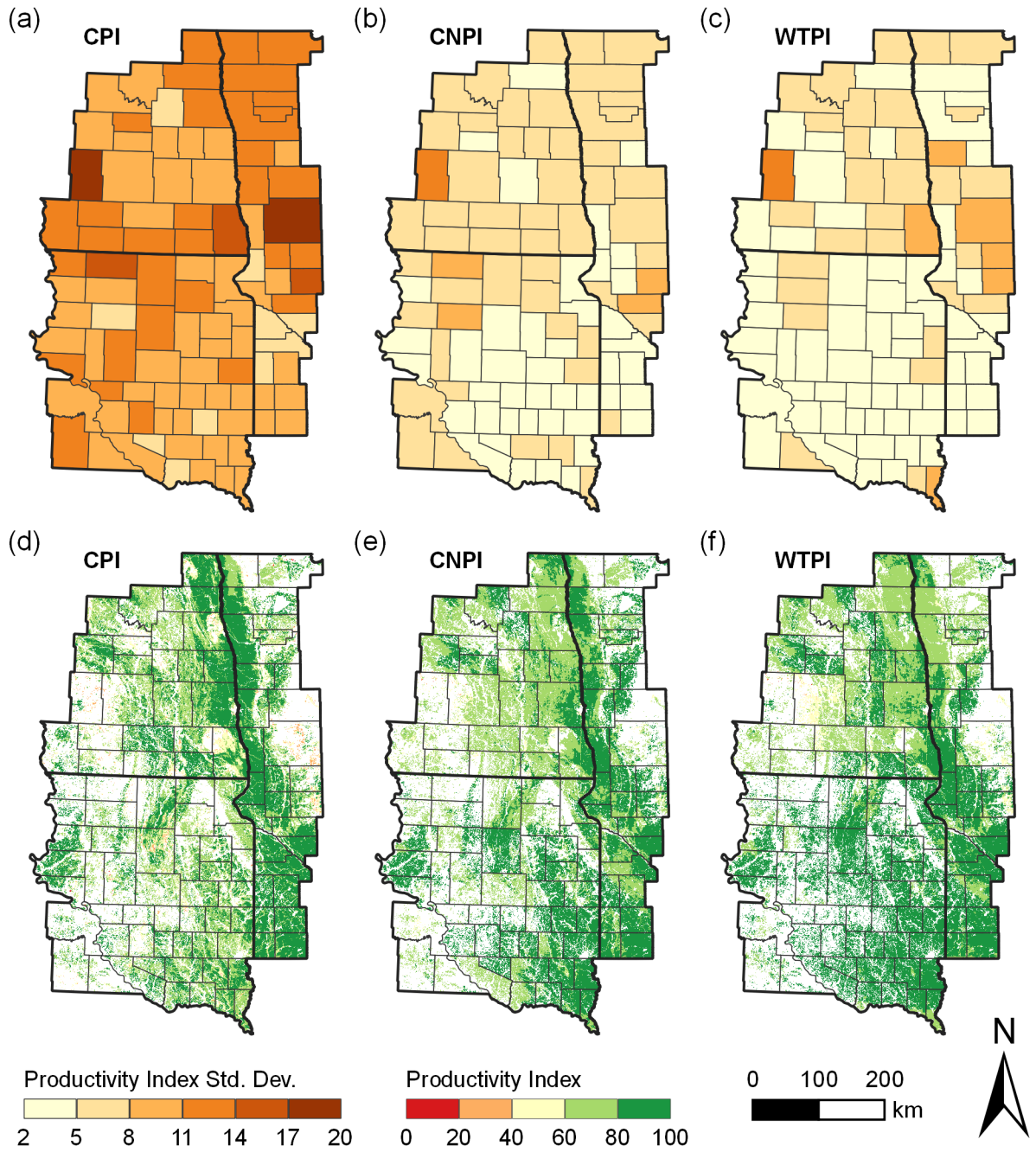


Figure 20. For parcels with CDL-indicated corn or wheat production from 2006 to 2015 (see Figure 10), county-specific standard deviations of (a) crop productivity index (CPI), (b) ALMANAC-derived corn productivity index (CNPI), and (c) ALMANAC-derived wheat productivity index (WTPI). (d – f) Corresponding parcel-specific values of CPI, CNPI, and WTPI.

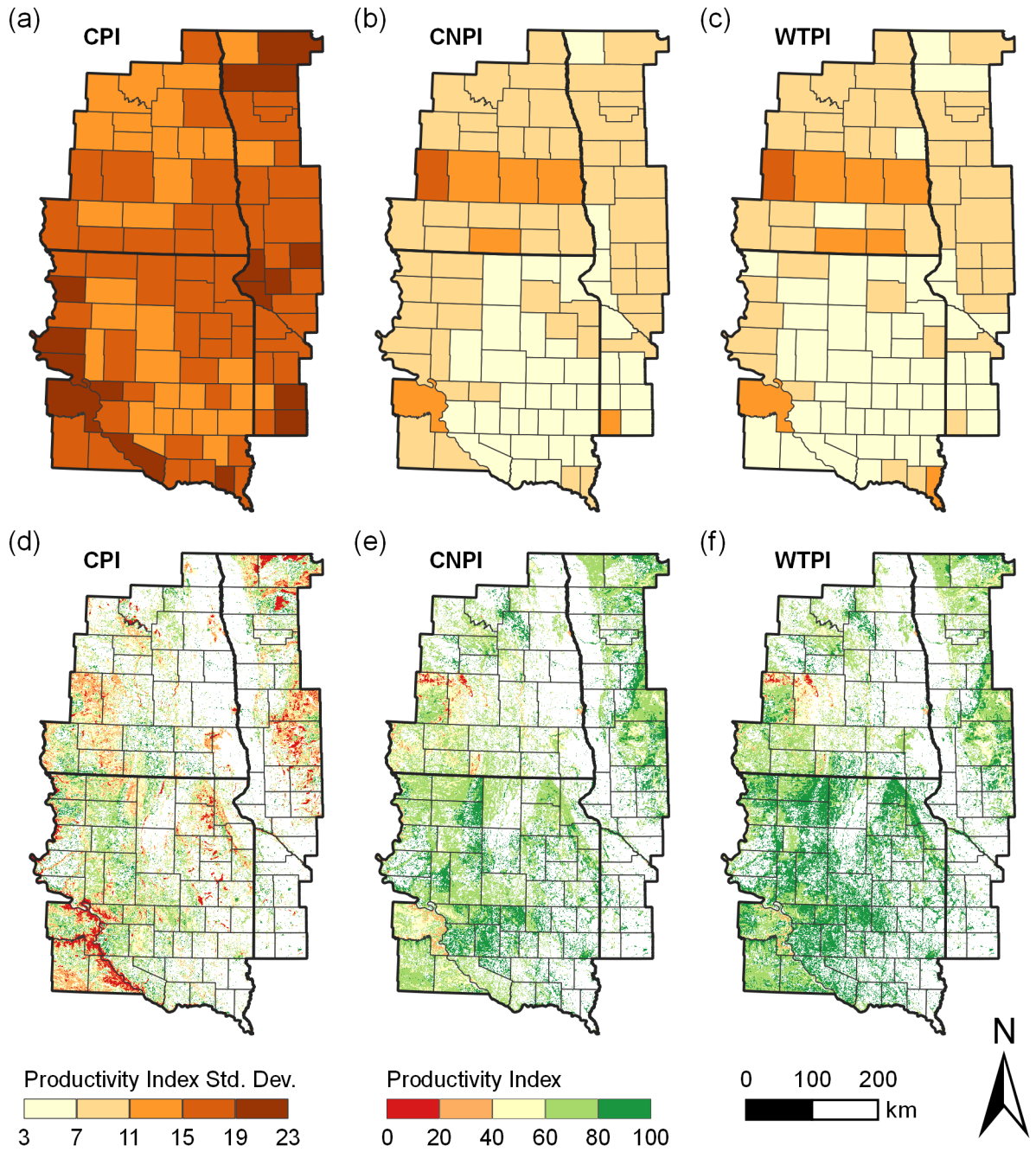


Figure 21. For parcels without CDL-indicated corn or wheat production from 2006 to 2015 (see Figure 10), county-specific standard deviations of (a) crop productivity index (CPI), (b) ALMANAC-derived corn productivity index (CNPI), and (c) ALMANAC-derived wheat productivity index (WTPI). (d – f) Corresponding parcel-specific values of CPI, CNPI, and WTPI.

3.4.2. 2. *CPI, CNPI, and WTPI by LCC*

While ALMANAC has been shown to simulate less parcel-by-parcel corn and wheat yield variability than would be expected according to CPI, this effect seems to be more pronounced for parcels without a recent history of corn or wheat production. To further evaluate ALMANAC performance on parcels of varying land use suitabilities, CPI, CNPI, and WTPI were evaluated by LCC. Land capability classification shows, in a general way, the suitability of soils for most types of field crops (Soil Survey Staff, 2018). Class is the broadest grouping of LCC and is designated by numbers 1 through 8, with progressively higher numbers indicating progressively greater limitations and narrower choices for practical use. Soils in classes 1 through 4 are generally considered suitable for cultivated cropping, while soils in classes 5 through 7 feature severe or very severe limitations that restrict their use mainly to pasture, rangeland, grazing, forestland, or wildlife habitat. Since class 8 soils have limitations that preclude commercial plant production, this investigation only considers soils from classes 1 to 7.

The study area is dominated by LCC 2 and 3 (Figure 22a), which constitute 64% and 16% of all study area parcels, respectively (Table 8). Corresponding values for corn or wheat production parcels are 80% and 12% for LCC 2 and 3, with LCC 1 constituting an additional 4.2% of all production parcels. When considering distributions of CPI, CNPI, and WTPI by LCC (Figure 22b), it appears that ALMANAC was more effective at simulating within-county variability among corn and wheat production parcels because ALMANAC is relatively effective at simulating yield variability for parcels of LCC 1 to 3. For parcels of LCC 1, distributions of CPI, CNPI, and WTPI largely overlap and have respective median values of 96, 90, and 91, with CNPI and WTPI only slightly skewed towards lower values than CPI. Similarly, distributions of CPI, CNPI, and WTPI for parcels of LCC 2 overlap around median values from 80 to 86, with only a slight skew towards lower values for WTPI. Distributions of CPI and WTPI for LCC 3 parcels also largely overlap about a median near 65, although the distribution of CNPI values is centered on a distribution with a median of 76. When considering

that parcels with LCC of 1 to 3 represent 96% of corn and wheat production parcels (Table 8), these results help to explain the accuracy of ALMANAC-estimated multiyear-average corn and wheat yields by county (Figures 16 and 18).

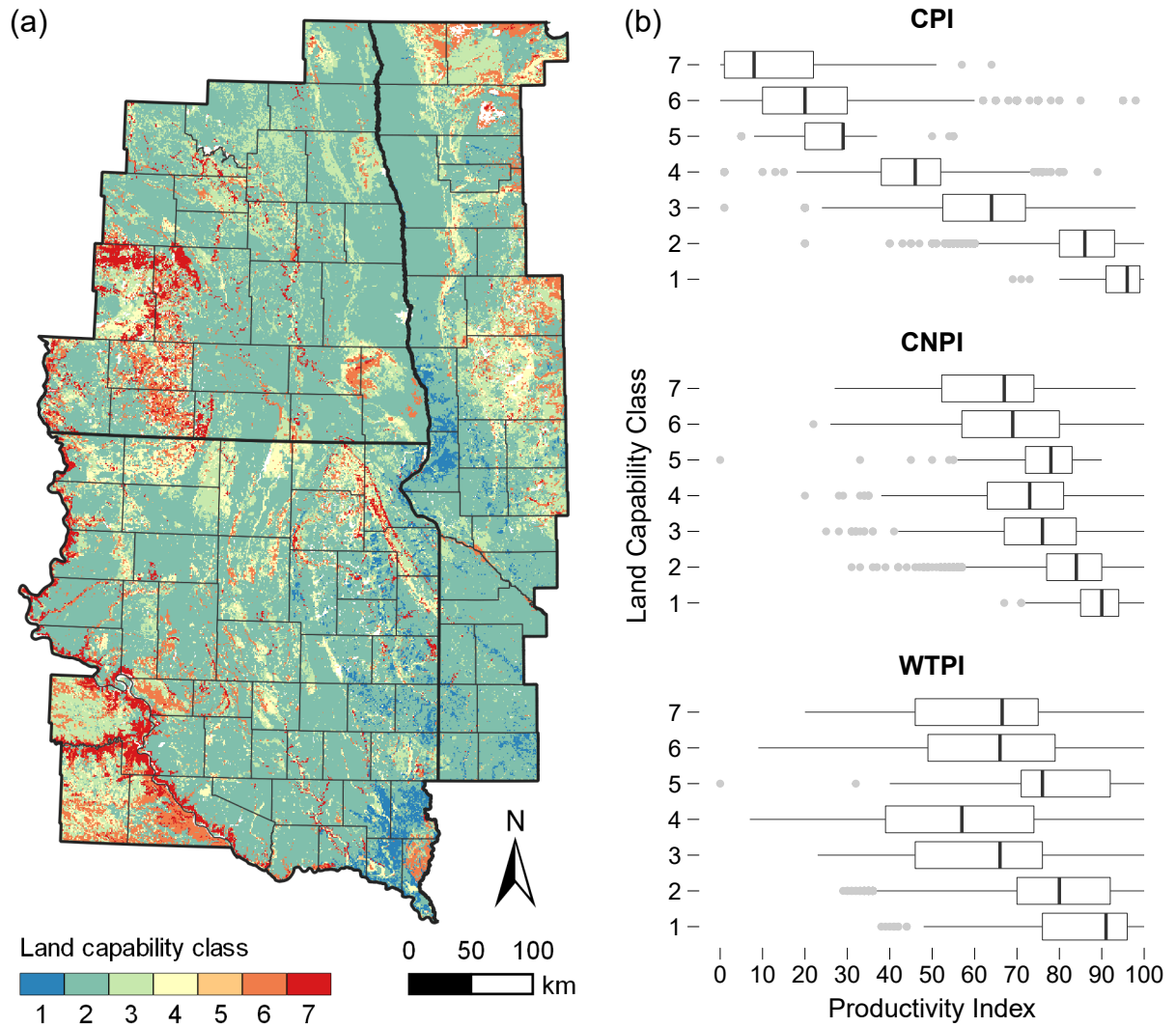


Figure 22. (a) Land capability classes for all study area parcels. (b) Distributions of crop productivity index (CPI) and ALMANAC-derived corn productivity (CNPI) and wheat productivity (WTPI) indexes, grouped by land capability class.

While CPI, CNPI, and WTPI displayed relative agreement for parcels with LCC of 1 to 3, distributions of CNPI and WTPI values for parcels in LCC 4 to 7 compare poorly to distributions of CPI. Median CPI values for LCC 4 to 7 are 46, 29, 20, and 8, respectively

Table 8. Tabulation of study area parcels by land capability class (LCC) for all parcels, parcels with corn or wheat (C/W) production, and parcels without C/W production.

LCC	All Parcels		C/W Prod. Parcels		Non C/W Prod. Parcels	
	n	% of total	n	% of total	n	% of total
1	10,035	2.7	8812	4.2	1223	0.75
2	236,982	64	167,237	80	69,745	43
3	58,000	16	24,324	12	33,676	21
4	25,647	6.9	6073	2.9	19,574	12
5	965	0.26	237	0.11	728	0.45
6	26,940	7.3	2576	1.2	24,364	15
7	13,133	3.5	244	0.12	12,889	8.0

(Figure 22b). Corresponding median values of CNPI and WTPI range from 57 to 78. Therefore, ALMANAC seems to greatly overestimate the yield potential of parcels with LCC 4 to 7, which possess very severe limitations for field crop production or are restricted to uses other than crop production. Since these parcels are primarily used for purposes other than corn or wheat production throughout the study region (Table 8), the relative inability of ALMANAC to accurately estimate yields for these parcels has limited impact on ALMANAC estimates of county-average corn and wheat yields.

3.4.2. 3. Soils of field-scale ALMANAC investigations

Published accounts of ALMANAC corn simulation in the US (Kiniry and Bockholt, 1998; Kiniry et al., 1997, 2004; Xie et al., 2001) identify the series name for simulation soils but do not include LCC descriptions. Since most of these soil series describe several soils differing in slope, the exact soils used in each of these investigations cannot be identified. Nonetheless, characterizing the LCC of all possible soils provides insight on the relative cropping suitability of soil series used in previous ALMANAC model testing. Among the 65 soils within the 35 soil series across these four investigations, there were 2, 40, 19, 3, and 1 soils in LCC 1 to 5, respectively. Thus, 65% of all soils were in LCC 1 and 2 and 94% of all soils were in LCC 1 to

3. Similarly, among 14 possible soils used in published accounts of EPIC wheat simulation in the US and Canada (Kiniry et al., 1995; Moulin and Beckie, 1993; Touré et al., 1995), 11 (79%) were classified as suitable for intensive agriculture while 3 (21%) were classified as suitable only for perennial species.

Unlike empirical models, which cannot be extrapolated outside the conditions used for parameter estimation, dynamic system models can generally be extrapolated across a wide range of soil types, weather conditions, and management practices due to their mechanistic and functional subroutines (Jones et al., 2016; Thornton et al., 1991). Nonetheless, this investigation indicates that ALMANAC may perform poorly when simulating intensive cropping on soils considered poorly suited for this purpose, and these soils represent an extrapolation from the agricultural soils used extensively in model development and testing. In the US, LCC values are accompanied by one of four subclasses designating the main hazard for field crop production: risk of erosion unless close-growing plant cover is maintained; water in or on the soil interfering with plant growth or cultivation; shallow, stony, or droughty soil; or climate that is very cold or very dry. In Canada, the Land Suitability Rating System (Bock et al., 2018) defines one most limiting component among two climate components (heat supply, moisture supply), five soil components (moisture supply, nutrient supply, physical conditions, chemical conditions, drainage), and three landscape components (erodability potential, management factors, flooding potential). For improved ALMANAC corn and wheat simulations in nonagricultural soils, further field-scale testing is warranted in these soils where one or more of these limitations precludes intensive cropping.

3.4.3. Moisture stress and yield estimation biases

Rainfed agriculture is predominant throughout the study area, with estimated irrigated acreage constituting just 3.1% of all corn harvested area and 0.16% of all wheat harvested area in the latest available Census of Agriculture (USDA NASS, 2012a). Thus, soil moisture conditions exert a large influence on year-to-year yield variability throughout the study region. In order to accurately estimate year-to-year variability across the study area, ALMANAC must

accurately estimate yield under a wide range of soil moisture conditions.

3.4.3. 1. Relating ALMANAC biases to a drought index

To evaluate the effect of soil moisture on the bias of ALMANAC county-average yield estimates against NASS values, annual ALMANAC yield biases were compared to corresponding mean growing season DSCI (Drought Severity Coverage Index) values from 2006 to 2015 (Figure 23). A zero value for DSCI indicates that no area of the county experienced drought conditions at any time throughout the growing season, while increasing DSCI values indicate increasing areal coverage or intensity of drought conditions. Since DSCI is a function of intensity and areal extent of drought conditions (Equation [25]), a given DSCI value could represent an array of drought outcomes experienced over the course of a growing season. Nonetheless, county-wide presence of abnormally dry, moderate drought, and severe drought conditions throughout the entire growing season would represent conceptual examples of 100, 200, and 300 DSCI, respectively.

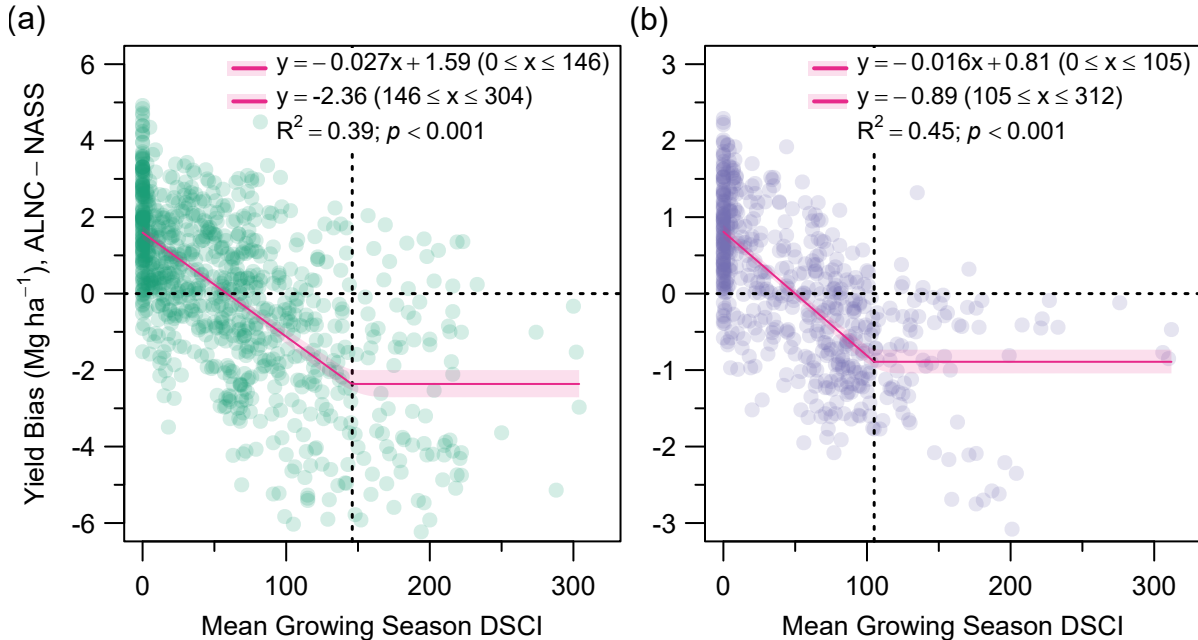


Figure 23. For (a) corn and (b) wheat, ALMANAC yield bias vs. mean growing season drought severity and coverage index (DSCI). Each point represents a county-average value for a single year.

Although R^2 values of 0.39 for corn and 0.45 for wheat indicate that other factors also influence the annual variability in ALMANAC yield bias, there was a clear linear-plateau relationship between increasing drought and ALMANAC yield bias (Figure 23). Under no drought stress (DSCI = 0), the ALMANAC model almost exclusively overestimated county-average corn and wheat yields, with average yield bias estimates of 1.59 Mg ha^{-1} for corn and 0.81 Mg ha^{-1} for wheat. With increasing values of DSCI up to the breakpoint indicated by a linear-plateau regression (Section 3.3.4), 146 for corn and 105 for wheat, ALMANAC increasingly underestimated county-average yield when compared to NASS. ALMANAC predominately underestimated county-average yield at DSCI values above the breakpoint, but increasing DSCI was not associated with further changes in ALMANAC yield bias.

3.4.3. 2. Relationships among ALMANAC outputs

Simulated water stress in ALMANAC is the ratio of simulated water use to potential plant water evaporation, summed across all soil layers (Sharpley and Williams, 1990; Williams et al., 1989). Water stress affects crop growth in three ways: reduced progression of LAI development, reduced biomass assimilation, and reduced HI if water stress occurs when 45 to 60% of the maximum potential heat units have accumulated (Section 3.3.1). To further investigate ALMANAC yield biases with varying water stress, annual ALMANAC yield biases were compared to anomalies of ALMANAC-simulated crop available water, water stress days, and HI, with results segregated into groups where DSCI equaled zero (i.e. no water stress), DSCI was between zero and the linear-plateau regression breakpoint (Figure 23), and DSCI was greater than the breakpoint. Anomalies were used to correct for geospatial differences in simulated variables across the study area and were calculated on a county-by-county basis by subtracting annual values from the multiyear average.

In corn and wheat, most counties from 2006 to 2015 featured DSCI between zero and the regression breakpoint. Among these counties, relationships among variables were similar for the two crops, with crop available water and harvest index positively correlated with ALMANAC yield bias, corresponding to a negative correlation between water stress

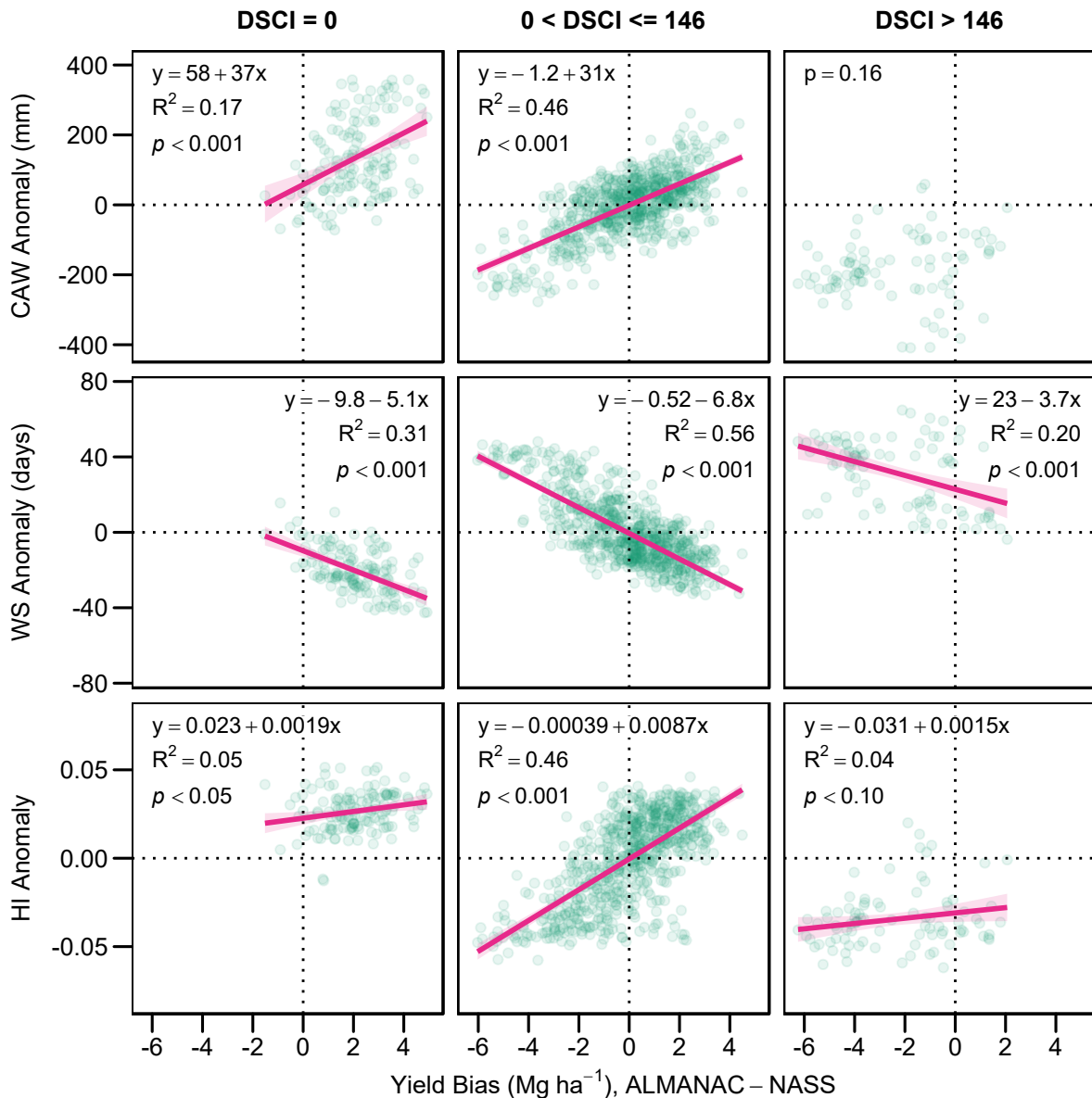


Figure 24. For corn, crop available water (CAW), water stress (WS), and harvest index (HI) anomalies vs. ALMANAC yield bias, grouped by drought severity and coverage index (DSCI; see Figure 23). Each point represents a county-average value for a single year.

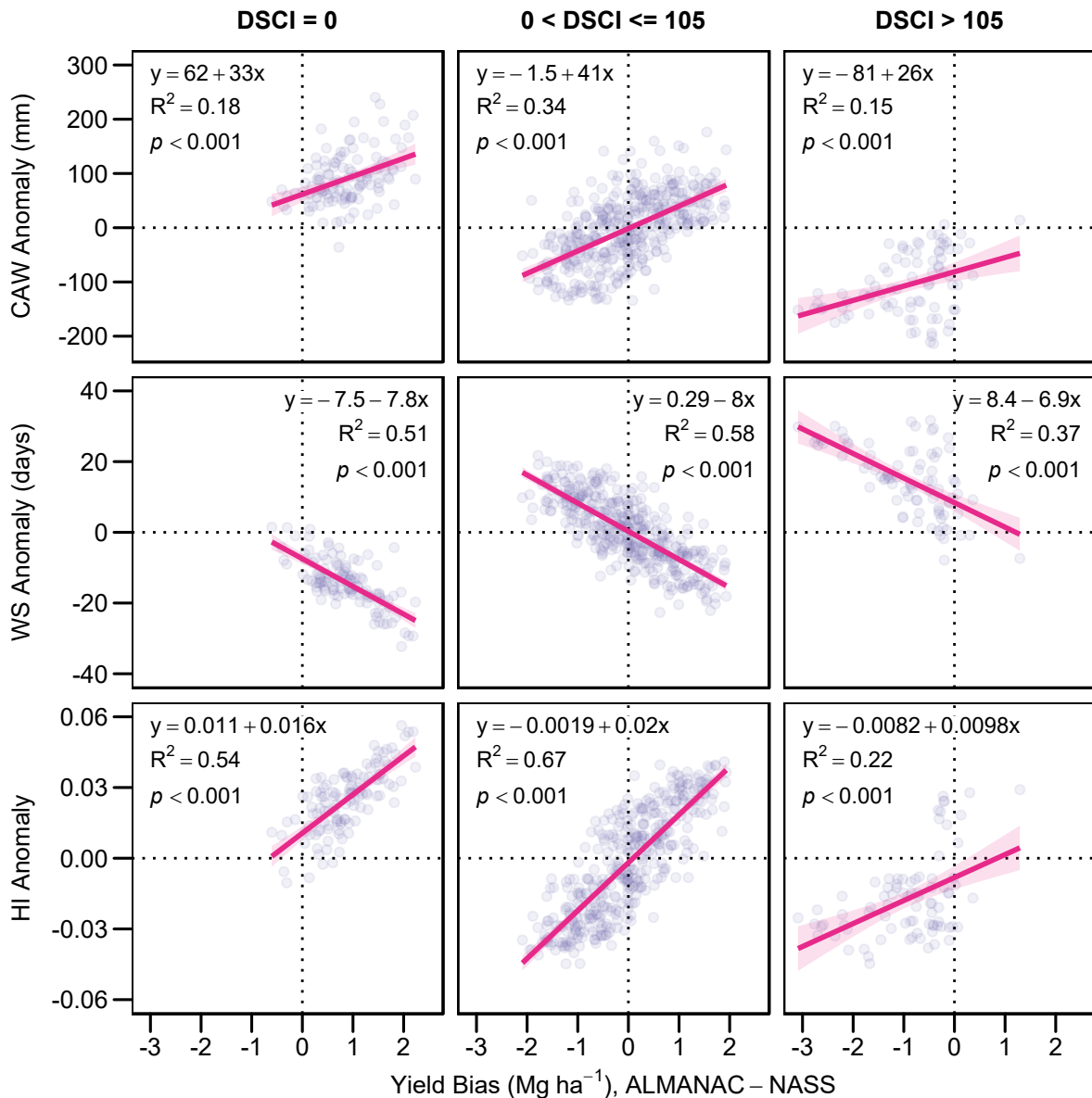


Figure 25. For wheat, crop available water (CAW), water stress (WS), and harvest index (HI) anomalies vs. ALMANAC yield bias, grouped by drought severity and coverage index (DSCI; see Figure 23). Each point represents a county-average value for a single year.

and yield bias (Figures 24 and 25, ' $0 < \text{DSCI} \leq 146$ '). Thus, simulated crop available water is clearly a primary determining factor in the accuracy of ALMANAC-simulated yields within most counties and years: above-average crop available water was strongly associated with positively-biased ALMANAC yield estimates, below-average crop-available water was strongly associated with negatively-biased yield estimates, and these relationships were modulated by the ALMANAC water stress estimation subroutine.

Relationships among these variables were largely similar in counties where DSCI equaled zero, although without a strong influence on harvest index in corn (Figures 24 and 25, ' $\text{DSCI} = 0$ '). Considering the water stress routine of ALMANAC influenced yield estimates in counties where DSCI estimated no soil moisture limitation, and that ALMANAC tends to overestimate county-average yields when soil moisture is not limiting (Figure 23), it seems that ALMANAC is not accurately estimating water stress in these types of environments.

The ALMANAC water stress routine seems to also be active under drought-limited environments where DSCI exceeds 146 in corn and 105 in wheat, as evidenced by negative correlations between water stress and yield bias in these subgroups (Figure 24, ' $\text{DSCI} > 146$ '; Figure 25, ' $\text{DSCI} > 105$ '), but the reduced R^2 values and slopes of these regression relationships suggests that the ALMANAC water stress routine exerts less influence on yield in severely-water limited environments than in environments with little to no water limitation. Finally, the similar relationships between DSCI and ALMANAC yield bias for corn and wheat suggest that the soil water subroutines of ALMANAC are responsible for these outcomes, rather than any crop-specific parameterization. Collectively, these results suggest that improved ALMANAC water stress estimation is necessary for improved year-to-year yield estimation at a regional scale.

3.4.4. Sensitivity analyses

In simulation modeling, sensitivity analyses (SA) indicate how uncertainty in model inputs affects uncertainty in model outputs, and indicates which parameters require the greatest attention when parameterizing the model for future investigations. Sensitivity analyses outlined

in Table 6 demonstrate the relative impacts of ALMANAC parameterization changes on simulated corn and wheat yields.

Distributions of the normalized sensitivity parameter (NSP) are shown in Figure 26. The NSP expresses the magnitude change in simulated yield response as a proportion of the magnitude change of a given parameter. The relative influence of each parameter on simulated yield outcomes is obtained by sorting on the absolute value of the NSP. Since parameterization changes could not be quantified in the SA evaluating crop sequencing and planting/harvest dates, these parameters were excluded from comparisons of the NSP.

Evaluations of simulated yield and water stress outputs provide further insight into the impact of SA parameterization changes on ALMANAC model function. Figures 27 and 29 compare two ALMANAC biases for corn and wheat, respectively: the bias of county-average yield or water stress days from SA comparison parameterizations relative to baseline parameterizations, and the bias of county-average yields from SA baseline parameterizations relative to NASS yields. Baseline parameterizations are identical to the parameterizations of final corn and wheat simulations for all SA except the one examining EXTINC in corn (Table 6), which had a negligible impact on yield and water stress outcomes. Thus, Figures 27 and 29 illustrate how the SA comparison parameterizations would have modulated the annual yield biases of the final corn and wheat parameterizations.

Utilizing parcel-specific yields rather than county-average yields, Figures 28 and 30 evaluate differences in SA responses when classified by calibration area (see Figure 10) and soil quality. To reduce the number of comparisons for these analyses, a qualitative variable was created to simplify the seven LCC used in this study into categorizations of soils as good ('G'), fair ('F'), or poor ('P') for corn and wheat production. Soils with LCC of 1 or 2 have no or slight limitations restricting agricultural use (Soil Survey Staff, 2018) and were assigned 'G'. Soils with LCC of 3 or 4 have severe or very severe limitations restricting agricultural use and were assigned 'F'. Soils with LCC of 5 to 7 are limited primarily to pasture, rangeland, forestland, or wildlife habitat and were assigned 'P'. Even with this simplification, Figures 28

and 30 feature 162 and 108 comparisons, respectively. Thus, minimalist boxplots in the style of Tufte (2001) are used to display these distributions.

3.4.4. 1. Parameters defining maximum productivity – corn

Parameterizing ALMANAC for corn simulations involved the adjustment of two parameters that influence maximum productivity: harvest index (HI) and light extinction coefficient (EXTINC). The maximum productivity of a simulated crop in ALMANAC is determined by its LAI development curve, the efficiency in which leaf area intercepts photosynthetically active radiation as defined by EXTINC, and the efficiency in converting intercepted light into biomass as defined by RUE. Harvest index represents the fraction of simulated biomass that is allocated to grain (Kiniry et al., 1992). Thus, while HI does not influence maximum biomass production, it does influence maximum potential grain yield. In corn, this investigation used the default ALMANAC values for LAI and RUE, and used the default EXTINC for corn with 76 cm row spacing (0.53) in management zones 4 to 6 (Figure 12a). Due to the tendency for growers within the study area to utilize narrower row spacings at higher latitudes due to increased yield potential (Stahl et al., 2009), corn in management zones 1 to 3 was assigned EXTINC for 56 cm row spacings (0.57). The SA for EXTINC contrasted values of 0.53 and 0.57 across the entire study region (Table 6). A maximum HI of 0.56 and minimum limit of HI of 0.48 were used in this investigation, as estimated across 13 growing seasons in east-central Minnesota (Linden et al., 2000), as compared to ALMANAC defaults of 0.53 and 0.30, respectively (Table 6).

With an NSP of 1.00, decreasing harvest index (HI) has the greatest relative impact on corn yield (Figure 26a). Since HI simply represents the fraction of simulated biomass that is allocated to grain, any change in HI results in a proportionate change in grain yield. Thus, since the SA for HI contrasted the lower default value (0.53) against the higher modified value (0.56), a yield decrease was observed in all instances (Figure 27a, 'HI'). However, the minimum limit to HI is only relevant in those environments with water stress during the early reproductive periods of tasseling, silking, pollination, and fertilization (45 to 60% of accumulated seasonal

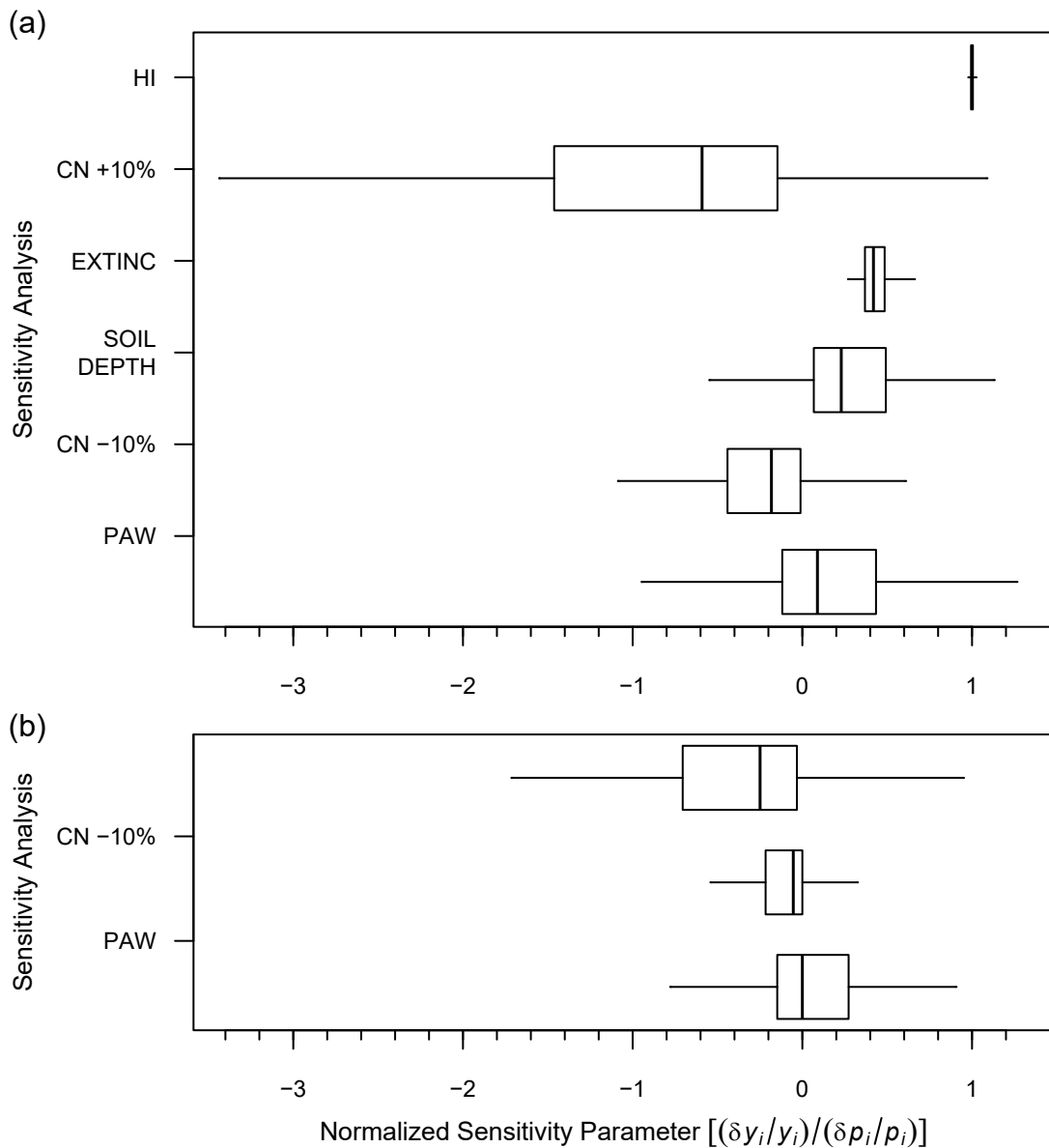


Figure 26. Distributions of the normalized sensitivity parameter for sensitivity analyses (Table 6) across (a) 80,207 corn simulation units and (b) 60,433 wheat simulation units. For clarity, outliers (points extending beyond the whiskers) were omitted. HI = harvest index, CN = runoff curve number, EXTINC = light extinction coefficient, PAW = plant-available water.

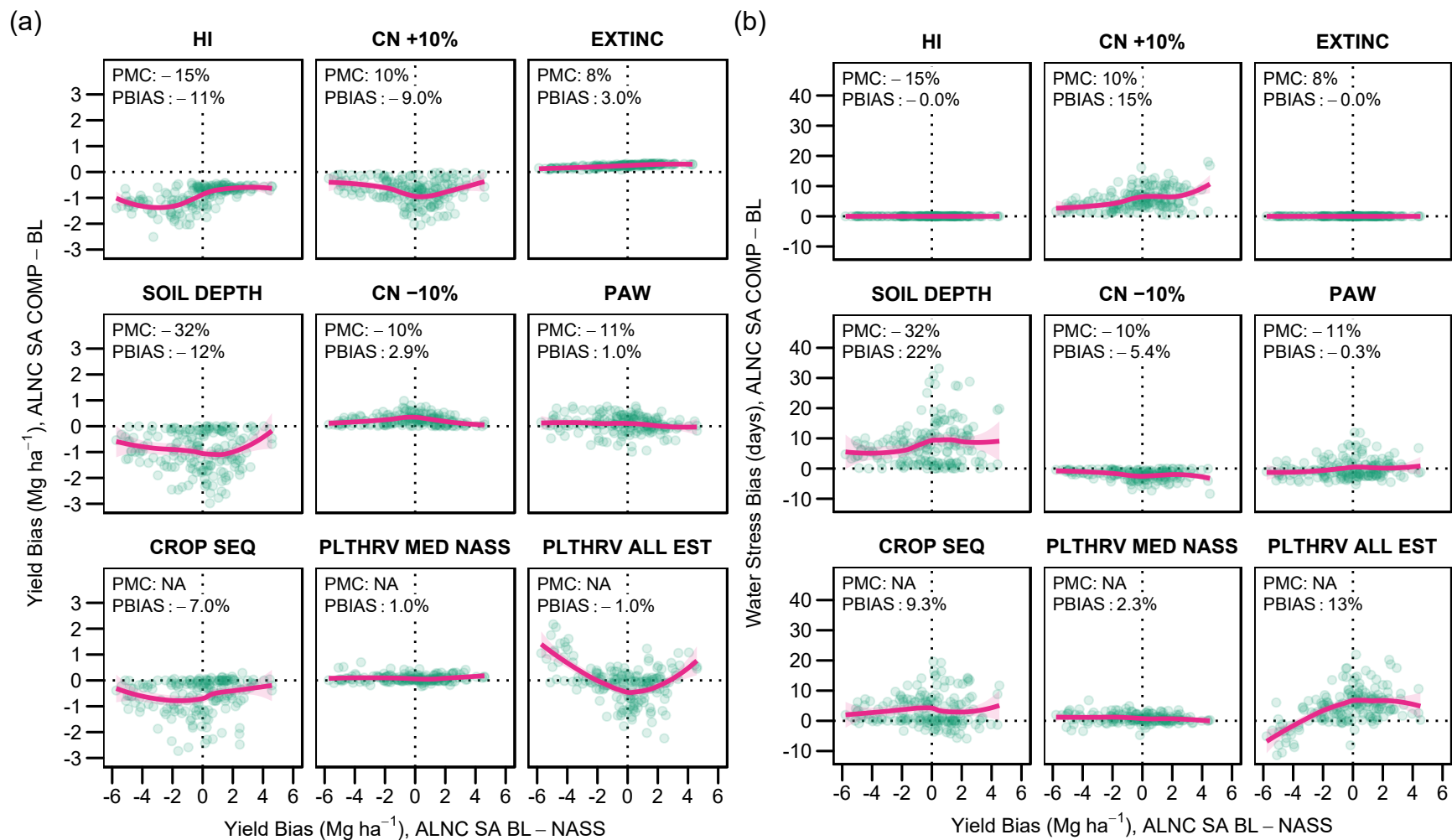


Figure 27. For corn, (a) Yield bias and (b) water stress bias of ALMANAC sensitivity analysis (ALNC SA) comparison parameterization (COMP) minus baseline parameterization (BL) (see Table 6) vs. yield bias of ALMANAC sensitivity analysis baseline parameterization minus USDA NASS. Each point represents a county-average value. HI = harvest index, CN = runoff curve number, EXTINC = light extinction coefficient, PAW = plant-available water, CROP SEQ = crop sequencing, PLTHRV MED NASS = median NASS planting and harvest dates, PLTHRV ALL EST = all estimated planting and harvest dates. PMC = parameter mean change, PBIAS = percent mean bias.

heat units; Xie et al., 2001). In the ‘HI’ SA, decreasing the minimum limit of HI from 0.48 to 0.30 resulted in even worse yield estimations in the water-limited situations where the final corn parameterization underestimated county-average yields, with further grain yield decreases of 1 Mg ha⁻¹ or greater (Figure 27a, ‘HI’). In contrast, reducing the maximum HI from 0.56 to 0.53 would have reduced estimated yields by up to 1 Mg ha⁻¹ in those environments where water was not limiting and the final corn parameterization overestimated county-average yields by up to 5 Mg ha⁻¹. Thus, it appears that increasing the minimum limit of HI was justified in this investigation, while increasing the maximum HI may not have been.

Due to a low-magnitude parameter value change (from 0.53 to 0.57), increasing EXTINC had the next largest relative impact on yield outcomes (median NSP = 0.42; Figure 26a). However, the absolute change in yield estimation was minimal, as increasing EXTINC from 0.53 to 0.57 increased yield by an average of only 3.0% (Figure 27a, ‘EXTINC’). In this investigation, EXTINC varied across corn management zones (Figure 12a). When evaluating its SA across calibration areas spanning these zones (Figure 10a), there is no discernible pattern from one calibration area to another (Figure 28, ‘EXTINC’). Thus, it seems that varying EXTINC across space was unnecessary for accurate yield estimation.

3.4.4. 2. Parameters defining environmental responses – corn

All other modifications for corn simulations (CN+10%, CN-10%, SOIL DEPTH, PAW, CROP SEQ, PLTHRV MED NASS, PLTHRV ALL EST) involved changes to crop or management parameters influencing crop response to environmental conditions. Considering that soil moisture status was the predominant environmental factor influencing the accuracy of corn simulations (Section 3.4.3), the outcomes of these sensitivity analyses are evaluated based on yield and water stress responses.

With an NSP of 0.23, decreasing soil depth was ranked fourth out of six parameters in the relative sensitivity analysis for corn (Figure 26a). In absolute terms, the SA decreasing soil depth from the modified values to SSURGO defaults (Table 6) resulted in the largest average yield change of any SA (-12%; Figure 27a, ‘SOIL DEPTH’). This was accompanied by a 22%

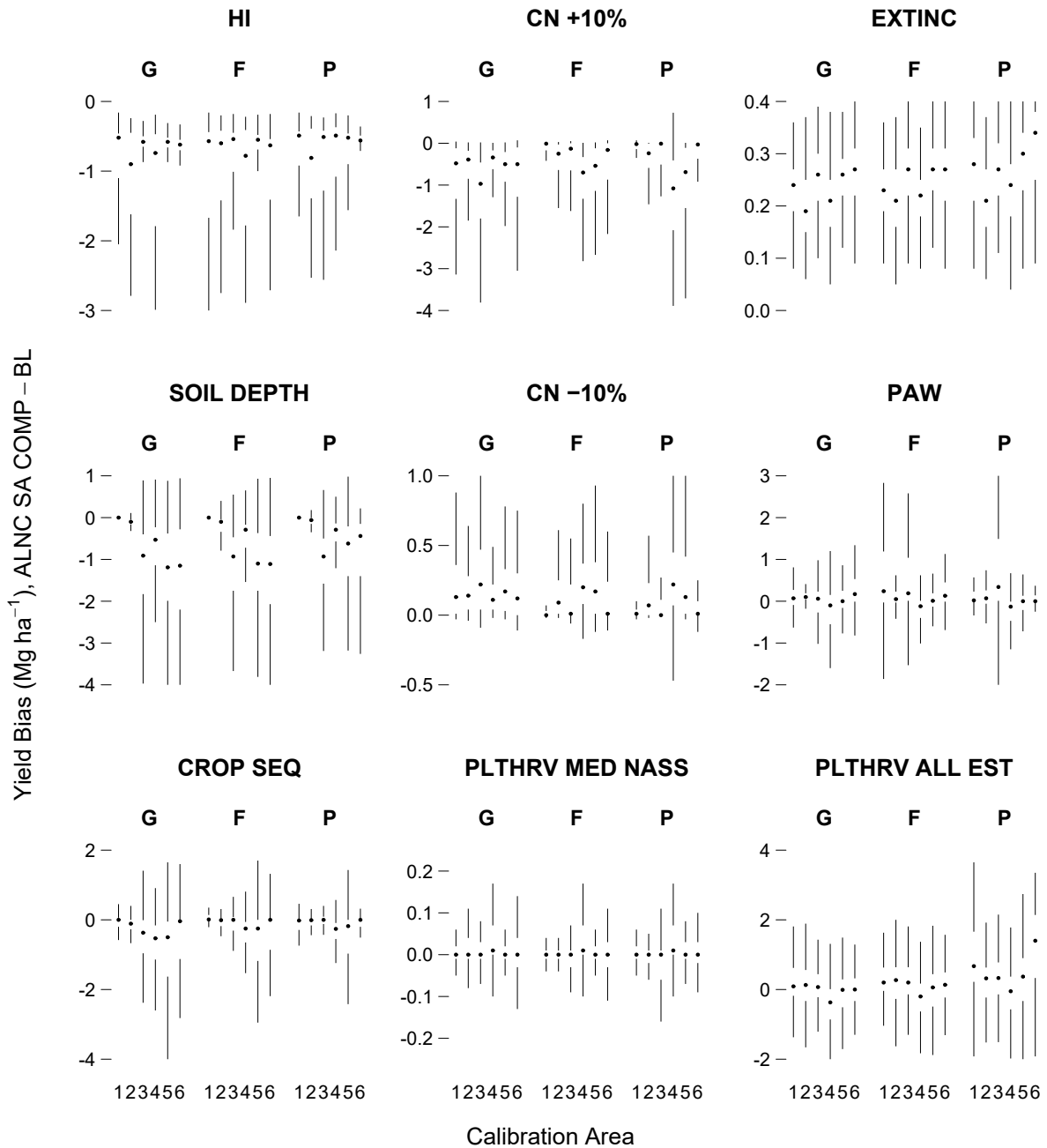


Figure 28. For 80,207 corn simulation units, yield bias distributions for ALMANAC sensitivity analysis (ALNC SA) comparison parameterization (COMP) minus baseline parameterization (BL; see Table 6), grouped by land suitability for cropping (G = good, F = fair, P = poor) and calibration area (see Figure 10). In these box and whisker plots, a dot represents the median, vertical lines represent the whiskers, and the gap between lines represents the interquartile range. For clarity, outliers (points extending beyond the whiskers) were omitted. HI = harvest index, CN = runoff curve number, EXTINC = light extinction coefficient, PAW = plant-available water, CROP SEQ = crop sequencing, PLTHRV MED NASS = median NASS planting and harvest dates, PLTHRV ALL EST = all estimated planting and harvest dates.

increase in water stress on average (Figure 27b, 'SOIL DEPTH'), as the shallower soil offered less water-holding capacity to support corn growth. The effect of modifying crop sequencing seemed to have a similar effect as modifying soil depth, albeit to a lesser magnitude. For 2006 to 2015 weather conditions, the SA for crop sequencing compared the results of 10 separate simulations with one soybean spinup year each to simulations encompassing the entire 10-year corn-soybean rotation (Table 6). This resulted in an average yield decrease of 7.0% (Figure 27a, 'CROP SEQ') and an average water stress increase of 9.3% (Figure 27b, 'CROP SEQ').

When evaluating SA outcomes by calibration area and land use capability, simulated corn yield was especially sensitive to soil depth and crop sequencing parameterization changes in the central and southern portions of the study region. Calibration areas 1 and 2 (Figure 10a) are located within corn management zone 1 (Figure 12a), where the default soil depths from SSURGO (most often 1.52 m) were extended to a uniform depth of 2.0 m (Section 3.3.2). Within these areas, sensitivity analyses decreasing soil depth from 2.0 m to SSURGO defaults had minimal impact on simulated yield, resulting in median changes near 0 Mg ha⁻¹ and narrow distributions of yield change values around the medians (Figure 28, 'SOIL DEPTH'). Similarly, simulating corn growth within a 10-year corn-soybean rotation had a minimal impact on yield outcomes in calibration areas 1 and 2 (Figure 28, 'CROP SEQ'). In contrast, calibration areas 3 to 6 (Figure 10a) are located within corn management zones 2 to 5 (Figure 12a), where the default soil depths from SSURGO were extended to a uniform depth of 2.7 m (Section 3.3.2). Within these areas, sensitivity analyses decreasing soil depth from 2.7 m to SSURGO defaults resulted in median yield decreases of 1 Mg ha⁻¹ in several instances, and yield decreases as large as 3 to 4 Mg ha⁻¹ within individual parcels (Figure 28, 'SOIL DEPTH'). Similarly, parcels in calibration areas 3 to 6 exhibited a greater range in yield responses due to crop sequencing changes (Figure 28, 'CROP SEQ'), especially in soils classified as 'G' or 'F' for cropping suitability (i.e. LCC of 1 to 4); although median yield changes in response to crop sequencing changes were modest, individual parcels exhibited yield decreases as large as 2 to 4 Mg ha⁻¹.

Setting soil depth to 2.7 m clearly increased final corn yield estimates throughout the southern portions of the study region, due to reduced water stress in response to the increased water holding capacity of a deeper soil. Parameterization of crop sequencing is also an important consideration in these areas, as a continuous 10-year rotation in areas of increased soil depth oftentimes resulted in yield decreases. When considering the increased water stress associated with this altered crop sequencing (Figure 27b, 'CROP SEQ'), it appears that corn simulations in soils 2.7 m deep oftentimes caused soil water depletion that could not be fully replenished by precipitation in subsequent years, thereby resulting in increased water stress and decreased yields in subsequent corn simulations. Parameterizing corn simulations with a single model spinup year of soybean production avoided this outcome.

Second only to HI, the SA increasing runoff curve number (CN) had the next greatest impact on yield, as the distribution of NSP values from the 'CN+10%' SA has a median of -0.59 and a skew to values less than -3 (Figure 26a). Decreasing CN (CN-10%) had a more modest impact on simulated yields, with a median NSP of -0.18 . In absolute terms, increasing CN by 10% resulted in an average yield decrease of 9.0% due to an average water stress increase of 15% (Figure 27a,b 'CN+10%'). In contrast, decreasing CN by 10% resulted in an average yield increase of 2.9% due to an average water stress decrease of 5.4% (Figure 27a,b 'CN-10%'). A unitless empirical parameter ranging from 0 to 100 (Cronshey et al., 1986), CN partitions water between infiltration and runoff following precipitation events. Increasing CN results in increased runoff, while decreasing CN results in increased infiltration. In the water-limited environments of the study region, modifying CN to increase runoff had a three-fold greater impact on yield and water stress than did modifying CN to increase infiltration. Since the 'CN+10%' SA featured values similar to the default values of CN within ALMANAC (Table 6), CN adjustments for this investigation had a meaningful impact on final yield estimates.

In contrast to adjusting soil depth and crop sequencing or increasing CN, the method for estimating plant-available water-holding capacity of study area soils had minimal impact

on estimations of yield and water stress. The SA using SSURGO values instead of those according to the methods of Saxton and Rawls (2006) affected yield by just 1% on average and water stress by just 0.3% on average (Figure 27a,b 'PAW'). Although yield biases ranging from -2 to 3 Mg ha^{-1} are observed when evaluating outcomes by land suitability and calibration area, the distributions of yield biases are centered around a median of zero with no discernible patterns across calibration areas (Figure 28, 'PAW'). Thus, it appears that SSURGO values of plant-available water-holding capacity would have been suitable for accurate yield estimation across the study region.

Finally, the methodology for estimating spatially-explicit planting and harvest dates was tested in two SA. As described in Section 3.3.3, each simulation unit was assigned the most prevalent planting-harvest date pair among all estimated options (e.g. Figure 11c). This methodology was tested against a simplification of planting and harvest dates, where all simulation units were assigned the median statewide dates according to USDA NASS, and a methodology with increased complexity where county-average yields were calculated on the weighted average of yield simulations under all estimated date-pair combinations. Simplifying the estimation of planting and harvesting dates had a negligible impact on overall yield and water stress (Figure 27a,b 'PLTHRV MED NASS') and resulted in no discernible differences in yield estimation across calibration areas and land use capabilities (Figure 28, 'PLTHRV MED NASS'), suggesting that use of spatially-explicit planting and harvest dates did not improve the accuracy of the final corn parameterization. In contrast, using the weighted average of yield simulations under all estimated date-pair combinations had a modest impact on yield estimates (Figure 27a, 'PLTHRV ALL EST'). In situations where the final corn parameterization underestimated NASS yields by 4 to 6 Mg ha^{-1} , this method increased ALMANAC yield estimates by 0.5 to 2 Mg ha^{-1} . Similarly, this method decreased several county-average yield estimates by 1 to 2.5 Mg ha^{-1} where the final corn parameterization overestimated yield by 1 to 3 Mg ha^{-1} . However, this method oftentimes resulted in a negative yield bias where the final parameterization resulted in little or no yield bias, and

generally resulted in yield changes symmetrical around a median near zero when examined by calibration area and land suitability (Figure 28, 'PLTHRV ALL EST'). When also considering that this method greatly increases the number of simulations to be conducted, as all estimated planting and harvest date-pair combinations would be simulated, there is no strong evidence for recommending this practice in future regional yield simulations.

3.4.4. 3. Parameters defining environmental responses – wheat

With the exception of soil depth, which was not modified from default SSURGO values in the final wheat parameterization (Section 3.3.2), the same parameters responsible for determining corn response to environmental conditions were also tested in wheat.

Adjusting CN had the largest impact of any tested parameters, but the impacts of adjusting CN were modest relative to corn. Increasing CN had the greatest relative impact on yield, with a median NSP of -0.25 for the 'CN+' SA (Figure 26b). In absolute terms, increasing CN decreased yield by 5.2% on average (Figure 29a, 'CN+10%') due to an increase in simulated water stress of 10% on average (Figure 29b, 'CN+10%'). When compared to corresponding corn values of 9.0% for yield and 15% for water stress (Figure 27a,b 'CN+10%'), it is clear that wheat yield estimation was less sensitive to increased runoff than was corn yield estimation. Similar to corn, increasing infiltration resulted in modest wheat yield and water stress effects (Figure 29a,b 'CN -10%') relative to the effects of increasing runoff (Figure 29a,b 'CN+10%').

Similar to corn, utilizing SSURGO estimates of soil PAW instead of Saxton and Rawls (2006) estimates resulted in minimal yield bias; the NSP was 0.00 (Figure 26b), the average yield increase was 0.4% (Figure 29a, 'PAW'), and the average water stress decrease was 1.8% (Figure 29b, 'PAW'). Nonetheless, yield decreases of 0.5 to 1 Mg ha⁻¹ were observed in some situations where the final wheat parameterization overestimated yield by 0.5 to 2 Mg ha⁻¹ (Figure 29a, 'PAW'). Also similar to corn, assigning the median statewide planting and harvest dates from USDA NASS resulted in a negligible impact on county-average yield (Figure 29a, 'PLTHRV MED NASS') and water stress (Figure 29b, 'PLTHRV MED NASS') estimation, as

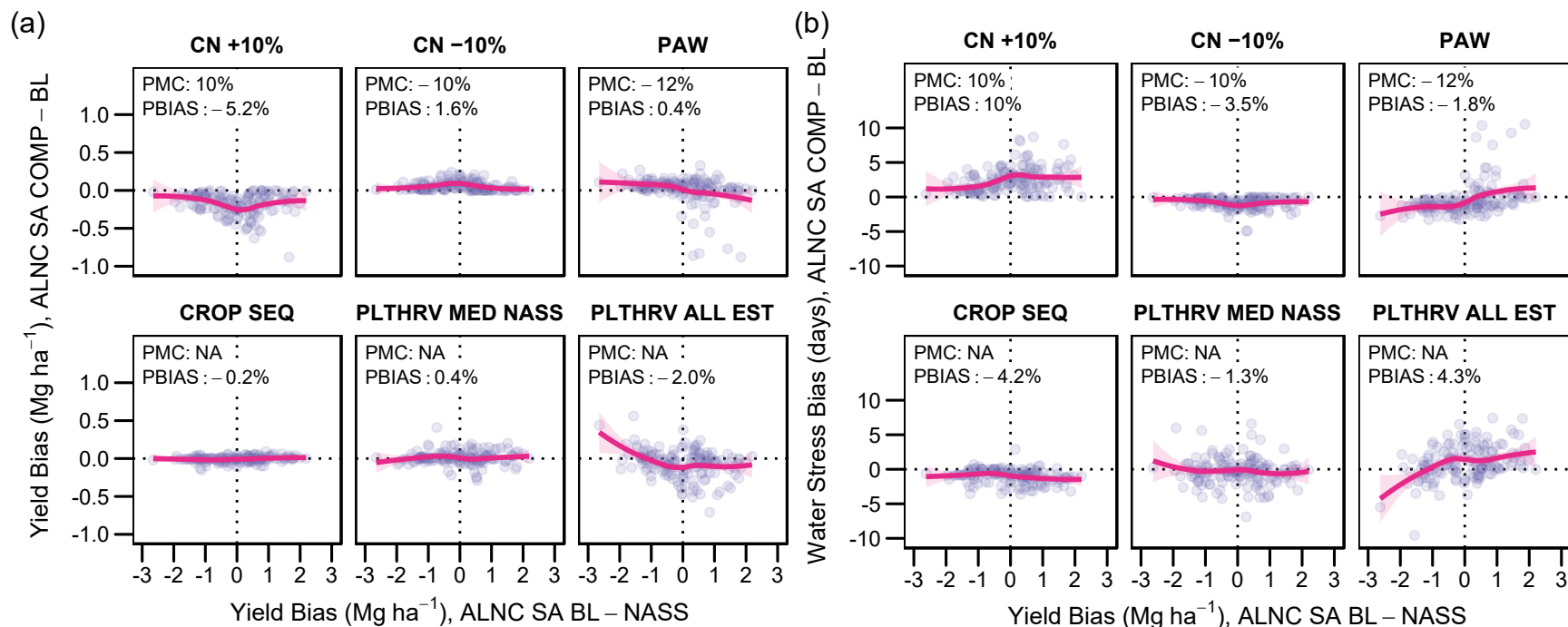


Figure 29. For wheat, (a) Yield bias and (b) water stress bias of ALMANAC sensitivity analysis (ALNC SA) comparison parameterization (COMP) minus baseline parameterization (BL; see Table 6) vs. yield bias of ALMANAC sensitivity analysis baseline parameterization minus USDA NASS. Each point represents a county-average value. CN = runoff curve number, PAW = plant-available water, CROP SEQ = crop sequencing, PLTHRV MED NASS = median NASS planting and harvest dates, PLTHRV ALL EST = all estimated planting and harvest dates. PMC = parameter mean change, PBIAS = percent mean bias.

did using the weighted average of yield simulations for all estimated planting and harvest date-pair combinations (Figure 29a,b, 'PLTHRV ALL EST'). When considering that distributions of planting and harvest date SA yields also exhibited narrow distributions surrounding a median near zero when aggregated by calibration area and land suitability (Figure 30, 'PLTHRV MED NASS' and 'PLTHRV ALL EST'), it seems that the estimation of spatially-explicit planting and harvest dates is unnecessary for accurate county-average wheat yield estimation.

Finally, unlike with corn, simulating wheat growth within a 10-year rotation with soybean did not have a considerable impact on yield and water stress estimation, neither for county-average estimates (Figure 29, 'CROP SEQ') nor when aggregated by calibration area and land suitability (Figure 30, 'CROP SEQ'). This suggests that ALMANAC is not particularly sensitive to crop sequencing by itself, but rather to the impacts of crop sequencing on soil moisture status over the duration of the simulated time period.

3.4.5. Improving ALMANAC estimates

For non-irrigated corn in soils representative of nine counties in Texas, Xie et al. (2003) found that yield estimation was most sensitive to CN and rainfall, and recommended that accurate CN, rainfall, and soil depth are critical for accurate yield simulations. The analyses presented herein generally support these conclusions. Other than altering HI in corn, sensitivity analyses that increased CN had a greater relative impact on simulated yield outcomes than modifications of any other parameter. Furthermore, differential responses to increased or decreased CN in both corn and wheat illustrate the water-limited nature of corn and wheat production in the rainfed environments of the study region. A unitless empirical parameter ranging from 0 to 100 (Cronshey et al., 1986), CN partitions water between infiltration and runoff following precipitation events, with increasing CN values resulting in increased runoff. For both corn and wheat, simulated yield was much more sensitive to increased CN (i.e. increased runoff) than decreased CN (i.e. increased infiltration). Finally, the results of corn sensitivity analyses indicate that the other parameterization changes resulting in the largest decreases in simulated yield (decreased minimum limit of HI, decreased soil depth, crop

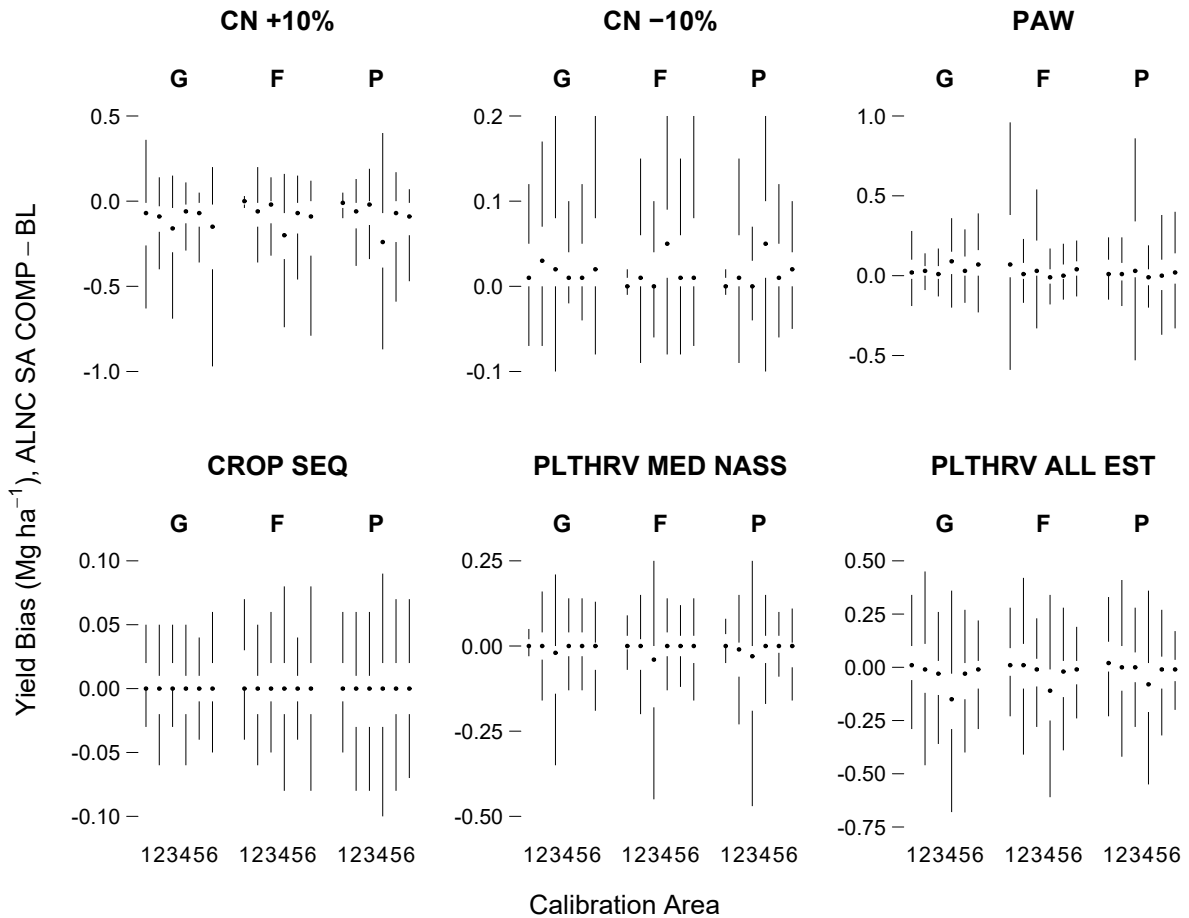


Figure 30. For 60,433 wheat simulation units, yield bias distributions for ALMANAC sensitivity analysis (ALNC SA) comparison parameterization (COMP) minus baseline parameterization (BL; see Table 6), grouped by land suitability for cropping (G = good, F = fair, P = poor) and calibration area (see Figure 10). In these box and whisker plots, a dot represents the median, vertical lines represent the whiskers, and the gap between lines represents the interquartile range. For clarity, outliers (points extending beyond the whiskers) were omitted. CN = runoff curve number, PAW = plant-available water, CROP SEQ = crop sequencing, PLTHRV MED NASS = median NASS planting and harvest dates, PLTHRV ALL EST = all estimated planting and harvest dates.

sequencing within a 10-year rotation with soybean) were associated with increases in simulated water stress.

Results presented in Figures 23 to 25 suggest that improving the agreement of ALMANAC-simulated water stress with real-world water stress indices, such as the US Drought Monitor, should result in improved accuracy of regional yield simulations. While modifications of CN and soil depth may improve the agreement between simulated soil moisture and real-world conditions, several other ALMANAC parameters influence the simulated crop response to moisture stress. Through its inclusion in the Penman-Monteith equation (Allen et al., 1998), stomatal conductance is one of the factors influencing simulated evapotranspiration in ALMANAC. Stomatal conductance in ALMANAC is insensitive to atmospheric vapor pressure deficit until reaching a threshold value specified by the user (VPTH), after which stomatal conductance can increase up to a user-specified maximum (GSI). Simulated stomatal conductance may therefore have a significant effect on simulated plant water use and subsequent yield; for example, GSI modifications had one of the largest relative impacts on simulated yield for the modified switchgrass parameterization presented in Chapter II (Figure 8). In addition to evapotranspiration impacts, ALMANAC modifies simulated radiation use efficiency as a function of vapor pressure deficit. At vapor pressure deficits exceeding VPTH, radiation use-efficiency declines according to a user-specified slope (VPD2) of the relationship between radiation use efficiency and vapor pressure deficit (Kiniry et al., 1998; Stockle and Kiniry, 1990). Characterizing this relationship is critical for accurate yield estimation under water-limited conditions, and the nature of this relationship has been subject to debate (Kiniry, 1999; Sinclair and Muchow, 1999a).

Results presented in Figure 23 also suggest that ALMANAC overestimates corn and wheat yields in environments without soil moisture limitations (i.e. where DSCI = 0). Thus, modifications of parameters defining the maximum productivity of corn and wheat would also be necessary to realize improved ALMANAC yield estimation. In ALMANAC, maximum crop productivity is determined by maximum radiation use efficiency under nonstress conditions

(RUE), maximum potential LAI (DMLA), the shape of the LAI development curve (defined by DLAI, DLAP1, DLAP2, and RLAD), and the rate of decline for radiation use efficiency at the end of the growing season (RBMD). An example of the impacts associated with modifications of these parameters is presented in the modified switchgrass parameterization of Chapter II, as modified RUE and LAI had some of the largest relative impacts on simulated yield among all parameterization changes (Figure 8).

Efforts to improve ALMANAC parameterizations of corn and wheat would require detailed measurements of crop growth under field conditions. Alternatively, improved regional-scale yield estimation may be realized by incorporating remote sensing estimates of plant-soil dynamics, such as soil moisture, LAI, and vegetation indices (e.g. NDVI), into ALMANAC model simulations. Assimilation of remote sensing data into crop models has been an area of active research since the 1970s (Dorigo et al., 2007; Fischer et al., 1997; Jin et al., 2018; Moulin et al., 1998), with at least one example specific to ALMANAC in the literature. After defining the relationship between field-measured fraction of photosynthetically active radiation intercepted by plants (FIPAR) and NDVI measurements from the advanced very high-resolution radiometer (AVHRR) sensor onboard the NOAA-14 satellite, Kiniry et al. (2004) used NDVI to replace daily FIPAR values simulated by ALMANAC. In two of three counties, the biases of resulting yield estimations were reduced from 1.16 and 2.06 Mg ha⁻¹ to 0.28 and 1.57 Mg ha⁻¹. Similar efforts with the EPIC and CERES-Maize (Crop Environment Resource Synthesis-Maize) models have integrated satellite-measured NDVI (Doraiswamy et al., 2003), LAI (Fang et al., 2008), or LAI and NDVI (Fang et al., 2011) to improve the accuracy of corn yield estimation. When integrated into the CERES-Maize, WOFOST (World Food Studies), and DSSAT (Decision Support System for Agrotechnology Transfer) CROPGRO models, soil moisture estimates from satellite microwave sensors have resulted in improved wheat (de Wit and van Diepen, 2007), corn (Ines et al., 2013), and soybean (Chakrabarti et al., 2014) yield estimations, particularly in years with limited rainfall. Within these investigations, remote sensing inputs characterizing vegetative characteristics featured spatial resolutions of 30 m to

1 km (Doraiswamy et al., 2003; Fang et al., 2008, 2011; Kiniry et al., 2004). Soil moisture products featured spatial resolutions of 25 or 50 km (Chakrabarti et al., 2014; de Wit and van Diepen, 2007; Ines et al., 2013), but were downscaled to 1 km by Chakrabarti et al. (2014). Thus, these approaches are suitable for regional-scale estimates at a resolution similar to the current study, where outputs were aggregated to approximately 800 m resolution and simulation units were defined by the intersection of SSURGO soil polygons and a climate grid with approximately 4 km resolution.

3.5. Conclusions

A summary of findings is presented in Table 9. At the county scale, ALMANAC successfully estimated multiyear-average corn and wheat yields across the prevailing production areas of the eastern Dakotas and western Minnesota (Section 3.4.1). However, annual yield estimates were much less precise than multiyear-average estimates. Compared to a relative productivity index provided by SSURGO (CPI), relative productivity indices developed from simulated corn (CNPI) and wheat (WTPI) yields showed similar distributions across parcels featuring corn or wheat production from 2006 to 2015 (Section 3.4.2). This indicated that ALMANAC provided a reasonable estimate of within-county yield variability for these production parcels. However, CNPI and WTPI values were much higher than CPI values for nonproduction parcels, indicating that ALMANAC appears to overestimate yields in soils that are typically considered unsuitable for cropping. Soil moisture status was the primary factor influencing the accuracy of annual ALMANAC yield simulations, as ALMANAC overestimated yield in years with adequate soil moisture and underestimated yield in years with soil moisture limitations (Section 3.4.3). In corn, increasing soil depths to 2.7 m in the southern study region, simulating corn with only one soybean spinup year, increasing the minimum limit of HI from 0.30 to 0.48, and decreasing CN were necessary to increase soil moisture storage, minimize water stress, and improve grain yield estimation in water-stressed environments (Section 3.4.4). In contrast, wheat yield and moisture stress estimation was less sensitive to adjustments in CN. In corn and wheat, estimating spatially-explicit planting and harvest

dates did not improve the accuracy of yield estimation, nor did using the methods of Saxton and Rawls (2006) to estimate plant-available water holding capacity of study region soils. In summary, this investigation demonstrated success in generating multiyear-average regional-scale yield estimates at moderate spatial resolution, as needed for the comparative feasibility analysis presented in Chapter IV. Nonetheless, ALMANAC users should exercise caution when generating annual yield estimates or yield estimates in parcels generally considered unsuitable for cropping.

Table 9. Summary of findings from Chapter III results (Section 3.4).

Section	Finding
3.4.1	<p>ALMANAC approximated the spatial pattern of county-average corn yields across the study region (IOA = 0.93, RMSE = 0.71 Mg ha⁻¹, PBIAS = 1.9%)</p> <p>ALMANAC approximated the spatial pattern of county-average wheat yields across the study region, but only when removing 19 southernmost counties with positively-biased yields (IOA = 0.85, RMSE = 0.28 Mg ha⁻¹, PBIAS = 2.8%)</p> <p>annual yield estimates were less precise than multiyear average estimates, with 200% greater RMSE in corn (2.13 vs. 0.71 Mg ha⁻¹) and 246% greater RMSE in wheat (0.97 vs. 0.28 Mg ha⁻¹)</p>
3.4.2	<p>across parcels highly suitable for cultivated cropping (LCC of 1 to 3), ALMANAC approximated within-county yield variability in corn and wheat</p> <p>across parcels less suitable for cultivated cropping (LCC of 4 to 7), ALMANAC generally overestimated corn and wheat yields</p>
3.4.3	<p>ALMANAC overestimated county-average corn yield and wheat yield when soil moisture was not limiting (Drought Severity Coverage Index [DSCI] = 0)</p> <p>ALMANAC underestimated county-average corn yield in moisture-limited conditions (DSCI ≥ 146 in corn, DSCI ≥ 105 in wheat)</p>
3.4.4	<p>in corn, increasing the minimum limit of HI (harvest index) from 0.30 to 0.48 was necessary to improve grain yield estimation in water-limited environments</p> <p>in corn, increasing soil depths to 2.7 m in the southern study region, simulating corn with only one soybean spinup year, and decreasing runoff curve number (CN) were necessary to increase soil moisture storage and minimize water stress</p> <p>changes in wheat yield and water stress estimation in response to altered CN were of 30 to 50% lesser magnitude than comparative corn responses</p>

Table 9. cont.

Section	Finding
---------	---------

	the accuracy of yield estimation was not improved by methodologies for (i) estimating spatially-explicit planting and harvest dates and (ii) estimating plant-available water holding capacity of study region soils
--	--

CHAPTER IV

BIOMASS AVAILABILITY IN THE EASTERN DAKOTAS AND WESTERN MINNESOTA: FEASIBILITY AND BENEFITS OF SUBSTITUTING SWITCHGRASS FOR EXISTING CORN AND WHEAT RESOURCES

4.1. Abstract

Despite the delayed development of a commercial industry, the production of cellulosic biofuels remains a goal of US federal renewable energy policy. For a 99-county area of the eastern Dakotas and western Minnesota with a dynamic history of land-use conversions between grasslands and agriculture, this investigation quantifies the existing resource base of corn (*Zea mays* L.) and wheat (*Triticum aestivum* L. ssp. *aestivum*) biomass and evaluates the technical, economic, and environmental impacts of switchgrass (*Panicum virgatum* L.) production on existing corn and wheat lands. Yields, revenue, expenses, soil erosion, nitrogen runoff, and soil carbon sequestration of corn, wheat, and switchgrass systems were estimated at approximately 800 m spatial resolution. Cellulosic biorefineries utilizing corn and wheat biomass are feasible only within 90 km of the Minnesota-Dakotas border under conventional tillage, but reduced tillage and no-till systems allow suitable biomass harvest across most of the study region. Biomass prices of \$30 to \$60 Mg⁻¹ would allow corn and wheat residue harvest in quantities sufficient to support biorefineries, but switchgrass requires biomass prices of \$100 to \$180 Mg⁻¹ to be economically competitive with corn or wheat. Annual subsidies of \$120 to \$230 million would be necessary to convert 410,000 ha of existing corn or wheat parcels to switchgrass production. Prioritizing parcels where switchgrass provides the greatest environmental benefit relative to corn or wheat, as opposed to the greatest increase in biomass yield, would increase resulting soil retention, N retention, and soil C sequestration by up to 420%, 210%, and 120%, respectively.

4.2. Introduction

The modern era of US biofuel production began with the Energy Policy Act of 2005. This act established the Renewable Fuel Standard, which mandated that US transportation fuels contain a minimum of 15 GL biofuel in 2006 and 28 GL biofuel by 2012 (Tyner, 2008). Biofuel usage requirements were expanded in the Energy Independence and Security Act of 2007, as the second Renewable Fuel Standard (RFS2) mandated the use of 34 GL in 2008 and 136 GL by 2022 (Bracmort, 2019a). These government mandates for biofuel use, coupled with rising oil prices in the 2000s, spurred rapid growth in domestic biofuel production (Tyner, 2008). Corn (*Zea mays* L.) grain ethanol currently dominates the U.S. biofuels industry, representing 84% of the 56 GL of biofuel produced between January and October 2018 (US EPA, 2019). Production of this first-generation biofuel has essentially been a mature industry since 2011, as production volumes met or exceeded RFS2 usage limits of 48, 52, 53, and 55 GL in 2011, 2014, 2015, and 2016, respectively, and were within 2%, 5%, and 1% of respective RFS2 limits for 2012, 2013, and 2017 (Bracmort, 2019a; US EPA, 2019). As mandated by RFS2, corn grain ethanol use has been capped at 57 GL since 2016 and will remain capped at this level through 2022 (Bracmort, 2019a).

By requiring cellulosic biofuel usage of 380 ML in 2010 and 61 GL by 2022 (Bracmort, 2019a), RFS2 was intended to encourage a transition from first-generation corn ethanol to second-generation cellulosic biofuels. However, the US cellulosic biofuel industry has developed slowly. There were no commercial-scale ($\geq 76 \text{ ML yr}^{-1}$) cellulosic biofuel facilities through 2013, but nine projects employing six different processing pathways were expected to be operational by 2014 (Brown and Brown, 2013). Five of the nine projects were never built (US NREL, 2019), with two of the companies involved declaring bankruptcy (Fehrenbacher, 2015; Lane, 2017), while one of the completed facilities is operational only as a 946,000 L yr⁻¹ pilot-scale ethanol plant (US NREL, 2019). Thus, just three commercial-scale plants were constructed. Abengoa opened a 95 ML yr⁻¹ cellulosic ethanol plant in Hugoton, KS in October 2014, using corn stover as a feedstock, before closing the plant in December 2015

(Aust, 2015; US DOE, 2014). The facility was sold out of bankruptcy in December 2016 (Voorhis, 2016), with no announced plans for its future operation as of May 2018 (Crooks, 2018). DuPont opened a 114 ML yr⁻¹ cellulosic ethanol plant in Nevada, IA in October 2015, using corn stover as a feedstock, before closing the facility in November 2017 (DuPont, 2015; Eller, 2017). The plant and a portion of DuPont's corn stover inventory were sold to German bioenergy producer VERBIO in November 2018, who by summer 2020 plan to produce compressed biomethane as transportation fuel using corn stover and other cellulosic materials as feedstocks (Maniatis et al., 2017; VERBIO, 2018). POET-DSM has been operating a 76 ML yr⁻¹ cellulosic ethanol biorefinery in Emmetsburg, IA since September 2014, using corn cobs as a feedstock (POET-DSM, 2014). Although this facility neared its conversion goal of 300 L Mg⁻¹ in 2017 (Sapp, 2017), and subsequently implemented an improved enzymatic pretreatment process (POET-DSM, 2017), it has yet to reach its nameplate capacity.

As a result of the delayed commercialization of cellulosic biofuel production, the US Environmental Protection Agency has used its waiver authority to reduce usage requirements throughout the entire tenure of RFS2 (Bracmort, 2019b). Relative to initial RFS2 requirements ranging from 380 ML in 2010 to 21 GL in 2017, revised requirements were 25 ML in 2010 and 1.2 GL in 2017. Actual production volumes have fallen short of these revised mandates, ranging from nil in 2010 to 33 ML in 2014 and 251 ML in 2017 (US EPA, 2019). Although biofuel production volumes have accelerated recently, only 38 ML of cellulosic ethanol was produced in 2017; the remaining 213 ML represents landfill gas compressed or liquefied for use as transportation fuel (Retka Schill, 2018; US EPA, 2019). Experts involved throughout the cellulosic biorefinery supply chain have identified high production costs, policy uncertainty, and competition with petroleum fuels as continued barriers to the commercialization of cellulosic biofuels (Chen and Smith, 2017, 2018). Nonetheless, production of dedicated cellulosic energy crops (Mitchell et al., 2016; Robertson et al., 2017; Tilman et al., 2009; U.S. Department of Energy, 2016) and sustainable harvest of cellulosic agricultural residues (Karlen et al., 2014; Mabee et al., 2011; Mitchell et al., 2016; Muth et al., 2013; Tan et al., 2012; Tilman

et al., 2009; U.S. Department of Energy, 2016) are critically important for a projected future where biofuels displace a considerable portion of petroleum-based transportation fuels.

Switchgrass (*Panicum virgatum* L.), corn stover, and wheat (*Triticum aestivum* L. ssp. *aestivum*) straw are leading candidates to supply biomass for second-generation biofuels. Switchgrass was identified as a model biomass crop by the US Department of Energy in 1992 (Wright and Turhollow, 2010) and is the most advanced herbaceous perennial bioenergy feedstock in terms of its agronomic development (Mitchell et al., 2012). Corn stover is the most abundant crop residue in the US, as Muth et al. (2013) estimated that 124 Tg of corn stover could be harvested in 2011 while maintaining soil carbon (C) and limiting soil erosion to within tolerable limits; this represented 82% of all available crop residues. Wheat straw is the next most abundant crop residue, representing 15% of available residues in 2011, and is more abundant than corn stover in the far northern US (Muth et al., 2013). Consistent with widespread supply, corn stover has served as the feedstock for all commercial-scale cellulosic ethanol plants to date (DuPont, 2015; POET-DSM, 2014; US DOE, 2014). When combined with no-till farming, moderate stover removal can mitigate traditional residue management problems and allow for slightly increased grain yield (Halvorson and Stewart, 2015; Karlen et al., 2014). Nonetheless, sustainable stover removal rates are site-specific (Muth et al., 2012) and field studies have documented increased soil erosion (Acharya and Blanco-Canqui, 2018; Jin et al., 2015; Kenney et al., 2015), reduced soil nutrients (Acharya and Blanco-Canqui, 2018; Blanco-Canqui and Lal, 2009a; Halvorson and Stewart, 2015) and accelerated loss of soil organic C (Blanco-Canqui, 2013; Halvorson and Stewart, 2015; Kochsiek and Knops, 2012) with excessive corn stover removal. Although studied less extensively, the environmental concerns of excessive wheat straw removal are similar to those for corn (Blanco-Canqui, 2013; Powlson et al., 2011; Tarkalson et al., 2011). Relative to corn, switchgrass managed for biomass harvest has shown reduced nitrogen (N) leaching (Jungers et al., 2019; McIsaac et al., 2010; Smith et al., 2013), N runoff (Nyakatawa et al., 2006), and soil erosion (Blanco-Canqui et al., 2017), as well as greater soil C sequestration (Abraha et al., 2018; Al-Kaisi et al., 2005; Eichelmann et al., 2016;

Follett et al., 2012; Omonode and Vyn, 2006), improved wildlife habitat (Landis et al., 2018), and enhanced biodiversity (Landis et al., 2018; Werling et al., 2014).

To minimize competition with food crops and the potential for land clearing, marginal lands are oftentimes proposed as the most suitable lands for dedicated biomass crops (Dale et al., 2014; Mitchell et al., 2016; Robertson et al., 2017; Tilman et al., 2009). As reviewed by Kang et al. (2013b), Shortall (2013), and Lewis and Kelly (2014), many definitions of ‘marginal’ land have emerged in the literature, such as unproductive land, waste land, idle cropland, abandoned cropland, degraded cropland, land unsuitable for food production, physically marginal land, or economically marginal land. Alternatively, Richards et al. (2014) argue that ‘marginal’ is often used to subjectively describe less-than-ideal land and propose that “authors reporting on marginal soils and marginal lands clearly state the context, definition, and specifics of marginality.” Offering clear definitions of marginal lands is especially important for bioenergy research, as research of marginal lands in the context of bioenergy production makes up an increasing proportion of marginal lands research since the mid 2000s (Richards et al., 2014).

This investigation considers the overlap between economic and physical marginality among a subset of existing corn and wheat parcels converted to switchgrass production. Physical marginality is characterized by USDA Land Capability Classification (LCC) (Soil Survey Staff, 2018), which provides a general measure of the suitability of soils for most types of field crops. Land Capability Classification is designated by numbers 1 through 8, with progressively higher numbers indicating progressively greater limitations and narrower choices for practical use. Using LCC to identify physically marginal land for bioenergy production is a common approach. For example, in a GIS analysis within a 40-km road network of an existing corn grain ethanol plant in eastern Nebraska, Uden et al. (2013) estimated that 14,000 ha of land in irregularly-shaped dryland fields, large dry-land fields with an LCC of 3 or greater, and the non-irrigated corners of fields with center-pivot irrigation would be eligible for conversion to switchgrass. This compared to 132,000 ha where corn stover could be collected. In another

example, Gelfand et al. (2013) identified marginal lands as those with LCC of 5 to 7 with slope gradients of 20% or less, and proposed mixed prairie as a biomass crop in those areas where at least 653 Gg yr^{-1} could be produced within an 80-km radius.

Economically marginal land in this investigation is defined as those areas where switchgrass can earn equivalent economic return as corn or wheat with spatially-explicit residue removal, at the biomass price that provides only enough revenue for corn or wheat residue harvest to cover its associated harvest and transport expenses (i.e. at the corn or wheat biomass breakeven price). This investigation builds upon previous research comparing switchgrass returns to those of existing crops without residue harvest (Bangsund et al., 2008), with residue harvest at a fixed removal rate (Krohn, 2015), or using a single set of representative yields for switchgrass and its competing crop (James et al., 2010). In addition, by estimating outcomes at a moderate spatial resolution ($\approx 800 \text{ m}$), this investigation should identify finer-scale variations in economic return than past investigations conducted at the county scale (Jain et al., 2010; U.S. Department of Energy, 2016).

The focus of this investigation is the eastern Dakotas and western Minnesota. Influenced by declining precipitation from east to west and increasing temperature from north to south (PRISM Climate Group, 2019), this region features gradients in land use and native vegetative cover. Cultivated cropland dominates the study region (Figure 31a), with corn, soybean, and spring wheat as the predominant crops. While soybean production is widespread throughout the study region, corn and wheat production vary across a gradient featuring wheat-dominated lands in the northwest and corn-dominated lands in the southeast (Figure 31d,e). Native vegetative cover for the study region ranges from mixed prairie in the west to tallgrass prairie in the east, with forested areas bordering the northeastern portion of the study region. Very little native prairie remains, as agricultural conversion has removed over 99% of the tallgrass prairie in Minnesota, North Dakota, and South Dakota and approximately 70% of the mixed grass prairie in North and South Dakota (Samson et al., 1998). Nonetheless, widespread areas of the western study region and isolated portions of the eastern study

region feature cultivated cropland intermixed with various forms of perennial grasslands, primarily remnant prairie, rangeland (i.e. pasture and hay), and retired cropland enrolled in the USDA Conservation Reserve Program (CRP). Although this region has experienced increased grassland cover and decreased agricultural use between 1973 and 2000 (Sleeter et al., 2013), land-use changes from the mid-2000s to early 2010s have been characterized by an increase in cultivated cropland at the expense of grassland cover (Faber et al., 2012; Johnston, 2014; Lark et al., 2015, 2018; Wright and Wimberly, 2013). Corn, soybean, and wheat are commonly planted as the first crop after conversion from grassland (Lark et al., 2015; Morefield et al., 2016) and production of corn grain ethanol appears to be one driver of these land-use changes (Wright et al., 2017). Given its existing resource base of corn and wheat production and the dynamic nature of its land-use conversions between grasslands and agriculture, this region is well-suited for a comparative feasibility analysis of corn, wheat, and switchgrass biomass production.

Within the study region, the objectives of this investigation are to (i) estimate the ability of current corn and wheat biomass inventories to supply cellulosic biorefineries, (ii) approximate the minimum biomass price necessary for delivery of corn and wheat biomass to biorefineries, (iii) quantify the economic and environmental outcomes of switchgrass production relative to corn or wheat production, and (iv) contrast the economic and environmental outcomes for two methods of prioritizing economically marginal corn or wheat lands for switchgrass production. This investigation considers the amount of sustainably harvestable corn and wheat residue under three tillage intensities, and contrasts low-cost (LC) and high-cost (HC) scenarios for switchgrass establishment. This investigation draws upon the procedures and parameterizations for switchgrass, corn, and wheat developed in Chapters II and III, and uses ALMANAC to generate spatially-explicit estimates of yield, N runoff, and soil erosion across the study region.

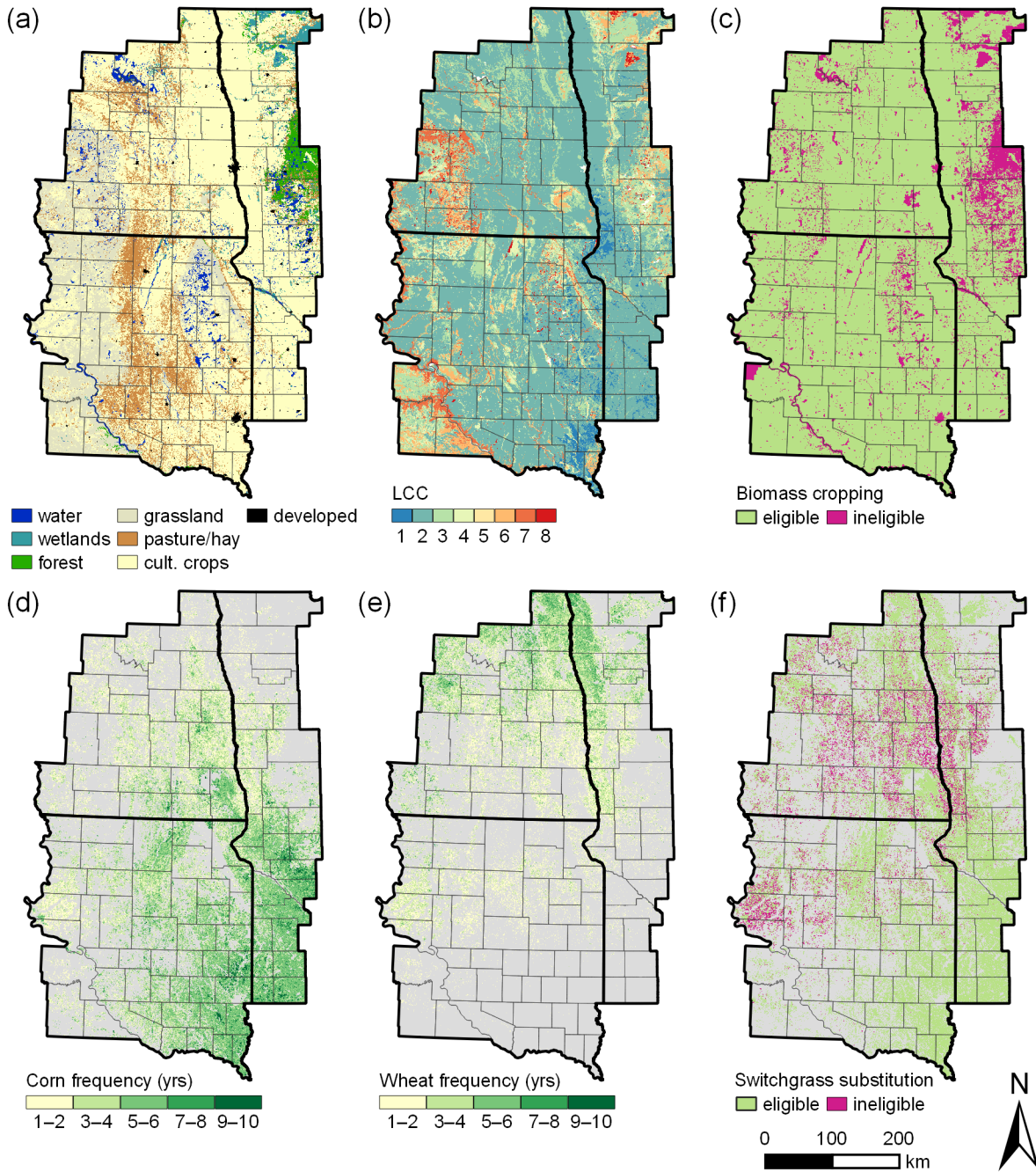


Figure 31. Characterizing study region land-use/land-cover (LULC). (a) Generalized LULC from 2011 National Land Cover Database. (b) Land capability classification (LCC). (c) Parcels considered eligible for biomass cropping. Frequency of (d) corn and (e) wheat production from 2006 to 2015, as indicated by USDA Cropland Data Layers. (f) Existing corn and wheat parcels considered eligible for substitution with switchgrass.

4.3. Materials and Methods

This study evaluates the technical feasibility, economic competitiveness, and environmental outcomes of switchgrass, corn stover, and wheat straw as cellulosic feedstocks for ethanol production. Across a 99-county area of eastern North Dakotas and western Minnesota, the analyses presented herein utilize moderate-resolution estimates of corn and wheat grain yields; corn, wheat, and switchgrass cellulosic biomass yields; and soil erosion, N runoff, and soil C sequestration associated with each cropping system. Grain yields are expressed on a market moisture basis (155 g kg^{-1} for corn, 135 g kg^{-1} for wheat) while biomass yields are expressed on a dry weight basis. For corn and wheat, comparisons are made among conventional tillage (CT), reduced tillage (RT), and no-till (NT) systems, as the quantity of biomass that can be sustainably removed generally increases with decreasing tillage intensity (Muth et al., 2013). The amount of harvestable corn and wheat biomass under each tillage system, assuming current land use patterns, was estimated in an analysis of potential biorefinery locations (Section 4.3.2). For switchgrass, comparisons are made between LC and HC establishment scenarios (Table 10, Section 4.3.4) with (+F) and without (-F) supplemental fertilizer (Sections 4.3.1 and 4.3.4), with establishment scenarios developed from varying accounts of successful stand establishment procedures within field-scale switchgrass production systems (Hoque et al., 2015; Mitchell et al., 2012; Perrin et al., 2008). Economic variables featured in the analyses include corn and wheat input costs and grain prices (Section 4.3.3), switchgrass input costs (Section 4.3.4), and environmental service valuations for soil erosion prevention, N loss mitigation, and C sequestration associated with switchgrass production (Section 4.3.7). To account for economic variables gathered from several sources representing various time periods, all dollar values presented herein were adjusted to 2010 USD using a Gross Domestic Product chain-type price index (U.S. Bureau of Economic Analysis, 2019).

All biophysical variables except soil C sequestration were simulated using the Agricultural Land Management Alternative with Numerical Assessment Criteria (ALMANAC)

Table 10. Comparison of assumptions for the low-cost (LC) and high-cost (HC) switchgrass establishment scenarios.

Item	LC	HC
Cover crop	none	seeded in fall prior to establishment year
Pesticides	applied in establishment year	applied in all years
Reseeding	none	10% of area reseeded in the year after establishment
Biomass yield: Est. year (Year 1)	50% of fully-established yield	none
Biomass yield: Year 2	100% of fully-established yield	50% of fully-established yield
Biomass yield: Years 3 to 10	100% of fully-established yield	100% of fully-established yield

model, utilizing crop parameters, soil characterizations, and climate variables described in Sections 2.3 and 3.3. Reported outcomes represent the average of 2006 to 2015 weather conditions. Simulations were conducted for 12,464 unique soils deemed suitable for biomass cropping (Figure 31c). Following Gelfand et al. (2013), simulations were performed for soils with LCC of 1 to 4 and soils with LCC of 5 to 7 along with slope gradients of less than 20% (Figure 31b). In addition, simulations were limited to those soils currently classified as cultivated cropland, pasture/hay, or grassland (Figure 31a). Simulation units were defined by the intersection of SSURGO mapunit polygons and the spatial resolution (4 km) of the climate dataset (gridMET; University of Idaho Climatology Lab, 2018). An output variable for a given simulation unit represents an area-weighted average across all primary soil components as defined by SSURGO. In total, there were 561,166 simulation units. Corn and wheat simulations featured grain and biomass harvest, with each soil assigned one of five biomass harvest systems representing the use of existing equipment and methods to remove residues from the field (Table 11). Assignment of residue removal systems to each soil was according to the analysis

of Muth et al. (2013), where a maximum sustainable residue removal rate was determined for each agricultural soil in the coterminous US (I.J. Bonner, personal communication, 2015). Specifically, a residue removal rate is considered sustainable if the combined soil loss from wind and water erosion is less than the tolerable limit defined by the USDA Natural Resources Conservation Service (NRCS), and soil organic matter is not being depleted. Three models were used to estimate these biophysical outputs: RUSLE2 (Revised Universal Soil Loss Equation 2), WEPS (Wind Erosion Prediction System), and SCI (Soil Conditioning Index). Due to differences in study methodologies, residue removal rates from Muth et al. (2013) were directly applicable to just 44% of the soils in the current study. Thus, each remaining soil was assigned a biomass removal rate from a soil in the same survey area with a similar LCC, soil loss tolerance factor, texture, and/or slope.

Switchgrass was simulated in a continuous monoculture. Two-year rotations with soybean were chosen to represent current corn and wheat cropping systems. Although this decision represents a simplification of current conditions, a cropping frequency analyses of USDA National Agricultural Statistics Service (NASS) Cropland Data Layer (CDL) maps from 2006 to 2015 indicates that these systems are a reasonable proxy for current cropping systems. This approach utilized CDL data to establish 10-year crop rotations across the study area. The 2010 to 2015 CDLs were scaled from 30 m to 56 m resolution to match the 2006 to 2009 CDLs, resulting in crop rotation maps at 56 m resolution. All pixels featuring land cover category changes between agricultural and non-agricultural uses were removed. For the 6.98 Mha featuring at least one year of corn (i.e. 22.26 million pixels), there were nearly 1.1 million unique cropping sequences. A strict corn-soybean (or soybean-corn) rotation was predominant on these parcels, featured on 1.35 Mha (19% of total), while 3.08 Mha (44% of total) exclusively featured corn and soybean. Nearly balanced rotations of corn and soybean were also widespread, as an additional 880,000 ha (13% of total) featured corn in 4 or 6 years of the sequence with soybean in all other years. For the 4.37 Mha featuring at least one year of wheat, there were over 1.2 million unique cropping sequences. Unlike corn, sequences

Table 11. Description, approximate residue removal rates, areal harvest costs (AHC), and yield-based harvest costs (YHC) for the five residue harvest systems used in this study. Systems adapted from (Muth et al., 2013).

Harvest system	Residue collection equipment and process	Collection rate (%)	AHC (\$ ha ⁻¹)	YHC
No residue harvest (NRH)	Combine harvester functions as normal	0	—	—
Harvest grain and cobs (HGC)	Combine harvester internal mechanisms are set to break apart cobs and collect them with the grain (corn only)	22	117.63 [†]	6.41 [‡]
Moderate residue harvest (MRH)	Combine harvester residue chopper and spreader are disengaged, leaving a windrow behind the machine. In a second pass a baler picks up the windrow, making 3' × 4' × 8' square bales.	35	—	14.28 [§]
Moderately high residue harvest (MHH)	Combine harvester residue chopper and spreader are disengaged, leaving a windrow behind the machine. A rake is used to collect additional surface residue into a single windrow. In a third pass a baler picks up the windrow, making 3' × 4' × 8' square bales.	52	10.76 [¶]	14.28 [§]
High residue harvest (HRH)	Combine harvester residue chopper and spreader are disengaged, leaving a windrow behind the machine. A flail shredder is used to cut standing stubble and to collect surface residue into a single windrow. In a third pass a baler picks up the windrow, making 3' × 4' × 8' square bales.	83	27.76 [#]	14.28 [§]

[†] 45.74 for cob collection (Maung and Gustafson, 2013) and 71.89 for reduced harvester efficiency (Lazarus, 2011, 2012, 2013, 2014, 2015; Lazarus and Smale, 2010; Maung and Gustafson, 2013)

[‡] \$ Mg-biomass⁻¹; 'moving large round bales to storage' (Edwards et al., 2013; Plastina et al., 2015)

[§] \$ bale⁻¹; 11.19 for 'straw or corn stalk baling, large square without wrap' and 3.09 for 'moving large round bales to storage' (Edwards and Johanns, 2010; Edwards et al., 2013; Plastina et al., 2015)

[¶] 'hay raking' (Aakre, 2014; NDSU, 2016; USDA NASS, 2010a)

[#] 'shredding corn stalks' (Aakre, 2014; NDSU, 2016; USDA NASS, 2010a)

featuring anywhere from 1 to 5 years of wheat production were common. Therefore, while a strict wheat-soybean (or soybean-wheat) rotation was predominant, it was featured on just 124,000 ha (3% of total). However, among the 1.61 Mha where wheat was a predominant crop in the sequence, 326,000 ha (20%) featured wheat and soybean in an equal number of years and 328,000 ha (20%) featured a difference of just one year between wheat and soybean. Thus, alternations between wheat and soybean appear to be fairly prevalent across the study area.

All output variables were aggregated to an approximately 800 m grid created by subdividing the 4 km resolution climate dataset. Thus, with an area of approximately 64 ha, each cell in the output datasets approximates a quarter section within the US Public Land Survey System. Hereafter, each cell in a gridded dataset is referred to as a ‘parcel’. Continuous variables were aggregated by taking the area-weighted average across simulation units within a parcel. Categorical variables were aggregated by assigning the value occupying the greatest area within a parcel. All maps were created in QGIS (QGIS Development Team, 2018) and projected using the USA Contiguous Albers Equal Area Conic USGS version (Spatial Reference, 2018). R statistical software (R Core Team, 2018) was used for statistical analysis and creating all other figures.

4.3.1. ALMANAC simulations

Corn and wheat simulations were conducted within a two-year rotation with soybean and under each of the three tillage systems. Tillage system operations (Appendix B) were defined using the standard management database (USDA NRCS, 2004) and definitions for no-till and reduced tillage systems (USDA NRCS, 2014a,b) from the USDA NRCS. Within each year, planting and harvest dates were assigned the predominant planting-harvest date pair of all combinations estimated using the methods described in Section 3.3.3. Within a given year, each simulation unit lacking wheat or corn production history was assigned the planting-harvest date pair of its nearest neighbor using the ‘RANN’ package of R (Arya et al., 2017). Two differing simulation approaches were used – one to simulate yield and a second to simulate environmental outcomes (soil erosion and N runoff).

As described in Section 3.3.3, each year's corn and wheat yield simulations were conducted following a single year of soybean production but separately from all other corn and wheat years. Thus, 60 sets of yield simulations were conducted to encompass all combinations of the two crops, three tillage systems, and ten years. In contrast, environmental outcomes simulations encompassed the entire 2006 to 2015 time frame, with 2005 included as a model spin up year. Each crop-tillage combination was simulated twice – once with soybean as the first crop in the rotation and once with corn or wheat as the first crop in the rotation. Thus, twelve sets of environmental outcome simulations were conducted to encompass all combinations of the two crops, three tillage systems, and two possible rotation sequences. Reported soil erosion and N runoff values represent the average across both crops and all years of the corn-soybean and wheat-soybean systems. Lastly, the average N fertilizer rates defined for the yield simulations (Section 3.3.3) were 34% and 19% higher than reported average 2006 to 2015 rates across Minnesota, North Dakota, and South Dakota for corn and wheat, respectively (USDA NASS, 2018). Thus, N fertilizer rates for the environmental outcome simulations were normalized so that the average rates across the study region were equal to the reported rates.

Switchgrass simulations were designed to estimate the multiyear average yield of a fully established switchgrass stand. Simulations were parameterized with 2005 as the establishment year and 2006 to 2015 as harvest years, using parameters described in Chapter II for upland switchgrass ecotypes grown in the US northern Great Plains. Plant population was set to 32 plants m^{-2} (Reitsma et al., 2011). Nitrogen fertilizer was assigned to simulation units at a rate of 14 $\text{kgN ha}^{-1} \text{ yr}^{-1}$ for each Mg of anticipated biomass yield, to a maximum of 112 $\text{kgN ha}^{-1} \text{ yr}^{-1}$, in accordance with published recommendations (Mitchell et al., 2015; Perrin et al., 2008). Anticipated biomass yield for each simulation unit was defined as the ALMANAC-simulated switchgrass yield from a preliminary model run featuring a N fertilizer rate of 135 kgN ha^{-1} . Phosphorus fertilization rates were 20, 10, and 5 kgP ha^{-1} for respective Olsen soil test P values of 0 to 3, 4 to 7, and 8 to 14 mg kg^{-1} ('very low', 'low', and 'medium')

P index values; Mitchell et al., 2015), with Olsen soil test P values estimated as described in Section 3.3.3. Soils with soil test P values of 15 mg kg⁻¹ or greater ('high' P index values) were assigned no P fertilizer. Although not used by ALMANAC, we estimated potassium (K) fertilizer rates for inclusion in switchgrass variable cost estimates (Section 4.3.4). Considering the lack of recommended potassium (K) fertilizer rates in Mitchell et al. (2015), we assumed that soil K index values would be similar to those for soil P and set switchgrass K rates to 3.2 times the P rates. This assumption is based on the relationship between recommended P and K rates for corn in Minnesota (Kaiser et al., 2018), as K fertilizer rates for soils with 'very low', 'low', and 'medium' K index values are 3.2 times higher than corresponding P rates for soils with 'very low', 'low', and 'medium' P index values. Estimated switchgrass N, P, and K fertilizer rates are shown in Figure 32.

All other management factors were accordant with those for corn. Switchgrass planting dates, in the establishment year, were set to three weeks prior to corn planting (McGuire and Rupp, 2013); in subsequent years, N fertilizer was applied on these same dates. Harvest occurred on the same dates as corn harvest, assuming a harvest efficiency of 95%, with no switchgrass harvested in the establishment year. Consistent with observations of switchgrass phenology varying by latitude (Casler, 2012), potential heat units (base 5°C) varied by corn management zone. Corn management zones (Chapter III, Figure 12a) characterize the expected potential heat units for corn production across the study region; a single switchgrass value for each zone was calculated using gridMET (University of Idaho Climatology Lab, 2018), averaging across years and raster cells within each zone. Switchgrass potential heat units were 2083, 2225, 2356, 2425, 2485, and 2566, respectively, for corn management zones 1 to 6. Lastly, to estimate switchgrass yields in the '-F' fertilizer option, a second set of simulations was conducted with no applied fertilizer and all other methods as described above.

Required computations for this study were conducted in parallel on a multi-core personal computer running the Windows operating system. R (R Core Team, 2018) was used to store ALMANAC input tables, write ALMANAC input files, invoke the command-

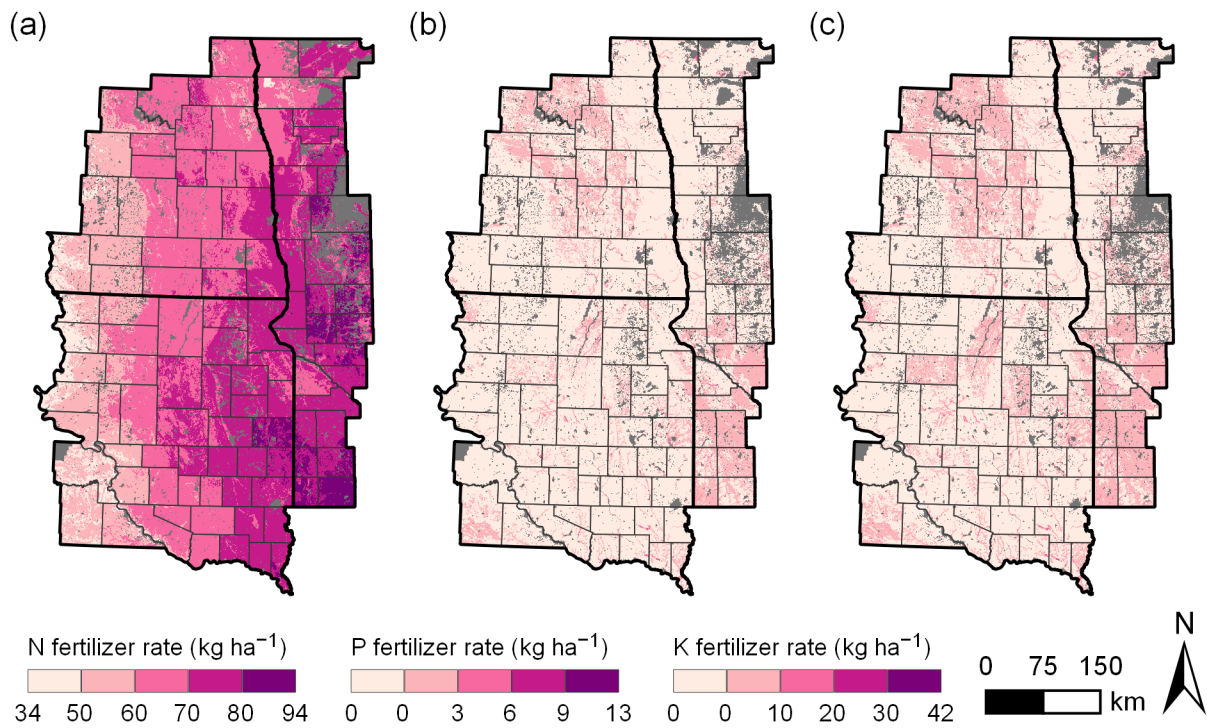


Figure 32. Estimated fertilizer rates for switchgrass (a) nitrogen (N), (b) phosphorus (P), and (c) potassium (K).

line ALMANAC interface, and extract desired results from ALMANAC output files. A local PostgreSQL database with a PostGIS extension was used to store ALMANAC outputs, the SSURGO spatial and tabular datasets, and other spatial datasets associated with this study. Using the parameterizations described above, 9% of the simulations conducted for this investigation featured a combination of soil parameters that resulted in ALMANAC errors. For these erroneous instances, simulations were rerun with parameters from a similar soil that did not result in a simulation error. For each error instance, the selected replacement soil was from the same county, with the same biomass harvest routine, and with a similar slope, plant-available water capacity, and USDA Crop Productivity Index as the error-producing soil. Following this routine, the number of simulation errors was reduced to 0.1% of all simulations. These instances were treated as missing values within all subsequent analyses.

4.3.2. Potential biorefinery locations

Following Gelfand et al. (2013), the values of mean corn and wheat biomass productivity obtained from ALMANAC were used to identify the location of potential cellulosic ethanol biorefineries. Potential biorefineries were limited to areas with combined corn and wheat biomass supply of at least 258.5 Gg yr^{-1} , under current spatial extents of corn and wheat production (Figure 31d,e), within a transportation distance of 8 to 112 km. The upper value of this range represents twice the biomass collection radius of a commercial-scale cellulosic ethanol plant in Emmetsburg, IA (POET-DSM, 2015). For this procedure, two moving-window algorithms were applied over the study region.

The first algorithm aggregated corn and wheat biomass yields from their respective production areas into circles with radii ranging from 8 to 112 km in 8-km increments. Areas of corn and wheat production were estimated using CDLs for 2006 to 2015 (USDA NASS, 2006, 2007, 2008, 2009, 2010b, 2012b, 2013, 2014, 2015a), modified by aggregating to 800 m resolution and removing all corn and wheat pixels not identified as cropland in 2011 National Land Cover Database (NLCD; Homer et al., 2012). To account for bias due to the spatial arrangement of corn and wheat fields within a given year, a separate moving-window tabulation was performed for each CDL. Only circles meeting the minimum biomass threshold for all ten CDLs were considered in the subsequent procedure.

The second algorithm identified non-overlapping circles as sites for potential biorefinery locations. The algorithm progressed through radii from 8 to 112 km in 8-km increments, identifying the smallest area needed to produce the minimum biomass supply threshold. To identify locations likely to produce more than the minimum threshold even in poor-yielding years, a potential biorefinery location was acceptable only if the lower limit of its 99% prediction interval for biomass productivity was greater than 258.5 Gg yr^{-1} . To account for the correlation among yields within a biorefinery collection area, the variance associated with each biorefinery collection area was calculated as the sum of all encompassed parcels' variances and twice the covariance among these parcels (Lane et al., 2019). Each parcel's

variance was defined as ALMANAC-simulated biomass production variance for 2006 to 2015 weather conditions. The 99% prediction interval was calculated using a t-distribution with 9 degrees of freedom. Covariance calculations were computationally intensive, and it was infeasible to calculate covariance for all potential biorefinery locations. Thus, for each radius, the necessary number of calculations was reduced by stratifying potential biorefinery locations into 10 quantiles ranging from lowest to highest biomass production variance. The algorithm then ranged from highest to lowest biomass productivity within each strata, moving on to the next strata on the first instance of a biorefinery location that did not meet the minimum biomass production threshold.

4.3.3. Corn and wheat expenses and revenue

Corn and wheat economic variables were gathered from several sources and generally represent the average of 2010 to 2015 values for Minnesota, North Dakota, and South Dakota. Whenever feasible, input costs represent actual values from growers within the 99-county study area, provided through consultations with farm financial management professionals (FINBIN, 2019). Considering the lack of widespread commercial harvest for corn or wheat cellulosic biomass, corresponding harvest costs were based on machinery cost estimates for Minnesota (Lazarus, 2011, 2012, 2013, 2014, 2015; Lazarus and Smale, 2010) and estimates of custom rates in North Dakota (Aakre, 2014; NDSU, 2016; USDA NASS, 2010a) and Iowa (Edwards and Johanns, 2010; Edwards et al., 2013; Plastina et al., 2015). Consistent with the standard approach for partial enterprise budget analysis of agronomic experiments (CIMMYT, 1988), the capital budget approach used here omits direct input costs invariant across the various systems. Examples of such costs are land rent, hired labor, marketing, and utilities. Thus, while the results presented here are valid for comparisons across the systems included, they do not account for all costs incurred by growers. Equations [28] to [34] and Figure 33 describe the estimation of corn and wheat revenue and expenses; a companion summary is presented in Table 12.

Figure 33 illustrates the general processes for calculating grain revenue, grain expense,

Table 12. For those equations within Sections 4.3.3 to 4.3.5 describing calculations of economic variables, summary of relevant crop(s), output variables, input variables, reference figures, and prerequisite equations. Output variables from prerequisite equations are used as input variables for Equations [38] to [41] and [43].

Eq.	Crop [†]	Output Variable	Input Variables	Ref. Figure	Prereq. Eq.
28	c/w	<i>GR</i> (grain revenue)	<i>GY</i> (grain yield), <i>GP</i> (grain profit)	33a	—
29–31	c/w	<i>GE</i> (grain expense)	<i>SC</i> (seed cost), <i>FC</i> (fertilizer cost), <i>CC</i> (chemicals cost), <i>DC</i> (drying cost), <i>MC</i> (machinery cost)	33b	—
32	c/w	<i>HE</i> (harvest expense)	<i>AHC</i> (areal harvest cost), <i>YHC</i> (yield-based harvest cost), <i>NRC</i> (nutrient removal cost), <i>BY</i> (biomass yield), <i>HS</i> (harvest system)	33c	—
33–34	c/w	<i>TE</i> (transport expense)	<i>LDC</i> (loading cost), <i>TC</i> (transport cost), <i>TD</i> (transport distance), <i>LW</i> (load weights), <i>BY</i> , <i>HS</i>	33d	—
36	swg	<i>PE</i> (production expense)	<i>SC</i> , <i>FC</i> , <i>CC</i> , <i>MC</i> , <i>AHC</i> , <i>YHC</i> , <i>BY</i>	35a	—
37	swg	<i>TE</i>	<i>LDC</i> , <i>TC</i> , <i>TD</i> , <i>LW</i> , <i>BY</i>	35b	—
38	swg	<i>SPP</i> (switchgrass parity price)	<i>VCS</i> (switchgrass variable cost), <i>OCD</i> (defender system opportunity cost), <i>BYS</i> (switchgrass biomass yield), <i>BYD</i> (defender system biomass yield)	—	39–44
39–41	c/w	<i>OCD</i>	<i>GR</i> , <i>GE</i> , <i>HE</i> , <i>TE</i> , <i>SBR</i> (soybean revenue), <i>SBE</i> (soybean expense)	—	28–34
42	c/w	<i>BYD</i>	<i>BY</i>	—	—
43	swg	<i>VCS</i>	<i>PE</i> , <i>TE</i>	—	36–37
44	swg	<i>BYS</i>	<i>BY</i>	—	—

[†] c/w = corn/wheat, swg = switchgrass

biomass harvest expense, and biomass transport expense in corn and wheat. Grain revenue (GR ; Figure 33a) was estimated as

$$GR_{ijk} = GY_{ijk} \times GP_j \quad [28]$$

where i is a soil growing crop j under tillage system k , GY is ALMANAC-simulated grain yield (Section 4.3.1), and GP is the average of 2010 to 2015 grain prices from FINBIN. Grain prices represent aggregate values across study area counties and were \$174 Mg-corn⁻¹ (\$4.42 bushel⁻¹) and \$234 Mg-wheat⁻¹ (\$6.38 bushel⁻¹).

Grain expense (GE ; Figure 33b) was characterized as the sum of five direct expenses:

$$GE_{ijk} = \begin{cases} SC_{ijk} + FC_{ijk} + CC_{jk} + DC_{jk} + MC_{jk} & \text{for } j = \text{corn} \\ SC_{jk} + FC_{ijk} + CC_{jk} + DC_{jk} + MC_{jk} & \text{for } j = \text{wheat} \end{cases} \quad [29]$$

where i is a soil growing crop j under tillage system k , SC_{ijk} and FC_{ijk} are soil-specific seed cost and fertilizer cost, and SC_{jk} , CC_{jk} , DC_{jk} , and MC_{jk} represent study region average values for seed, crop chemical, drying, and machinery costs (Table 13). When $j = \text{corn}$, soil-specific seed cost (SC_{ijk}) was estimated as a function of average seed cost (SC_{jk}):

$$SC_{ijk} = \left[\left(\frac{PD_{ij}}{\frac{1}{n} \sum_i^n PD_{ij}} \right) \times SC_{jk} \right] \quad [30]$$

where i is a soil growing crop j under tillage system k and PD is the planting density previously estimated for ALMANAC modeling (Chapter III, Figure 14c). In corn and wheat, soil-specific fertilizer cost (FC_{ijk}) was estimated as a function of average fertilizer cost (FC_{jk}):

$$FC_{ijk} = \left[NF_j \times \left(\frac{NR_{ij}}{\frac{1}{n} \sum_i^n NR_{ij}} \right) \times FC_{jk} \right] + [(1 - NF_j) \times FC_{jk}] \quad [31]$$

where i is a soil growing crop j under tillage system k , NF is the estimated N fraction of a producer's fertilizer costs, and NR is the N fertilizer rate. NR was previously estimated for

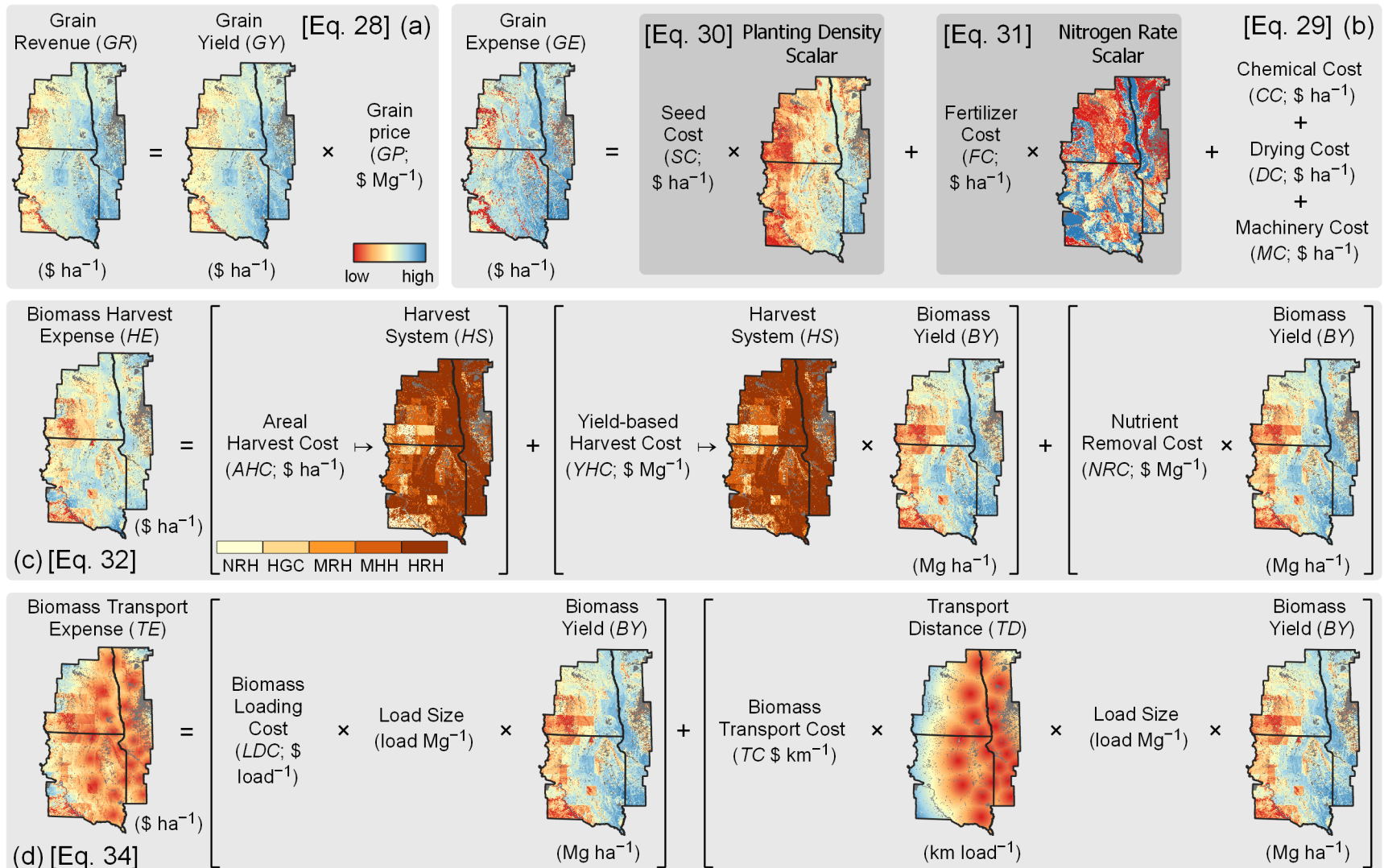


Figure 33. Illustrations for generalized calculations of corn (a) grain revenue, (b) grain expense, (c) biomass harvest expense, and (d) biomass transport expense. Wheat calculations were similar, but with a constant seed cost.

ALMANAC modeling (Chapter III, Figure 13a,c). NF was estimated using 2010 to 2015 US fertilizer price data (DTN, 2018) and the USDA Agricultural Resource Management Survey (USDA ERS, 2009, 2010) values for average N, P, and K fertilizer rates in the Northern Great Plains region. For example, corn fertilizer rates and prices are 155, 17, and 9 kg ha⁻¹ and \$1.09, \$3.14, \$1.19 kg⁻¹ for N, P, and K, respectively. With a N fertilizer cost of \$169 ha⁻¹ and a total fertilizer cost of \$233 ha⁻¹, the NF for corn was 0.72. With wheat fertilizer rates of 84, 14, and 4 kg ha⁻¹ for N, P, and K, respectively, the NF for wheat was 0.65.

While FINBIN is a valuable source for actual on-farm financial information, the methodologies used to estimate GE reflect two challenges in using the FINBIN dataset for fine-grained, spatially-explicit modeling of input costs. First, while the FINBIN interface allows for data aggregation by tillage system, only the Minnesota dataset featured examples from CT (Moldboard), RT (Chisel/Reduced), and NT systems in both corn and wheat. Thus, differences in grain production input costs among tillage systems (Table 13) are a function of tillage system scalars developed from Minnesota values. Scalars were developed by normalizing the 2006 to 2015 multiyear-average seed, fertilizer, crop chemicals, crop drying, and machinery cost values for CT, RT, and NT systems in Minnesota by the mean values across tillage systems. Values from 2006 to 2009 were included to increase the number of observations; for corn, there were 129, 2161, and 45 observations for the CT, RT, and NT systems, respectively, while there were 11, 1487, and 52 such observations for wheat. The resulting scalars were then multiplied by their corresponding input costs, which represented 2010 to 2015 multiyear-average seed, fertilizer, crop chemicals, crop drying, and machinery costs across all tillage systems and study region counties. The final results are the tillage-specific input cost estimates of Table 13.

The second challenge with using FINBIN values is that county is the smallest level of spatial aggregation within FINBIN, and many counties lacked sufficient observations to generate robust single- or multi-year cost estimates. Aggregating county-level FINBIN data into agricultural districts, as defined by the USDA for each state (USDA NASS, 2019), increases the number of observations per unit but results in abrupt differences in expenses

Table 13. Study-region average input costs for corn and wheat grain production, biomass harvest, and biomass transport within conventional tillage (CT), reduced tillage (RT), and no-till (NT) systems.

Input cost	Corn			Wheat		
	CT	RT	NT	CT	RT	NT
Grain production	\$ ha ⁻¹					
Seed	221.27	242.01	230.49	55.36	51.14	51.67
Fertilizer	288.89	312.97	300.93	228.45	209.41	196.72
Crop chemicals	56.79	55.02	65.08	79.18	69.19	64.91
Crop drying	17.23	18.23	24.17	1.40	1.40	2.47
Machinery	302.62	323.59	269.66	193.63	182.46	182.46
Subtotal	886.80	951.82	890.33	558.02	513.60	498.23
Biomass harvest [†]						
NRH	0.00	0.00	0.00	0.00	0.00	0.00
HGC	129.21	127.80	127.01	—	—	—
MRH	65.91	63.11	—	52.56	51.12	60.46
MHH	113.91	103.73	105.49	89.67	90.09	84.16
HRH	177.03	188.26	181.99	146.88	155.43	153.58
Biomass transport [†]						
NRH	0.00	0.00	0.00	0.00	0.00	0.00
HGC	55.19	38.89	32.22	—	—	—
MRH	58.44	35.24	—	62.48	29.26	19.88
MHH	74.68	49.49	40.54	76.43	40.24	42.86
HRH	132.65	63.44	64.49	146.07	55.11	53.76

[†] From Table 11; NRH = no residue harvest, HGC = harvest grain and cobs, MRH = moderate residue harvest, MHH = moderately high residue harvest, HRH = high residue harvest

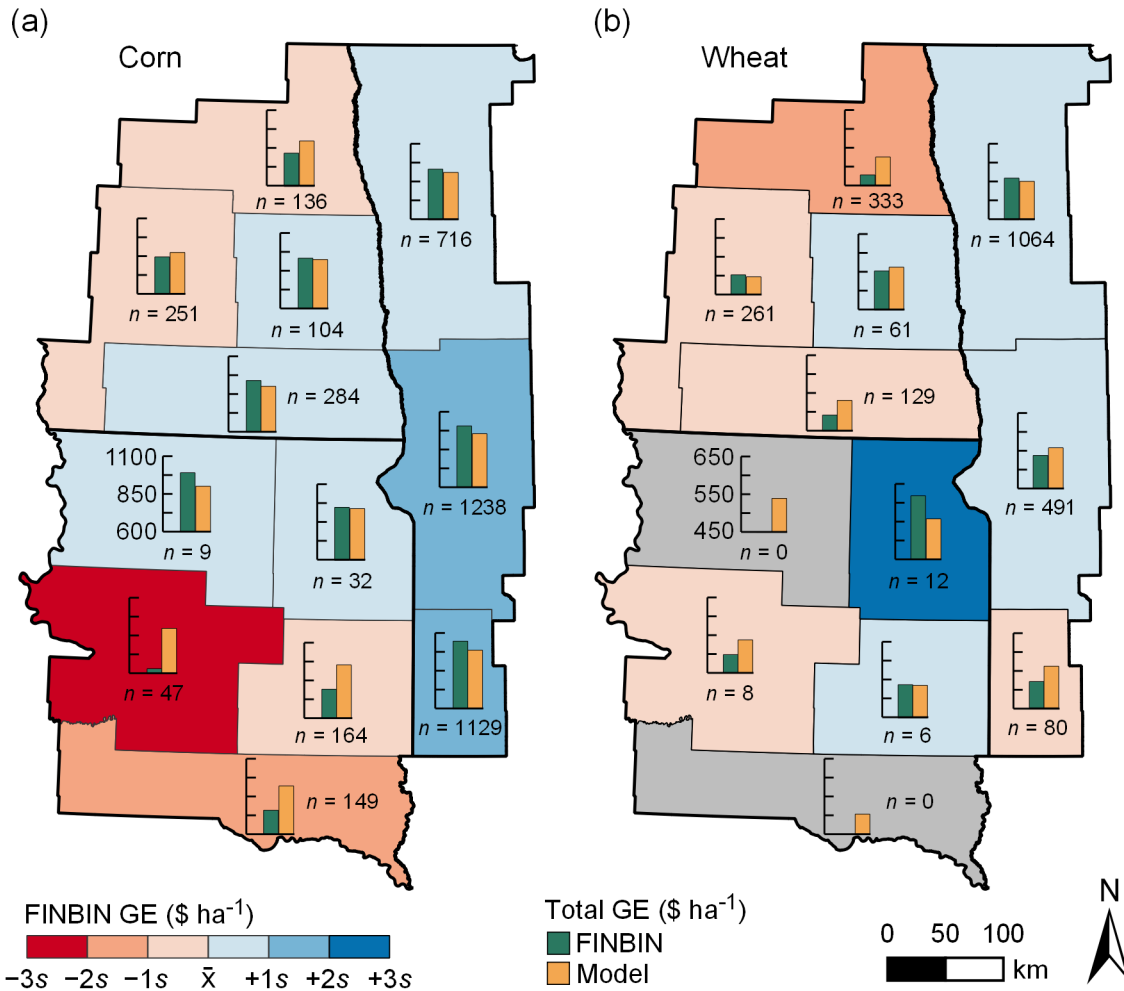


Figure 34. Comparison of FINBIN and model-derived grain production expenses (GE) for (a) corn and (b) wheat, aggregated by USDA Agricultural District. Expenses are averaged across tillage systems.

among certain neighboring districts (Figure 34). Considering that the number of observations varies widely among districts, from 9 to 1238 for corn and 0 to 1064 for wheat, these differences are most likely due to sampling and aggregation effects within each district in addition to any real differences in expenses among districts. Thus, parcel-specific estimates of grain expense (*GE*; Figure 33b) are a function of spatially-explicit fertilizer and corn seed costs but include study-area averages for all other costs. This methodology does not allow for spatial variations in the cost of crop chemicals, crop drying, machinery, and wheat seed, even though these variables are likely to vary dependent on local conditions, yields, and practices.

Nonetheless, when aggregated by USDA Agricultural District, *GE* estimates are similar to FINBIN (Figure 34). Wheat *GE* estimates are within 10% of FINBIN values in all districts, while corn *GE* estimates are within 10% of FINBIN values in 9 of 12 districts and 20% of FINBIN values in an additional 2 districts. The largest deviation is for corn *GE* 43% higher than the FINBIN estimate for central South Dakota, but this may be partly due to the low sample size used to generate the FINBIN estimate. Furthermore, in any district where *GE* differs by more than 5% from FINBIN, the net effect is that *GE* estimates are closer to the study-region average than are FINBIN estimates.

Expenses associated with corn and wheat residue removal were categorized as biomass harvest and transport expenses. Biomass harvest expense (*HE*; Figure 33c) was calculated as follows:

$$\begin{aligned}
 HE_{ijk} &= AHC_{ijk} + YHC_{ijk} + NRC_{ijk}, \\
 \text{where } AHC_{ijk} &\begin{cases} 117.63 & \text{for } HS_{ijk} = HGC \\ 10.76 & \text{for } HS_{ijk} = MHH \\ 27.76 & \text{for } HS_{ijk} = HRH \\ 0.00 & \text{otherwise} \end{cases}, \\
 YHC_{ijk} &\begin{cases} BY_{ijk} \times 6.41 & \text{for } HS_{ijk} = HGC \\ [BY_{ijk}/0.80/0.60] \times 11.19 & \text{otherwise} \end{cases}, \\
 NRC_{ijk} &= BY_{ijk} \times 8.94,
 \end{aligned} \tag{32}$$

i is a soil growing crop *j* under tillage system *k*, *AHC* is areal harvest cost, *YHC* is yield-based harvest cost, *NRC* is nutrient replacement cost, *HS* is biomass harvest system, and *BY* is biomass yield. *NRC* includes a nutrient replacement price of \$8.94 Mg-biomass⁻¹, which represents the sum of values for P (\$2.04) and K (\$6.90) and is derived from nutrient removal values of 0.65 kgP Mg-biomass⁻¹ and 5.8 kgK Mg-biomass⁻¹ (Edwards, 2014) and average fertilizer prices from 2010 to 2015 of \$3.14 kgP⁻¹ and \$1.19 kgK⁻¹ (DTN, 2018). Omitting N from this analysis is consistent with the approach of Edwards (2014), as residue

removal can increase N availability in certain soils through increased mineralization of soil organic matter. *AHC* and *YHC* operations within the MRH, MHH, and HRH systems feature equipment commonly used for baling hay or straw (Table 11). Based on focus group surveys of North Dakota farmers conducted in late 2010 to early 2011 (Maung et al., 2012), it is assumed that farmers would utilize custom hire for harvest and transportation of biomass within these systems. Custom hire rates were assigned the multiyear-average values from 2010, 2013, and 2016 custom rate surveys for North Dakota or Iowa. Since custom hire does not currently exist for simultaneous harvest of corn grain and cobs, *AHC* for the HGC system includes cost estimates for cob collector operation following Maung and Gustafson (2013). Cob collection cost includes a 50% reduction in harvest efficiency (Maung and Gustafson, 2013) and the costs associated with increased harvest time are taken from machinery use cost estimates for Minnesota (Lazarus, 2011, 2012, 2013, 2014, 2015; Lazarus and Smale, 2010). Custom rates for *YHC* are presented on a per-bale basis; conversion of *BY* from Mg-biomass to bales assumes that each harvested bale contains 800 g kg⁻¹ dry matter and weighs 0.60 Mg (Edwards, 2014).

Calculations of biomass transport expense assume that biomass harvested from each parcel will be hauled to market in as many full tractor-trailer loads as possible, with any remaining biomass hauled in a partial load. Therefore, each parcel is represented by a set of load weights (*LW*; in Mg) calculated as follows:

$$LW_{ijk} \begin{cases} \{ 14.05 \times L_{ijk}, BY_{ijk}/0.80 - L_{ijk} \times 14.05 \} & \text{for } HS_{ijk} = \text{HGC} \\ \{ 21.60 \times L_{ijk}, BY_{ijk}/0.80 - L_{ijk} \times 21.60 \} & \text{otherwise} \end{cases}, \quad [33]$$

$$\text{where } L_{ijk} \begin{cases} \lfloor BY_{ijk}/0.80/14.05 \rfloor & \text{for } HS_{ijk} = \text{HGC} \\ \lfloor BY_{ijk}/0.80/21.60 \rfloor & \text{otherwise} \end{cases},$$

i is a soil growing crop *j* under tillage system *k*, *L* is the number of full tractor-trailer loads, *BY* is biomass yield, and *HS* is biomass harvest system. The assumed tractor-trailer capacity for corn cobs is 14.05 Mg, based on a standard silage trailer with capacity of 65 m³ and average

corn cobs density of 216 kg m^{-3} (Tapco Inc, 2019). The assumed capacity for bales of corn stover or wheat straw is 21.60 Mg, which assumes standard large square bales with dimensions of $0.91 \text{ m} \times 1.22 \text{ m} \times 2.44 \text{ m}$ and weighing 0.60 Mg each (Edwards, 2014), and that 36 bales can fit a standard flatbed trailer 2.47 m wide and 14.63 m long. Also, we assume that harvested bales and corn cobs contain 800 g kg^{-1} dry matter. Subsequently, biomass transport expense (TE ; Figure 33d) was calculated as follows:

$$TE_{ijk} = \sum_{l=1}^{L_{ijk}+1} [LDC_{ijkl} + (TC_{ijkl} \times TD_i)],$$

$$\text{where } LDC_{ijkl} \begin{cases} 24.28 & \text{for } LW_{ijkl} < 9 \\ 24.79 & \text{for } 9 \leq LW_{ijkl} \leq 18, \\ 27.41 & \text{for } LW_{ijkl} > 18 \end{cases}, \quad [34]$$

$$TC_{ijkl} \begin{cases} 2.88 & \text{for } LW_{ijkl} < 9 \\ 3.10 & \text{for } 9 \leq LW_{ijkl} \leq 18, \\ 3.16 & \text{for } LW_{ijkl} > 18 \end{cases}$$

i is a soil growing crop j under tillage system k , l is a tractor-trailer load, L is the number of full tractor-trailer loads, LDC is the loading cost for a tractor-trailer load, TC is the transport cost for a tractor-trailer load ($\$ \text{ km}^{-1}$), TD is the transportation distance to the nearest potential biorefinery location (Section 4.3.2), and LW is the set of tractor-trailer load weights. Values for LDC and TC are average North Dakota custom rates averaged across 2010, 2013, and 2015 (Aakre, 2014; NDSU, 2016; USDA NASS, 2010a).

4.3.4. Switchgrass expenses

The switchgrass budget was patterned after Hoque et al. (2015) and considers establishment, production, harvest, and transport costs over 10 years. A 10-year time period is appropriate for switchgrass, as it does not reach its full yield potential for several years and usually features a stand life of 10 years or longer (Mitchell et al., 2015). Pre-establishment costs, such as preparation of non-agricultural land for switchgrass production, are not included as it is assumed these costs would be invariant across all biomass cropping systems. All

production tasks prior to harvest are assumed to be performed by the farmer. Equipment costs for these operations were average machinery operation direct costs for Minnesota from 2010 to 2015 (Lazarus, 2011, 2012, 2013, 2014, 2015; Lazarus and Smale, 2010). Consistent with the corn and wheat residue harvest systems, it is assumed that custom hire would be utilized for all switchgrass harvest and transport operations. Equations [36] and [37] and Figure 35 describe the estimation of switchgrass expenses; a companion summary is presented in Table 12.

Switchgrass budget items are encompassed within two expenses, production and transport, with each expense expressed as the annualized net present value assuming a discount rate of 5% and a time frame of 10 years. Using a discount rate of 5% follows James et al. (2010) and is supported by Erickson et al.'s (2004) finding that U.S. farms averaged a 5% rate of return on capital from 1960 to 2001. Annualized net present value (*ANPV*) was calculated by applying a standard financial annuity formula to the net present value of 10-year returns:

$$ANPV = NPV \left[\frac{r(1+r)^T}{(1+r)^T - 1} \right], \quad [35]$$

where *NPV* is the net present value of 10-yr returns, *r* is the interest rate (5%), and *T* is the time horizon (10 yrs). Figure 35 illustrates the general process for calculating each switchgrass expense.

Biomass production expense (*PE*; Figure 35a) includes all switchgrass production activities up to the parcel edge, and the net present value of *PE* was estimated as follows:

$$NPV(PE_{imm}) = \sum_{t=1}^T \left(\frac{SC_m^x + FC_{in} + CC_m^x + MC_{mn}^x + AHC_m^x + YHC_{imm}^x}{(1+r)^t} \right),$$

where $x \begin{cases} t & \text{for } t \leq 2 \\ 3 & \text{otherwise} \end{cases}$,

$$SC_m \begin{cases} (140.46, 0.00, 0.00) & \text{for } m = LC \\ (140.46, 14.05, 0.00) & \text{for } m = HC \end{cases}$$

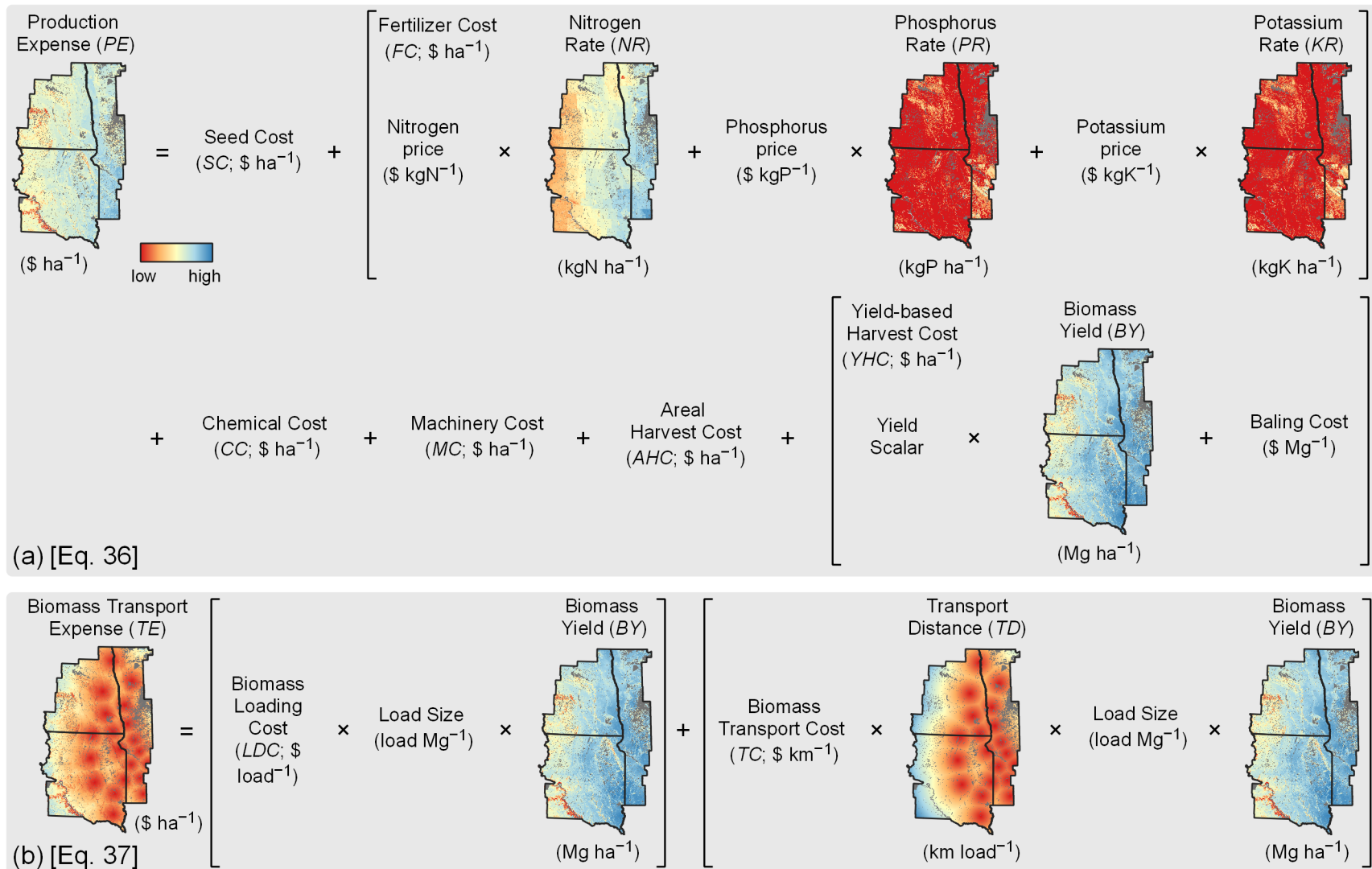


Figure 35. Illustrations for generalized calculations of switchgrass (a) biomass production expense and (b) biomass transport expense.

$$\begin{aligned}
FC_{in} & \begin{cases} 0.00 & \text{for } t = 1 \text{ or } n = -F \\ [NR_i \times 1.09] + [PR_i \times 3.14] + [KR_i \times 1.19] & \text{for } t \geq 2 \text{ and } n = +F \end{cases} \\
CC_m & \begin{cases} (43.31, 0.00, 0.00) & \text{for } m = LC \\ (67.66, 15.33, 15.33) & \text{for } m = HC \end{cases}, \\
MC_{mn} & \begin{cases} (65.97, 0.00, 0.00) & \text{for } m = LC \text{ and } n = -F \\ (65.97, 13.98, 13.98) & \text{for } m = LC \text{ and } n = +F \\ (173.52, 14.99, 10.49) & \text{for } m = HC \text{ and } n = -F \\ (173.52, 28.97, 24.47) & \text{for } m = HC \text{ and } n = +F \end{cases}, \\
AHC_m & \begin{cases} (36.95, 36.95, 36.95) & \text{for } m = LC \\ (0.00, 36.95, 36.95) & \text{for } m = HC \end{cases}, \\
YHC_{imn}^x & = [YS_m^x \times BY_{in}/0.80/0.68] \times 12.64, \\
YS_m & \begin{cases} (0.5, 1.0, 1.0) & \text{for } m = LC \\ (0.0, 0.5, 1.0) & \text{for } m = HC \end{cases},
\end{aligned} \tag{36}$$

i represents a soil growing switchgrass under establishment scenario m (LC or HC) and fertilizer option n ($-F$ or $+F$); FC is fertilizer cost; NR , PR , and KR are fertilizer rates for N, P, and K, respectively; BY is biomass yield; and the x^{th} elements of SC , CC , MC , AHC , YHC , and YS are seed cost, crop chemicals cost, machinery cost, areal harvest cost, yield-based harvest cost, and a yield scalar, respectively, for the t^{th} year of production. Details of CC and MC are presented in Table 14. SC for $t = 1$ is the product of a 5.6 kg ha^{-1} seeding rate (Hoque et al., 2015) and a seed price of $\$25 \text{ kg}^{-1}$, which is the average from 2010 to 2015 price lists of Shooting Star Native Seed in Spring Grove, MN. Under HC establishment, SC for $t = 2$ is 10% of SC for $t = 1$, representing reseeding for 10% of switchgrass area. Spatially-explicit estimates of NR , PR , and KR were developed for ALMANAC modeling (Figure 32). Average 2010 to 2015 fertilizer prices of $\$1.09 \text{ kgN}^{-1}$, $\$3.14 \text{ kgP}^{-1}$, and $\$1.19 \text{ kgK}^{-1}$ (DTN, 2018) were multiplied by NR , PR , and KR , respectively, with FC defined as the sum of

these products. Consistent with recommended best management practices for switchgrass (Mitchell et al., 2015), no fertilizer was applied in the establishment year ($t = 1$) under either fertilization option. *AHC* combines average hay harvest costs across 2010, 2013, and 2016 for ‘mowing and conditioning’ (\$26.19 ha⁻¹) and ‘raking’ (\$10.76 ha⁻¹; Aakre, 2014; NDSU, 2016; USDA NASS, 2010a). *YHC* represents average costs across 2010, 2013, and 2015 for ‘baling large square hay’ (\$9.56 bale⁻¹; Edwards and Johanns, 2010; Edwards et al., 2013; Plastina et al., 2015), with conversion of *BY* from Mg-biomass to bales assuming that each harvested bale contains 800 g kg⁻¹ dry matter and weighs 0.68 Mg (Hoque et al., 2015). Finally, *YS* implements the delayed realization of full yield potential under HC establishment when compared to LC establishment. Complete study region average input costs under the HC and LC scenarios and –F and +F fertilizer options are presented in Table 15.

Biomass transport expense estimates the costs included for transporting switchgrass biomass from a parcel to the nearest biorefinery (Section 4.3.2). Similar to corn and wheat (Equation [33]), calculations of biomass transport expense assume that biomass harvested from each parcel will be hauled to market in as many full tractor-trailer loads as possible, with any remaining biomass hauled in a partial load. Therefore, each parcel is represented by a set of load weights (*LW*; in Mg), which are used in the calculation of transport expense (*TE*; Figure 35b). The net present value of *TE* was calculated as follows:

$$NPV (TE_{imn}) = \sum_{t=1}^T \left(\frac{\sum_{l=1}^{L_{imn}^x+1} [LDC_{imnl}^x + (TC_{imnl}^x \times TD_i)]}{(1+r)^t} \right),$$

$$\text{where } x \begin{cases} t & \text{for } t \leq 2 \\ 3 & \text{otherwise} \end{cases},$$

$$YS_m \begin{cases} (0.5, 1.0, 1.0) & \text{for } m = \text{LC} \\ (0.0, 0.5, 1.0) & \text{for } m = \text{HC} \end{cases},$$

$$L_{imn}^x = \lfloor BY_{imn} \times YS_m^x / 0.80 / 24.48 \rfloor, \quad [37]$$

$$LW_{imn}^x = \left\{ 21.60 \times L_{imn}^x, BY_{imn} \times YS_m^x / 0.80 - L_{imn}^x \times 24.48 \right\},$$

Table 14. Detailed crop chemicals and machinery cost estimates for the low-cost (LC) and high-cost (HC) establishment scenarios in year 1 (YR1), year 2 (YR2), and subsequent years (YR3+) of switchgrass production.

Input cost	LC			HC		
	YR1	YR2	YR3+	YR1	YR2	YR3+
Crop chemicals (CC) [†]	\$ ha ⁻¹					
cover crop burndown [‡]	—	—	—	24.35	—	—
preemergence [§]	27.98	—	—	27.98	—	—
postemergence [¶]	15.33	—	—	15.33	15.33	15.33
Subtotal	43.31	—	—	67.66	15.33	15.33
Machinery (MC)						
cover crop aerial seeding [#]	—	—	—	97.06	—	—
prairie grass drill ^{††}	44.99	—	—	44.99	4.50	—
sprayer – burndown ^{‡‡}	—	—	—	10.49	—	—
sprayer – preemergence ^{‡‡}	10.49	—	—	10.49	—	—
sprayer – postemergence ^{‡‡}	10.49	—	—	10.49	10.49	10.49
fertilizer spreader ^{§§}	—	13.98	13.98	—	13.98	13.98
Subtotal	65.97	13.98	13.98	173.52	28.97	24.47

[†] prices from Zollinger (2010, 2011, 2012, 2013, 2014, 2015), chemical choices from Mitchell et al. (2015)

[‡] glyphosate (Roundup PowerMAX; \$19.12 ha⁻¹), adjuvant (Class Act NG; \$5.23 ha⁻¹)

[§] quinclorac (Facet/Paramount; \$17.84 ha⁻¹), atrazine (Atrazine 4L; \$10.14 ha⁻¹)

[¶] 2,4-D amine

[#] \$44.89 ha⁻¹ for seeding, \$52.17 ha⁻¹ for oats at 3.4 kg ha⁻¹ (USDA NRCS, 2010)

^{††} Lazarus (2011, 2012, 2013, 2014, 2015); Lazarus and Smale (2010)

^{‡‡} average of 'boom sprayer, self-propelled' and 'boom sprayer, pull-type' (Lazarus, 2011, 2012, 2013, 2014, 2015; Lazarus and Smale, 2010)

^{§§} 'boom sprayer, self-propelled' (Lazarus, 2011, 2012, 2013, 2014, 2015; Lazarus and Smale, 2010)

Table 15. Study-region average input costs for combinations of establishment scenario (low-cost [LC], high-cost [HC]) and fertilizer option (-F, +F) in year 1 (YR1), year 2 (YR2), and subsequent years (YR3+) of switchgrass production. Transport costs are to the nearest biorefinery, with biorefinery locations determined by available corn and wheat biomass under conventional tillage (CT), reduced tillage (RT), and no-till (NT) systems.

Input cost	LC			HC		
	YR1	YR2	YR3+	YR1	YR2	YR3+
-F fertilizer option	\$ ha ⁻¹					
Seed (SC)	140.46	—	—	140.46	14.05	—
Fertilizer (FC)	—	—	—	—	—	—
Crop chemicals (CC)	43.31	—	—	67.66	15.33	15.33
Machinery (MC)	65.97	—	—	173.52	14.99	10.49
Areal harvest (AHC)	36.95	36.95	36.95	—	36.95	36.95
Yield-based harvest (YHC)	66.08	131.97	131.97	—	66.08	131.97
Subtotal	352.77	168.92	168.92	381.64	147.40	194.74
Biomass transport: CT	112.73	221.72	221.72	—	112.73	221.72
Biomass transport: RT	56.13	110.40	110.40	—	56.13	110.40
Biomass transport: NT	49.67	97.69	97.69	—	49.67	97.69
+F fertilizer option						
Seed (SC)	140.46	—	—	140.46	14.05	—
Fertilizer (FC)	—	80.48	80.48	—	80.48	80.48
Crop chemicals (CC)	43.31	—	—	67.66	15.33	15.33
Machinery (MC)	65.97	13.98	13.98	173.52	28.97	24.47
Areal harvest (AHC)	36.95	36.95	36.95	—	36.95	36.95
Yield-based harvest (YHC)	92.93	186.02	186.02	—	92.93	186.02
Subtotal	379.62	317.43	317.43	381.64	268.71	343.25
Biomass transport: CT	160.97	318.93	318.93	—	160.97	318.93
Biomass transport: RT	80.07	158.27	158.27	—	80.07	158.27
Biomass transport: NT	70.61	139.78	139.78	—	70.61	139.78

$$LDC_{imnl}^x \begin{cases} 24.28 & \text{for } LW_{imnl}^x < 9 \\ 24.79 & \text{for } 9 \leq LW_{imnl}^x \leq 18 \\ 27.41 & \text{for } LW_{imnl}^x > 18 \end{cases},$$

$$TC_{imnl}^x \begin{cases} 2.88 & \text{for } LW_{imnl}^x < 9 \\ 3.10 & \text{for } 9 \leq LW_{imnl}^x \leq 18 \\ 3.16 & \text{for } LW_{imnl}^x > 18 \end{cases}.$$

i represents a soil growing switchgrass under establishment scenario m (LC or HC) and fertilizer option n ($-F$ or $+F$), L is the number of full tractor-trailer loads, l is a tractor-trailer load, LDC is the loading cost for a tractor-trailer load, TC is the transport cost for a tractor-trailer load ($\$ \text{ km}^{-1}$), TD is the transportation distance to the nearest potential biorefinery location (Section 4.3.2), the x^{th} element of YS is a yield scalar for the t^{th} year of production, BY is biomass yield, r is the interest rate (5%), and T is the time horizon (10 yrs). Calculations of L and LW assume that a full tractor-trailer has a capacity of 24.48 Mg (36 bales weighing 0.68 Mg each; Hoque et al., 2015) and that harvested bales contain 800 g kg^{-1} dry matter. Values for LDC and TC are average North Dakota custom rates across 2010, 2013, and 2015 (Aakre, 2014; NDSU, 2016; USDA NASS, 2010a). Finally, YS implements the delayed realization of full yield potential in the HC scenario when compared to the LC scenario. Study region average transportation expenses under the HC and LC scenarios and $-F$ and $+F$ fertilizer options are presented in Table 15.

4.3.5. Switchgrass parity price

Following James et al. (2010), the economic competitiveness of switchgrass is characterized by the biomass price required for switchgrass to generate the same net return as a defender system (i.e. corn or wheat produced for grain and biomass, in a balanced rotation with soybean produced for grain). Equations [38] to [44] describe the estimation of the switchgrass parity price; a companion summary is presented in Table 12.

The formula to calculate the switchgrass parity price (SPP , in $\$ \text{ Mg}^{-1}$) of cellulosic

biomass is adapted from Hilker et al. (1987):

$$SPP_{ijkmn} = \frac{[ANPV(VCS_{imn}) + ANPV(OCD_{ijk})]}{[ANPV(BYS_{imn}) - ANPV(BYD_{ijk})]} \quad [38]$$

where i is a soil growing switchgrass under establishment scenario m and fertilizer option n or growing corn or wheat j under tillage system k , $ANPV$ is the annualized net present value (e.g. Equation [35]), VCS is the variable cost of producing switchgrass as a biomass crop ($\$ \text{ ha}^{-1}$), OCD is the opportunity cost of lost net revenue from the defender system, BYS is the biomass yield for switchgrass (Mg ha^{-1}), and BYD is the biomass yield for the defender system. In the denominator, BYD is subtracted from BYS to measure switchgrass' net gain in cellulosic biomass above what the defender system would offer, assuming equal prices across cellulosic biomass sources.

In Equation [38], OCD is defined as the grain-only revenue above all costs associated with the production and harvest of both grain and stover. Since corn and wheat cropping systems were represented by two-year rotations with soybean, the net present value (NPV) of OCD was estimated as

$$NPV(OCD_{ijk}) = \sum_{t=1}^{T/2} \left[\left(\frac{GR_{ijk} - GE_{ijk} - HE_{ijk} - TE_{ijk}}{(1+r)^{(2t-1)}} \right) + \left(\frac{SBR_{ijk} - SBE_{ijk}}{(1+r)^{2t}} \right) \right] \quad [39]$$

where GR is grain revenue (Equation [28], Figure 33a), GE is grain expense (Equation [29], Figure 33b), HE is biomass harvest expense (Equation [32], Figure 33c), TE is biomass transport expense (Equation [34], Figure 33d), SBR is soybean revenue, SBE is soybean expense, t is the time of cash flow, and T is the time horizon (10 yrs). While corn and wheat ALMANAC simulations included soybean as a rotational crop, ALMANAC did not effectively simulate spatial patterns in soybean yield across the study area (data not shown). Thus, SBR and SBE were defined by linear regression relationships derived from 2010 to 2015 FINBIN data (FINBIN, 2019). With revenue defined as the 'total product return per acre' variable returned by FINBIN and expenses defined as the sum of the five direct expenses used to estimate GE

(Equation [29]), annual 2010 to 2015 revenue and expenses for corn, wheat, and soybean were queried from FINBIN with USDA Agricultural Districts (USDA NASS, 2019) as aggregation units. Subsequently, simple linear regressions were performed for corn and wheat variables against corresponding soybean variables. The resulting regression equations (Appendix C, Figure 71) were used to predict SBR and SBE as a function of GR and GE :

$$SBR_{ijk} = \begin{cases} GR_{ijk} \times 0.42 + 402 & \text{for } j = \text{corn}; p < 0.0001; R^2 = 0.57 \\ GR_{ijk} \times 1.01 + 109 & \text{for } j = \text{wheat}; p < 0.0001; R^2 = 0.55 \end{cases}, \text{ and} \quad [40]$$

$$SBE_{ijk} = \begin{cases} GE_{ijk} \times 0.27 + 214 & \text{for } j = \text{corn}; p < 0.0001; R^2 = 0.50 \\ GE_{ijk} \times 0.52 + 173 & \text{for } j = \text{wheat}; p < 0.0001; R^2 = 0.52 \end{cases}. \quad [41]$$

As the defender system assumes a balanced rotation with soybean, the biomass yield of the defender system (BYD ; Equation [38]) includes no biomass yield in the years where soybean is grown. Therefore, the net present value (NPV) of BYD was calculated as

$$NPV (BYD_{ijk}) = \sum_{t=1}^{T/2} \left[\left(\frac{BY_{ijk}}{(1+r)^{(2t-1)}} \right) + \left(\frac{0}{(1+r)^{2t}} \right) \right] \quad [42]$$

where i represents a soil growing crop j under tillage system k , BY is the average biomass yield for 2006 to 2015 weather conditions (Section 4.3.1), r is the interest rate of 5%, t is the time of realized yield, and T is the time horizon of 10 yrs.

The net present value of the variable cost of producing switchgrass as a biomass crop ($NPV (VCS)$; Equation [38]) was calculated as

$$NPV (VCS_{imm}) = NPV (PE_{imm}) + NPV (TE_{imm}) \quad [43]$$

where i is a soil growing switchgrass in establishment scenario m (LC or HC) and fertilizer option n ($-F$ or $+F$), $NPV (PE)$ is the net present value of production expense (Equation [36]), and $NPV (TE)$ is the net present value of transport expense (Equation [37]). As described

in Table 10, biomass yields under LC and HC establishment reflect the varying levels of stand establishment success chronicled in the literature. Thus, the net present value (*NPV*) of switchgrass biomass yield (*BYS*; Equation [38]) was calculated as

$$NPV (BYS_{imm}) = \sum_{t=1}^T \left(\frac{YS_m^x \times BY_{imn}}{(1+r)^t} \right),$$

$$\text{where } x \begin{cases} t & \text{for } t \leq 2 \\ 3 & \text{otherwise} \end{cases}, \quad [44]$$

$$YS_m \begin{cases} (0.5, 1.0, 1.0) & \text{for } m = \text{LC} \\ (0.0, 0.5, 1.0) & \text{for } m = \text{HC} \end{cases},$$

i represents a soil growing switchgrass under establishment scenario *m* (LC or HC) and fertilizer option *n* (−F or +F), *r* is the interest rate of 5%, *t* is the time of realized yield, *T* is the time horizon of 10 yrs, *BY* is the average biomass yield for 2006 to 2015 weather conditions (Section 4.3.1), and the *x*th element of *YS* is a yield scalar for the *t*th year of production.

Several treatment factors are embedded in the four variables used to calculate *SPP* (Equation [38]). Calculations of *OCD* (Equation [39]) and *BYD* (Equation [42]) include three tillage systems (conventional tillage [CT], reduced tillage [RT], and no-till [NT]) and two cropping systems (corn-soybean and wheat-soybean) as treatment factors. Meanwhile, calculations of *VCS* (Equation [43]) and *BYS* (Equation [44]) include two switchgrass establishment scenarios (LC and HC) and two fertilization options (−F and +F) as factors. Therefore, this factorial treatment arrangement resulted in 24 separate *SPP* datasets. For display in the Results and Discussion (Section 4.4), these 24 separate datasets were consolidated into 6 composites. Figure 36 illustrates the process for consolidating the eight RT outcomes into two. First, a composite dataset was created to combine the *SPP* estimates across its competing corn-soybean and wheat-soybean systems (Figure 36a); for each cell, the competing system with a greater *SPP* is displayed. This effectively compares switchgrass to the system that is most economically competitive with switchgrass production. Subsequently, a composite dataset was

created to combine the *SPP* outputs from Figure 36a across the two switchgrass fertilization options; for each cell, the lesser *SPP* estimate is displayed (Figure 36b). This effectively displays the switchgrass fertilization option that is most economically competitive with its competing corn-soybean or wheat-soybean system. Figures 72 and 73 (Appendix C) display the analogous processes of generating composite datasets for *SPP* relative to competing CT and NT systems. These six composite datasets were used for all derivative analyses including *SPP* as an input.

4.3.6. Environmental outcomes

Environmental outcomes of corn-soybean, wheat-soybean, and switchgrass cropping systems were evaluated by their effects on soil erosion by water, N runoff, and C sequestration. Soil erosion was estimated by the Revised Universal Soil Loss Equation within ALMANAC. Nitrogen runoff was defined as the sum of ALMANAC outputs for organic N loss with sediment (YON) and nitrate loss in surface runoff (YNO3), with YNO3 converted to an elemental N basis. Raster datasets of soil erosion and N runoff under corn-soybean and wheat-soybean systems were subsequently subtracted from a corresponding switchgrass raster; all subsequent analyses consider soil erosion mitigation and N runoff mitigation for switchgrass relative to a competing corn-soybean or wheat-soybean system.

Carbon sequestration was estimated by the inventory method of West et al. (2008). Briefly, this method assumes that the soil C concentrations from SSURGO represent steady-state values following decades of cropping under CT. The expected accumulation in soil C following decreased tillage intensity is assumed to occur at a linear rate. The linear rates of soil C accumulation are expressed as a fraction of soil C and are adjusted for baseline (i.e. SSURGO) soil C values. Higher baseline soil C values result in decreased rates of soil C accumulation. For initial soil C of 2 to 10 kgC m⁻², the C accumulation adjustment factor ranged from 1.2 to 0.3; adjustment factors were bound by these extremes when baseline soil C values fell outside this range. In this investigation, the soil C accumulation rate for CRP grassland was used to represent switchgrass, and soil C accumulation rates associated with

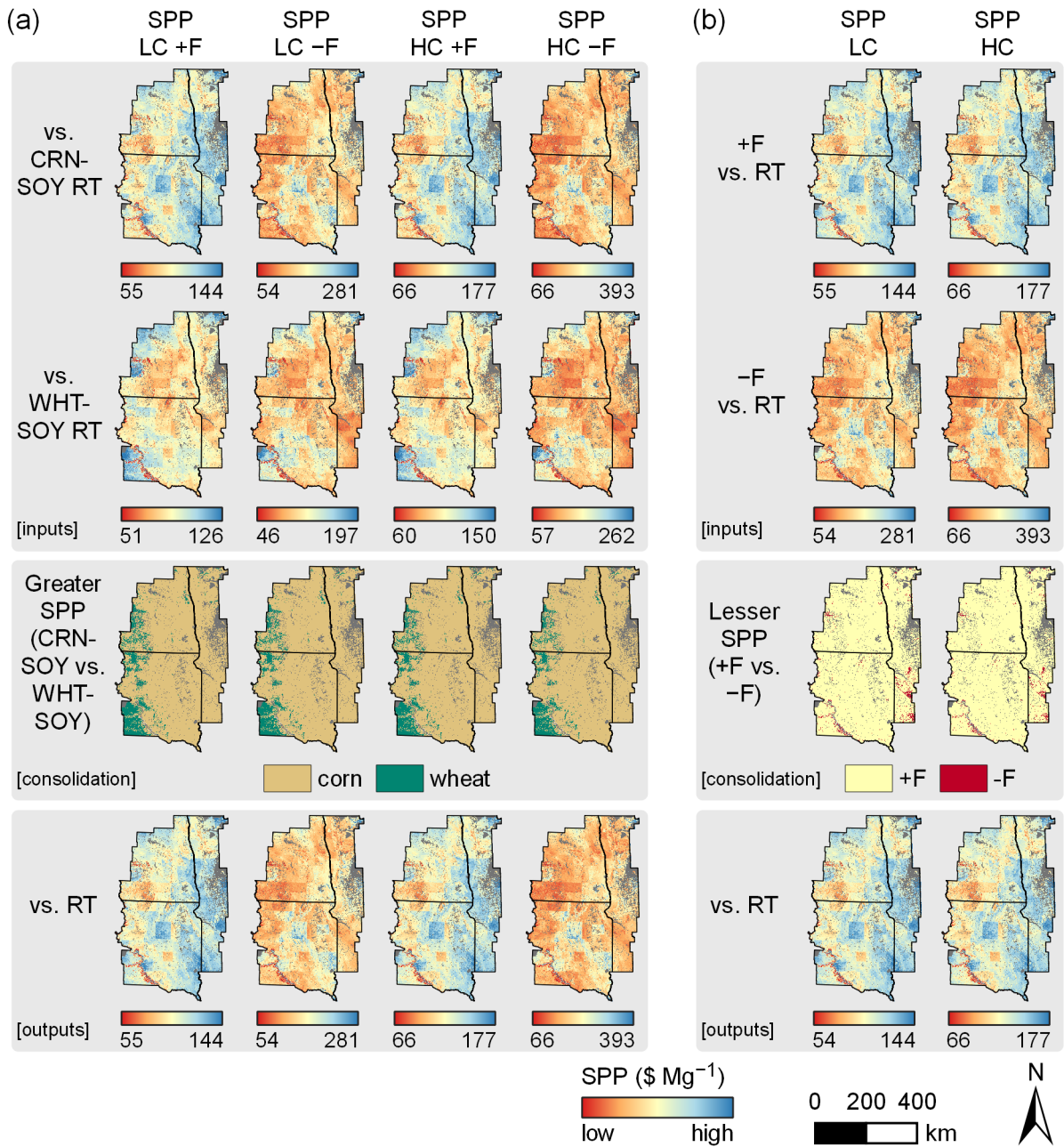


Figure 36. Consolidation of switchgrass parity price (SPP) estimates across (a) its competing cropping systems in a reduced tillage (RT) system and (b) management systems with (+F) or without (-F) fertilizer applications. In (a), SPP estimates for all combinations of establishment scenario (low-cost [LC] or high-cost [HC]) and fertilizer application are consolidated by keeping the competing cropping system requiring the greatest SPP (corn-soybean [CRN-SOY] or wheat-soybean [WHT-SOY]). In (b), the LC and HC outputs from (a) are consolidated to keep the lowest SPP across the +F and -F options.

switchgrass production were expressed relative to a competing corn or wheat system. The unadjusted soil C accumulation rate for switchgrass was $31.4 \text{ g kg}^{-1} \text{ yr}^{-1}$ (West et al., 2008). Corresponding rates for corn were $0 \text{ g kg}^{-1} \text{ yr}^{-1}$ for CT, $5.2 \text{ g kg}^{-1} \text{ yr}^{-1}$ for RT, and $10.4 \text{ g kg}^{-1} \text{ yr}^{-1}$ for NT, while corresponding rates for wheat were $0 \text{ g kg}^{-1} \text{ yr}^{-1}$ for CT, $4.7 \text{ g kg}^{-1} \text{ yr}^{-1}$ for RT, and $9.3 \text{ g kg}^{-1} \text{ yr}^{-1}$ for NT. Spatially-explicit estimates of switchgrass soil C sequestration relative to corn or wheat ($CSEQ$) were calculated as

$$CSEQ_{ijk} = \sum_{y=1}^n [(31.4 - AR_{jk}) \times BD_{iy} \times D_{iy}] \quad [45]$$

where y is a layer in soil i , 31.4 is the soil C accumulation rate for switchgrass, AR is the soil C accumulation rate for corn or wheat j in tillage system k , BD is soil bulk density, and D is soil depth. Soil bulk density and depth were provided by SSURGO. Consistent with the method of West et al. (2008), the bottom layer of each soil was extended to a depth of 3 m.

4.3.7. Supplanting corn or wheat with switchgrass

This investigation considers the outcomes from converting 82, 164, 246, 328, or 410 ha $\times 10^3$ of existing corn or wheat lands to switchgrass production, which represents 1 to 5% of all corn and wheat parcels assumed eligible for conversion to switchgrass. The upper limit of this range was chosen to align with recent estimates of net grassland-to-agriculture conversions for Minnesota, North Dakota, and South Dakota: Wright and Wimberly (2013) estimated net grassland conversion to corn and soybean of 351,000 ha from 2006 to 2011, while Lark et al. (2015) estimated net grassland conversion to cropland of 357,000 ha from 2008 to 2012. We assume that corn and wheat lands eligible for conversion to switchgrass belong to two broad categories: lands highly suitable for cultivated cropping and oftentimes planted to corn and wheat, and physically marginal lands (i.e. lands less suitable for cultivated cropping) with any recent history of corn or wheat production. Specifically, eligible parcels were those with an LCC of 1 or 2 and at least five years of corn or wheat production from 2006 to 2015, along with those having an LCC of 3 or greater and at least one year of corn or wheat production

from 2006 to 2015 (Figure 31f). Areas of corn and wheat production were identified using the modified CDLs described in Section 4.3.2. For switchgrass to supplant existing corn or wheat parcels, we assume that it would need to generate the same economic returns as its competing corn-soybean or wheat-soybean system at a biomass price of \$60 Mg⁻¹. The switchgrass subsidy (*SS*; in \$) necessary to ensure this outcome was calculated as

$$SS_{ijkmn} = (SPP_{ijkmn} - 60) \times ANPV(BYS_{imn}) \quad [46]$$

where *SPP* is the parity price (Equation [38]) for switchgrass grown in parcel *i* under establishment scenario *m* and fertilizer option *n* relative to corn or wheat *j* under tillage system *k*, and *ANPV*(*BYS*_{*imn*}) is the annualized net present value of 10-year switchgrass biomass yields (Equations [35] and [44]).

This investigation contrasts two methods for prioritizing corn and wheat parcels for conversion to switchgrass. The first method indexes parcels based on the marginal gain in biomass production per dollar spent on *SS*. The subsidized biomass production index (*SBPI*) was calculated as

$$SBPI_{ijkmn} = SS_{ijkmn} / [ANPV(BYS_{imn}) - ANPV(BYD_{ijk})] \quad [47]$$

where *SS* is the subsidy for switchgrass grown in parcel *i* under establishment scenario *m* and fertilizer option *n* relative to corn or wheat *j* under tillage system *k*, *ANPV*(*BYS*_{*imn*}) is the annualized net present value of 10-year switchgrass biomass yields (Equations [35] and [44]), and *ANPV*(*BYD*_{*ijk*}) is the annualized net present value of 10-year defender system (corn-soybean or wheat-soybean) biomass yields (Equations [35] and [42]).

The second method for prioritizing conversions of corn and wheat lands indexes parcels based on the gain in environmental services from growing switchgrass. This necessitated the estimation of baseline environmental service valuations for the soil erosion mitigation, N loss mitigation, and C sequestration associated with switchgrass production. The baseline

valuation of soil erosion mitigation is \$4.55 Mg-soil⁻¹ and represents the mean valuation across the 99 study region counties for 13 items impacted by soil erosion (irrigation ditches and canals, marine recreational fishing, freshwater fisheries, marine fisheries, flood damages, road drainage ditches, municipal and industrial water use, municipal water treatment, steam power plants, soil productivity, water-based recreation, navigation, and reservoir services). County-level valuations were taken from Hansen and Ribaudo (2008), who provide regional dollar-per-ton estimates of soil conservation benefits for each county in the contiguous US. Sobota et al. (2015) provides low, median, and high damage cost estimates of anthropogenic reactive N release for the coterminous US. The baseline valuation for mitigation of N runoff in this investigation is \$19.32 kgN⁻¹, which is the summation of median damage cost estimates from Sobota et al. (2015) for three drinking water system variables (undesirable odor and taste, nitrate contamination, increased colon cancer risk) and four freshwater system variables (declining waterfront property value, loss of recreational use, loss of endangered species, increased eutrophication) impacted by surface freshwater N loading. We used \$118 MgC⁻¹ as the baseline valuation of C sequestration, which is the mean value from the United States Interagency Working Group (2016) for 2010 assuming a discount rate of 3%. With social cost of C estimates ranging widely in the literature, from under \$35 MgC⁻¹ to over \$669 MgC⁻¹ (Tol, 2011), we chose this value as a reasonable proxy for potential C payments by a US government agency. The three environmental services valuations were then used to calculate the subsidized environmental services index (*SESI*) as follows:

$$SESI_{ijkmn} = SS_{ijkmn} / [(SMIT_{ijkn} \times 4.55) + (NMIT_{ijkn} \times 19.32) + (CSEQ_{ijk} \times 118)] \quad [48]$$

where *SS* is the subsidy for switchgrass grown in parcel *i* under establishment scenario *m* and fertilizer option *n* relative to corn or wheat *j* under tillage system *k*, and *SMIT*, *NMIT*, and *CSEQ* are the soil erosion mitigation, N runoff mitigation, and C sequestration (Equation [45]) of switchgrass production.

It is assumed that the parcels with the lowest values of *SBPI* and *SESI* would be the first converted to switchgrass production. Given a parcel size of approximately 64 ha, the values for the levels of *SBPI* and *SESI* necessary to convert 82, 164, 246, 328, and 410 ha $\times 10^3$ to switchgrass (1 to 5% of eligible corn and wheat parcels) were determined by extracting the 1278, 2557, 3836, 5115, and 6394th elements of *SBPI* and *SESI* vectors sorted in ascending order. For further analyses characterizing the impacts of these conversions, the spatial positions of cells with *SBPI* or *SESI* at or below these thresholds were used to extract values from corresponding raster datasets of biomass production, soil erosion, N runoff, C sequestration, and LCC.

4.3.8. Embedded assumptions

Results presented in Sections 4.4.1 to 4.4.7 reflect several assumptions embedded within the methods presented in Sections 4.3.2 to 4.3.7. The technical availability of corn and wheat biomass is defined as the amount of biomass available within collection areas of potential biorefineries (Section 4.4.1). The methodology for estimating the locations of feasible biorefineries uses spatial patterns of corn and wheat production from 2006 to 2015 (Section 4.3.2) and assumes that all available corn or wheat biomass is harvested. The economic availability of corn and wheat biomass is defined by the biomass breakeven price (Section 4.4.2), which represents the biomass price necessary to cover expenses associated with crop residue collection and transportation of crop residues to the nearest biorefinery (Section 4.3.3). Estimation of transportation expenses assumes a straight-line distance to the biorefinery (i.e. does not consider existing road networks).

Estimated switchgrass substitutions of existing corn and wheat parcels (Section 4.4.5) consider the biomass price necessary for switchgrass to earn economic returns equivalent to a competing corn-soybean or wheat-soybean system (i.e. the switchgrass parity price). The switchgrass parity price contrasts the annualized net present value of 10-year switchgrass returns to the annualized net present value of 10-year returns from a competing corn-soybean or wheat-soybean system (Section 4.3.5). Thus, it is assumed that economic return over 10 years

is the sole criterion for determining the conversion of corn or wheat parcels to switchgrass production. For the competing corn-soybean or wheat-soybean system, this methodology assumes constant revenue and expenses and no cropping sequence alterations over the 10-year time period. Although switchgrass substitutions were limited to a subset of existing corn and wheat parcels (Section 4.3.7), substitutions were not limited to biorefinery collection areas. This allowed for the estimation of switchgrass proliferation across the study region, and the estimation of biorefinery proliferation across the study region in response to expanded switchgrass production (Section 4.4.6).

4.4. Results and Discussion

4.4.1. Technical availability of corn and wheat biomass

Removal of crop residues for biomass harvest involves tradeoffs between energy production and environmental services such as reduced erosion by wind and water, decreased runoff and non-point agricultural pollution, soil water retention, maintained or improved soil organic matter, promotion of healthy soil biological activity, and maintenance of agricultural productivity (Blanco-Canqui and Lal, 2009b). Thus, one aspect of technical biomass availability is the maximum amount of residue that can be removed from fields while maintaining soil organic C and limiting soil erosion from wind and water (Muth and Bryden, 2013; Muth et al., 2013). Nonetheless, the spatial distribution of available crop residues is also important, as cellulosic biorefineries require sufficient availability of nearby biomass to meet their annual production goals. Although corn and wheat biomass yields are displayed for all parcels containing soils deemed suitable for biomass cropping, this investigation defines technically-available biomass as the biomass available within biorefinery collection areas. Biorefinery collection areas feature collection radii from 8 to 112 km in 8-km intervals and are supplied by corn and wheat residue, assuming sustainable residue removal rates (Muth et al., 2013) and remotely-sensed spatial patterns of corn and wheat production from 2006 to 2015.

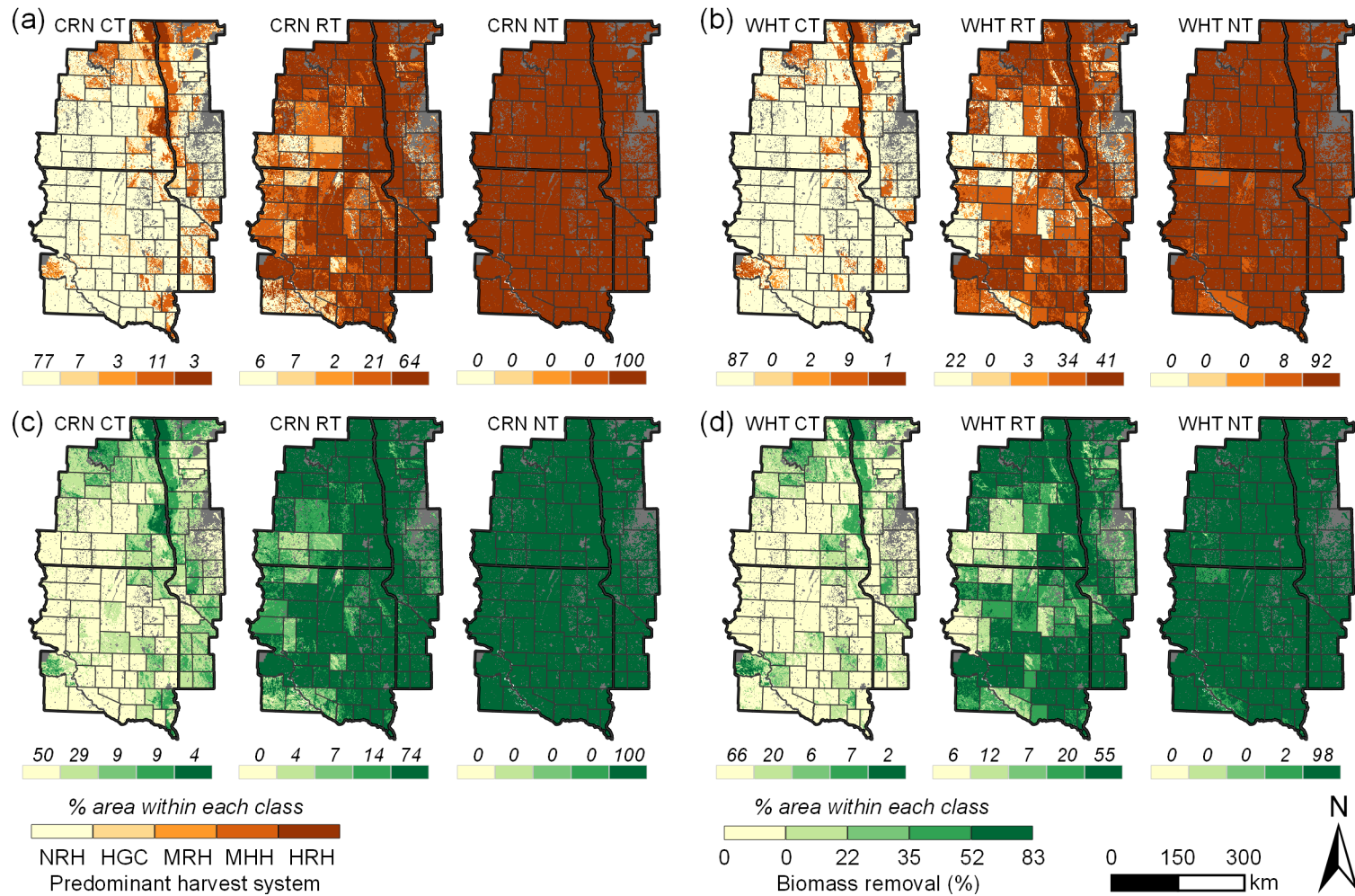


Figure 37. For (a) corn (CRN) and (b) wheat (WHT), the predominant harvest system (see Table 11) within each parcel and the percent of parcels within each classification under conventional tillage (CT), reduced tillage (RT), and no-till (NT) systems. For (c) CRN and (d) WHT, the percent biomass removal within each parcel and the percent of parcels within each classification under the CT, RT, and NT systems. Percent biomass removal is a continuous variable due to the mixing of biomass harvest systems within parcels.

4.4.1. 1. Residue harvest systems

Study region allocations of biomass harvest systems (Table 11) and residue removal rates are shown in Figure 37. Collectively, the CT, RT, and NT systems represent a broad range of possible biomass removal outcomes. The CT system represents a conservative approach to biomass collection, with no corn or wheat residue collection over 50% and 66% of the study region, respectively, and residue removal allocated primarily to the high-productivity areas along the border of Minnesota and the Dakotas (Figure 37c, ‘CRN CT’; Figure 37d, ‘WHT CT’). Residue removal rates of 0 to 22% are predominant among harvestable parcels in the CT system, consistent with residue removal rates of 20 to 25% currently recommended for commercial-scale corn biomass harvest (Wirt, 2014) and slightly higher than the residue removal rates of 0 to 16% acceptable for CT wheat with grain yields similar to those estimated in this study (Johnson et al., 2006; Tarkalson et al., 2011). In contrast, the NT system features residue removal rates of 52 to 83% across the entire study area for corn (Figure 37c, ‘CRN NT’) and 98% of the study area for wheat (Figure 37d, ‘WHT NT’), thus representing a best-case scenario for crop residue availability. The RT system features residue removal rates intermediate of the CT and NT rates, with the highest possible residue removal rates across most of the study area but lesser rates in the lower-yielding western areas of the study region (Figure 37c, ‘CRN RT’; Figure 37d, ‘WHT RT’).

4.4.1. 2. Biomass yields

Estimated grain yields and biomass removal for corn and wheat are displayed in Figure 39. Grain yields for each crop are similar across tillage systems but decrease from east to west across the study region, ranging from 10.94 to 4.56 Mg ha⁻¹ for corn (Figure 39a) and 4.17 to 2.36 Mg ha⁻¹ for wheat (Figure 39b). These spatial patterns are consistent with those of USDA county-average yields (Section 3.4.1) and are expected due to the drier climate of the western study region (PRISM Climate Group, 2019). The median corn grain yield of 7.75 Mg ha⁻¹ is more than twice the median wheat yield of 3.33 Mg ha⁻¹, due to the greater simulated radiation-use efficiency and harvest index of corn relative to wheat

(39.0 vs. 28.0 kg ha⁻¹ MJ⁻¹ m⁻², 0.56 vs. 0.42). However, due to the greater allocation of aboveground biomass towards grain production in corn, the median biomass removal for corn is only modestly greater than wheat (4.35 vs. 3.52 Mg ha⁻¹).

Gradients in biomass removal across the study region and among tillage practices reflect the agricultural productivity of the landscape and the estimated residue removal rates of the CT, RT, and NT systems. Due to low residue removal rates (Figure 37c, 'CRN CT' and Figure 37d, 'WHT CT'), biomass removal is almost entirely below the median value under the CT system, ranging from 1.40 to 4.35 Mg ha⁻¹ in corn (Figure 39c, 'CT') and 1.54 to 3.52 Mg ha⁻¹ in wheat (Figure 39d, 'CT'). With increasing residue removal rates (Figure 37c, 'CRN RT', 'CRN NT'; Figure 37d, 'WHT RT', 'WHT NT'), biomass removal exceeding the median value becomes more prevalent under the RT system and is predominant in all areas outside the far western portion of the study area under the NT system. The greatest biomass removal in the NT system ranges from 5.19 to 6.39 Mg ha⁻¹ in corn (Figure 39c, 'NT') and 4.03 to 4.55 Mg ha⁻¹ in wheat (Figure 39d, 'NT'). Estimated corn biomass removal rates are supported by the field observations of Karlen et al. (2014), where a moderate removal treatment yielded an average of 2.5 to 4.2 Mg ha⁻¹ across nine southern Minnesota locations and one eastern South Dakota location from 2008 to 2012; corresponding biomass yields for a high removal treatment were 6.0 to 12.4 Mg ha⁻¹. Similar to this investigation, average grain yield across the nine Minnesota sites and one South Dakota site of Karlen et al. (2014) was unaffected by residue removal. This is consistent with unchanged to slightly increased grain yields observed across the full dataset spanning 239 site-years of field research at 36 sites in seven different states (Karlen et al., 2014).

4.4.1. 3. Potential biorefineries

Estimated locations of potential biorefineries (Figure 38) identify existing corn and wheat production areas with the potential to support bioenergy production. Each location identifies a collection area necessary to supply a consistent annual supply of 258.5 Gg biomass from areas of existing corn and wheat production (Figure 31d,e). Potential biorefineries with

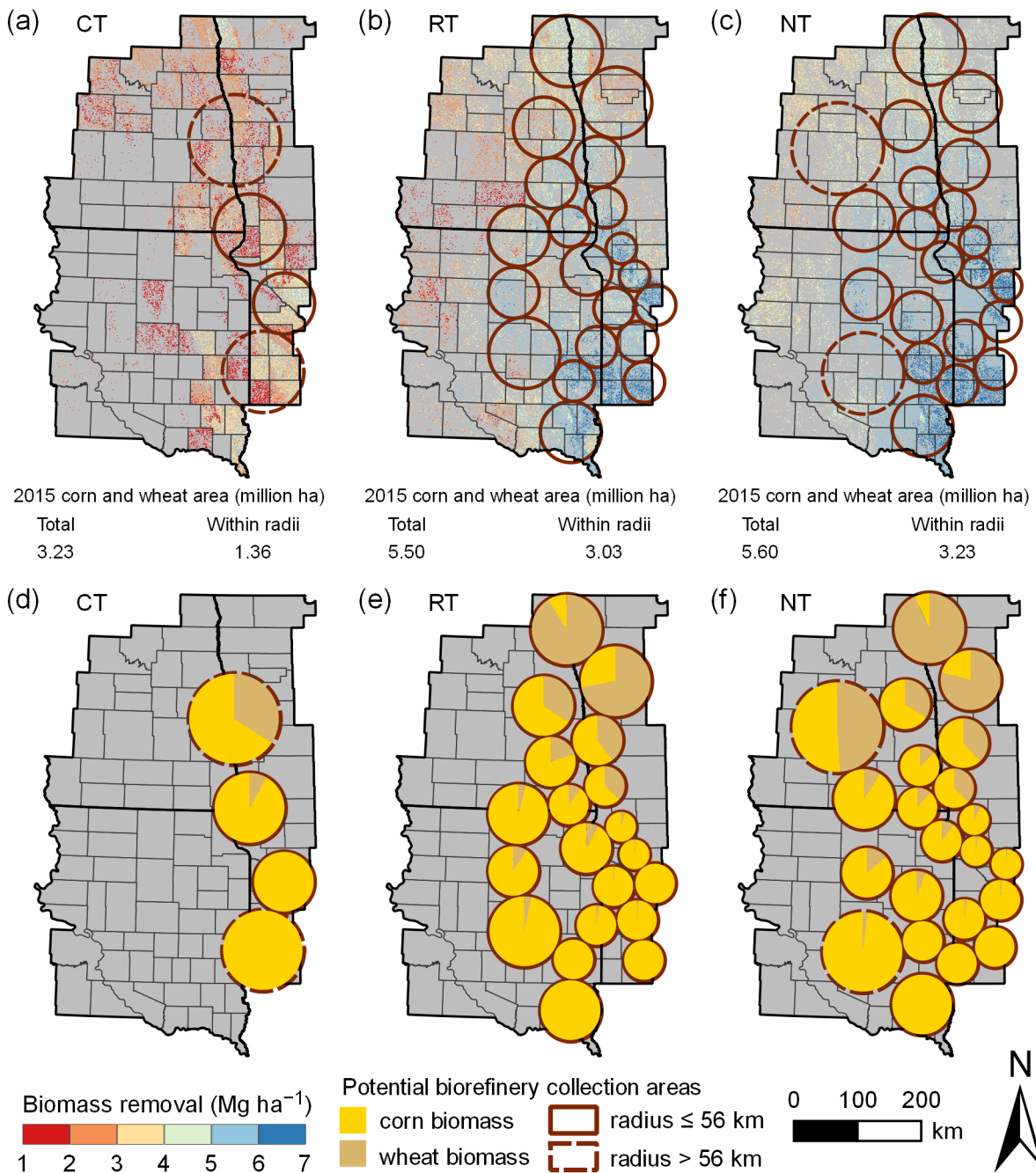


Figure 38. Collection areas for potential biorefineries under (a) conventional tillage (CT), (b) reduced tillage (RT), and (c) no-till (NT) systems. As an example of biomass harvest extent for a single year, corn or wheat biomass removal (from Figure 39) is displayed for each parcel with corn and wheat production according to the 2015 Cropland Data Layer. (d – f) Under each tillage system, the relative fractions of corn and wheat biomass supplying each potential biorefinery location.

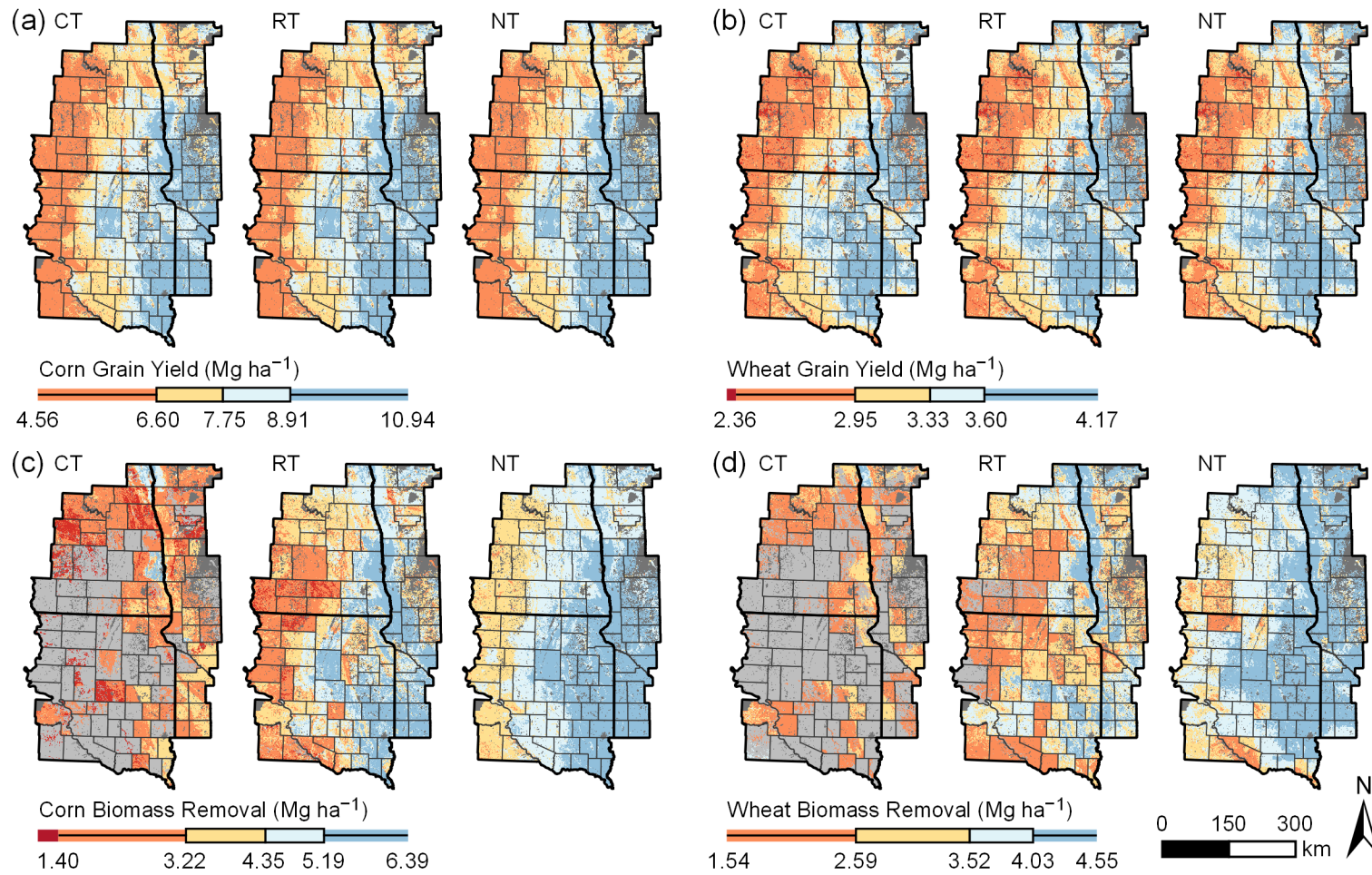


Figure 39. Simulated (a) corn and (b) wheat grain yield under conventional tillage (CT), reduced tillage (RT), and no-till (NT) systems. Simulated (c) corn and (d) wheat biomass removal under the CT, RT, and NT systems. Biomass removal reflects the harvest systems in Figure 37.

a collection radius of 56 km or less match the biomass requirement and collection radius of PoetDSM Project LIBERTY, an existing cellulosic ethanol refinery in Emmetsburg, IA utilizing corn biomass as a feedstock (POET-DSM, 2015). Potential biorefineries with collection radii greater than 56 km feature an adequate annual supply of biomass, but may be less viable than biorefineries requiring a smaller collection radius. Biorefinery collection areas occur across a limited spatial extent in the CT system, within 90 km to the east or west of the Minnesota-Dakotas border (Figure 38a). The RT and NT systems allow for biomass collection across a much greater spatial extent, with collection radii of 56 km or less extending across almost all of western Minnesota and up to 185 km west of the Minnesota-Dakotas border (Figure 38b,c). In the NT system, further westward expansion is allowed under collection radii greater than 56 km. With the exception of potential biorefineries in far northwest Minnesota under RT and NT systems, corn is the primary biomass source across the study region for all tillage systems (Figure 38d-f). Nonetheless, wheat provides a portion of the biomass for each potential biorefinery except for those in far southeast South Dakota and southwest Minnesota.

This analysis demonstrates that existing areas of corn and wheat production can provide sufficient biomass for commercial-scale biofuel production, especially under the biomass collection rates assumed for RT and NT systems. Mean annual biomass production is 2.32 Tg within the four CT collection radii, with 0.90 Tg available within the two radii having a radius of 56 km or less. Biorefinery collection radii contain an annual supply of 13.98 Tg under RT and 16.48 Tg under NT, with 14.29 Tg within NT radii having a collection radius of 56 km or less. Assuming a commercially attainable ethanol conversion rate of 0.29 L kg^{-1} (Sapp, 2017), which is conservative relative to the estimate of 0.38 L kg^{-1} cited elsewhere (e.g. Gelfand et al., 2013; Schmer et al., 2008), cellulosic ethanol production of 0.65, 4.05, and 4.78 GL is possible within the CT, RT, and NT biorefineries. If used to produce E85 transportation fuel, this is equivalent to 0.56 to 4.13 GL of gasoline on an equivalent energy basis (US DOE, 2019), which represents 4 to 33% of mean annual gasoline consumption for the transportation sector in Minnesota, North Dakota, and South Dakota from 2006 to 2015 (US EIA, 2019).

Clearly, there exists a sufficient technical supply to provide meaningful biofuel production to the region.

4.4.2. Economic availability of corn and wheat biomass

In addition to requiring a sufficient supply of biomass to meet annual production goals, cellulosic bioenergy companies will require biomass at prices that enable profitable operation of their biorefineries. Establishing reasonable prices for cellulosic biomass is difficult, as no commercial marketplace for cellulosic biomass currently exists. Nonetheless, comparisons in this investigation assume that biomass prices of \$30 to \$60 Mg⁻¹ are a reasonable proxy for market value. In this investigation, the economic availability of corn and wheat biomass is defined as the quantity of biomass available within biorefinery collection areas at a given breakeven price. Breakeven price represents the minimum biomass price necessary to cover harvest and transport expenses associated with biomass collection, and its calculation is dependent on the biomass yields described in Section 4.4.1.

4.4.2. 1. Estimated revenue and expenses

Figures 40 and 41 show the spatial patterns of grain revenue, expense, and profit in corn and wheat, as well as the spatial extents of biomass harvest expense, transport expense, and breakeven price. Spatial patterns in grain revenue (Figure 40a–c and Figure 41a–c, ‘GR’) are the same as those for grain yield (Figure 39a,b), with decreasing values from east to west across the study region and little difference across the CT, RT, and NT systems. Spatial patterns in grain expense (Figure 40a–c and Figure 41a–c, ‘GE’) reflect estimated N fertilizer rates for corn and wheat (Section 3.3.3; Figure 13a,c) and planting rates for corn (Section 3.3.3; Figure 14c), and also reflect differences in estimated grain expenses across the CT, RT, and NT systems (Section 4.3.3).

When spatial patterns of grain expense are subtracted from grain revenue, the resulting patterns of grain profit are similar to those of grain revenue. Median corn profitability is \$422 ha⁻¹, with values ranging from \$422 to \$923 ha⁻¹ in the eastern study region and from \$–60 to \$422 ha⁻¹ in the western study region (Figure 40a–c, ‘GPF’). Wheat is generally less

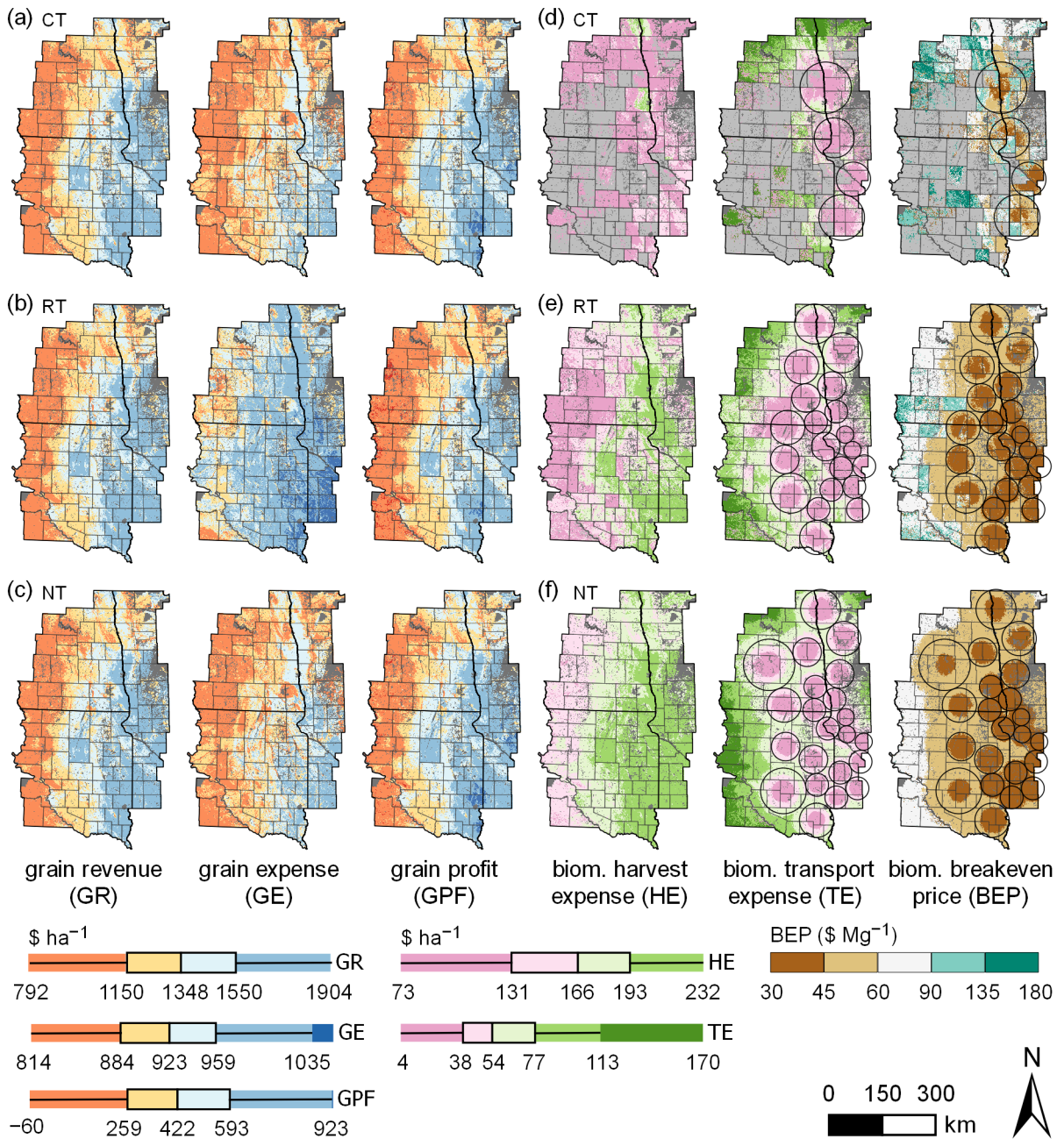


Figure 40. Estimated revenue, expense, and profit for corn grain production under (a) conventional tillage (CT), (b) reduced tillage (RT), and (c) no-till (NT) systems. Estimated harvest expense, transport expense, and breakeven price for corn biomass production under (d) CT, (e) RT, and (f) NT systems. Overlain on transport expense and breakeven price are the biorefinery collection areas from Figure 38.

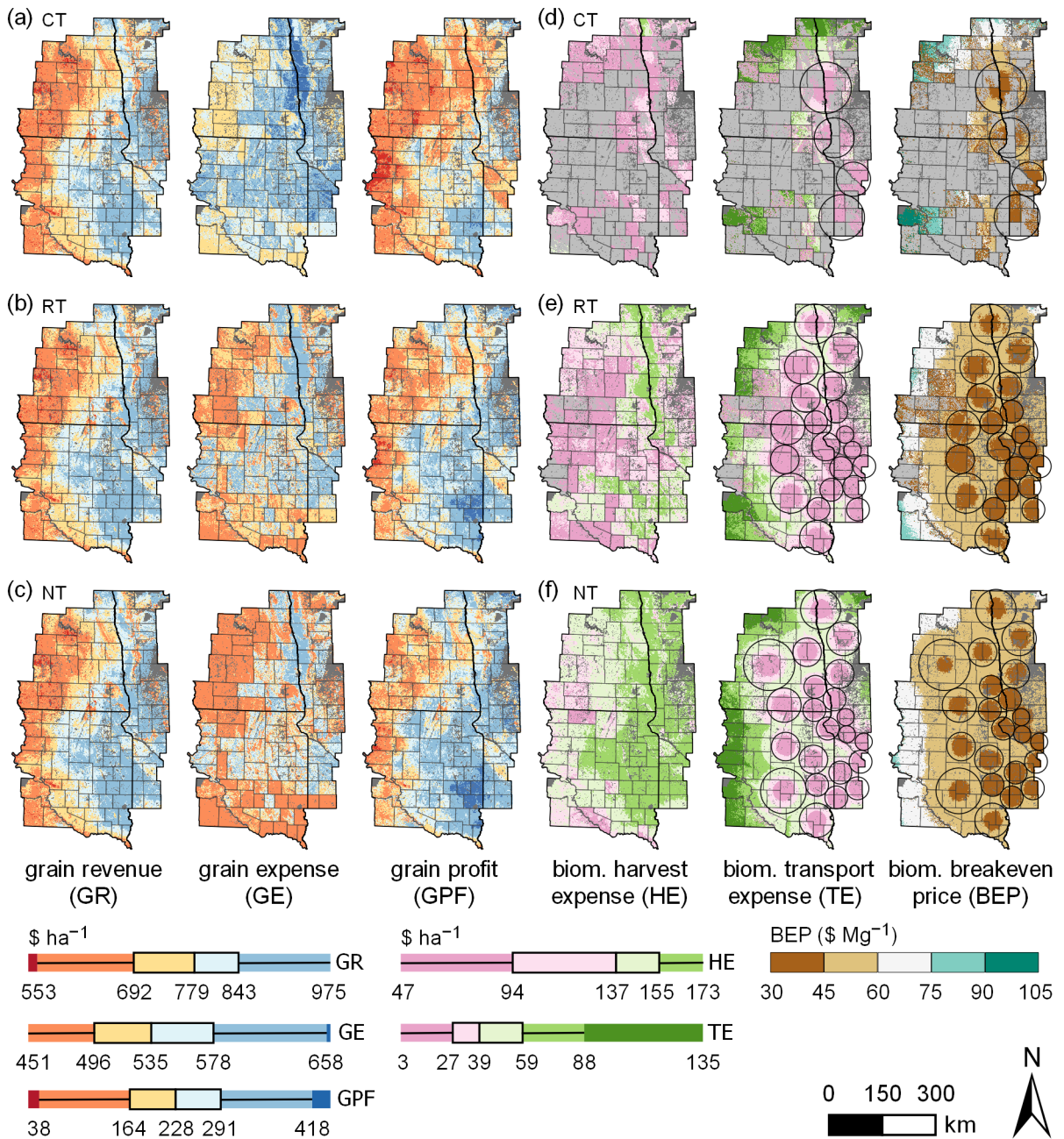


Figure 41. Estimated revenue, expense, and profit for wheat grain production under (a) conventional tillage (CT), (b) reduced tillage (RT), and (c) no-till (NT) systems. Estimated harvest expense, transport expense, and breakeven price for wheat biomass production under (d) CT, (e) RT, and (f) NT systems. Overlain on transport expense and breakeven price are the biorefinery collection areas from Figure 38.

profitable than corn across the study region, with a median profitability of \$228 ha⁻¹ ranging up to \$418 ha⁻¹ in the eastern study region and down to \$38 ha⁻¹ in the western study region (Figure 41a–c, ‘GPF’).

Biomass harvest expense (Figure 40d–f and Figure 41d–f, ‘HE’) displays identical spatial patterns to biomass yield (Figure 39c,d). Biomass harvest expense increases with decreasing tillage intensity and from east to west across the study region. Median values are similar for corn and wheat, \$166 versus \$137 ha⁻¹, and values range up to \$232 ha⁻¹ for corn and \$173 ha⁻¹ for wheat. In contrast, biomass transport expense is primarily a function of distance to potential biorefinery locations within each tillage system (Figure 40d–f and Figure 41d–f, ‘TE’); values within biorefinery collection radii range from \$4 to \$77 ha⁻¹ in corn and from \$3 to \$59 ha⁻¹ in wheat.

4.4.2. 2. Biomass breakeven price

The biomass breakeven price (Figure 40d–f and Figure 41d–f, ‘BEP’) also displays a pattern dependent on distance to potential biorefinery locations. In this investigation, the economic availabilities of corn and wheat biomass were calculated by executing spatial queries of the biomass yields for each crop (Figure 39c,d) and the frequency of corn and wheat production from 2006 to 2015 (Figure 31d,e) for a given set of biomass breakeven prices. The validity of the economic availability estimates is tested by comparisons to US Department of Energy estimates (U.S. Department of Energy, 2016) developed using the Policy Analysis System (POLYSYS) simulation model (De La Torre Ugarte and Ray, 2000).

The breakeven price for biomass within biorefinery collection areas mostly ranges from \$30 to \$45 Mg⁻¹ (Figure 40d–f and Figure 41d–f, ‘BEP’). Biorefineries collecting CT, RT, and NT residue can supply 1.23, 10.82, and 12.18 Tg of biomass at a price of \$45 Mg⁻¹ or less. Since most of the study region features RT or NT tillage systems, with just 16% of corn area (USDA ERS, 2010) and 2% of wheat area (USDA ERS, 2009) featuring CT in the Northern Plains, the biomass availability estimates under RT and NT are consistent with the estimated 12.00 Tg of corn stover and wheat straw available within study region counties at a farmgate

price of \$45 Mg⁻¹ in 2015 (U.S. Department of Energy, 2016). At a price of \$60 Mg⁻¹ or less, which encompasses all breakeven prices within biorefinery collection areas (Figure 40d–f and Figure 41d–f, ‘BEP’), all biomass within biorefinery collection areas is economically available (2.32, 13.98, 16.48 Tg for CT, RT, and NT, respectively). These values are consistent with the value of 13.46 Tg estimated by U.S. Department of Energy (2016).

Although not a direct comparison, as the estimates of U.S. Department of Energy (2016) only consider transportation to the field edge, our estimates of corn and wheat economic availability are similar. The similarity of our estimated outcomes to those developed with a completely different methodology suggests that the amounts of economically-available corn and wheat biomass presented herein are reasonable. In addition, although the estimated biomass breakeven prices for wheat are greater than the \$28 Mg⁻¹ price previously estimated for Minnesota (Gallagher et al., 2003), the predominant corn biomass prices are consistent with previous estimates for Minnesota of \$42 to \$48 Mg⁻¹ (Petrolia, 2006) and \$58 to \$70 Mg⁻¹ (Petrolia, 2008) and are well within the range of \$19 to \$86 Mg⁻¹ reported in the literature review of Carriquiry et al. (2011).

4.4.3. Switchgrass economic competitiveness

Dedicated energy crops represent an alternative source of biomass for bioenergy production. Switchgrass is considered a model bioenergy crop due to its adaptedness across large regions of the US, relatively high yields, and long history of research and development (Sanderson et al., 1996; Wright and Turhollow, 2010). Furthermore, switchgrass production typically supplies a greater quantity of biomass than does residue removal from corn or wheat croplands. In this investigation, the economic availability of switchgrass biomass is defined by the switchgrass parity price (SPP). The SPP represents the minimum biomass price necessary for switchgrass to earn a net return equal to that of combined grain and biomass harvest in corn or wheat. Calculation of the SPP considers the corn and wheat biomass yields described in Section 4.4.1 and the revenue and expense information described in Section 4.4.2, as well as the biomass yields, production expense, and transport expense associated with switchgrass

production. Switchgrass parity price is displayed for all parcels containing soils deemed suitable for biomass cropping.

4.4.3. 1. Estimated yield and expenses

Estimated switchgrass biomass yields for the study region are shown in Figure 42a. Similar to corn and wheat (Figure 39c,d), switchgrass yields decreased from east to west across the study region. Consistent with published literature (Boyer et al., 2012; Fike et al., 2017; Heaton et al., 2004; Lemus et al., 2008; Madakadze et al., 1999b; Muir et al., 2001), switchgrass yields were highly responsive to fertilizer applications. Estimated yields from switchgrass grown without fertilizer ranged from 2.70 to 7.41 Mg ha⁻¹ across most of the study area (Figure 42a, 'LC, -F' and 'HC, -F'), compared to yields of 7.41 to 11.87 Mg ha⁻¹ with applied fertilizer (Figure 42a, 'LC, +F' and 'HC, +F').

To a lesser extent, yields also varied between LC and HC establishment. With no applied fertilizer, yields under LC establishment ranged from 2.70 to 5.89 Mg ha⁻¹ across the far western portions of the study region and from 7.41 to 11.87 Mg ha⁻¹ along the Minnesota-Dakotas border and into southwest Minnesota (Figure 42a, 'LC, -F'). Under HC establishment, yields ranging from 2.70 to 7.41 Mg ha⁻¹ were estimated across the Dakotas, with higher yields found only in a limited area of southwest Minnesota (Figure 42a, 'HC, -F'). With applied fertilizer, yields under LC establishment ranged from 9.03 to 11.87 Mg ha⁻¹ across nearly the entire study region (Figure 42a, 'LC, +F'), while yields under HC establishment ranged from 7.41 to 9.03 Mg ha⁻¹ across the northern and west-central portions of the study region and from 9.03 to 11.87 Mg ha⁻¹ in eastward areas (Figure 42a, 'HC, +F'). Overall, fertilized switchgrass under LC or HC establishment (Figure 42a, 'LC, +F' and 'HC, -F') can provide approximately 4 to 7 Mg ha⁻¹ of additional biomass relative to corn or wheat in a NT system (Figure 39c,d).

Although switchgrass management practices necessary for high yields have been documented for the study region (McGuire and Rupp, 2013; Mitchell et al., 2015; Reitsma et al., 2011) and many other regions of the US (Bughrara et al., 2007; Drinnon et al., 2015;

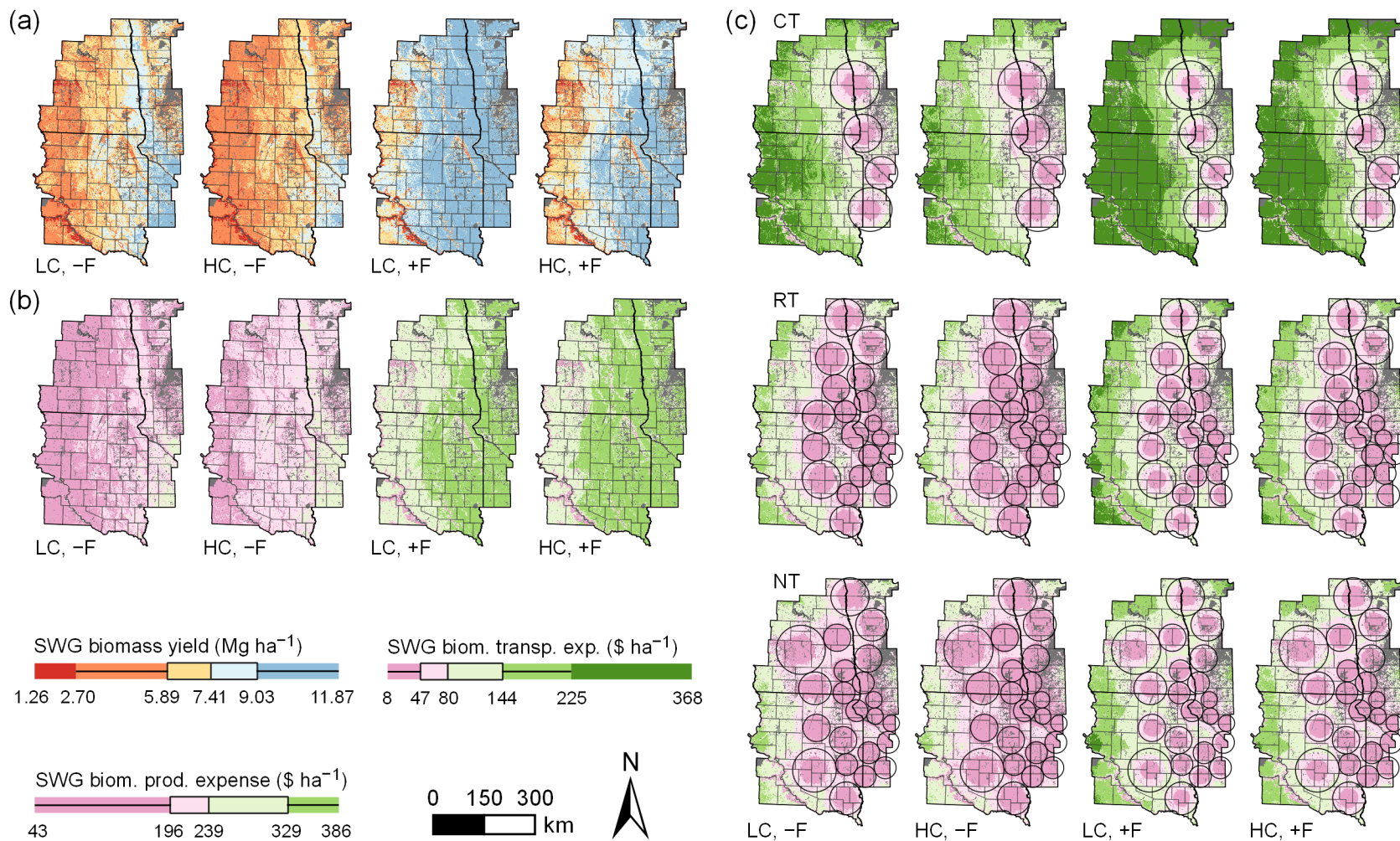


Figure 42. Under the low-cost (LC) and high-cost (HC) establishment scenarios, with (+F) and without (-F) fertilizer applications, the estimated (a) yield, (b) production expense, and (c) transport expense associated with switchgrass (SWG) biomass production. Overlain on transport expense are the biorefinery collection areas from Figure 38. All values represent the annualized net present value of 10-year returns with a discount rate of 5%.

Garland, 2008; Hancock, 2017; Holman et al., 2011; Mitchell et al., 2015; Newman et al., 2014; Shankle and Garrett, 2014; Teel et al., 2003), switchgrass must generate net returns comparable to existing crops in order to be utilized across the landscape. Estimated production and transportation expenses for switchgrass production are displayed in Figure 42b,c. Production expenses are dependent on biomass yield, ranging from \$43 to \$239 ha⁻¹ for unfertilized switchgrass (Figure 42b, 'LC, -F' and 'HC, -F') and from \$239 to \$386 ha⁻¹ for fertilized switchgrass (Figure 42b, 'LC, +F' and 'HC, +F'). Similar to corn and wheat (Figure 40d-f, 'TE' and Figure 41d-f, 'TE'), switchgrass transportation expenses are primarily dependent on distance to the nearest potential biorefinery (Figure 42c). For fertilized switchgrass (Figure 42c, 'LC, +F' and 'HC, +F'), transportation expenses range from \$8 to \$47 ha⁻¹ in the immediate vicinity of potential biorefineries and from \$47 to \$144 ha⁻¹ within the remaining portions of biorefinery collection areas. Due to its relatively high biomass yields, switchgrass transportation expense ranges from \$225 to \$368 ha⁻¹ in areas greater than 100 to 150 km from a potential biorefinery (e.g Figure 42c 'CT', 'LC, +F', and 'HC, +F'), which is approximately twice the expense of corn or wheat biomass transportation over a similar distance (Figure 40d-f, 'TE' and Figure 41d-f, 'TE').

4.4.3. 2. *Switchgrass parity price*

The economic competitiveness of switchgrass production relative to corn or wheat is expressed using the SPP (Figure 43a-c and Figure 44a-c), which utilizes the following variables as inputs: corn and wheat biomass yields (Figure 39c,d); corn and wheat grain revenue, grain expense, biomass harvest expense, and biomass transport expense (Figures 40 and 41); and switchgrass biomass yields, biomass production expense, and biomass transport expense (Figure 42).

At the SPP, growers would realize a positive economic return to switchgrass production over nearly the entire study region (Figure 43d-f and Figure 44d-f), with profits ranging from \$0 to \$400 ha⁻¹ in western areas, from \$400 to \$800 ha⁻¹ throughout most of the central and eastern study region, and from \$800 to \$1200 ha⁻¹ in several areas along the Minnesota-

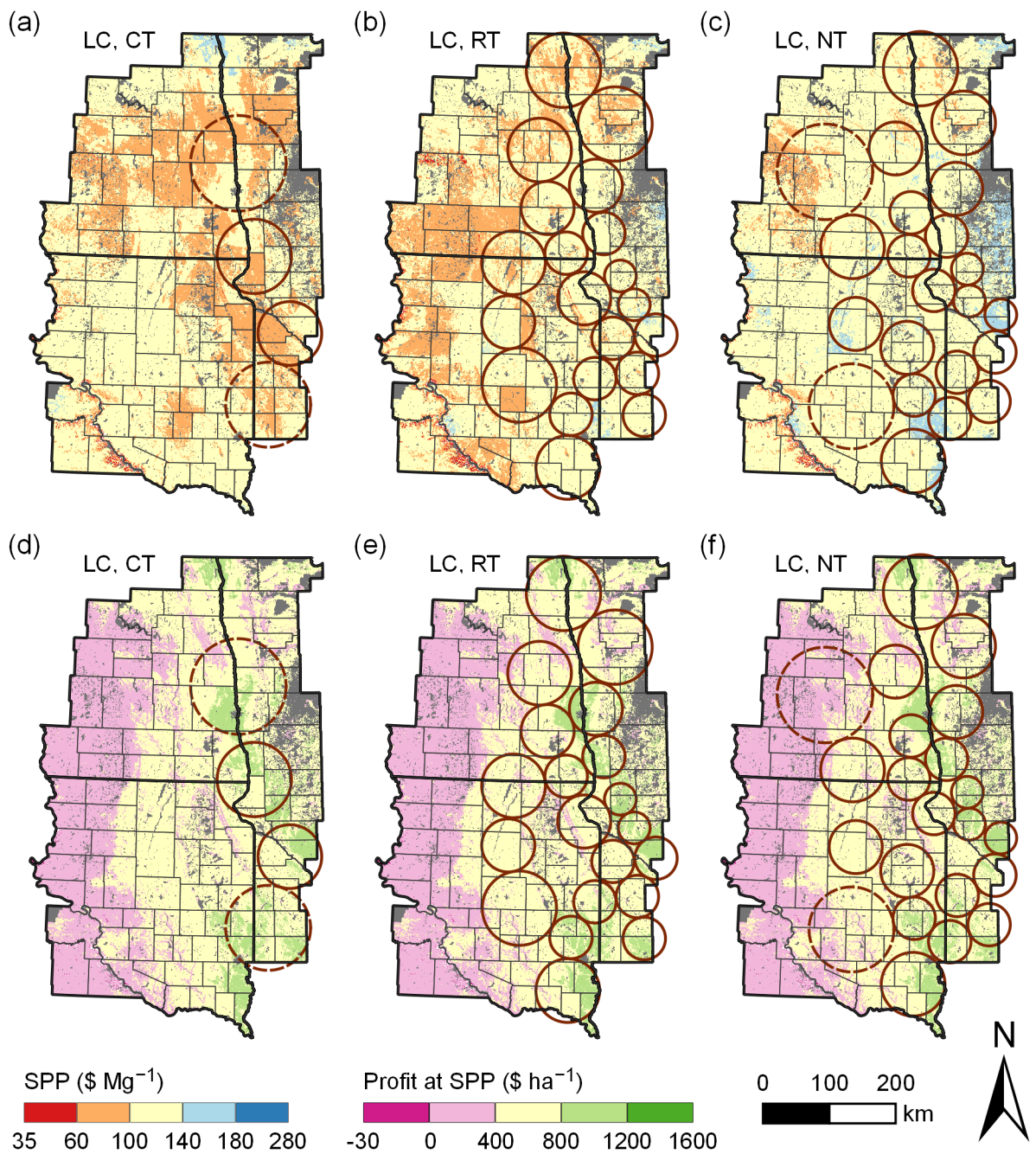


Figure 43. For the low-cost (LC) establishment scenario, the biomass price necessary for switchgrass to generate the same net return as a competing corn or wheat system (SPP, switchgrass parity price) under (a) conventional tillage (CT), (b) reduced tillage (RT) or (c) no-till (NT). (d – f) The net return of switchgrass production at the SPP.

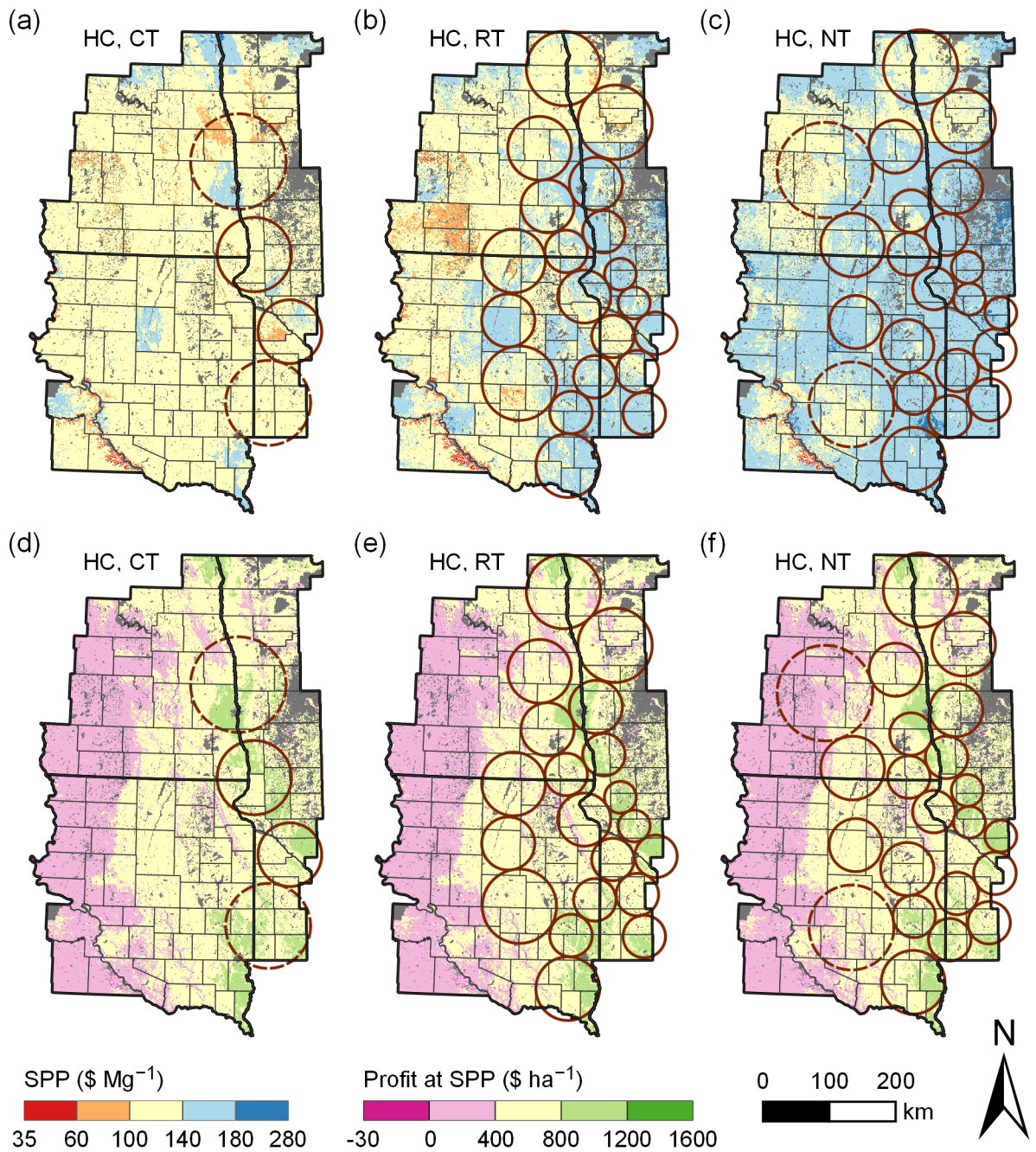


Figure 44. For the high-cost (HC) establishment scenario, the biomass price necessary for switchgrass to generate the same net return as a competing corn or wheat system (SPP, switchgrass parity price) under (a) conventional tillage (CT), (b) reduced tillage (RT) or (c) no-till (NT). (d – f) The net return of switchgrass production at the SPP.

Dakotas border. However, whether under LC or HC establishment, the only areas with an SPP of \$35 to \$60 Mg⁻¹ are a limited number of parcels along the Missouri river in the southwest portion of the study region (Figure 43a–c and Figure 44a–c). Thus, switchgrass is not economically competitive at prices feasible for corn or wheat biomass harvest (Figure 40d–f, ‘BEP’ and Figure 41d–f, ‘BEP’). Under LC establishment, the SPP relative to competing CT and RT systems ranges from \$60 to \$100 Mg⁻¹ across large portions of the study region, but primarily outside potential biorefinery collection areas (Figure 43a,b). Relative to competing RT and NT systems, the SPP within biorefinery collection areas ranges from \$100 to \$140 Mg⁻¹ (Figure 43b,c). Switchgrass under HC establishment (Figure 44a–c) is even less economically competitive, with the SPP within biorefinery collection areas mostly ranging from \$100 to \$140 Mg⁻¹ relative to CT and \$140 to \$180 Mg⁻¹ relative to RT and NT. Under all combinations of switchgrass establishment cost and competing tillage system presented herein, switchgrass production must be financially incentivized in order to be competitive with corn or wheat biomass harvest.

Estimated SPP values across combinations of switchgrass establishment cost and competing tillage system are within the range of values estimated by others for the northern US. In a three-county area of southern North Dakota, Bangsund et al. (2008) estimated that switchgrass would be competitive with existing cropping at a price of \$47 to \$95 Mg⁻¹ in soils varying from low to high productivity and across multiple projections of switchgrass yield, competing crop prices, and input costs. For contrasting low-cost and high-cost scenarios, Jain et al. (2010) estimated that switchgrass would be economically competitive with a corn-soybean rotation harvested for grain at \$150 to \$195 Mg⁻¹ in Minnesota, \$132 to \$168 Mg⁻¹ in Wisconsin, and \$106 to \$148 Mg⁻¹ in Michigan. In Michigan, James et al. (2010) estimated that switchgrass would be economically competitive with continuous corn featuring 38% biomass removal at a biomass price of \$119 Mg⁻¹. Collectively, these comparisons suggest that the SPP estimates presented herein are reasonable. Nonetheless, SPP estimates are highly sensitive to the assumption that biomass producers would evaluate switchgrass

profitability relative to the net present value of a competing system over a 10-year time period. For example, SPP estimates are as high as \$350 Mg⁻¹ if biomass producers would evaluate annualized switchgrass returns relative to a single year of corn or wheat production (Appendix C, Figure 74).

4.4.4. Switchgrass environmental benefits

Although switchgrass biomass production is not economically competitive with combined grain and biomass production in corn or wheat, environmental services provided by perennial switchgrass cropping are an additional benefit not offered by annual crops such as corn or wheat. This investigation quantifies mitigated soil erosion, mitigated N runoff, and C sequestration advantage relative to corn or wheat production as environmental services offered by switchgrass cropping. Figure 45 presents environmental services of switchgrass production under LC establishment and the most profitable fertilization option (+F vs. -F) relative to the most competitive defender system (corn-soybean vs. wheat-soybean; e.g. Figure 36). Outcomes under HC establishment are nearly identical, and are presented in Figure 75 (Appendix C). Switchgrass environmental services are displayed for all parcels containing soils deemed suitable for biomass cropping.

4.4.4. 1. Soil erosion mitigation

Across all parcels and tillage systems, the median soil erosion mitigation is 0.47 Mg ha⁻¹ yr⁻¹ (Figure 45a). The amount of mitigated soil erosion decreases with decreasing tillage intensity of its competing system, with most of the study region ranging from 0.47 to 1.76 Mg ha⁻¹ yr⁻¹ relative to CT (Figure 45a, 'LC, CT') and from 0.04 to 0.47 Mg ha⁻¹ yr⁻¹ relative to NT (Figure 45a, 'LC, NT'). Regardless of competing tillage system, study region areas most susceptible to erosion have mitigation values ranging from 1.07 to 9.05 Mg ha⁻¹ yr⁻¹ (Figure 45a), corresponding to areas with slope gradients ranging from 5 to 20% (Figure 45d).

When expressed as a percentage of its competing corn-soybean or wheat-soybean system, relative soil erosion mitigation ranged from 80 to 100% of its competing crop, with

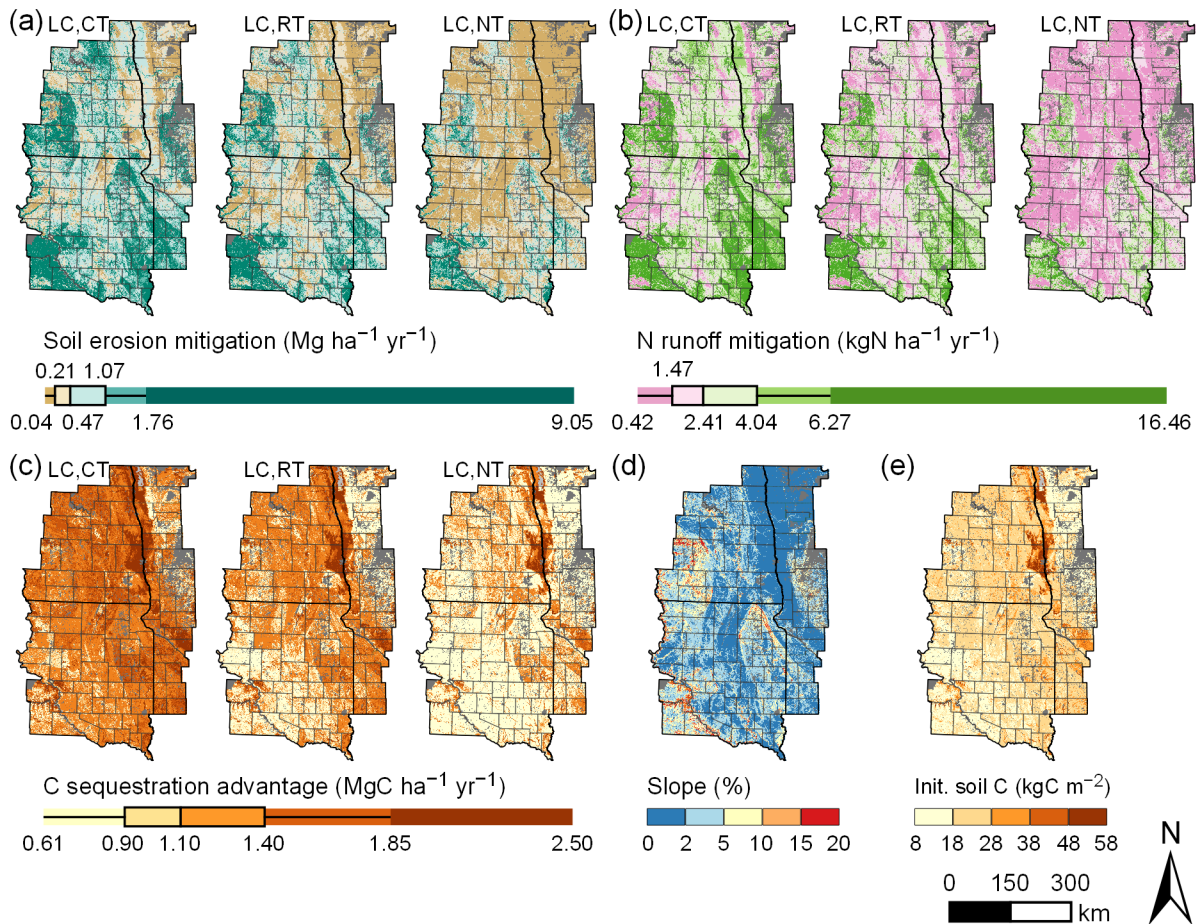


Figure 45. Environmental benefits of switchgrass production relative to corn or wheat and under the most profitable fertilization option (e.g. Figure 36) for the low-cost (LC) establishment scenario: (a) mitigation of soil erosion, (b) mitigation of nitrogen (N) runoff into surface water, and (c) carbon (C) sequestration. Maps of (d) slope and (e) initial soil C from SSURGO are provided to provide context to the spatial patterns of a – c.

an average of over 99% (data not shown). Although these relative values are at the high end of the range in sediment reduction of 53 to 99% reported for 17 studies of switchgrass-containing filter strips, buffer strips, and riparian buffers (Acharya and Blanco-Canqui, 2018), these estimates are consistent with observations of soil erosion near nil in established perennial sod crops (Kort et al., 1998). In addition, mean estimated soil erosion values for corn and wheat in this study are consistent with those from literature, and much lower than those reported by the USDA for cultivated cropland. Considering only parcels identified as cultivated cropland in the 2011 NLCD (Homer et al., 2012), estimated soil erosion values for corn in this study

ranged from 0.01 to 7.12 Mg ha⁻¹, with a mean of 0.74 and median of 0.39 (data not shown). In a review reporting 19 multi-year observations from systems with grain and biomass harvest, sediment loss in corn ranged from 0.03 to 3.50 Mg ha⁻¹, with a mean of 0.64 and median of 0.40 (Acharya and Blanco-Canqui, 2018). Estimated soil erosion values for wheat in this study ranged from 0.01 to 6.76 Mg ha⁻¹, with a mean of 0.67 and median of 0.36 (data not shown). Comparatively, reported sediment loss across 10 multi-year observations in wheat ranged from 1.00 to 13.50 Mg ha⁻¹, with a mean of 6.50 and median of 6.25 (Acharya and Blanco-Canqui, 2018). Average USDA soil erosion estimates for cultivated cropland from 2007 to 2015 were 4.53, 2.20, and 3.54 Mg ha⁻¹ for Minnesota, North Dakota, and South Dakota, respectively (USDA, 2018), which are approximately 3 to 6 times greater than our corn and wheat estimates. Collectively, published literature supports that the soil erosion mitigation estimates presented herein are a reasonable approximation of field conditions, and may be conservative estimates.

4.4.4. 2. N loss mitigation

Since ALMANAC simulations of soil erosion and N runoff depend on many of the same variables (Sharpley and Williams, 1990), patterns of N runoff mitigation (Figure 45b) are similar to soil erosion mitigation (Figure 45a). First, N runoff mitigation decreases with decreasing intensity of the competing tillage system. Relative to CT, much of the study region features N runoff mitigation above the median value of 2.41 kgN ha⁻¹ yr⁻¹ (Figure 45b, 'LC, CT'). Relative to NT, corresponding values range from 0.42 to 2.41 kgN ha⁻¹ yr⁻¹ (Figure 45b, 'LC, NT'). Second, the highest levels of N runoff mitigation are found in study region areas with the highest slopes (Figure 45d); values in these areas range from 4.04 to 16.46 kgN ha⁻¹ yr⁻¹ regardless of the competing tillage system (Figure 45b). Third, switchgrass was estimated to be highly effective in mitigating N runoff mitigation. When expressed as the percent reduction in N runoff relative to its competing crop, relative switchgrass N mitigation estimated for this study ranged from 52 to 100%, with a mean of 95% (data not shown).

Relative N runoff mitigation values are greater than the reduction in nitrate runoff of 43% reported by Nyakatawa et al. (2006) across five years of a study comparing no-till

corn to switchgrass production, and are at the high end of N runoff reductions of 45 to 94% reported for switchgrass-containing filter strips, buffer strips, and riparian buffers (Acharya and Blanco-Canqui, 2018). When also considering corn and wheat N runoff amounts reported in literature, our estimates of N runoff mitigation may be less conservative than our estimates of soil erosion mitigation. In a review reporting 14 multi-year observations across seven soils supporting corn grain and biomass harvest, Acharya and Blanco-Canqui (2018) reported N runoff ranging from 0.12 to 18.91 kgN ha⁻¹, with mean and median values of 2.51 and 1.11, respectively. Considering only those parcels identified as cultivated cropland in the 2011 NLCD (Homer et al., 2012), corresponding values in this study ranged from 0.25 to 15.31 kgN ha⁻¹, with a mean of 3.02 and median of 2.30 (data not shown). Across 10 multi-year observations on one soil supporting wheat grain and biomass harvest, reported N runoff ranged from 1.36 to 2.55 kgN ha⁻¹, with a mean of 2.02 and median of 2.00 (Acharya and Blanco-Canqui, 2018). Corresponding values in this study ranged from 0.16 to 14.31 kgN ha⁻¹, with a mean of 2.69 and median of 2.05 (data not shown). Although greater than mean N runoff values reported in literature, our mean values are conservative relative to those reported by the USDA Small Watershed Nutrient Forecasting Tool (SWIFT; USDA ARS, 2019b). Designed to rapidly estimate nutrient loads from small watersheds for a given ecoregion in the US, SWIFT estimates annual field edge N export of 5.03 and 7.78 kgN ha⁻¹ for the ‘Northern Glaciated Plains’ and ‘Lake Agassiz Plain’ ecoregions that constitute the majority of our study region. These values are approximately 1.5 to 2.5 times greater than our mean N runoff estimates from corn or wheat featuring grain and biomass harvest.

4.4.4. 3. C sequestration advantage

Estimated spatial patterns of C sequestration advantage (Figure 45c) differ from those of soil erosion and N runoff mitigation, as values are dependent on initial soil C estimates from SSURGO (Figure 45e) rather than soil slope. Similar to mitigation of soil erosion and N runoff, however, switchgrass C sequestration advantage decreases with decreasing tillage intensity of its competing system. Carbon sequestration advantage relative to CT ranges from

1.10 to 1.85 MgC ha⁻¹ yr⁻¹ across much of the study region (Figure 45c, ‘LC, CT’), but decreases to a range of 0.61 to 1.10 MgC ha⁻¹ yr⁻¹ relative to NT (Figure 45c, ‘LC, NT’). Across all parcels and tillage systems, the median C sequestration advantage of switchgrass relative to its competing system ranges from 0.61 to 2.50 MgC ha⁻¹ yr⁻¹, with a median of 1.10 (Figure 45c).

Although published literature contains conflicting reports on the relative abilities of corn, wheat, and switchgrass systems to sequester C, our estimates are well within the range of values from comparative experiments of switchgrass and annual crops established on existing cropland. Across 10 years in western Iowa, Al-Kaisi et al. (2005) reported a switchgrass C sequestration advantage of 0.69 MgC ha⁻¹ yr⁻¹ from 0 to 15 cm soil depth relative to a competing corn-soybean-alfalfa system. In 13 eastern Indiana fields with a paired corn-soybean system and 1 field with a paired corn-soybean-wheat system, Omonode and Vyn (2006) reported an average switchgrass C sequestration advantage of 2.10 MgC ha⁻¹ yr⁻¹ from 0 to 100 cm. Abraha et al. (2018) reported a C sequestration advantage of 0.77 MgC ha⁻¹ yr⁻¹ over seven years in southwest Michigan, as eddy covariance measurements showed average emissions of 0.10 MgC ha⁻¹ yr⁻¹ for continuous NT corn while switchgrass sequestered 0.67 MgC ha⁻¹ yr⁻¹. Eichelmann et al. (2016) reported switchgrass C sequestration advantages of 4.59 and 7.65 MgC ha⁻¹ for a single year of eddy covariance measurements in southwest Ontario, as switchgrass sequestered 0.66 MgC ha⁻¹ while RT corn with grain harvest emitted 3.93 MgC ha⁻¹ and RT corn with grain and stover harvest emitted 6.99 MgC ha⁻¹. Although NT corn has also been reported to result in similar amounts of C sequestration as switchgrass (Follett et al., 2012), these results collectively support the reasonableness of the comparative C sequestration estimates presented herein.

4.4.5. Scenarios for subsidizing switchgrass production

Under all combinations of establishment scenario and competing tillage system, switchgrass biomass production is not price competitive with corn or wheat harvested for biomass and grain. For all combinations of establishment scenario and competing tillage

system, Figure 46 summarizes the amount of subsidy necessary for switchgrass to supplant 1 to 5% of eligible corn or wheat parcels, under two land-use substitution scenarios. As described in Section 4.3.7, switchgrass land-use substitutions are limited to a subset of parcels with remotely-sensed corn or wheat production history from 2006 to 2015. Through benefit payments for its soil erosion mitigation, N runoff mitigation, and C sequestration relative to its competing system (Figure 45a–c), ‘subsidized environmental services’ (SES) prioritizes the conversion of those corn and wheat parcels where conversion to switchgrass offers the greatest environmental services benefit. Through increasing the biomass price above the assumed baseline value of \$60 Mg⁻¹, which represents a feasible biomass price for harvest of corn and wheat residues within biomass collection areas (Figures 40 and 41d–f, ‘BEP’), ‘subsidized biomass production’ (SBP) prioritizes the conversion of those corn and wheat parcels where conversion to switchgrass offers the greatest increase in biomass production. The total subsidy for each parcel equals the amount necessary for switchgrass to earn a net return equal to its competing system.

4.4.5. 1. Minimum required subsidies

Using subsidies to convert 1 to 5% of eligible corn and wheat parcels to switchgrass is not economically feasible under current levels of US government spending, whether by SBP or SES. To support the establishment and production of bioenergy crops in the US, the Biomass Crop Assistance Program (BCAP) was established in the Food, Conservation, and Energy Act of 2008 and reauthorized in the Agricultural Act of 2014 (McMinimy, 2015). More commonly known as the 2008 and 2014 Farm Bills, these acts primarily authorized funding for nutrition assistance, commodity programs, and conservation, with energy among one of several programs receiving lesser funding amounts. In nominal dollars, funding across the two Farm Bills totaled \$796 billion from 2008 through 2017, with \$600 billion for nutrition assistance, \$78 billion for commodity programs, \$83 billion for conservation, and \$1.8 billion for energy (Harl, 2014; Harris et al., 2008). As part of the \$1.8 billion allocated for energy, BCAP outlays totaled \$400 million (\$389 million in real dollars; McMinimy, 2015). Thus, BCAP spending

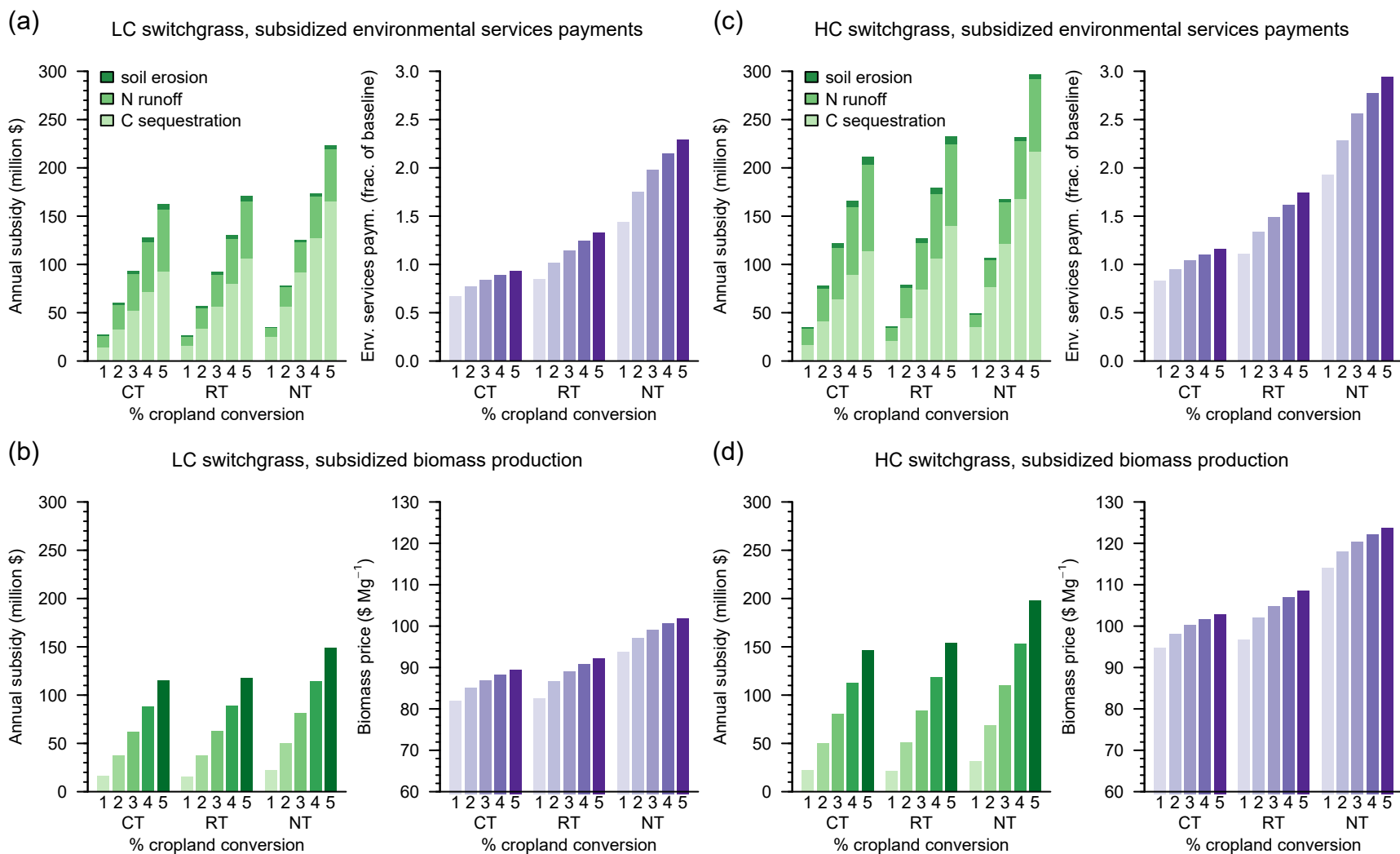


Figure 46. (a) For switchgrass with low-cost (LC) establishment; subsidized environmental services; and competing with corn or wheat in a conventional tillage (CT), reduced tillage (RT), or no-till (NT) system; required annual subsidy and environmental services payments to achieve 1 to 5% conversion of eligible corn and wheat parcels to switchgrass production. (b) The required annual subsidy and biomass price with subsidized biomass production. (c – d) Corresponding values for high-cost (HC) establishment.

represents a small fraction of the overall spending authorized by these acts.

The required funding to enable 1 to 5% switchgrass substitution over 10 years through SES is \$300 million to \$2.9 billion, which is 0.8 to 7.5 times the amount provided by BCAP to the entire US from 2008 through 2017. Under SES, switchgrass with LC establishment would require from \$30 to \$170 million annually to convert 1 to 5% of eligible CT or RT parcels to switchgrass, and \$40 to \$230 million annually to convert the same amount of NT parcels (Figure 46a, left panel). Under HC establishment, subsidies as high as \$210 to \$230 million are necessary to convert CT and RT parcels, while values as high as \$290 million are necessary to convert NT parcels (Figure 46c, left panel). Converting 1 to 5% of eligible CT parcels to switchgrass with LC establishment is possible at environmental service payments at or below the baseline values of \$4.55 Mg-soil⁻¹, \$19.32 kgN⁻¹, and \$118 MgC⁻¹ (Figure 45a, right panel). In contrast, respective values as high as 1.3 or 2.3 times the baseline would be necessary to convert RT and NT parcels. Assuming HC establishment, converting 5% of eligible corn and wheat parcels under CT, RT, and NT would require respective environmental services payments 1.2, 1.7, and 2.9 times the baseline values (Figure 45c, right panel). At 2.9 times the baseline values, environmental services payments would be \$13.20 Mg-soil⁻¹, \$56.03 kgN⁻¹, and \$342 MgC⁻¹. For comparison, this N valuation is nearly twice the upper-limit estimate of \$32.62 kgN⁻¹ presented by Sobota et al. (2015), while this C valuation falls between the 67th and 90th percentiles of a Fisher-Tippett distribution fitted to 311 published estimates of the social cost of C (Tol, 2011).

To convert the same number of cropland parcels, SBP requires less subsidy spending than SES. Compared to annual payments as large as \$230 million under SES (Figure 46a, left panel), switchgrass with SBP and LC establishment could replace 5% of eligible corn and wheat parcels under CT or RT with an annual outlay of \$120 million, and could replace 5% of eligible parcels under NT with an annual outlay of \$150 million (Figure 46b, left panel). With HC establishment, switchgrass with SBP requires \$150 to \$200 million to replace 5% of eligible parcels under CT, RT, and NT systems (Figure 46d, left panel), compared to values

as high as \$290 million under SES (Figure 46c, left panel). Nonetheless, the required funding to enable 1 to 5% switchgrass substitution over 10 years through SBP is \$155 million to \$2 billion, which represents 0.4 to 5.1 times the amount provided by BCAP to the entire US from 2008 through 2017 (McMinimy, 2015). Subsidized biomass prices necessary to encourage 5% conversion of eligible parcels range from \$90 to \$102 Mg⁻¹ for switchgrass with LC establishment (Figure 46b, right panel), and from \$104 to \$124 Mg⁻¹ for HC establishment (Figure 46d, right panel). Whether under LC or HC establishment, parcels with SBP will experience no cropland-to-switchgrass conversion at prices less than \$80 Mg⁻¹.

4.4.5. 2. Net gains in harvested biomass

The SES and SBP approaches would result in similarly modest increases in the net amount of newly-available biomass. Under SES and across LC and HC establishment, converting 1 to 5% of eligible corn or wheat parcels to switchgrass will allow for a net gain in total biomass production of 0.2 to 1.9 Tg, 0.2 to 1.5 Tg, and 0.4 to 1.7 Tg within CT, RT, and NT biomass collection areas, respectively (Figure 47a,c). This represents a 9 to 83% increase over the 2.3 Tg of corn and wheat biomass annually available under CT, where corn and wheat biomass is harvestable only from a limited area (Figure 37c, 'CRN CT' and Figure 37d, 'WHT CT'), but just a 1 to 11% increase over the 14.0 Tg available under RT and a 2 to 10% increase over the 16.5 Tg available under NT. Comparatively, converting 1 to 5% of eligible corn or wheat parcels to switchgrass via SBP will increase net biomass production by 0.4 to 2.4 Tg, 0.3 to 1.8 Tg, and 0.3 to 1.9 Tg within CT, RT, and NT biomass collection areas, respectively (Figure 47b,d), representing increases of 17 to 104%, 2 to 13%, and 2 to 12% over existing corn and wheat biomass.

Whether facilitated by SES or SBP, newly-available switchgrass biomass would yield only a modest increase in energy production. Assuming a commercially attainable ethanol conversion rate of 0.29 L kg⁻¹ (Sapp, 2017), the net gain of 0.2 to 2.4 Tg switchgrass biomass within biorefinery collection areas would yield 0.06 to 0.70 GL ethanol. If used to produce E85 transportation fuel, this is equivalent to 0.05 to 0.60 GL gasoline on an equivalent energy basis

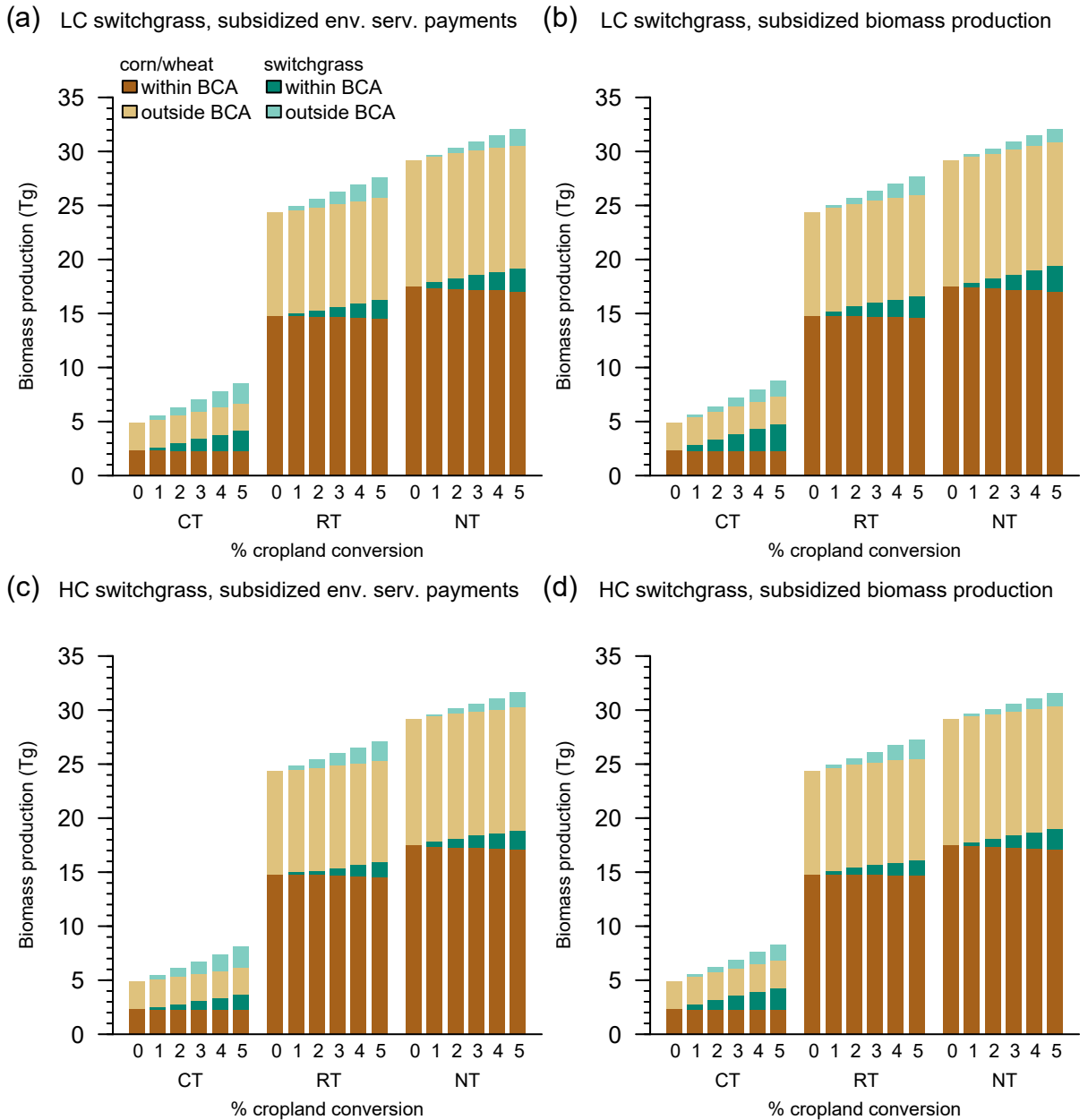


Figure 47. For switchgrass with low-cost (LC) establishment, subsidized (a) environmental services payments or (b) biomass production, and competing with corn or wheat in a conventional tillage (CT), reduced tillage (RT), or no-till (NT) system, the changes in biomass production within or outside a biorefinery collection area (BCA; Figure 38) when converting 1 to 5% of eligible corn or wheat parcels to switchgrass production. (c – d) Corresponding values for HC establishment.

(US DOE, 2019), which represents 0.4 to 4.8% of mean annual gasoline consumption for the transportation sector in Minnesota, North Dakota, and South Dakota from 2006 to 2015 (US EIA, 2019).

4.4.5. 3. Environmental outcomes

Although resulting in similar biomass production outcomes, SES results in much greater environmental benefits than SBP (Figure 48). For example, replacement of RT corn or wheat with LC or HC establishment switchgrass via SES (Figure 48a,c ‘RT’) resulted in 250 to 1000 Gg soil retention (top panels), 0.58 to 2.5 Gg N retention (middle panels), and 160 to 680 Gg C sequestration (bottom panels). Comparatively, replacement of RT corn or wheat via SBP (Figure 48b,d ‘RT’) resulted in 38 to 255 Gg soil retention (top panels), 0.13 to 0.90 Gg N retention (middle panels), and 76 to 433 Gg C sequestration (bottom panels). Estimated benefits of switchgrass substitutions for RT parcels are most relevant to current agronomic practices, as 56% of combined corn and wheat cropland across Minnesota, North Dakota, and South Dakota featured RT (22% residue cover) or mulch till (42% residue cover) in 2009/10 (USDA ERS, 2009, 2010), compared to 20% CT (9% residue cover) and 25% NT (66% residue cover).

With switchgrass substitutions for RT parcels under SES, significant improvements in environmental outcomes could be achieved. For example, the USDA Greenhouse Gas Inventory (USDA, 2016) estimates a net loss of mineral soil C from Minnesota, North Dakota, and South Dakota croplands of 1.25 Tg in 2013. Carbon sequestration due to SES substitutions on RT parcels (160 to 680 Gg C) would reduce this loss by 13 to 54%. In another example, the Minnesota Nutrient Reduction Strategy (MN Interagency Work Group, 2014) estimates that Minnesota agriculture contributes 77 Gg annual N loading to the Mississippi River and calls for a 18.2 Gg annual reduction in N load by 2025. Of the reduction target, 4.0 Gg of N retention is recommended to come from increased perennial cover on 650,000 ha. In this investigation, there are 75 HUC8 watersheds (USGS, 2019) intersecting the study region, with 56 of these watersheds within the Mississippi River drainage basin. Within these 56

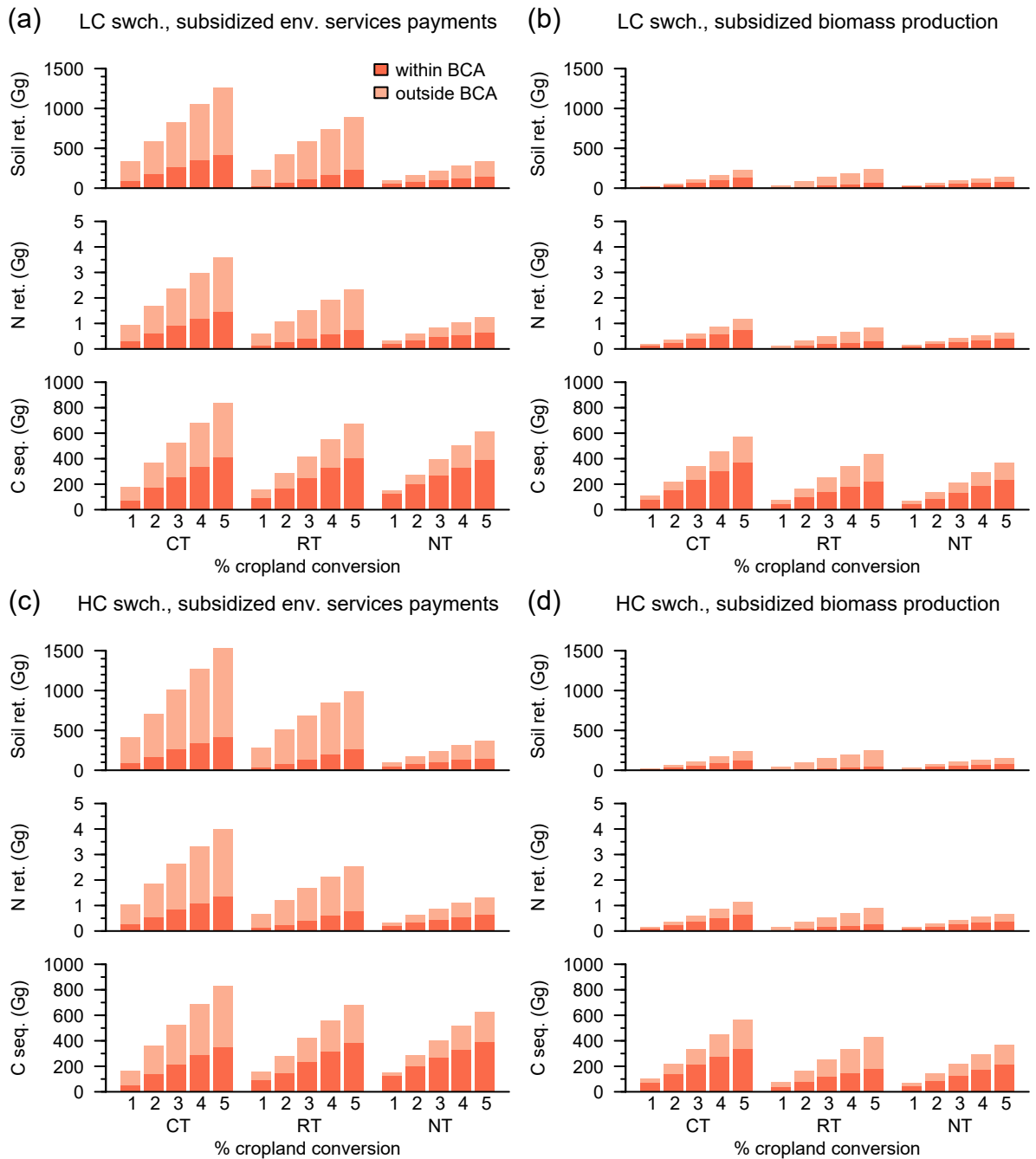


Figure 48. For switchgrass with low-cost (LC) establishment, subsidized (a) environmental services payments or (b) biomass production, and competing with corn or wheat in a conventional tillage (CT), reduced tillage (RT), or no-till (NT) system, the resulting soil retention, nitrogen (N) retention, and carbon (C) sequestration within or outside a biorefinery collection area (BCA; Figure 38) provided by converting 1 to 5% of eligible corn or wheat parcels to switchgrass production. (c – d) Corresponding values for HC establishment.

watersheds, the USDA National Load Estimating Tool (NLET; USDA ARS, 2019a) estimates annual N loadings from agriculture of 62 Gg under current land uses and cropping practices. Within the SES scenario converting 82,000 to 410,000 ha of RT corn or wheat to switchgrass (1 to 5% of eligible parcels), 62,000 to 285,000 ha of conversions occurred within these 56 parcels, resulting in 0.37 to 1.35 Gg N retention. Thus, these conversions could meet 9 to 34% of the reduction targeted by the Minnesota Nutrient Reduction Strategy.

While SES substitutions would provide considerable environmental benefit, the environmental outcomes displayed in Figure 48 also illustrate the diminishing environmental benefits of switchgrass substitution for corn and wheat grown in decreasingly intensive tillage systems. Compared to soil retention of 340 to 1500 Gg when SES introduces LC or HC establishment switchgrass onto CT parcels, soil retention declines to ranges of 250 to 1000 Gg relative to RT and 95 to 370 Gg relative to NT (Figure 48a,c top panels). Similarly, N retention ranges from 0.92 to 4.0 Gg relative to CT, 0.58 to 2.5 Gg relative to RT, and 0.34 to 1.3 Gg relative to NT (Figure 48a,c middle panels). Switchgrass C sequestration advantage is slightly less affected by competing tillage system, but still declines from a range of 170 to 840 Gg relative to CT to ranges of 160 to 680 Gg relative to RT and 150 to 620 Tg relative to NT (Figure 48a,c bottom panels). Growers continue to replace CT parcels with less-intensive tillage practices across Minnesota, North Dakota, and South Dakota, as the percentage of combined corn and wheat production areas featuring CT decreased from 48% in 1989 to 35% in 2004 (Baker, 2011) and 20% in 2009/10 (USDA ERS, 2009, 2010). As improved soil management practices continue to proliferate across the region, it becomes increasingly important to place switchgrass or other perennial biomass crops in the areas where they provide the greatest environmental benefit.

4.4.5. 4. *Relative outcomes summary*

Figure 49 summarizes the relative differences in annual subsidy (Figure 46); biomass production (Figure 47); and soil retention, N retention, and C sequestration (Figure 48) when comparing SES and SBP approaches to replacing 5% of eligible corn or wheat parcels with

switchgrass. The SES approach requires an annual subsidy up to 50% greater than SBP and results in up to 30% less biomass production (Figure 49a–d). However, these differences in annual subsidy and biomass production are almost always less than the proportionate increases in soil retention, N retention, and C sequestration from utilizing SES. Across the three tillage systems and two establishment scenarios, parcels within biorefinery collection areas feature 70 to 420% greater soil retention, 50 to 210% greater N retention, and 5 to 120% greater C sequestration under SES than SBP (Figure 49a,c) . When considering all parcels, SES results in 130 to 550% greater soil retention, 90 to 250% greater N retention, and 50 to 70% greater C sequestration relative to SBP (Figure 49b,d). Collectively, Figures 46 to 49 support the targeted placement of switchgrass on parcels where it would provide the greatest environmental benefit. Although SBP will result in modestly higher biomass production relative to SES, and for a lower annual subsidy, any gains in biomass production from introducing switchgrass to the landscape are modest relative to the corn and wheat biomass already available under RT or NT. Furthermore, for SES relative to SBP, the increases in environmental services are proportionally larger than the concomitant decreases in biomass production.

4.4.6. Land-use changes with subsidized switchgrass

The study region has a history of dynamic land use changes between agriculture and perennial grasslands (Section 4.2), features several areas with cultivated cropland and perennial land covers in close proximity to each other (Figure 31a), and currently features cultivated cropland on most of its parcels considered highly suitable for cropping (Figure 31a,b). Thus, it is important to consider possible land-use changes associated with introduction of switchgrass cropping to the landscape. While Section 4.4.5 considered the possible environmental implications of subsidized switchgrass production, this section addresses the relative suitability for cropping of those parcels converted to switchgrass and the possible impacts of expanded switchgrass cropping on existing perennial land covers. As in Section 4.4.5, switchgrass land-use substitutions are limited to a subset of parcels with remotely-sensed corn or wheat production history from 2006 to 2015.

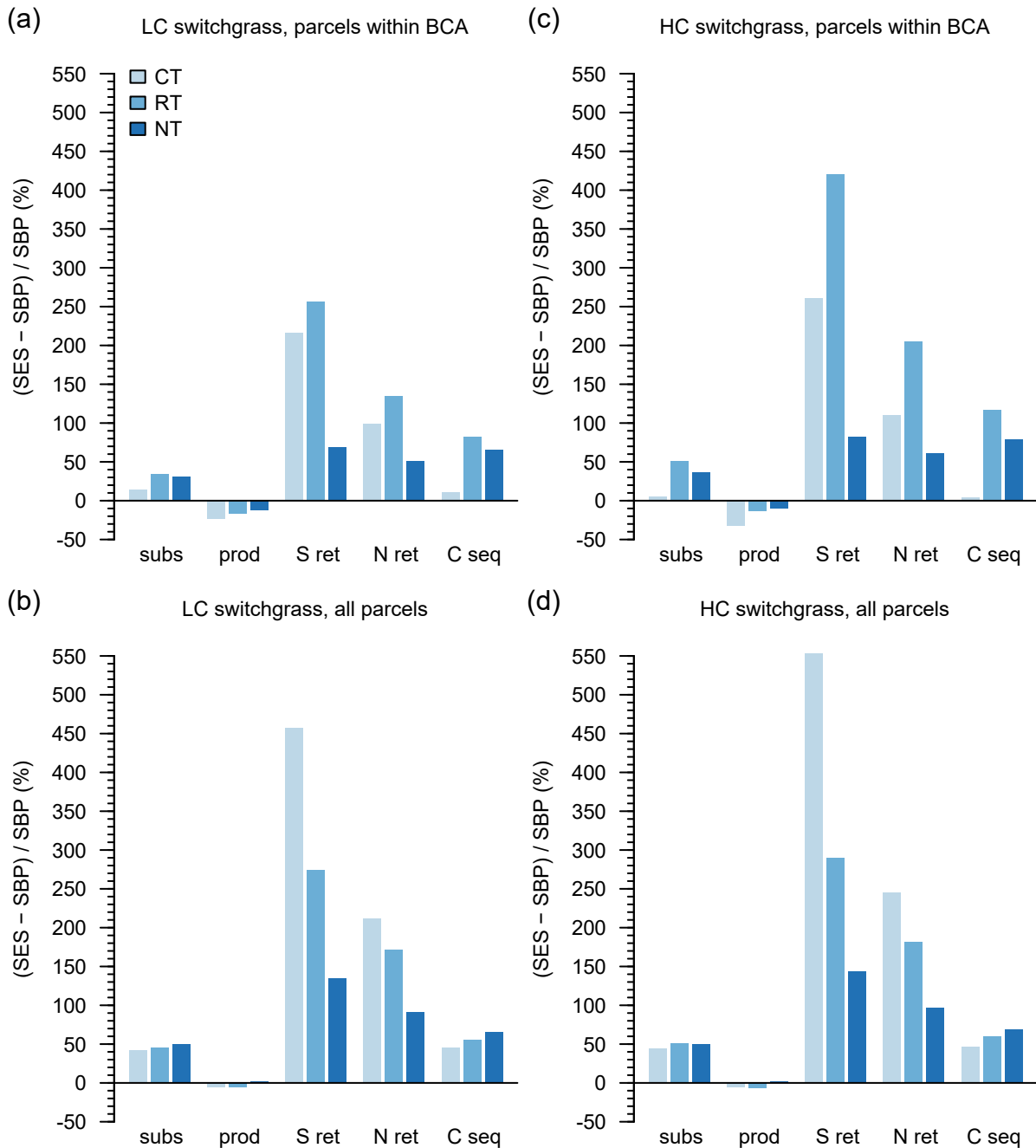


Figure 49. For switchgrass substitution on 5% of eligible corn or wheat parcels under conventional tillage (CT), reduced tillage (RT), or no-till (NT), the percent difference in annual subsidy (subs), biomass production (prod), soil retention (S ret), nitrogen retention (N ret), and carbon sequestration (C seq) between the subsidized environmental services (SES) and subsidized biomass production (SBP) approaches. (a) low-cost (LC) switchgrass establishment, parcels within biorefinery collection areas (BCA); (b) LC establishment, all parcels; (c) high-cost (HC) establishment, parcels within BCA; (d) HC establishment, all parcels.

4.4.6. 1. LCC of substituted parcels

The SES and SBP approaches differed greatly in the LCC of parcels converted into switchgrass production (Figure 50). Land capability classification shows, in a general way, the suitability of soils for most types of field crops (Soil Survey Staff, 2018). Soils in classes 1 through 4 are generally considered suitable for cultivated cropping, with class 1 soils having few limitations, class 2 soils having moderate limitations requiring moderate conservation practices, and class 3 and 4 soils having severe or very severe limitations requiring careful management. Soils in classes 5 through 7 are generally considered unsuitable for cultivated cropping, as they have severe or very severe limitations that restrict their use mainly to pasture, rangeland, grazing, forestland, or wildlife habitat. Class 8 soils have limitations that preclude commercial plant production, and are thus excluded from this investigation.

Across LC and HC establishment, the SES approach preferentially allocated switchgrass to those parcels least suitable for cultivated cropping. An LCC of 5, 6, or 7 is featured on less than 5% of corn and wheat parcels eligible for substitution (Figure 50a,c ‘ref’) but 10 to 30% of SES-converted parcels (Figure 50a,c ‘CT’, ‘RT’, and ‘NT’). Similarly, 24 to 48% of converted parcels have an LCC of 3 or 4 (Figure 50a,c ‘CT’, ‘RT’, and ‘NT’), compared to just 23% of corn and wheat parcels overall (Figure 50a,c ‘ref’). Similar to SES, the SBP approach converts a lesser proportion of LCC 1 and 2 parcels (Figure 50b,d ‘CT’, ‘RT’, and ‘NT’) than found among existing corn and wheat parcels (Figure 50b,d ‘ref’), thus leaving a greater proportion of these high-quality croplands for cultivated cropping. However, in comparison to SES (Figure 50a,c), SBP converts a greater proportion of LCC 3 and 4 parcels and a lesser proportion of LCC 6 and 7 parcels (Figure 50b,d). Thus, while SBP removes environmentally-sensitive lands from cultivated cropping, it is less effective than SES in converting the most sensitive parcels into switchgrass production.

4.4.6. 2. Marginal lands – Physical vs. Economic

This investigation assumes that harvested corn and wheat residue will be the primary feedstocks for emergent cellulosic bioenergy systems within the study region, and that

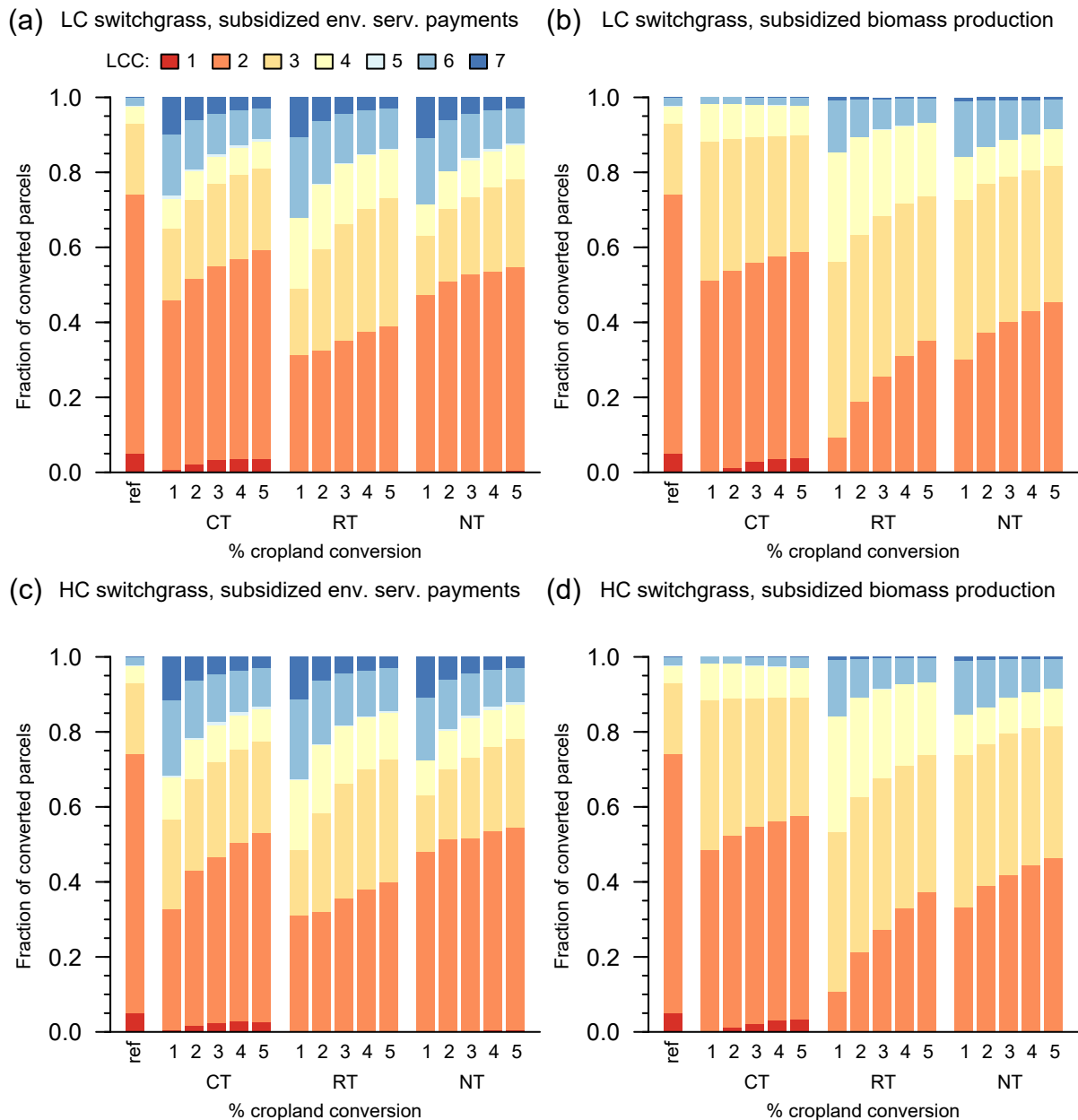


Figure 50. For switchgrass with low-cost (LC) establishment, subsidized (a) environmental services payments or (b) biomass production, and competing with corn or wheat in a conventional tillage (CT), reduced tillage (RT), or no-till (NT) system, the distribution of land capability classifications (LCC) among converted parcels when converting 1 to 5% of corn and wheat parcels considered eligible for switchgrass production. The reference (ref) column refers to the distribution of LCC among all corn and wheat production parcels eligible for conversion to switchgrass. (c – d) Corresponding values for HC establishment.

switchgrass could be produced on economically marginal lands if its profitability was equal to that of corn or wheat at a biomass price of \$60 Mg⁻¹ or less. By this definition, there are currently no marginal lands suitable for switchgrass production within the study region (Figures 43 and 44a–c); this concurs with previous analyses for this region (Jain et al., 2010; Krohn, 2015). Without biomass price supports or environmental services payments, switchgrass is not competitive with corn or wheat within areas featuring sufficient biomass for a 258,000 Mg yr⁻¹ biorefinery.

The subsequent analysis of switchgrass production subsidized through price support or environmental services payments was also designed to identify economically marginal parcels, as those parcels requiring the lowest biomass price or environmental services payments were the first to be converted to switchgrass production. This analysis revealed overlap between economically and physically marginal land, as parcels with a LCC of 3 to 7 were also disproportionately selected by the SES and SBP conversion scenarios (Figure 50). Nonetheless, the improved environmental outcomes of the SES scenario, which converted a higher proportion of LCC 6 and 7 parcels than SBP, illustrates that there are differing environmental outcomes to biomass cropping among these LCC classes. Although it is common to classify parcels within a range of LCC classes as ‘marginal’ (e.g. 3 to 8 [Feng et al., 2017; Uden et al., 2013]; 5 to 7 [Gelfand et al., 2013]; or 4 to 8 [Hamdar, 1999]), these results support the approach of considering land functionality to quantitatively identify marginal lands (e.g. Kang et al., 2013a). These observations also support the general conclusions of Richards et al. (2014): the use of marginal lands for biomass cropping should be predicated on the development of specific, verifiable, and comparable definitions for marginal land.

4.4.6. 3. Considerations of scale

The parcel size of 64 ha used in this investigation approximates a quarter-section of land in the Public Land Survey System, which represents a typical agricultural management unit within the study region. At this scale, there are clear environmental and land-use conversion benefits of SES switchgrass substitutions. However, as future cellulosic energy

systems develop, switchgrass placement decisions must consider a range of spatial scales. At a local scale, the amount of sustainably harvestable annual crop residue varies within fields (Muth et al., 2012), thus presenting opportunities for profitable switchgrass production within field areas where combined grain and residue harvest are unprofitable (Bonner et al., 2014). Similarly, within-field riparian buffers and grass waterways set aside for environmental protection could also provide cellulosic biomass (Coffin et al., 2016). At broader scales, landscape position has been shown to have no effect on switchgrass establishment or biomass yields within the first four years of establishment (Wilson et al., 2014), but Zilverberg et al. (2018) found that C sequestration rates on a farm undergoing transition to mixed grasslands were greatest in the most eroded landscape positions. Furthermore, favorable biodiversity outcomes provided by switchgrass and other forms of perennial agriculture, such as pest control (Liere et al., 2015; Meehan et al., 2011; Werling et al., 2011, 2014), pollination (Bennett and Isaacs, 2014; Werling et al., 2014), avian species richness (Meehan et al., 2010; Robertson et al., 2011b; Werling et al., 2014), and migratory bird habitat (Robertson et al., 2011a), are influenced by the positioning of these perennial crops on the landscape. Clearly, comprehensive land-use planning is essential to realize the desired energetic, environmental, social, and economic outcomes of switchgrass and other cellulosic biomass crops (Landis et al., 2018; McGranahan, 2014; Robertson et al., 2017).

4.4.6. 4. Proliferation of potential biorefineries

As switchgrass production is introduced into the study region, its increased biomass yields relative to corn and wheat allow for cellulosic biorefineries to be located in areas where corn and wheat biomass supply are insufficient. Figure 51 shows the progression of potential biorefineries into new areas if 5% of eligible corn and wheat parcels were replaced with LC establishment switchgrass having SES or SBP. Figure 52 is the corresponding figure for HC establishment switchgrass.

Although the estimated locations of potential biorefineries differ across the four possible combinations of LC, HC, SES, and SBP, the general trends are similar across these

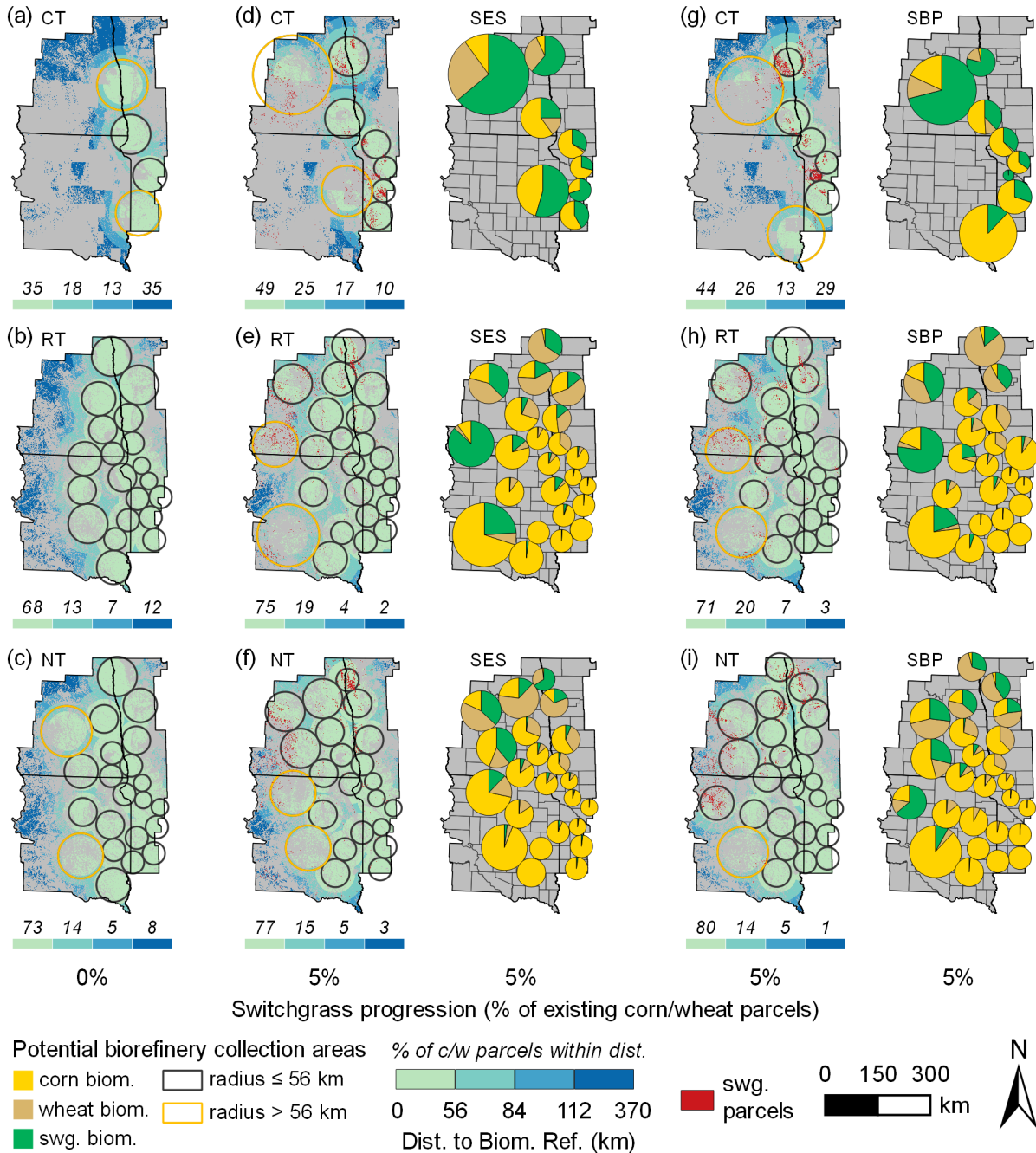


Figure 51. Distances from biomass-producing corn and wheat parcels to the nearest potential biorefinery under (a) conventional tillage (CT), (b) reduced tillage (RT), and (c) no-till (NT) systems (biorefineries from Figure 38). Distances from biomass-producing corn and wheat parcels to the nearest potential biorefinery and the proportions of corn, wheat, and switchgrass (swg.) biomass collected by each biorefinery where switchgrass with low-cost establishment and subsidized environmental services payments (SES) replaced 5% of eligible corn or wheat parcels under (d) CT, (e) RT, and (f) NT. (g – i) Same as (d – f), except for switchgrass with subsidized biomass production (SBP).

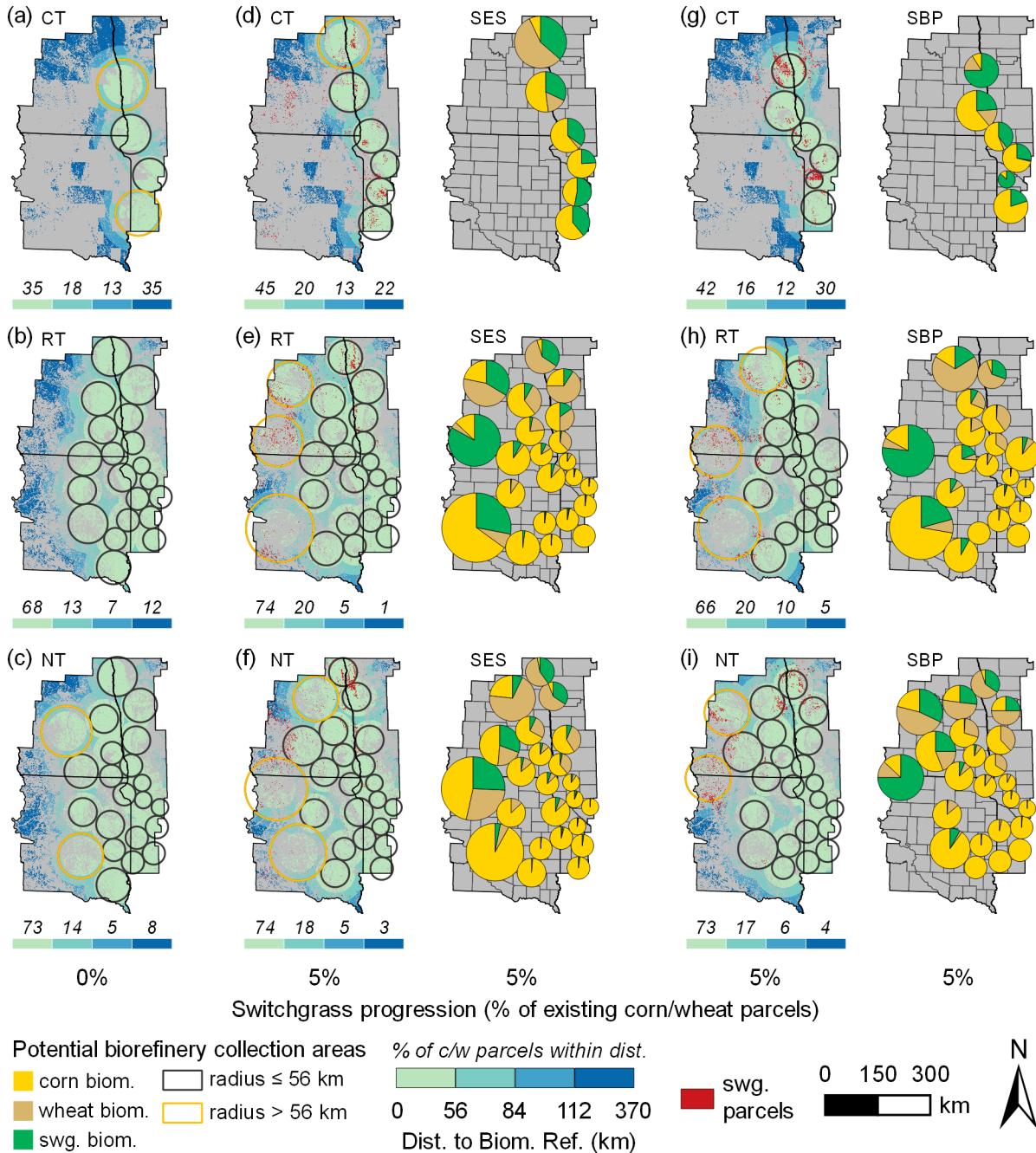


Figure 52. Distances from biomass-producing corn and wheat parcels to the nearest potential biorefinery under (a) conventional tillage (CT), (b) reduced tillage (RT), and (c) no-till (NT) systems (biorefineries from Figure 38). Distances from biomass-producing corn and wheat parcels to the nearest potential biorefinery and the proportions of corn, wheat, and switchgrass (swg.) biomass collected by each biorefinery where switchgrass with high-cost establishment and subsidized environmental services payments (SES) replaced 5% of eligible corn or wheat parcels under (d) CT, (e) RT, and (f) NT. (g – i) Same as (d – f), except for switchgrass with subsidized biomass production (SBP).

combinations. For switchgrass competing with CT, adding switchgrass to the landscape allows for additional biorefineries primarily within 120 km to the east or west of the Minnesota-Dakotas border (Figures 51 and 52, a vs. d and g). Any westward expansion beyond that distance is only possible with collection area radii of 96 to 112 km (e.g. Figure 51d,g). Due to the relatively low corn and wheat biomass yields associated with CT, switchgrass contributes 43% of biorefinery biomass on average (Figure 51d,g; Figure 52d,g). In contrast to CT, switchgrass in combination with RT or NT corn and wheat allows for biorefinery expansion further into the western study region. Under RT, potential biorefineries are technically feasible to the western edge of North Dakota counties with collection radii up to 72 km, and to the western edge of South Dakota counties with collection radii up to 96 km (Figures 51 and 52, b vs. e and h). Under NT, potential biorefineries with collection radii of 72 km or less are found over nearly the entire area with LC establishment switchgrass (Figure 51c vs. f and i), while radii up to 88 km are required to cover a similar extent when using HC establishment switchgrass (Figure 52c vs. f and i). Across all combinations featuring RT or NT corn and wheat, 81 to 87% of corn and wheat parcels are within 84 km of a biorefinery when corn and wheat are the sole biomass sources (Figures 51 and 52b,c); this increases to 86 to 94% of parcels when switchgrass is added to the landscape (Figures 51 and 52e,f,h,i – left panels). Switchgrass biomass generally constitutes a greater proportion of biorefinery biomass in the northern and western areas of the study region, where switchgrass biomass ranges from 7 to 87% of all biorefinery biomass (Figures 51 and 52e,f,h,i – right panels). Over the rest of the study region, switchgrass biomass ranges from 0 to 22% of all biorefinery biomass.

4.4.6. 5. Proliferation of switchgrass production

Although westward expansion of biorefineries would present enhanced opportunities for bioenergy production, it may also encourage further agricultural encroachment onto existing grasslands. Figure 53 provides an example of progression onto existing grassland that could occur when utilizing SBP to replace RT corn and wheat with LC establishment switchgrass. In this scenario, biomass prices from \$85 to \$93 Mg⁻¹ would be necessary to

convert from 82,000 to 410,000 ha of existing corn and wheat parcels (1 to 5% of eligible) to switchgrass (Figure 53a). At these prices, switchgrass would be profitable and economically competitive with corn and wheat on 690,000 to 1.43 million ha of existing perennial grasslands (Figure 53b), primarily in the western portion of the study region that features rangeland, pasture, CRP, and remnant prairie intermixed with cultivated cropland (Figure 31a). Thus, efforts to subsidize cellulosic bioenergy systems could result in conversions of grassland parcels similar to those already observed under existing bioenergy systems. Significant conversions of grasslands to cultivated cropping have been documented in the study region in the late 2000s and early 2010s (Faber et al., 2012; Johnston, 2014; Lark et al., 2015, 2018; Wright and Wimberly, 2013), and Wright et al. (2017) identified areas surrounding existing corn grain ethanol plants as land-use change hotspots.

Due to the difficulty in identifying different grass-dominated land covers in satellite imagery, many past investigations identified cropland-to-grassland conversions that may involve one or more types of grass-dominated land cover: native prairie, grass pasture and hay, and retired cropland converted to perennial grasses through CRP (Faber et al., 2012; Johnston, 2014; Wright and Wimberly, 2013). However, Lark et al. (2015) used long-term datasets to identify recent conversions of unimproved grasslands not used for cropping or pasture since at least the early 1970s, while Lark et al. (2018) combined satellite imagery, aerial photographs, and a field-based inventory to identify accelerated native prairie conversions in western Minnesota from 2008 to 2012. Such conversions of native prairie are highly concerning, as native prairie remnants within the study region belong to one of North America's most endangered ecosystems (Samson et al., 2004), provide critical habitat for grassland birds and migratory waterfowl (Brennan and Kuvlesky Jr., 2005; Johnson et al., 2010), and are a massive store of soil C (Euliss Jr. et al., 2006; Jobbágy and Jackson, 2000; Smith, 2014; Ward et al., 2016). In efforts to protect these ecosystems, the US Farm Bill implemented the Swampbuster provision in 1985 to preserve native prairie wetlands from agricultural conversion (Brady, 2000, 2005; Reynolds et al., 2006, 2007), while the Sodsaver provision for

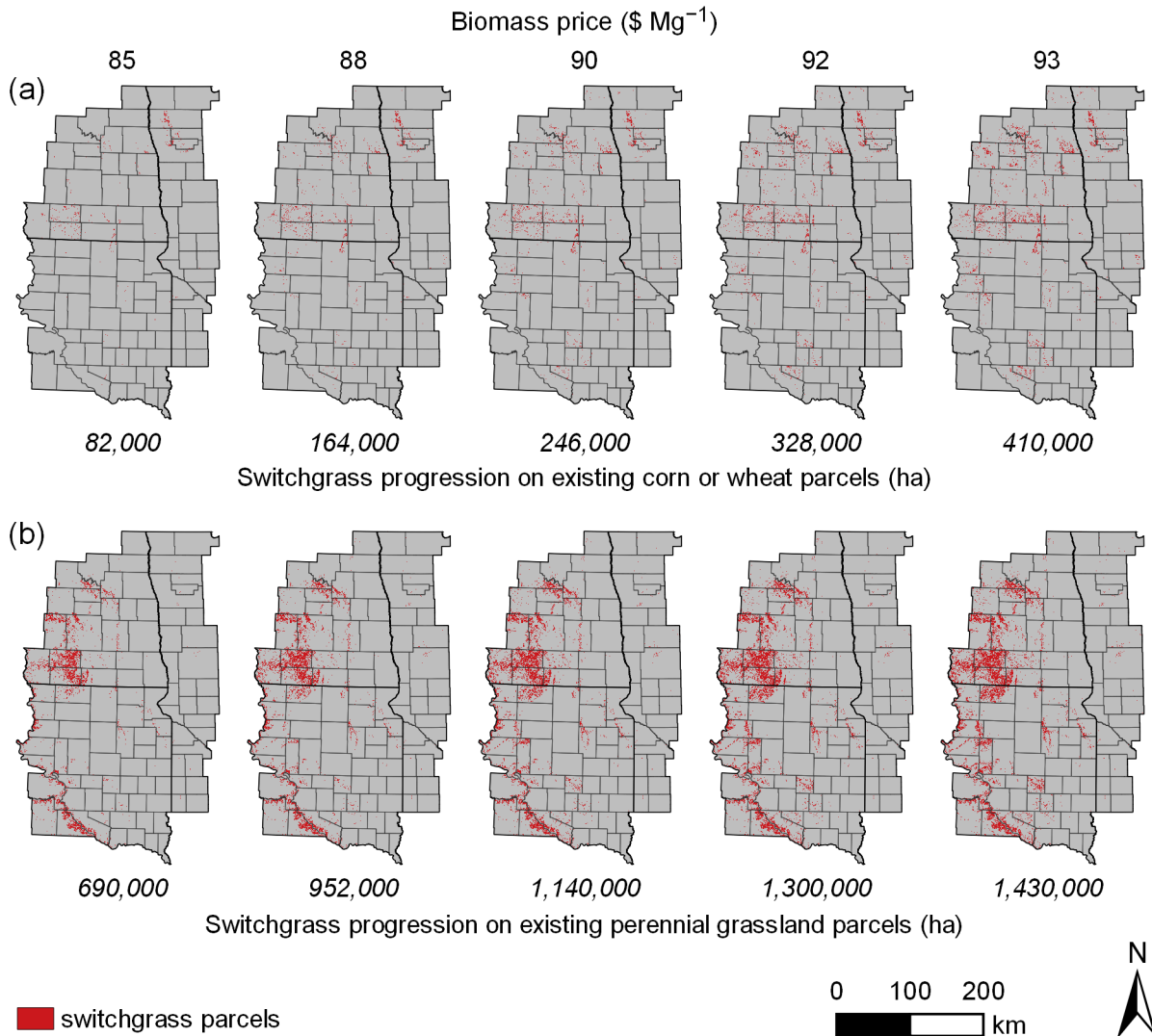


Figure 53. Under the biomass prices necessary to convert 1 to 5% of eligible corn or wheat parcels in a reduced tillage system to switchgrass production, (a) switchgrass progression across existing corn or wheat parcels assuming low-cost establishment and subsidized biomass production and (b) existing perennial grassland parcels where switchgrass would be profitable and economically competitive with corn or wheat production.

protection of native prairie grasslands was implemented in 2014 (Claassen et al., 2018; Miao et al., 2016). Opportunities exist to protect these ecologically important landscapes, already vastly modified by agricultural development, alongside cellulosic bioenergy development (Dale et al., 2014, 2010; Fargione et al., 2009; Robertson et al., 2017; Tilman et al., 2009).

In contrast to native prairie, CRP grasslands are oftentimes cited as a potential biomass resource (Jungers et al., 2013; Lee et al., 2007; Mulkey et al., 2006) or as candidates for conversion to switchgrass (LeDuc et al., 2017). Conservation Reserve Program grasslands are retired croplands subject to periodic disruptions as contracts expire; for example, total CRP enrollment in Minnesota, North Dakota, and South Dakota declined from 6.9 Mha in 2006 to 4.1 Mha in 2015 (USDA FSA, 2018). If biomass cropping were allowed on CRP lands, the additional revenue provided by biomass harvests could reverse this decline and keep these lands in perennial cover. Since CRP grasslands generally have lesser ecological function than undisturbed native prairie (Burke et al., 1995; Foster et al., 2003; McIntyre and Thompson, 2003), the environmental impacts of allowing cellulosic biomass harvest on CRP are far less concerning than those impacts resulting from native prairie conversions to agricultural uses. Nonetheless, CRP provides numerous environmental benefits, including wildlife habitat (Dunn et al., 1993; Haufler, 2005; Hohman and Halloum, 2000; McIntyre and Thompson, 2003; Reynolds et al., 2006, 2007), soil C storage (Burke et al., 1995; Gelfand et al., 2011; McLaughlin et al., 2006), and retention of soil and nutrients (Gleason et al., 2011; Hansen, 2007). Any conversions of CRP grasslands to other uses, including biomass cropping, should be managed carefully to minimize the disruption of these services (Abraha et al., 2018; Morefield et al., 2016; Wu and Weber, 2012). Just as comprehensive land-use planning will be essential to realize the benefits of switchgrass biomass cropping across multiple spatial scales, such planning will also be necessary to ensure that switchgrass cultivation does not further threaten existing ecosystems (Fletcher Jr. et al., 2011; Gelfand et al., 2011; Jungers et al., 2015; McGuire and Rupp, 2013; Werling et al., 2014).

4.4.7. Improving switchgrass competitiveness through increased yield

A possible alternative to subsidizing switchgrass production is to breed higher-yielding switchgrass cultivars, thus improving its economic competitiveness. Switchgrass production in the Northern Plains has been limited to upland ecotypes, which possess lower yield potential yet superior winter survival relative to lowland ecotypes (Mitchell et al., 2014). For example, a database of switchgrass yields from 1190 yield observations within 39 field trials (Wullschleger et al., 2010) showed that ‘Alamo’, ‘Kanlow’, and ‘Cave-in-Rock’ were the most widely-grown switchgrass cultivars in the US, with median biomass yields of 12.2, 14.2, and 9.6 Mg ha⁻¹, respectively. However, only ‘Cave-in-Rock’ has a production history in the northern US, with a mean yield of 8.5 Mg ha⁻¹ across 47 field observations (Maughan, 2011), as ‘Alamo’ and ‘Kanlow’ are lowland ecotypes unadapted to the Northern Plains. Furthermore, all three cultivars were released between 1960 and 1980 (Alderson and Sharp, 1994), prior to the 1992 selection of switchgrass as a model bioenergy crop within the US Department of Energy’s (DOE) Biofuels Feedstock Development Program (BFDP; Wright and Turhollow, 2010). According to Casler (2012), switchgrass breeders have likely increased yields by 20 to 30% since the inception of the US DOE BFDP.

Resulting from the breeding efforts of the US DOE BFDP, the USDA-sponsored CenUSA bioenergy project (<https://cenusa.iastate.edu/>) released ‘Liberty’ switchgrass in 2013 (Vogel et al., 2014). ‘Liberty’, a high-yielding lowland-type switchgrass cultivar, possesses winter survival similar to upland cultivars, yield increases of 25 to 40% relative to upland cultivars, and is adapted for areas north of 40° N latitude. To examine if ‘Liberty’ switchgrass could be economically competitive in the study region, Figure 54 shows the yield increases necessary for our simulated upland-type switchgrass to be economically competitive with corn or wheat under CT, RT, or NT at a biomass price of \$60 Mg⁻¹. In isolated areas of the study region, LC establishment switchgrass would be economically competitive with a yield increase of 15 to 40%, which should be attainable with ‘Liberty’ (Figure 54a–c). However, most of the region would require yield increases from 40 to 110% for LC establishment switchgrass to

be economically competitive. For HC establishment switchgrass, yield increases from 75 to 145% would be necessary for switchgrass to be competitive with corn or wheat (Figure 54d–f). Although high-yielding cultivars such as ‘Liberty’ are promising for switchgrass production in the Northern Plains, a strategy combining improved cultivars and financial incentives will be necessary for switchgrass to be economically competitive with corn or wheat under current technical and economic conditions.

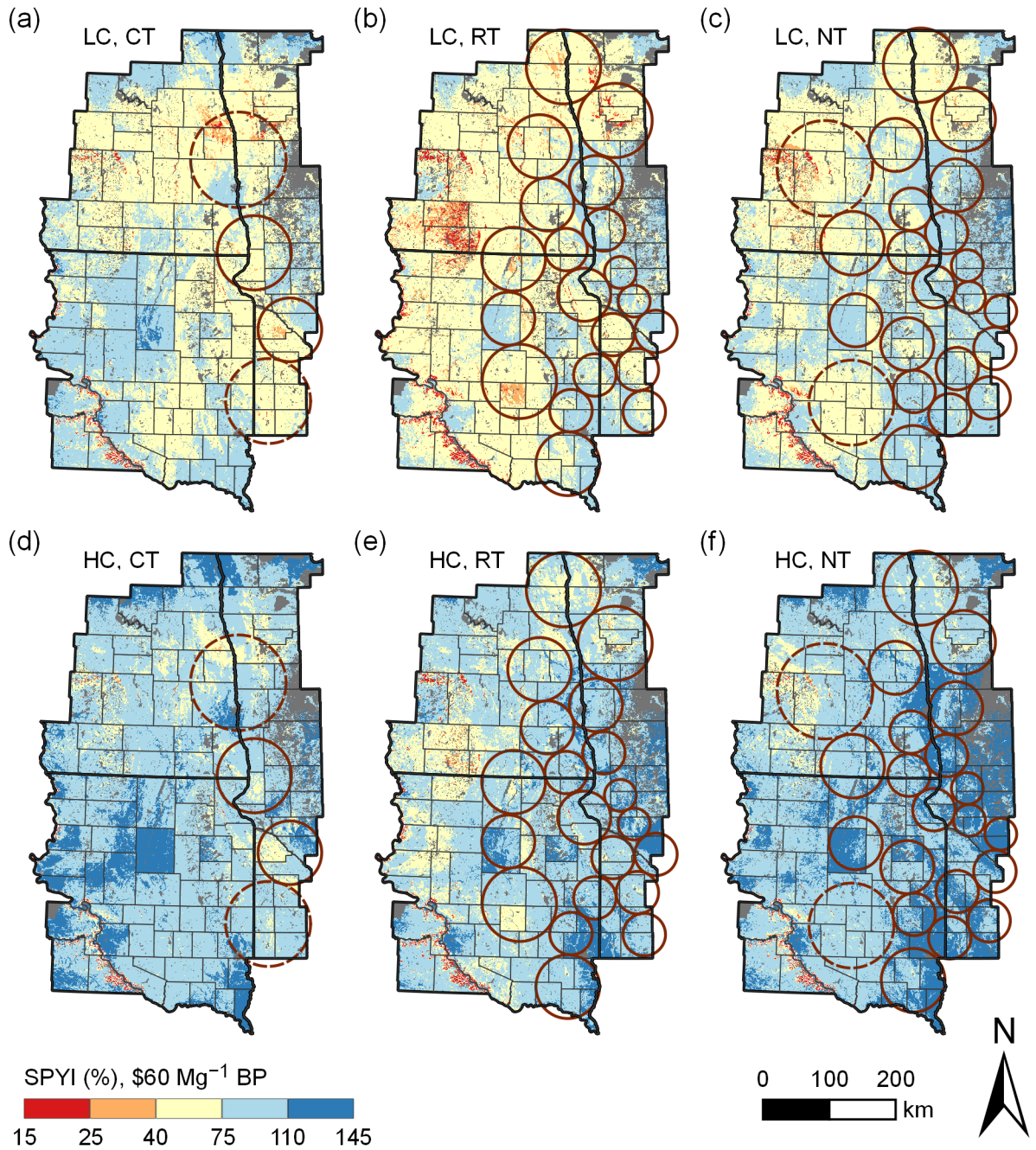


Figure 54. (a – c) For a biomass price (BP) of \$60 Mg⁻¹ and switchgrass production with low-cost (LC) establishment, the biomass yield increase necessary for switchgrass to generate the same net return as a competing corn or wheat system (SPYI, switchgrass parity yield increase) under conventional tillage (CT), reduced tillage (RT) or no-till (NT). (d – f) Corresponding values for high-cost (HC) establishment.

4.5. Conclusions

A summary of findings is presented in Table 16. Under RT or NT systems, there exists a sufficient amount of corn and wheat biomass to support cellulosic biofuel production across most of the study region (Section 4.4.1). The available biomass within potential biorefineries could produce sufficient ethanol to displace up to 33% of mean annual gasoline consumption for the transportation sector within study region states. Up to 74% of the technically-available corn and wheat biomass within potential biorefineries would be economically available at biomass prices of \$45 Mg⁻¹ or less, while all biomass would be economically available at biomass prices of \$60 Mg⁻¹ or less (Section 4.4.2). Switchgrass biomass is not economically competitive with corn and wheat biomass at these prices. To earn the same net return as its competing corn-soybean or wheat-soybean system in CT, RT, or NT, switchgrass would require biomass prices from \$60 to \$140 Mg⁻¹ under a LC establishment scenario and from \$100 to \$180 Mg⁻¹ under a HC establishment scenario (Section 4.4.3). Although switchgrass provides soil erosion mitigation, N loss mitigation, and C sequestration advantage when compared to corn or wheat (Section 4.4.4), and these benefits could be monetized through environmental services payments, subsidizing switchgrass production to achieve the conversion of 82,000 to 410,000 ha of existing corn and wheat parcels would require funding levels up to 7.5 times greater than past federal government expenditures for the entire US (Section 4.4.5). Nonetheless, opportunities may exist to reallocate funding from other areas to support switchgrass production, as financial support of biomass cropping represented just 0.05% of overall Farm Bill spending from 2008 through 2017.

When subsidizing switchgrass, prioritizing the conversion of corn and wheat parcels where switchgrass would offer the greatest environmental benefit, as opposed to the greatest increase in biomass production, would increase the resulting amount of soil retention, N retention, and soil C sequestration by up to 420%, 210%, and 120%, respectively. This approach would also preferentially convert corn and wheat parcels with LCC of 5 to 7 into switchgrass production, and these represent the current corn and wheat parcels least suitable

for cultivation (Section 4.4.6). Expanded switchgrass production could enable biorefineries to proliferate to the western edge of the study region, with switchgrass serving as a major biomass source, but may also encourage switchgrass production on up to 1.43 Mha of existing perennial grassland within the study region. The use of a newly-developed high-yielding switchgrass cultivar ('Liberty') would reduce the amount of financial support necessary for switchgrass production, but would be insufficient by itself to make switchgrass economically competitive with corn and wheat residue harvest (Section 4.4.7).

In conclusion, widespread switchgrass production is unlikely under current technical and economic conditions. Nonetheless, implementing switchgrass production on the most environmentally-sensitive parcels currently used for cultivated cropping results in considerable environmental benefits. Any payments to encourage switchgrass production should be designed to encourage switchgrass production in areas where it will provide the greatest environmental benefit, and to avoid further conversions of existing perennial grasslands.

Table 16. Summary of findings from Chapter IV results (Section 4.4).

Section	Finding
4.4.1	<p>under CT, RT, and NT systems, corn and wheat residues from 2006 to 2015 were sufficient to support biorefineries within the study region</p> <p>combined corn and wheat biomass availability within estimated biorefinery collection areas is 2.32, 13.98, and 16.48 Tg for CT, RT, and NT, respectively</p> <p>technically-available biomass could displace 4 to 33% of mean annual gasoline consumption for the transportation sector within the study region states</p>
4.4.2	<p>economically-available corn and wheat biomass within estimated biorefinery collection areas is 1.23, 10.82, and 12.18 Tg at \$45 Mg⁻¹ or less for CT, RT, and NT, respectively</p> <p>all corn and wheat biomass within estimated biorefinery collection areas is economically-available at \$60 Mg⁻¹ or less</p>
4.4.3	<p>for low-cost (LC) establishment switchgrass, the switchgrass parity price (SPP) within estimated biorefinery collection areas ranges from \$60 to \$140 Mg⁻¹</p> <p>for high-cost (HC) establishment switchgrass, the SPP within estimated biorefinery collection areas ranges from \$100 to \$180 Mg⁻¹</p>

Table 16. cont.

Section	Finding
4.4.4	<p>median estimates of soil erosion mitigation, N loss mitigation, and C sequestration advantage from switchgrass production are consistent with published field observations</p> <p>the soil erosion, N loss, and C sequestration benefits of switchgrass production decrease as competing tillage systems convert from CT to RT to NT</p>
4.4.5	<p>converting 410,000 ha of existing corn or wheat land to switchgrass through subsidized environmental services (SES) would require \$170 to \$290 million annually</p> <p>converting 410,000 ha of existing corn or wheat land to switchgrass through subsidized biomass production (SBP) would require \$120 to \$200 million annually</p> <p>relative to SBP, using SES to convert 410,000 ha of existing corn or wheat land to switchgrass would increase soil retention, N retention, and soil C sequestration by up to 420%, 210%, and 120%, respectively</p>
4.4.6	<p>relative to SBP, SES substitutions preferentially selects parcels least suitable for cultivated cropping (LCC of 5 to 7)</p> <p>switchgrass substitutions would allow biorefinery expansion to the western edge of the study region under RT and NT, where switchgrass would provide up to 87% of all biorefinery biomass</p> <p>subsidizing switchgrass production could encourage switchgrass production on up to 1.43 Mha of existing perennial grassland, primarily in western portions of the study region</p>
4.4.7	<p>‘Liberty’, a newly-developed high-yielding switchgrass cultivar, would require subsidy to be economically competitive with corn or wheat</p>

CHAPTER V

GENERAL DISCUSSION

For a 99-county area of the US northern Great Plains characterized by gradients in precipitation, temperature, native land cover, wheat cropping, and corn cropping, the preceding chapters of this dissertation provide (i) an improved method for using the ALMANAC model to simulate yields of upland switchgrass ecotypes adapted to the northern US (Chapter II), (ii) a methodology for using ALMANAC to simulate corn and wheat yields at a moderate resolution over a regional scale (Chapter III), and (iii) a comparative analysis of the technical supply, economic availability, and environmental outcomes of corn, wheat, and switchgrass biomass cropping (Chapter IV). Discussions embedded within each chapter (i) describe and validate ALMANAC switchgrass parameterization changes against field observations of switchgrass phenology, physiology, and productivity across the northern US and southern Canada (Section 2.5), (ii) contrast the regional-scale corn and wheat simulations to the protocols and outcomes of ALMANAC simulations using field-scale parameterizations of soil properties and weather conditions (Sections 3.4.1, 3.4.2 and 3.4.5), (iii) consider the potential for using remote sensing data to improve the accuracy of annual corn and wheat ALMANAC simulations at a regional scale (Section 3.4.5), (iv) compare the estimated technical, economic, and environmental outcomes for corn, wheat, and switchgrass to past field observations and simulation studies (Sections 4.4.1 to 4.4.4), (v) consider the energetic and environmental outcomes of biomass cropping within the contexts of current transportation energy use and ongoing initiatives to improve the environmental outcomes of agricultural systems (Sections 4.4.1 and 4.4.5), (vi) consider the subsidies necessary to support switchgrass production within the context of current government subsidies for biomass cropping (Section 4.4.5), (vii) discuss the possible land-use implications of switchgrass

cropping (Section 4.4.6), and (viii) discuss the potential of a new high-yielding switchgrass cultivar to improve its competitiveness relative to corn or wheat (Section 4.4.7).

The discussion provided in this concluding chapter is focused on two overarching themes from the preceding three chapters: (i) Methods for estimation of regional-scale biophysical outcomes at low-to-moderate resolution, and (ii) Moving from regional to local scales in estimating and incentivizing land-use outcomes. The discussion provided herein provides additional context to the preceding chapters, considers limitations of the chosen methodologies, and suggests opportunities for future work.

5.1. Methods for estimation of regional-scale biophysical outcomes at low-to-moderate resolution

5.1.1. Modeling overview

Synthesis of research understanding, cropping system decision management, and policy analysis are the three broad purposes for which crop models have been developed (Boote et al., 1996; Jones et al., 2016). Models to synthesize scientific understanding are typically mechanistic models, designed to simulate known or hypothesized physical, chemical, or biological processes occurring in crop production systems (Boote et al., 1996; Di Paola et al., 2016; Jones et al., 2016). These models tend to operate on fine time scales (instantaneous to hourly), include a large number of parameters, and require input information that may not be readily available for general applications. Therefore, fully mechanistic models are unsuitable for investigations of cropping system decision management and policy analysis, such as the investigation presented in Chapter IV.

In contrast to mechanistic models, empirical models and dynamic system simulation models (DSSMs) are broadly applicable to these types of investigations (Jones et al., 2016). Dynamic system simulation models, such as ALMANAC (Agricultural Land Management Alternative with Numerical Assessment Criteria; Kiniry et al., 1992) describe changes to cropping system states in response to external drivers such as weather conditions, management practices, and soil characteristics. These models typically integrate several mechanistic and

functional routines, with functional routines defined as empirical functions that approximate complex physical, chemical, or biological processes (Boote et al., 1996; Jones et al., 2016). Empirical crop models characterize statistical relationships between outcomes (e.g. crop yield) and predictive variables (e.g. temperature, rainfall, soil texture) with no consideration for the underlying biophysical processes responsible for the predicted outcomes. The computational efficiency of empirical models makes them particularly useful for predictions over a broad geographical scale, with the disadvantage that outcomes cannot be extrapolated “out of sample” because data used for parameter estimation do not represent soil, climate, and management practices encountered elsewhere (Jones et al., 2016).

5.1.2. Estimating biomass cropping outcomes

Shortly after the second Renewable Fuel Standard (RFS2) was adopted in 2007, which required cellulosic biofuel usage of 380 ML in 2010 and 61 GL by 2022 (Bracmort, 2019a), at least two investigations reported empirical models for predicting switchgrass biomass yields across the US. Wullschleger et al. (2010) compiled a database of 1190 switchgrass yield observations from 39 field trials across 17 states. Database yields were subsequently used to parameterize an empirical model predicting switchgrass yield as a function of four variables: annual average temperature, growing season precipitation, nitrogen (N) fertilization, and latitude. Finally, switchgrass yields were predicted across the contiguous US at a spatial resolution of 400 m. Jager et al. (2010) compiled a database of 1162 switchgrass yield observations from 31 locations across 17 states and 1 Canadian province, and subsequently parameterized empirical models predicting yields of upland and lowland switchgrass ecotypes as a function of nine variables: average growing season temperature, minimum winter temperature, total growing season precipitation, an index of soil wetness, total N fertilizer applied, an indicator variable for fertilizer application, depth to bedrock, number of harvests per year, and stand age. Finally, switchgrass yields were predicted across the US. The switchgrass yield estimates of Jager et al. (2010) and Wullschleger et al. (2010) were subsequently incorporated into the US Department of Energy Billion-Ton Update (U.S. Department of

Energy, 2011), thus informing US government bioenergy policy.

In contrast to empirical models, DSSMs can generally be extrapolated across a wide range of soil types, weather conditions, and management practices due to their mechanistic and functional subroutines (Jones et al., 2016; Thornton et al., 1991). Due to this characteristic, DSSMs are a powerful tool to predict crop yields and other biophysical variables under particular environmental characteristics and in response to specific management options and production scenarios (Di Paola et al., 2016). Thus, DSSMs are widely used to inform decision-making across a range of spatial scales, from management and enterprise decisions at the field and farm scales to economic optimization, environmental management, land use planning, and food security analysis at district, regional, national, and global scales (Boote et al., 2010; Jones et al., 2016).

As discussed in Chapters II and III, numerous investigations have used the ALMANAC model to predict corn and switchgrass yields at field scale in many regions of the US (Kiniry et al., 2005; Kiniry and Bockholt, 1998; Kiniry et al., 1996, 1997, 2004, 2008b; McLaughlin et al., 2006; Xie et al., 2001). Most of these investigations were published in the 1990s and 2000s. Recently, numerous investigations have advanced to using ALMANAC and other DSSMs to predict yield and other biophysical outcomes at regional-to-national scales, with results relevant to potential cellulosic bioenergy systems. Outcomes of these investigations include biomass yield of native prairie on physically-marginal land (Gelfand et al., 2013); switchgrass (Jain et al., 2010; Miguez et al., 2012; Thomson et al., 2009) and corn (Jain et al., 2010) yields under current climate and management conditions; switchgrass yield in response to projected climate change (Behrman et al., 2013); switchgrass primary production, CO₂ mitigation, N₂O emissions, and greenhouse gas (GHG) emissions under current conditions (Qin et al., 2015); soil erosion and losses of soil carbon (C), phosphorus (P), and N in switchgrass and corn cropping systems under conventional tillage and no-till (Powers et al., 2011); yield and soil organic C sequestration of corn and switchgrass under various land-use change scenarios (Davis et al., 2012; Qin et al., 2016a); yields, C sequestration, and soil erosion

of corn and switchgrass (Krohn, 2015); yields, GHG emissions, erosion, N loss, and P loss of corn, wheat, and switchgrass systems (Zhang et al., 2010); yield, GHG emissions, and soil organic C change with corn stover harvest (Jones et al., 2017a); water erosion, wind erosion, and soil conditioning index for residue removal from current crop rotations (Muth et al., 2013); and yields and soil C sequestration of corn and wheat (Zhang et al., 2015).

5.1.3. Calibration and validation of yield outcomes

Calibration and validation are essential steps for DSSM users, where calibration is the optimization process where model parameters are adjusted to improve model agreement with experimental observations or measurements, and validation is the process of confirming that the model predictions adequately represent measured or observed conditions within the model's domain of applicability (Di Paola et al., 2016). In order to extrapolate DSSM outputs beyond the environmental and management conditions inherent to the calibration dataset, the validation and calibration datasets must be independent of each other. In this dissertation, ALMANAC switchgrass parameters were calibrated to align with field observations of switchgrass growth from southern Canada and the Northern Great Plains states of Iowa, Minnesota, Nebraska, North Dakota, and South Dakota and validated against a separate set of field observations from 66 location-years of switchgrass production across 13 sites in the eastern Dakotas and western Minnesota (Chapter II). In contrast, corn and wheat parameters were calibrated to give county-level yield estimates consistent with a subset of 20 (corn) or 18 (wheat) study region counties, with the parameterizations subsequently validated against yields from the remaining study region counties (Chapter III). These switchgrass, corn, and wheat parameterizations were then used in the regional-scale analyses presented in Chapter IV.

A particular challenge for regional-scale investigations is to gather sufficient calibration and validation data to represent a geographically-broad study region. In switchgrass, several investigations have used extensive databases of switchgrass yield to calibrate and validate model performance in a manner similar to the procedure outlined in Chapter II. To calibrate and validate the BioCro model (Miguez et al., 2009) for switchgrass yield estimation across the

contiguous US, Miguez et al. (2012) used yield observations gathered from 58 locations across 20 states in the eastern and central US. For estimating switchgrass yield across the contiguous US with the EPIC (Erosion Productivity Impact Calculator) model (Williams et al., 1989), Thomson et al. (2009) used a dataset representing 1400 data points from 31 field trial locations; 67 data points from 10 states were drawn for the calibration procedure, with the remaining used for validation. Others have used considerably smaller datasets for model testing, with these small datasets usually featuring data points from a limited spatial extent. Using DAYCENT (daily version of CENTURY model; Parton et al., 1998) model parameters for switchgrass yield previously calibrated by Davis et al. (2010), Davis et al. (2012) validated DAYCENT with just 12 yield observations gathered from six locations in Illinois; subsequently, switchgrass yields were predicted across 21 states in the central and eastern US. Jain et al. (2010) estimated switchgrass yields across the contiguous US using the Integrated Science Assessment Model (ISAM; Jain, 2019), using parameters calibrated for one Illinois site and validated in six other Illinois sites. Krohn (2015) used 6 data points to validate the ALMANAC model for switchgrass yield estimation across six states in the north-central US, where these 6 data points represented averages across 193 location-years.

Although the author is unaware of a minimum number of data points considered acceptable for validating a DSSM, the quantity and spatial distribution of calibration and validation data points should be considered when assessing the validity of published DSSM parameterizations. Individual switchgrass ecotypes are known to have limited adaptability in areas more than approximately 2 degrees (≈ 220 km) north or south of their adapted range (Casler et al., 2004, 2007), and the investigation presented in Chapter II illustrates the inaccuracies that can arise when using parameters developed for an area far outside the study region. When considering that expansive datasets of switchgrass yields have been compiled for past investigations (Jager et al., 2010; LeBauer et al., 2018; Maughan, 2011; Wullschleger et al., 2010), and that these datasets feature yield from across much of the contiguous US, DSSM users should utilize these datasets to validate their parameterizations. For example,

the ALMANAC parameters for upland switchgrass developed in Chapter II were calibrated primarily from observations in southern Ontario, Canada and were validated in the eastern Dakotas and western Minnesota. Considering this, and that switchgrass ecotypes generally have broad adaptedness across longitudes (Casler et al., 2007), these ALMANAC parameters may be broadly applicable throughout the northern regions of the US considered suitable for upland ecotypes of switchgrass. Nonetheless, any future investigations utilizing the parameters developed in Chapter II outside the eastern Dakotas and western Minnesota should validate these parameters with field observations as near as possible to the study region.

The county-scale yields reported by the USDA National Agricultural Statistics Service (NASS) are spatially-consistent and date back to 1910 for corn and 1918 for wheat (USDA NASS, 2018). Thus, this dataset is a valuable resource for investigations requiring spatially-explicit crop yields. The methodologies presented in Chapter III, where USDA county yields were used for calibration and validation of ALMANAC corn and wheat yield parameters, are consistent with at least three examples from the literature. Zhang et al. (2010) did not modify the default EPIC parameters for estimating yield across nine counties in southwest Michigan, but used average USDA NASS yields from 1979 to 2003 to validate simulated corn, soybean, and winter wheat yields. Similarly, Zhang et al. (2015) did not calibrate the EPIC model for yield estimation across 12 states in the US Midwest, but validated EPIC yield outputs for corn, soybean, and winter wheat against average USDA NASS yields from 1991 to 2008. For estimating corn and soybean yields across six states in the US Midwest, Krohn (2015) calibrated ALMANAC for corn and soybean yield estimation using average 2004 to 2015 USDA NASS yields for 12 sample counties within the study region and validated ALMANAC parameters against USDA NASS yields for all study region counties. In a contrasting example, Jones et al. (2017a) compiled 1737 data points from ten experiments featuring corn with stover removal, in nine states across the US Midwest. Subsequently, EPIC was calibrated on 20% of the measurements and validated on the remaining dataset. When considering that the parameters developed in Chapter III estimated corn and wheat yields across three tillage

systems and four residue removal rates but were only validated against county-average yields from USDA NASS, further investigations utilizing an approach similar to Jones et al. (2017a) would further verify the outcomes presented in Chapter III.

5.1.4. Calibration and validation of environmental outcomes

For investigations estimating regional-scale erosion and N loss, it is common practice that the estimated outcomes are not validated against field measurements. In a nationwide assessment, Muth et al. (2013) estimated soil erosion across all agricultural soils using the RUSLE2 (Revised Universal Soil Loss Equation 2) and WEPS (Wind Erosion Prediction System) models, citing the preexisting use of these models for conservation planning within the USDA Natural Resources Conservation Service (NRCS) as justification for their use. In estimating soil erosion and soil N loss to surface water and groundwater for five Iowa soils with the APEX (Agricultural Policy/Environmental eXtender) model, Powers et al. (2011) cite extensive past evaluations of the APEX model as justification for its use. In an integrated modeling study over nine counties in southwest Michigan, Zhang et al. (2010) used the EPIC model to evaluate erosion, N loss, and P loss within 54 cropping system scenarios, citing that EPIC has been broadly tested and is capable of estimating these outcomes. Similarly, in this investigation, ALMANAC is used to estimate soil erosion and N runoff without validation against observed data.

In contrast to erosion and N loss, recent regional-scale evaluations of soil C dynamics have validated simulated outcomes against observational data. In modeling soil C sequestration with corn and switchgrass from 30 to 100 cm depth across the contiguous US, Qin et al. (2016a) validated simulated outcomes from a surrogate CENTURY model against a database of 328 field studies published by Qin et al. (2016b). Across nine states in the US Midwest, Jones et al. (2017a) validated EPIC simulations of soil organic C following corn with stover removal against nearly 1400 field observations. The inventory-based method of West et al. (2008) used in this investigation has been widely used elsewhere and was recently validated against spatially-explicit estimates across 12 Midwest US states from the EPIC model (Zhang et al.,

2015). Nonetheless, validating the soil C sequestration outcomes presented in this investigation would increase the confidence in associated inferences, particularly when comparing soil C sequestration across tillage systems (Section 4.4.4) and when considering that estimated environmental services payments for C sequestration are much greater than the estimated payments for soil erosion and N runoff (Figure 46a,c left panels).

5.1.5. Tradeoffs

Finally, the use of DSSMs for regional-scale investigations inevitably involves tradeoffs between model complexity, computational efficiency, spatial extent of the study region, and spatial resolution of model estimates. When using a complex field-scale DSSM such as ALMANAC or EPIC, the processing power necessary for a desired spatial resolution and spatial extent is a primary consideration. In order to conduct simulations at a moderate spatial scale (e.g. 30 m) over a broad spatial extent (e.g. multiple states to nationwide), supercomputing resources are necessary (Jones et al., 2017a; Muth et al., 2013; Zhang et al., 2015). Otherwise, a typical tradeoff is to limit spatial extent of the study region or the spatial resolution of model estimates. One common approach with field-scale models is to take a sampling of soils from across the study region, such as by randomly selecting soils from within a desired grid cell size (Behrman et al., 2013), selecting only certain types of soils from within simulation units (Gelfand et al., 2013; Thomson et al., 2009), using one set of weather conditions to represent all instances of a given soil within a survey area (Krohn, 2015), or selecting soils purported to be representative of a larger spatial extent (Powers et al., 2011). Alternatively, simulations may be conducted for all soils over a limited spatial extent (Zhang et al., 2010). Another approach is to use generalized inputs within a chosen DSSM, such as by averaging site-level soil characteristics within a desired grid cell size (Miguez et al., 2012) or by using gridded climate and soils datasets (Jain et al., 2010; Qin et al., 2015).

By simulating yields for all soils over a 99-county area, this investigation featured 561,166 simulation units. When considering the three crops (switchgrass, corn, wheat), three tillage systems for corn and wheat (CT, RT, NT), and ten separate simulations for

corn and wheat each featuring one soybean spinup year, this investigation required over 34 million simulations to generate the necessary yield outputs. This investigation did not use a supercomputing cluster to execute ALMANAC, but increased computing power or reduced spatial resolution of model outputs would be necessary to expand this methodology to a broader spatial extent.

5.2. Estimating and incentivizing land-use outcomes: Moving from regional to local scale

A primary feature of moderate-resolution regional assessments is the ability to evaluate interactions among factors such as crop productivity, environmental outcomes, and profitability at a spatial scale relevant to landowners or other land managers. These types of comparisons cannot be made when results of integrated assessments are instead aggregated to broader spatial scales such as county, watershed, or USDA agricultural district. Nonetheless, the results presented herein and in other moderate-resolution assessments are still an approximation of local conditions, as they cannot account for fine-grained variations within individual fields or account for the various interconnected factors affecting an individual farmers' decisions on adoption of a new innovation (see Abadi Ghadim and Pannell, 1999). This section of the discussion briefly considers how existing ethanol infrastructure, farmers' willingness to supply biomass, and precision agriculture decision support systems may influence the local adoption of cellulosic biomass cropping.

5.2.1. Existing ethanol infrastructure

In this investigation, technically-available corn and wheat biomass is defined as all biomass that can be harvested from within estimated biorefinery collection areas according to the removal rates provided by Muth et al. (2013). This estimate of technically-available biomass would benefit from consideration of existing infrastructure supporting corn grain ethanol production. Corn grain ethanol currently dominates the U.S. biofuels industry, as production of this first-generation biofuel has essentially been a mature industry since 2011 (Bracmort, 2019a; US EPA, 2019). There are currently 24 corn grain ethanol plants within the study region (US NREL, 2019), which represent considerable production and storage capacity

and feature access to additional necessary infrastructure such as road networks, railroad access, and water supplies. Co-location of grain ethanol and cellulosic ethanol plants produces lower-cost cellulosic ethanol than stand-alone cellulosic ethanol plants (Ou et al., 2014), and the only commercial-scale cellulosic ethanol plant currently operational in the US (PoetDSM Project LIBERTY in Emmetsburg, IA) is co-located with an existing corn grain ethanol plant in order to realize operational efficiencies (POET-DSM, 2018). Further refinement of the potential biorefinery locations presented in this investigation could be achieved by evaluating the spatially-explicit biomass production estimates in an approach similar to that of Uden et al. (2013), who analyzed biomass availability within a 40-km road network of an existing corn grain ethanol plant in eastern Nebraska. This should improve the accuracy of estimated biorefinery locations and thus improve estimates of technically-available biomass, and would provide useful information to corn grain ethanol manufacturers considering the co-location of cellulosic ethanol production at their facilities.

5.2.2. Farmers' willingness to supply biomass

Another limitation of this investigation is that all technically-available biomass within a biorefinery collection area is assumed to be available for conversion into cellulosic ethanol. Ultimately, the amount of cellulosic biomass available to biorefineries is dependent on the willingness of individual landowners to supply biomass for this purpose. In a focus group of 16 southeast North Dakota growers, Maung et al. (2012) found that 79% of respondents would be willing to contract most of their corn and wheat residue production while an additional 14% would be willing to contract 75% of their total production. However, grower and landowner surveys in southern Michigan (Skevas et al., 2016), southwest Wisconsin (Mooney et al., 2015), northern Wisconsin and northern Michigan (Swinton et al., 2017), and Iowa (Tyndall et al., 2011) have revealed that the quantity of biomass that farmers and landowners are willing to supply is far less than the quantity of biomass that is potentially available. Only 17% of Iowa farmers ($n = 594$) expressed a willingness to harvest corn stover (Tyndall et al., 2011). In north-central Iowa, which represents the area of the state with the greatest available supply of corn

stover, only 23% of farmers ($n = 185$) were willing to supply stover for bioenergy production. At rental rates double the prevailing land rental rate in the region, private landowners in northern Wisconsin and northern Michigan ($n = 1124$) were willing to rent land for bioenergy crops on only 21% of available land considered marginal for agricultural production and 23% of available cropland (Swinton et al., 2017). Similarly, private landowners in southern Michigan ($n = 599$) were willing to rent only 37% of all physically-marginal land for corn, switchgrass, or prairie at rental rates triple the prevailing rate of $\$247 \text{ ha}^{-1}$, with only 27% of marginal land available at the prevailing land rental rate (Skevas et al., 2016). Crop and livestock farmers in southwest Wisconsin ($n = 248$) were willing to supply corn stover or switchgrass biomass on no more than 30% of their cultivable land at biomass prices of up to $\$165 \text{ Mg}^{-1}$ (Mooney et al., 2015).

Clearly, future investigations would be strengthened by considering landowner willingness to supply land for biomass production, as measures of technical or economic availability may vastly overstate the quantity of available biomass. Furthermore, future investigations should contrast multiple scenarios regarding the spatial allocations of biomass parcels, as land parcels available for production of cellulosic biomass are likely to be spatially fragmented across the agricultural landscape (Mooney et al., 2015) and the intentions of individual landowners to rent land for bioenergy production are likely to be spatially dependent (Skevas et al., 2018).

5.2.3. Subfield allocation of cellulosic biomass cropping

Finally, this investigation presents outputs on a parcel size of 64 ha, which approximates a quarter-section of land in the US Public Land Survey System. Although a quarter-section of land is a typical management unit for cropping within the study region, this parcel size does not account for the fine-scale variability that farmers may encounter within their fields. Precision agriculture allows farmers to apply management practices at subfield scale, with clear implications for cellulosic biomass cropping. Precision agriculture would allow farmers to vary residue removal rates to match within-field variation in productivity, thereby optimizing

the amount of residue left behind to prevent soil erosion and loss of soil C, or to place perennial biomass crops in areas of fields where they will be most profitable or provide the greatest environmental benefit. For example, Bonner et al. (2014) found that up to 85% of corn producing fields in Hardin County, Iowa featured areas with negative net profits under current corn prices, presenting an opportunity for sub-field integration of switchgrass production. A similar analysis for all of Iowa estimated an upper bound of 4.3% of statewide corn-soybean cropland that would break even or realize increased profitability when converted to switchgrass production (Brandes et al., 2018). Conservation plantings on environmentally-sensitive portions of fields also represent a source of potential biomass (Coffin et al., 2016), especially in Minnesota where state law requires perennial vegetation buffers of up to 15 m along lakes, rivers and streams and of 5 m along public ditches (State of Minnesota, 2019).

Due to recent technological advances, farmers have a greater number of available tools to identify areas of fields suitable for perennial biomass cropping. The data limitations for running point-based crop models at small scales within fields are being overcome with new sensors, communication technologies, and algorithms (Jones et al., 2017b), as investments in precision agriculture data analytics are transforming US agriculture (Pham and Stack, 2018). In 2018, investors provided \$945 million to firms developing or providing agricultural data capturing devices, decision support software, or big data analytics, and these investments have shown year-over-year increases since at least 2012 (AgFunder, 2019). In an example specific to biomass cropping, the integrated modeling processes described by Muth et al. (2012), Muth et al. (2013), and Muth and Bryden (2013) for estimating sustainable removal of annual crop residues have been incorporated into the 'AgSolver' platform offered by EFC Systems (EFC Systems, 2019). Due to the availability of cloud computing services, another technology made available since the mid-2000s (Qian et al., 2009), AgSolver advertises the ability to estimate metrics of cropping system environmental performance such as erosion, soil C sequestration, CO₂ gas flux, N₂O gas flux, and NO₃ leaching at within-field spatial resolution of 3 m and with scalability across states, regions, or the entire US. With the proper incentives

and technical support, provided by entities such as the USDA NRCS or local soil and water conservation districts, exciting opportunities clearly exist for targeted placement of cellulosic biomass cropping within agricultural fields. Nonetheless, farmers must be willing to practice heterogeneous cropping practices for this strategy to be successful.

5.3. Conclusions

Chapter I presented six objectives for the research presented herein. The first objective was to present an improved parameterization for simulation of upland switchgrass ecotypes in ALMANAC. By utilizing switchgrass growth characterizations from southern Canada and the northern US, Chapter II provided an improved parameterization of upland ecotype switchgrass for the northern US. Reducing switchgrass maximum productivity, lengthening the growing season, and modifying parameters affecting switchgrass N, water, and frost stress responses improved the accuracy and precision of simulated annual and multiyear average yields relative to the default parameterization. The second objective was to characterize the accuracy and precision of the ALMANAC model for moderate-resolution estimation of corn and wheat yields. Chapter III demonstrated successful multiyear average yield estimation for corn and wheat across a study region spanning portions of three states. Accurate estimation of corn yields was dependent on increasing soil moisture storage and increasing the minimum limit of harvest index to maintain a high grain-to-biomass ratio under water-stressed conditions, while wheat yield estimation did not require these modifications. However, using ALMANAC for corn and wheat was found to produce imprecise annual yield estimates and to overestimate the productivity of parcels considered relatively unsuitable for cultivated cropping. These insights presented in Chapters II and III provide valuable information regarding ALMANAC model function and should prove valuable to future ALMANAC practitioners.

Chapter IV addressed the remaining objectives outlined in Chapter I. The third objective was to estimate the existing resource of corn and wheat biomass. Within estimated biorefineries, corn and wheat biomass can provide 2.32, 13.98, and 16.48 Tg of biomass under conventional tillage (CT), reduced tillage (RT), and no-till (NT) systems, respectively, which

can produce sufficient ethanol to displace up to 33% of mean annual gasoline consumption for the transportation sector within Minnesota, North Dakota, and South Dakota. Potential biorefineries are limited to areas within 90 km to the east or west of the Minnesota-Dakotas border under CT, but are feasible at up to 185 km west of the border under RT and NT. All of this biomass is available at a breakeven price of \$60 Mg⁻¹ or less. The fourth objective was to estimate the biomass prices necessary for switchgrass to be economically competitive with biomass harvest in corn or wheat. Required biomass prices range from \$60 to \$140 Mg⁻¹ under a low-cost establishment scenario and from \$100 to \$180 Mg⁻¹ under a high-cost establishment scenario. Thus, switchgrass cannot compete with corn or wheat residue harvest under any of the cost scenarios or tillage systems tested in this investigation. The fifth objective was to estimate the necessary incentives for switchgrass to supplant sufficient corn or wheat area to offset recent grassland-to-cropland conversions. To offset grassland-to-cropland conversions from the late 2000s and early 2010s would require subsidized biomass prices from \$90 to \$124 Mg⁻¹, dependent on competing tillage system and assumed establishment cost scenario. Alternatively, these conversions could be achieved with environmental services payments 1.2 to 2.9 times the baseline values of \$4.55 Mg-soil⁻¹, \$19.32 kgN⁻¹, and \$118 MgC⁻¹ estimated from the literature. Finally, the sixth objective was to evaluate possible land use and environmental implications of switchgrass production. Prioritizing parcels where switchgrass provides the greatest environmental benefit relative to corn or wheat, as opposed to the greatest increase in biomass yield, would increase resulting soil retention, N retention, and soil C sequestration by up to 420%, 210%, and 120%, respectively. This approach would also preferentially convert those corn and wheat parcels least suitable for cultivation. Expanded switchgrass production could enable biorefineries to proliferate to the western edge of the study region, with switchgrass serving as a major biomass source, but may also encourage switchgrass production on up to 1.43 Mha of existing perennial grassland within the study region. Any payments to encourage switchgrass production should be designed to avoid further conversions of existing perennial grasslands.

Simulated yield outputs were validated against switchgrass field data and county-average corn and wheat yields from USDA National Agricultural Statistics Service surveys. These methods are consistent with past investigations identified in the literature. Nonetheless, validating estimated corn yield, soil erosion, and N loss against field observations from stover removal studies represents a possible improvement for future investigations, as does validating soil C sequestration outcomes against field observations. Additional avenues for future work include refining estimates of technically-available biomass by characterizing transportation networks surrounding existing ethanol plants, modifying estimates of biomass availability by considering farmers' willingness to supply biomass, and quantifying the biomass resource base of within-field areas where switchgrass may provide economic or environmental benefits relative to corn or wheat.

APPENDICES

APPENDIX A
ALMANAC SWITCHGRASS DAILY OUTPUTS

ALMANAC stresses: ■ Water ■ Nitrogen ■ Temperature
 ALMANAC outputs: — LAI — AGPM
 ALMANAC yields: - - - MYA ■ 2007 ● 2008 ▲ 2009 ◆ 2010 ▲ 2011 ▼ 2012 * 2013
 Field yields: - - - - MYA ■ 2007 ● 2008 ▲ 2009 ◆ 2010 ▲ 2011 ▼ 2012 * 2013
 MYA Weather (Apr – Sep): 404 mm precipitation, 600 HU₁₂, 1984 HU₅

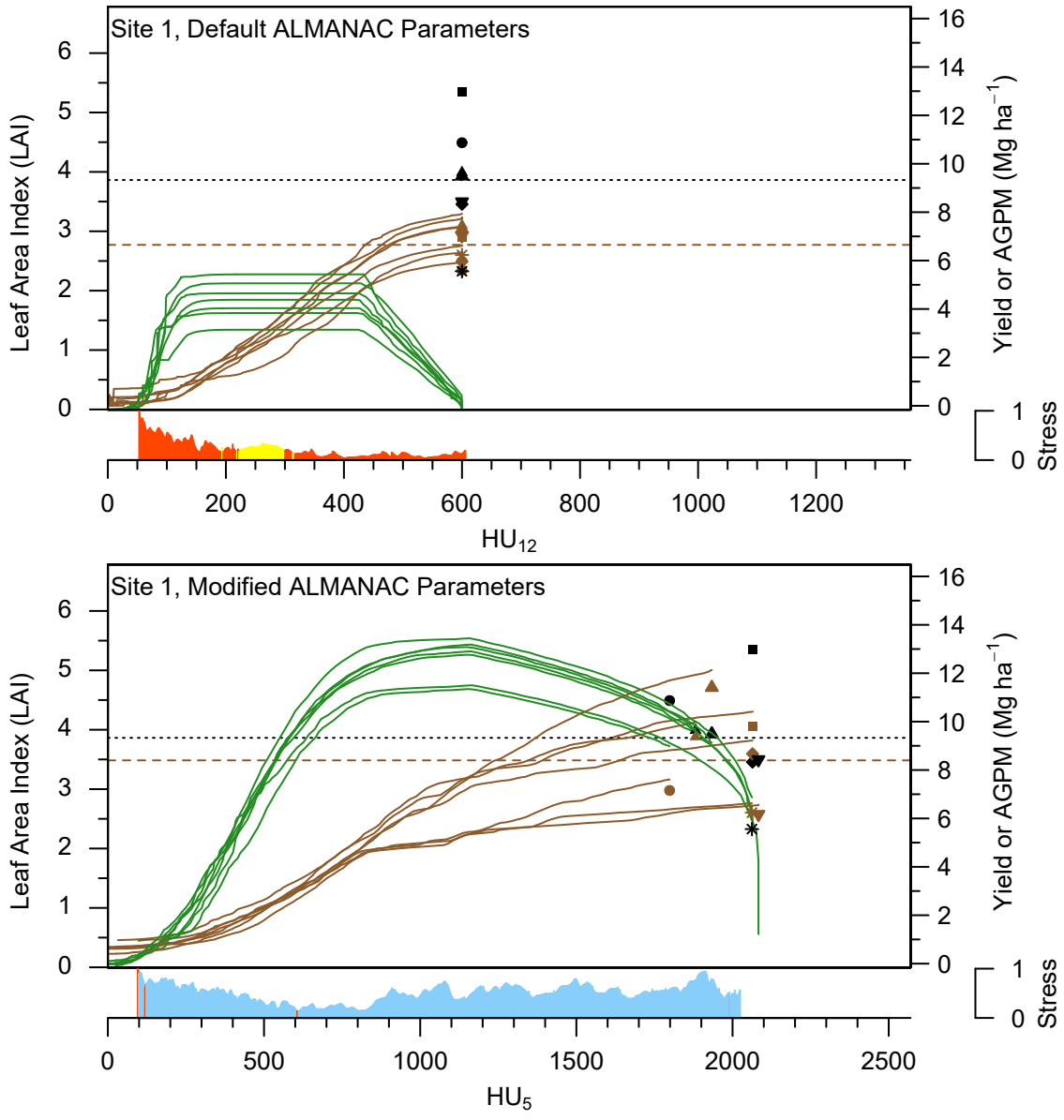


Figure 55. For Site 1 (Table 2), comparison of daily simulated leaf area index (LAI), aboveground plant mass (AGPM), and dominant plant growth stress for the default ALMANAC parameters and the modified parameters presented herein. Water, nitrogen, and temperature stress values represent the average over all simulation years. Superimposed on the daily outputs are annual and multiyear average (MYA) simulated and field-measured yields.

ALMANAC stresses: ■ Water ■ Nitrogen ■ Temperature
 ALMANAC outputs: — LAI — AGPM
 ALMANAC yields: - - - MYA ■ 2007 ● 2008 ▲ 2009 ◆ 2010 ▲ 2011 ▼ 2012 * 2013
 Field yields: - - - - MYA ■ 2007 ● 2008 ▲ 2009 ◆ 2010 ▲ 2011 ▼ 2012 * 2013
 MYA Weather (Apr – Sep): 396 mm precipitation, 600 HU₁₂, 1943 HU₅

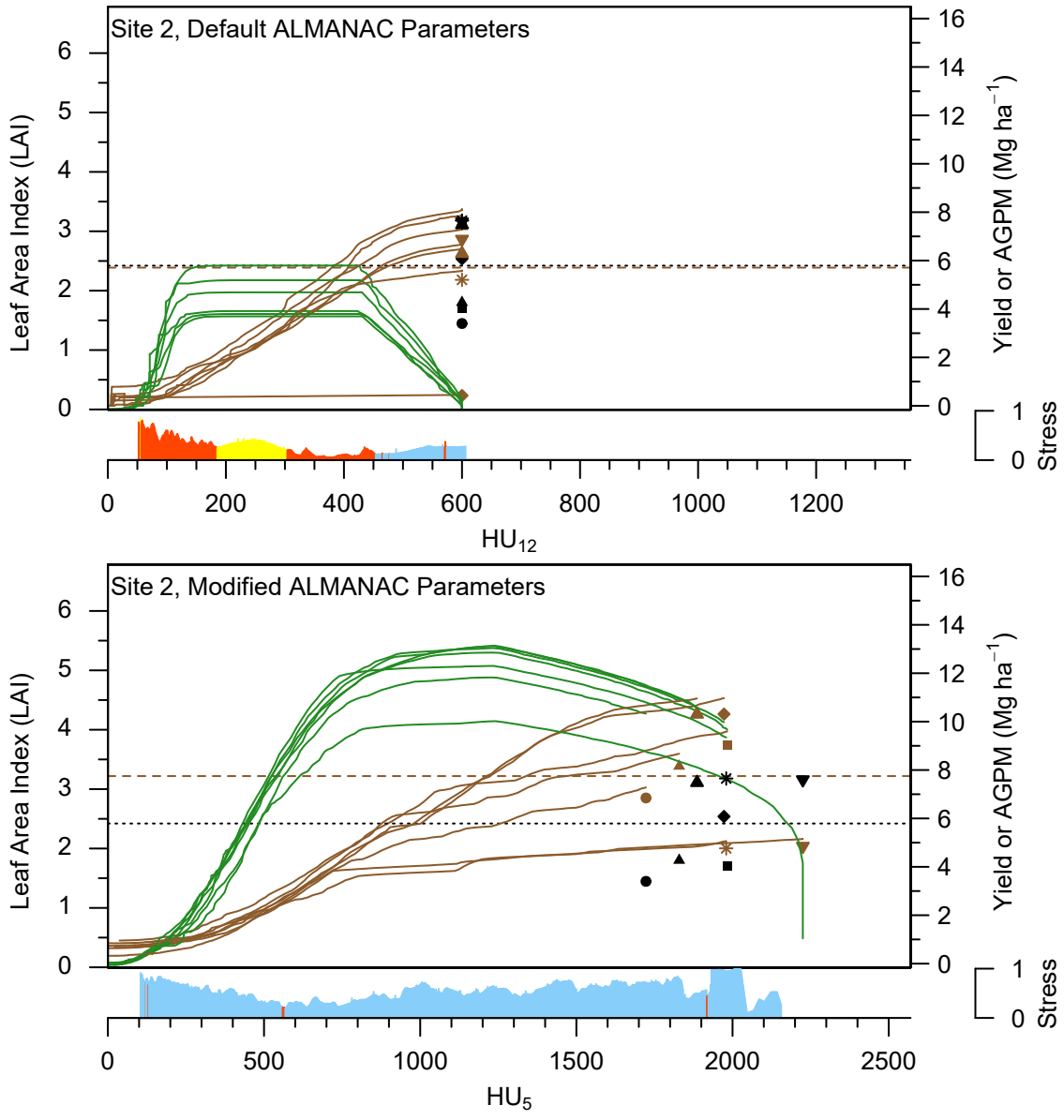


Figure 56. For Site 2 (Table 2), comparison of daily simulated leaf area index (LAI), aboveground plant mass (AGPM), and dominant plant growth stress for the default ALMANAC parameters and the modified parameters presented herein. Water, nitrogen, and temperature stress values represent the average over all simulation years. Superimposed on the daily outputs are annual and multiyear average (MYA) simulated and field-measured yields.

ALMANAC stresses: ■ Water ■ Nitrogen ■ Temperature
 ALMANAC outputs: — LAI — AGPM
 ALMANAC yields: - - - MYA ■ 2002 ● 2003 ▲ 2004 ◆ 2005
 Field yields: - - - - MYA ■ 2002 ● 2003 ▲ 2004 ◆ 2005
 MYA Weather (Apr – Sep): 392 mm precipitation, 590 HU₁₂, 1508 HU₅

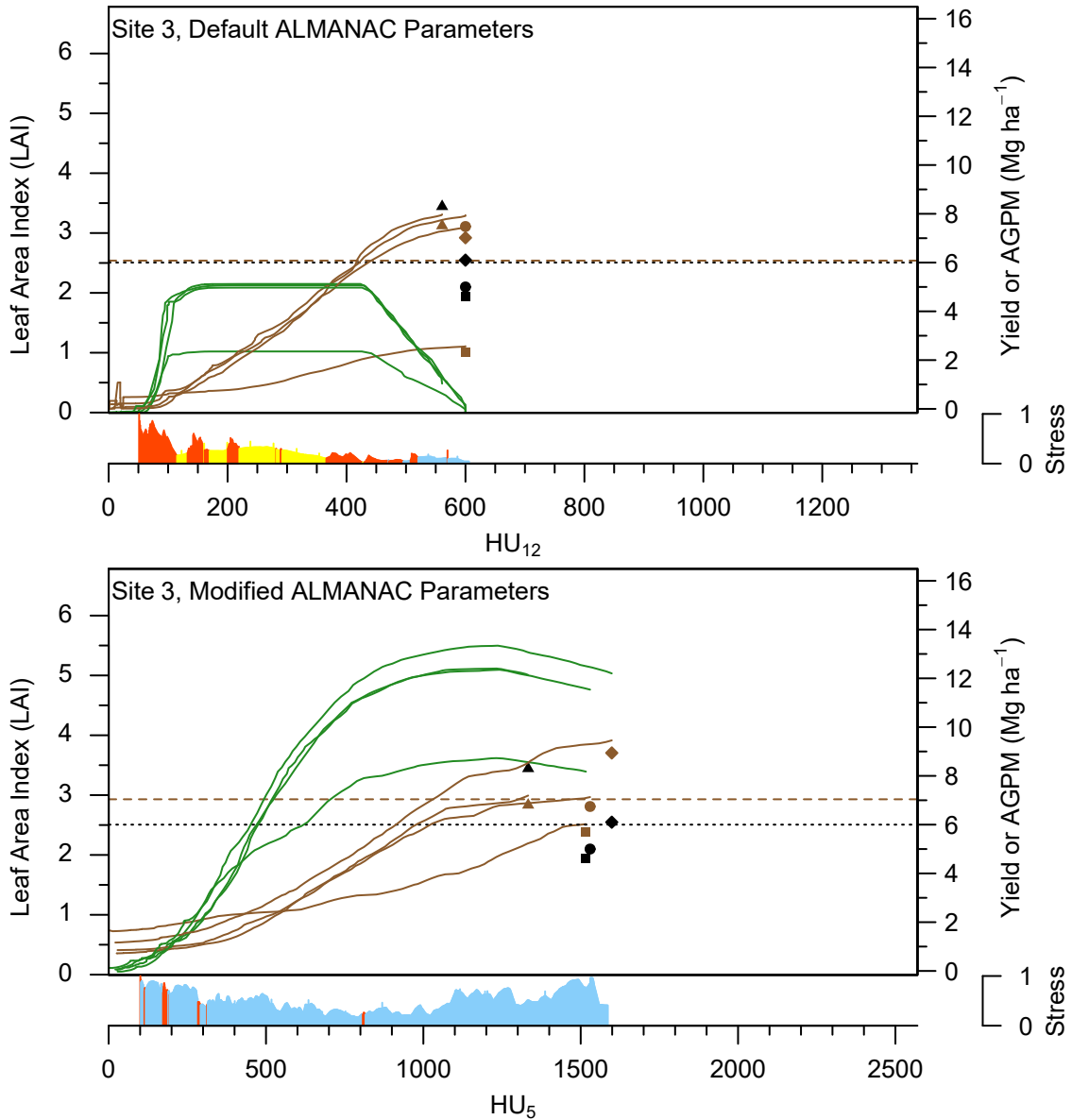


Figure 57. For Site 3 (Table 2), comparison of daily simulated leaf area index (LAI), aboveground plant mass (AGPM), and dominant plant growth stress for the default ALMANAC parameters and the modified parameters presented herein. Water, nitrogen, and temperature stress values represent the average over all simulation years. Superimposed on the daily outputs are annual and multiyear average (MYA) simulated and field-measured yields.

ALMANAC stresses: ■ Water ■ Nitrogen ■ Temperature
 ALMANAC outputs: — LAI — AGPM
 ALMANAC yields: - - - MYA ■ 1983 ● 1984 ▲ 1985 ◆ 1986 ▲ 1987
 Field yields: - - - - - MYA ■ 1983 ● 1984 ▲ 1985 ◆ 1986 ▲ 1987
 MYA Weather (Apr – Sep): 462 mm precipitation, 700 HU₁₂, 2159 HU₅

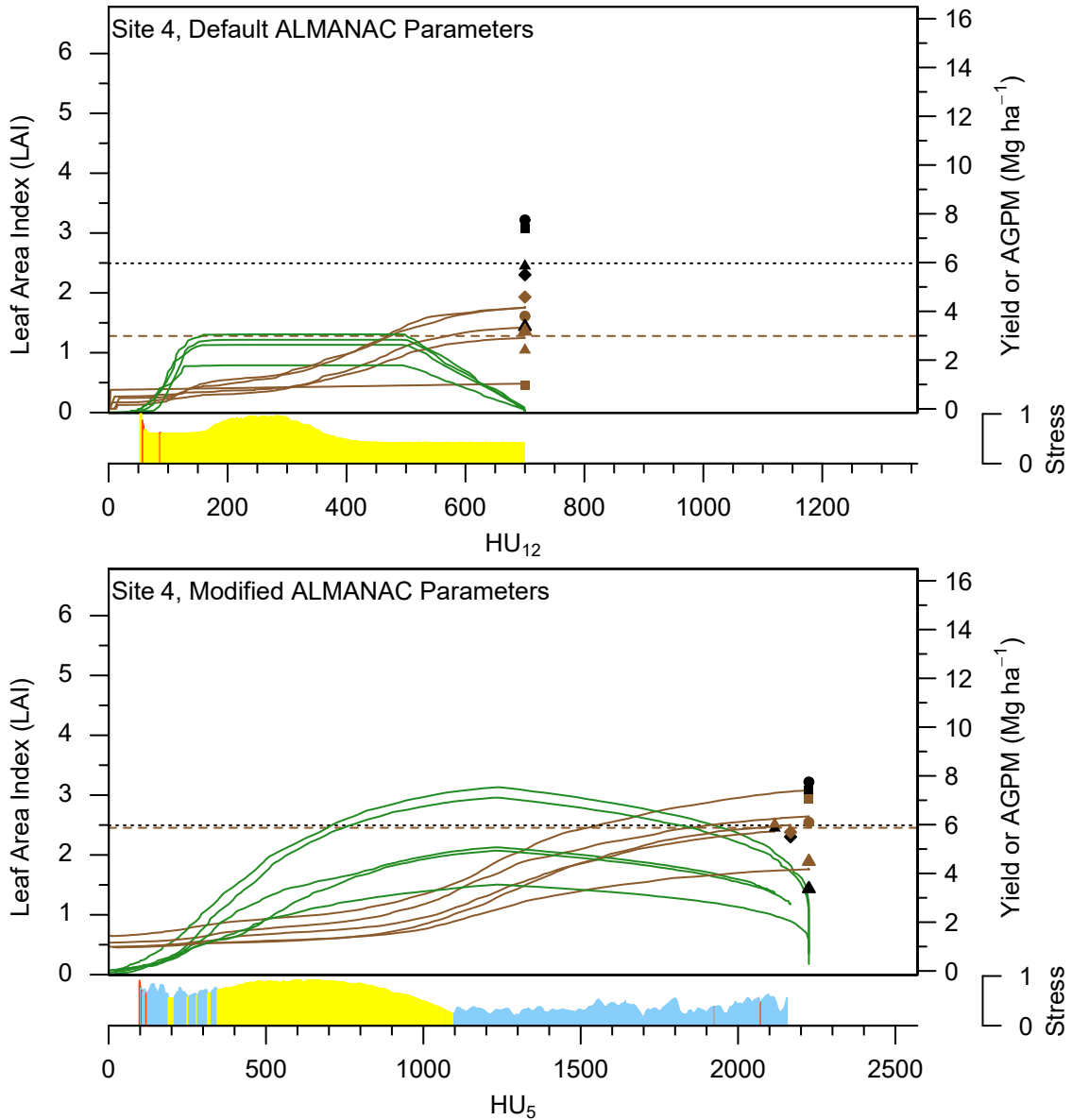


Figure 58. For Site 4 (Table 2), comparison of daily simulated leaf area index (LAI), aboveground plant mass (AGPM), and dominant plant growth stress for the default ALMANAC parameters and the modified parameters presented herein. Water, nitrogen, and temperature stress values represent the average over all simulation years. Superimposed on the daily outputs are annual and multiyear average (MYA) simulated and field-measured yields.

ALMANAC stresses: ■ Water ■ Nitrogen ■ Temperature
 ALMANAC outputs: — LAI — AGPM
 ALMANAC yields: - - - MYA ■ 2002 ● 2003 ▲ 2004 ◆ 2005
 Field yields: - - - - MYA ■ 2002 ● 2003 ▲ 2004 ◆ 2005
 MYA Weather (Apr – Sep): 450 mm precipitation, 800 HU₁₂, 2298 HU₅

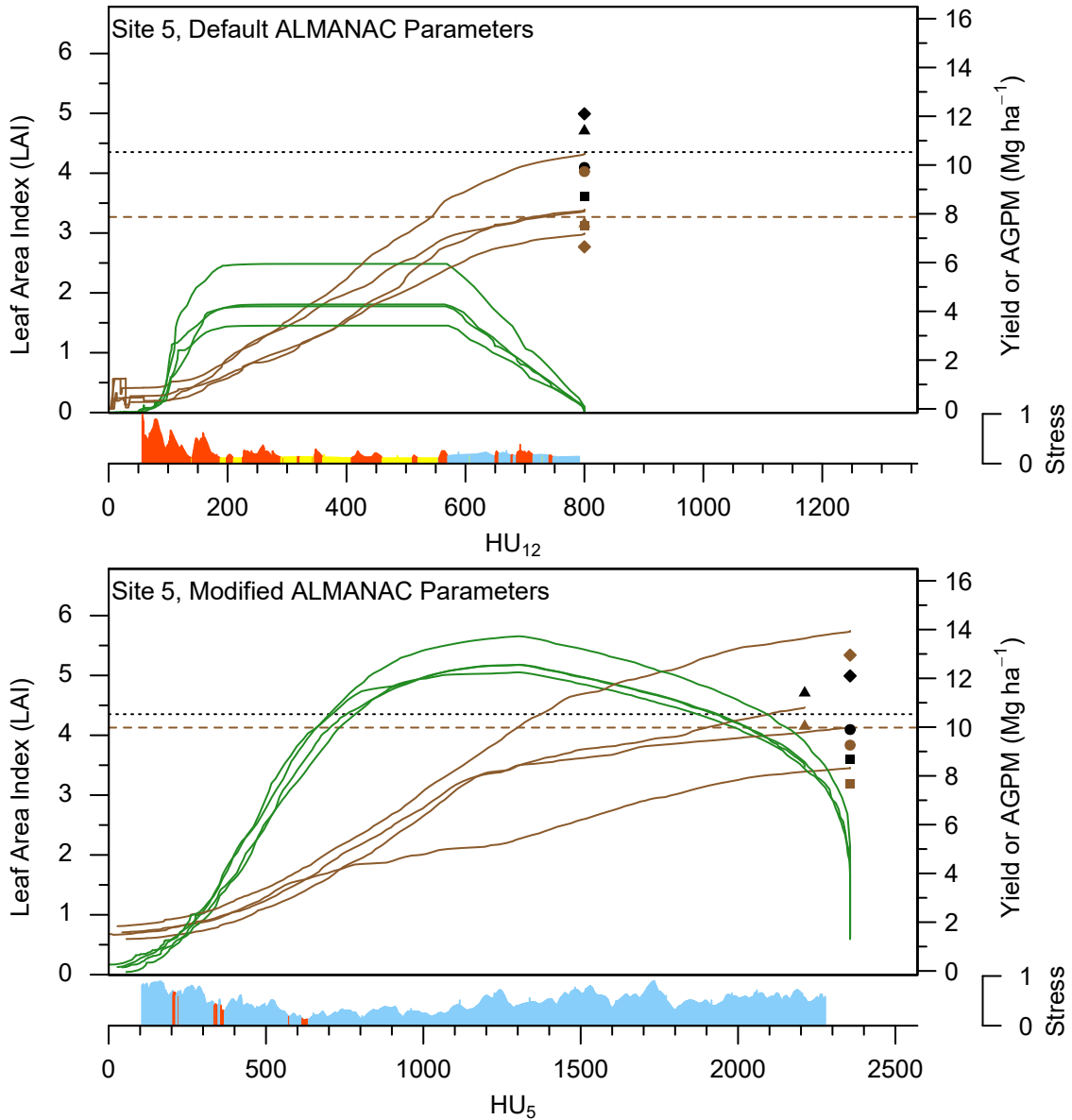


Figure 59. For Site 5 (Table 2), comparison of daily simulated leaf area index (LAI), aboveground plant mass (AGPM), and dominant plant growth stress for the default ALMANAC parameters and the modified parameters presented herein. Water, nitrogen, and temperature stress values represent the average over all simulation years. Superimposed on the daily outputs are annual and multiyear average (MYA) simulated and field-measured yields.

ALMANAC stresses: ■ Water ■ Nitrogen ■ Temperature
 ALMANAC outputs: — LAI — AGPM
 ALMANAC yields: - - - MYA ■ 1985 ● 1986 ▲ 1987 ◆ 1988 ▲ 1989
 Field yields: - - - MYA ■ 1985 ● 1986 ▲ 1987 ◆ 1988 ▲ 1989
 MYA Weather (Apr – Sep): 312 mm precipitation, 800 HU₁₂, 2225 HU₅

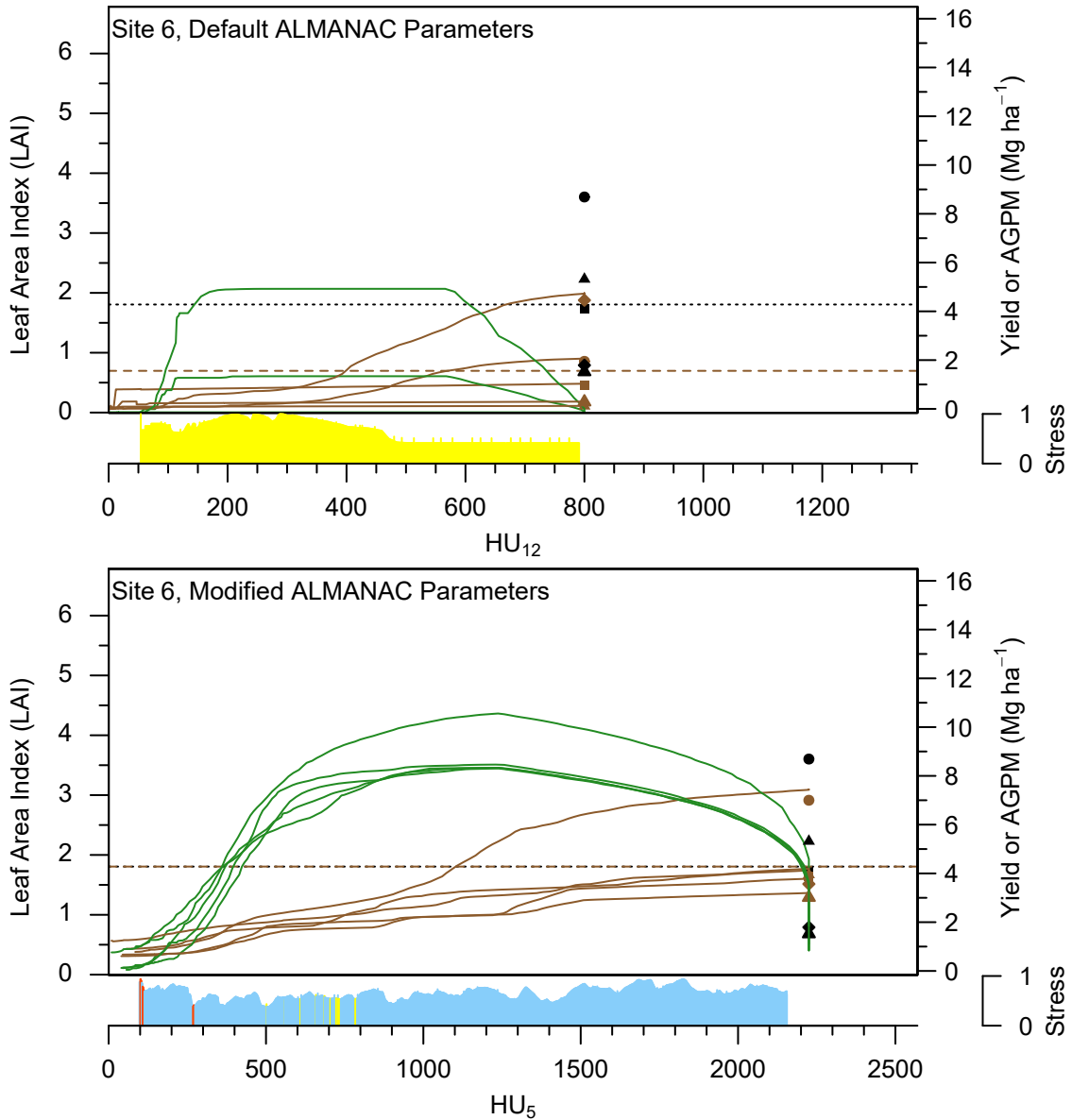


Figure 60. For Site 6 (Table 2), comparison of daily simulated leaf area index (LAI), aboveground plant mass (AGPM), and dominant plant growth stress for the default ALMANAC parameters and the modified parameters presented herein. Water, nitrogen, and temperature stress values represent the average over all simulation years. Superimposed on the daily outputs are annual and multiyear average (MYA) simulated and field-measured yields.

ALMANAC stresses: ■ Water ■ Nitrogen ■ Temperature
 ALMANAC outputs: — LAI — AGPM
 ALMANAC yields: - - - MYA ■ 2003 ● 2004 ▲ 2005
 Field yields: - - - - MYA ■ 2003 ● 2004 ▲ 2005
 MYA Weather (Apr – Sep): 423 mm precipitation, 785 HU₁₂, 1754 HU₅

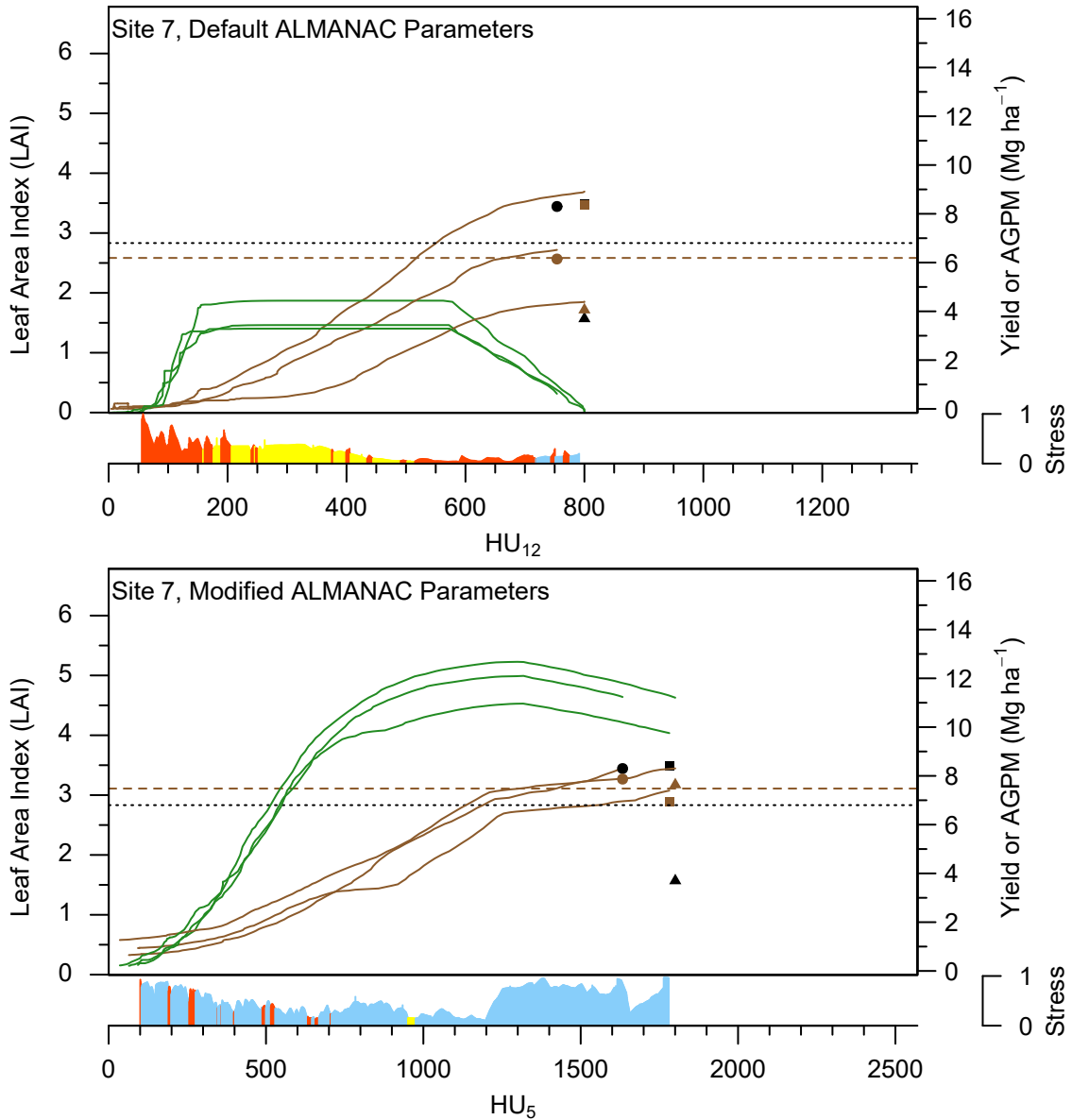


Figure 61. For Site 7 (Table 2), comparison of daily simulated leaf area index (LAI), aboveground plant mass (AGPM), and dominant plant growth stress for the default ALMANAC parameters and the modified parameters presented herein. Water, nitrogen, and temperature stress values represent the average over all simulation years. Superimposed on the daily outputs are annual and multiyear average (MYA) simulated and field-measured yields.

ALMANAC stresses: ■ Water ■ Nitrogen ■ Temperature
 ALMANAC outputs: — LAI — AGPM
 ALMANAC yields: - - - MYA ■ 2002 ● 2003 ▲ 2004 ◆ 2005
 Field yields: - - - - MYA ■ 2002 ● 2003 ▲ 2004 ◆ 2005
 MYA Weather (Apr – Sep): 411 mm precipitation, 795 HU₁₂, 1783 HU₅

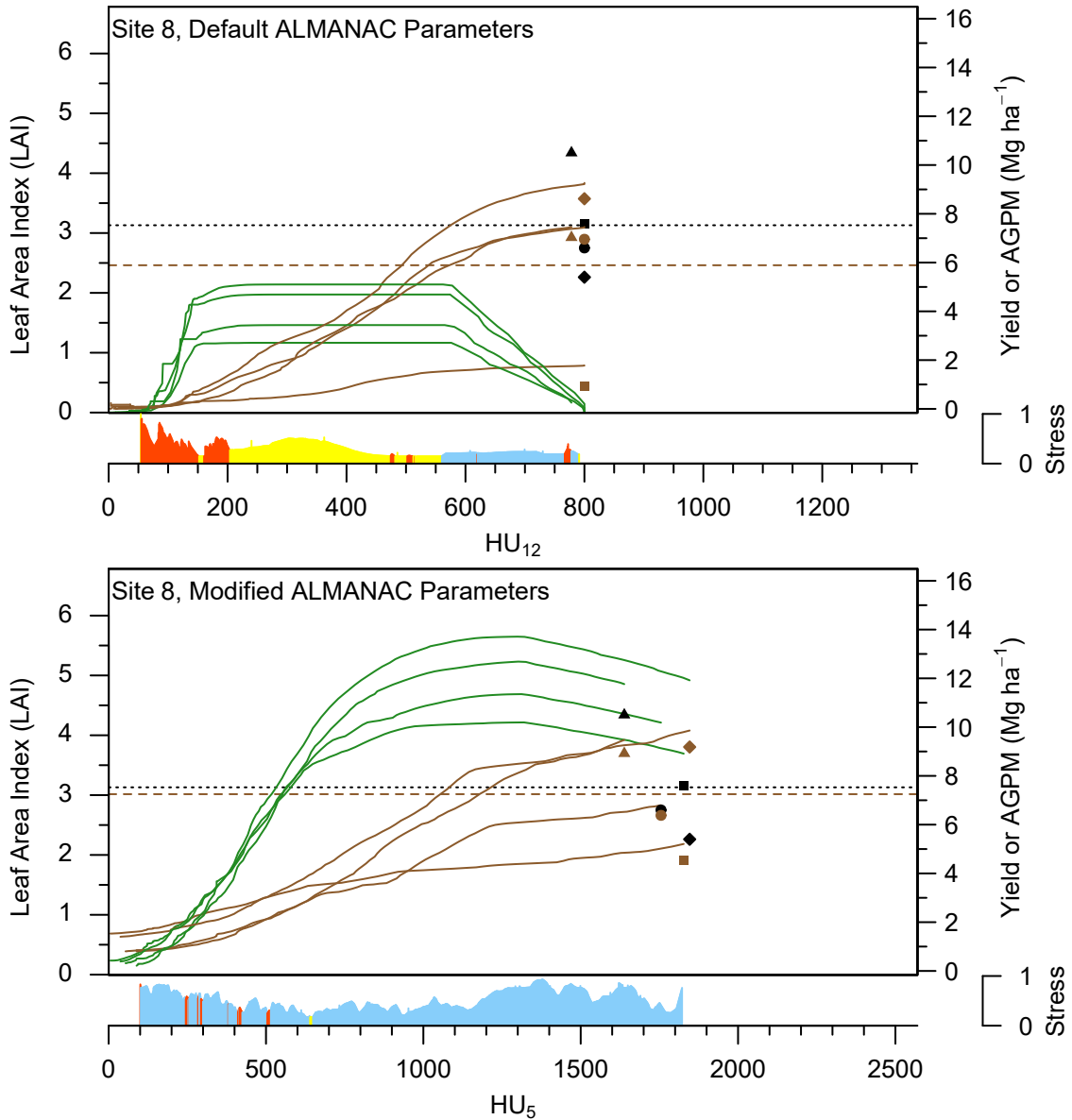


Figure 62. For Site 8 (Table 2), comparison of daily simulated leaf area index (LAI), aboveground plant mass (AGPM), and dominant plant growth stress for the default ALMANAC parameters and the modified parameters presented herein. Water, nitrogen, and temperature stress values represent the average over all simulation years. Superimposed on the daily outputs are annual and multiyear average (MYA) simulated and field-measured yields.

ALMANAC stresses: ■ Water ■ Nitrogen ■ Temperature
 ALMANAC outputs: — LAI — AGPM
 ALMANAC yields: - - - MYA ■ 2010 ● 2011
 Field yields: - - - - MYA ■ 2010 ● 2011
 MYA Weather (Apr – Sep): 636 mm precipitation, 800 HU₁₂, 2346 HU₅

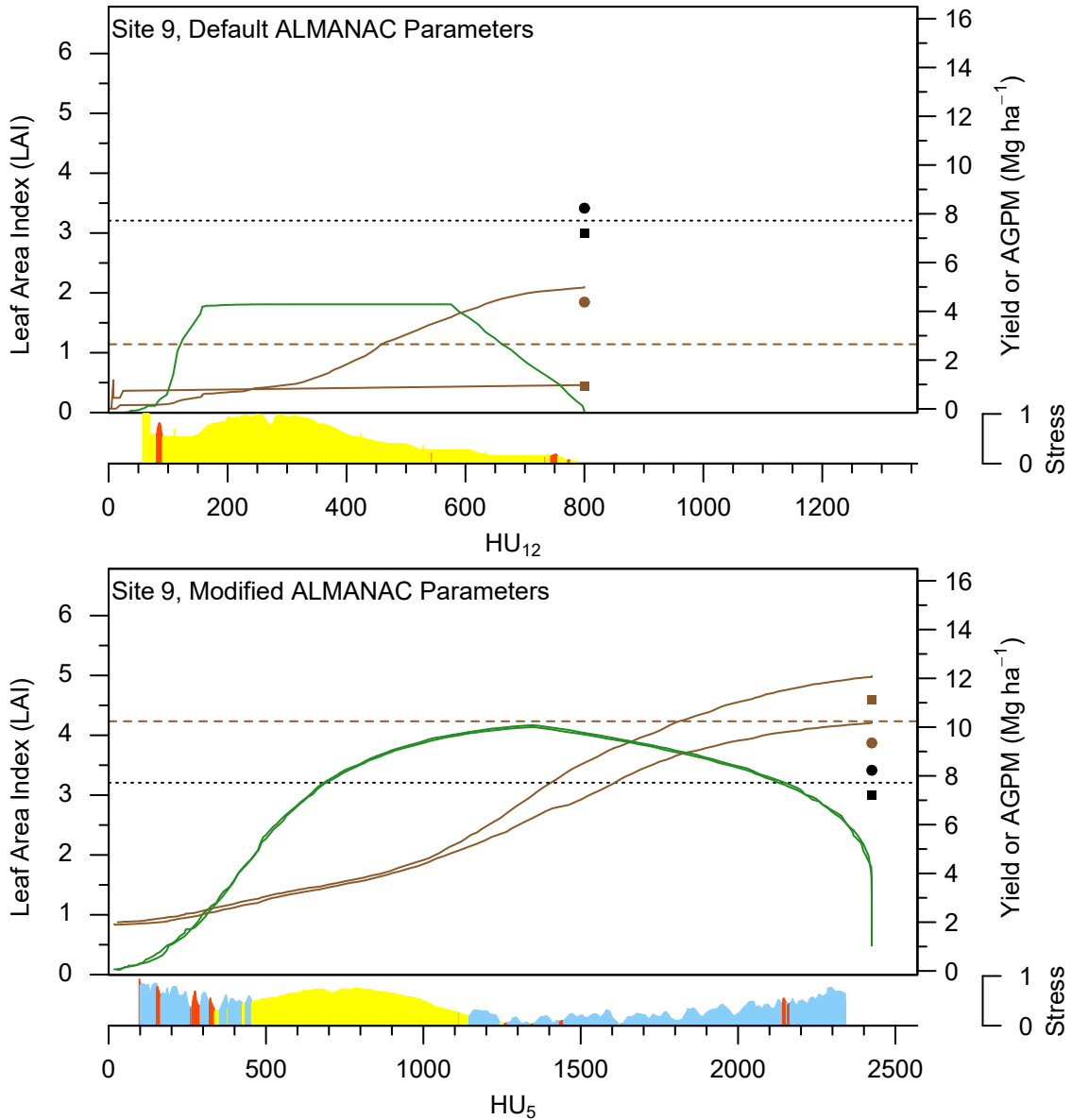


Figure 63. For Site 9 (Table 2), comparison of daily simulated leaf area index (LAI), aboveground plant mass (AGPM), and dominant plant growth stress for the default ALMANAC parameters and the modified parameters presented herein. Water, nitrogen, and temperature stress values represent the average over all simulation years. Superimposed on the daily outputs are annual and multiyear average (MYA) simulated and field-measured yields.

ALMANAC stresses: ■ Water ■ Nitrogen ■ Temperature
 ALMANAC outputs: — LAI — AGPM
 ALMANAC yields: - - - MYA ■ 1998 ● 1999 ▲ 2000 ◆ 2001
 Field yields: - - - - MYA ■ 1998 ● 1999 ▲ 2000 ◆ 2001
 MYA Weather (Apr – Sep): 436 mm precipitation, 800 HU₁₂, 2366 HU₅

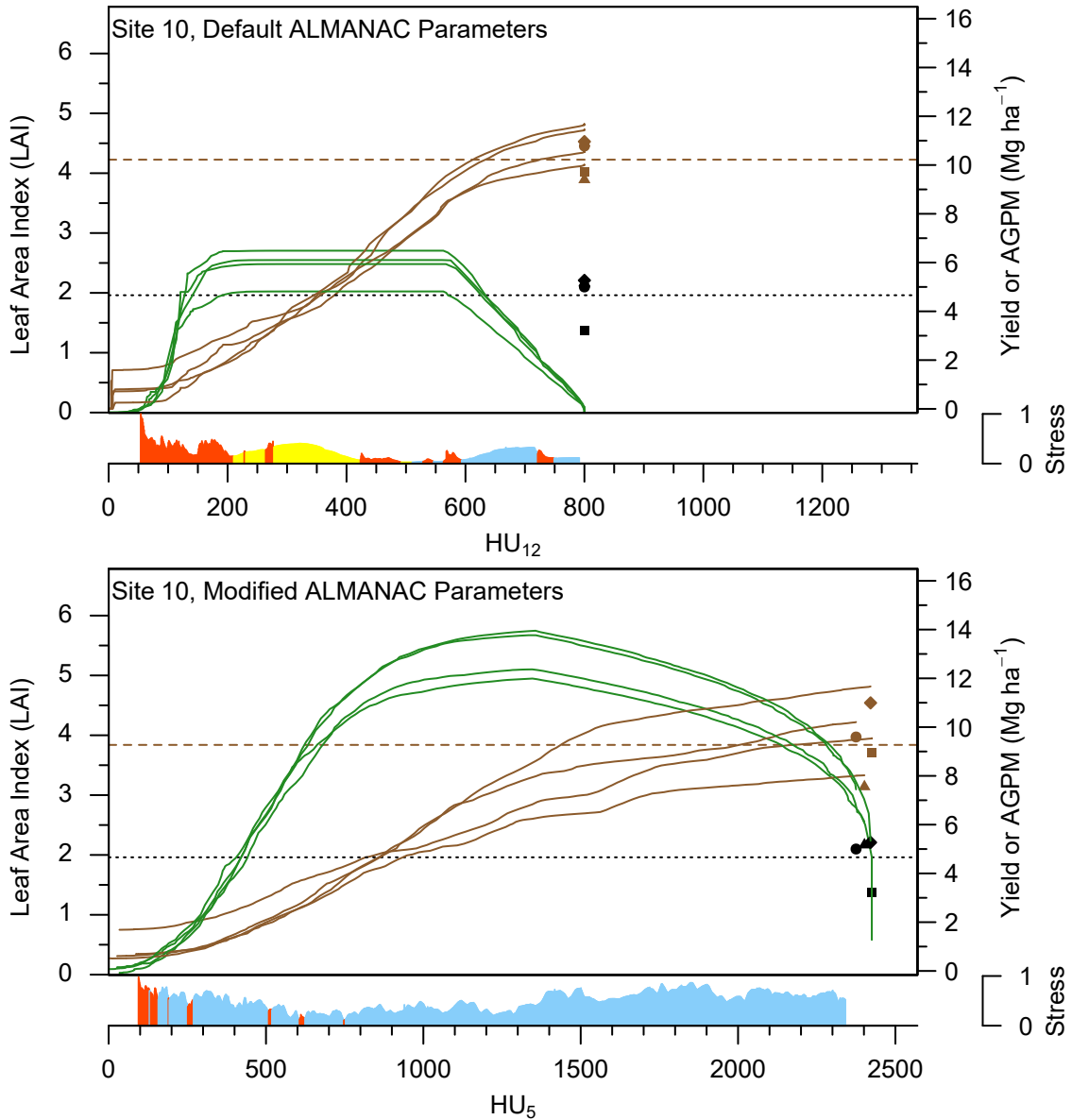


Figure 64. For Site 10 (Table 2), comparison of daily simulated leaf area index (LAI), aboveground plant mass (AGPM), and dominant plant growth stress for the default ALMANAC parameters and the modified parameters presented herein. Water, nitrogen, and temperature stress values represent the average over all simulation years. Superimposed on the daily outputs are annual and multiyear average (MYA) simulated and field-measured yields.

ALMANAC stresses: ■ Water ■ Nitrogen ■ Temperature
 ALMANAC outputs: — LAI — AGPM
 ALMANAC yields: - - - MYA ■ 2001 ● 2002 ▲ 2003 ◆ 2004
 Field yields: - - - - - MYA ■ 2001 ● 2002 ▲ 2003 ◆ 2004
 MYA Weather (Apr – Sep): 498 mm precipitation, 758 HU₁₂, 1622 HU₅

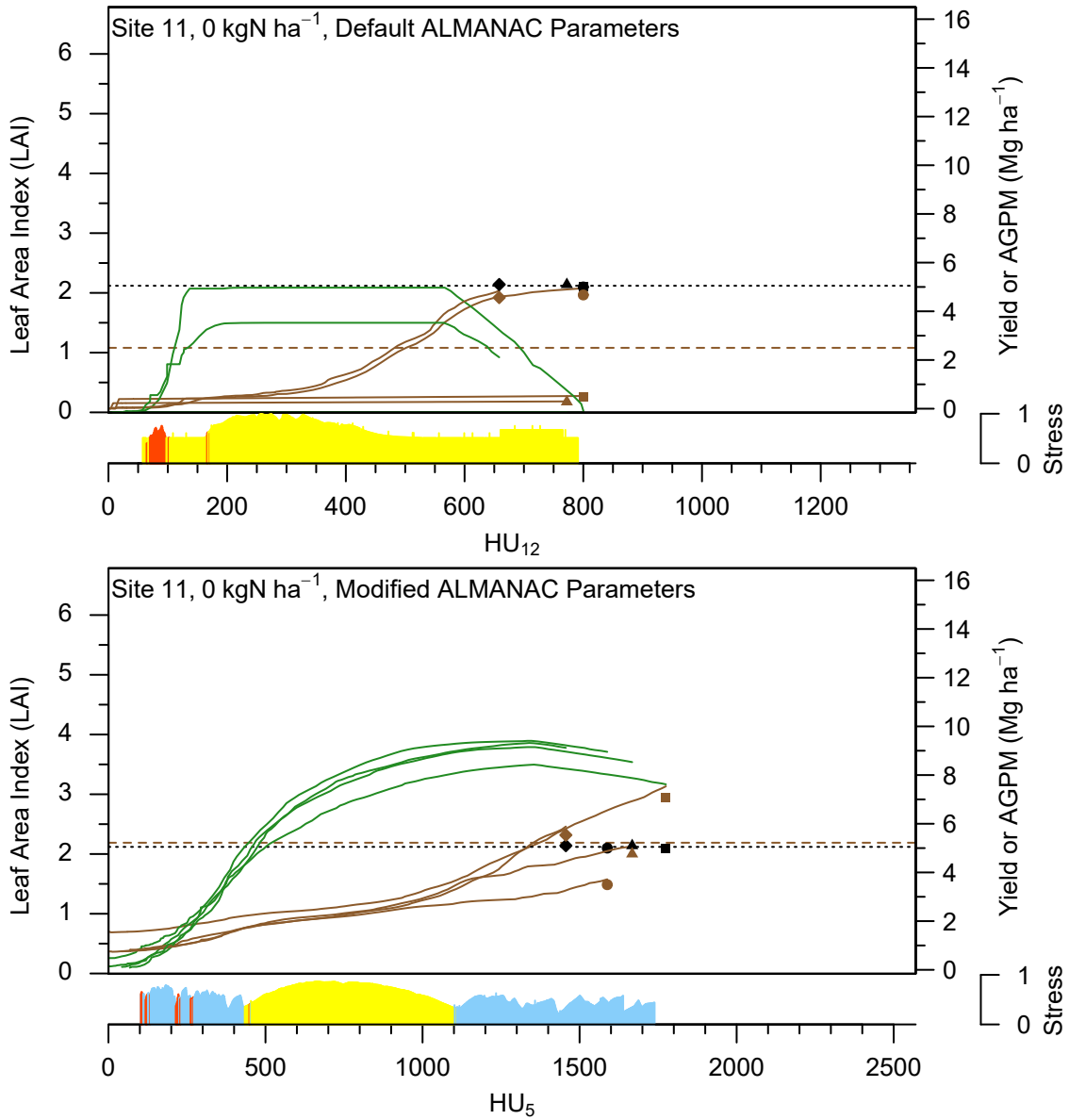


Figure 65. For Site 11 with no nitrogen fertilizer (Table 2), comparison of daily simulated leaf area index (LAI), aboveground plant mass (AGPM), and dominant plant growth stress for the default ALMANAC parameters and the modified parameters presented herein. Water, nitrogen, and temperature stress values represent the average over all simulation years. Superimposed on the daily outputs are annual and multiyear average (MYA) simulated and field-measured yields.

ALMANAC stresses: ■ Water ■ Nitrogen ■ Temperature
 ALMANAC outputs: — LAI — AGPM
 ALMANAC yields: - - - MYA ■ 2001 ● 2002 ▲ 2003 ◆ 2004
 Field yields: - - - - - MYA ■ 2001 ● 2002 ▲ 2003 ◆ 2004
 MYA Weather (Apr – Sep): 498 mm precipitation, 758 HU₁₂, 1622 HU₅

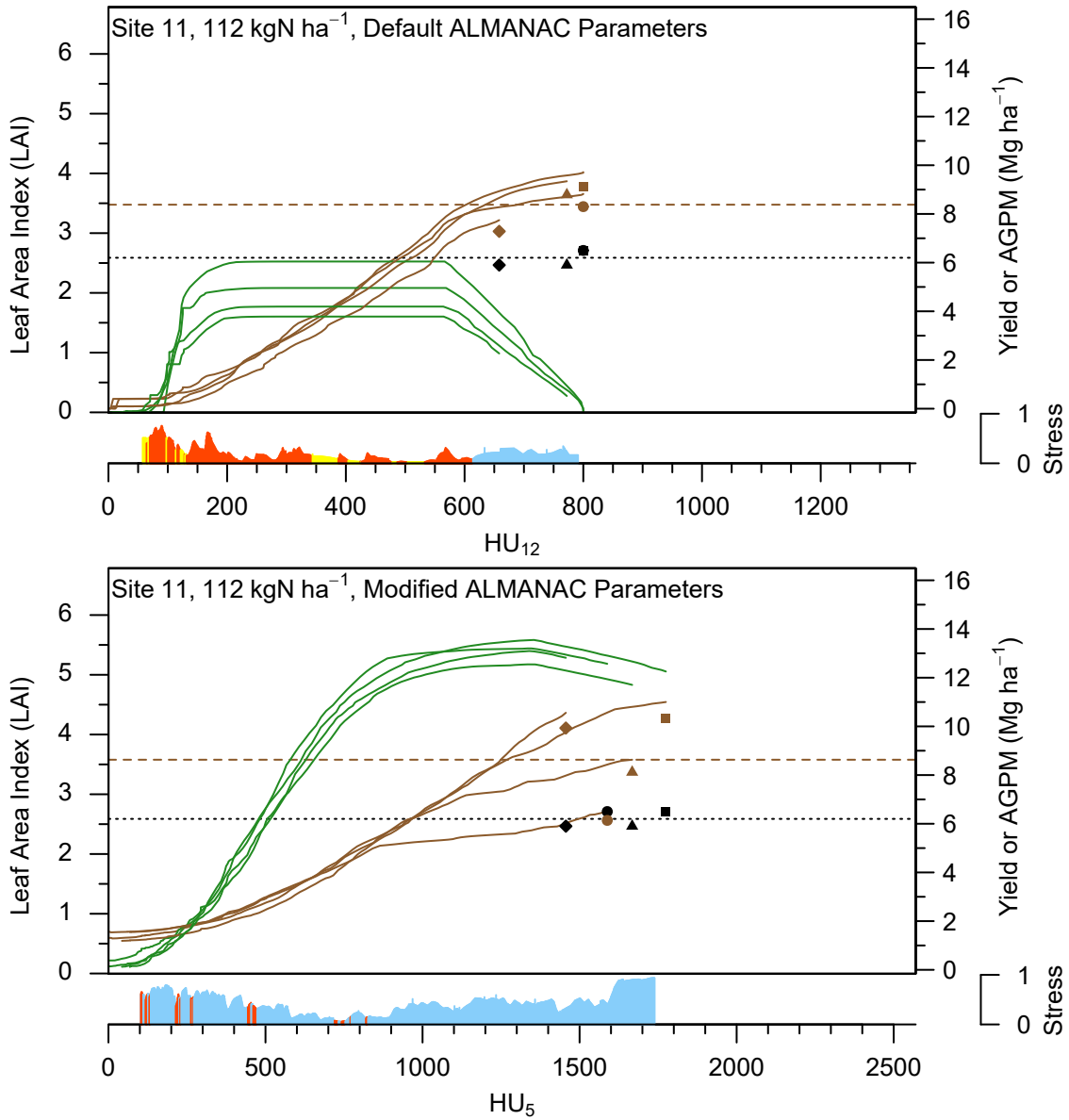


Figure 66. For Site 11 with 112 kgN ha⁻¹ fertilizer application (Table 2), comparison of daily simulated leaf area index (LAI), aboveground plant mass (AGPM), and dominant plant growth stress for the default ALMANAC parameters and the modified parameters presented herein. Water, nitrogen, and temperature stress values represent the average over all simulation years. Superimposed on the daily outputs are annual and multiyear average (MYA) simulated and field-measured yields.

ALMANAC stresses: ■ Water ■ Nitrogen ■ Temperature
 ALMANAC outputs: — LAI — AGPM
 ALMANAC yields: - - - MYA ■ 2001 ● 2002 ▲ 2003 ◆ 2004
 Field yields: - - - - - MYA ■ 2001 ● 2002 ▲ 2003 ◆ 2004
 MYA Weather (Apr – Sep): 498 mm precipitation, 758 HU₁₂, 1622 HU₅

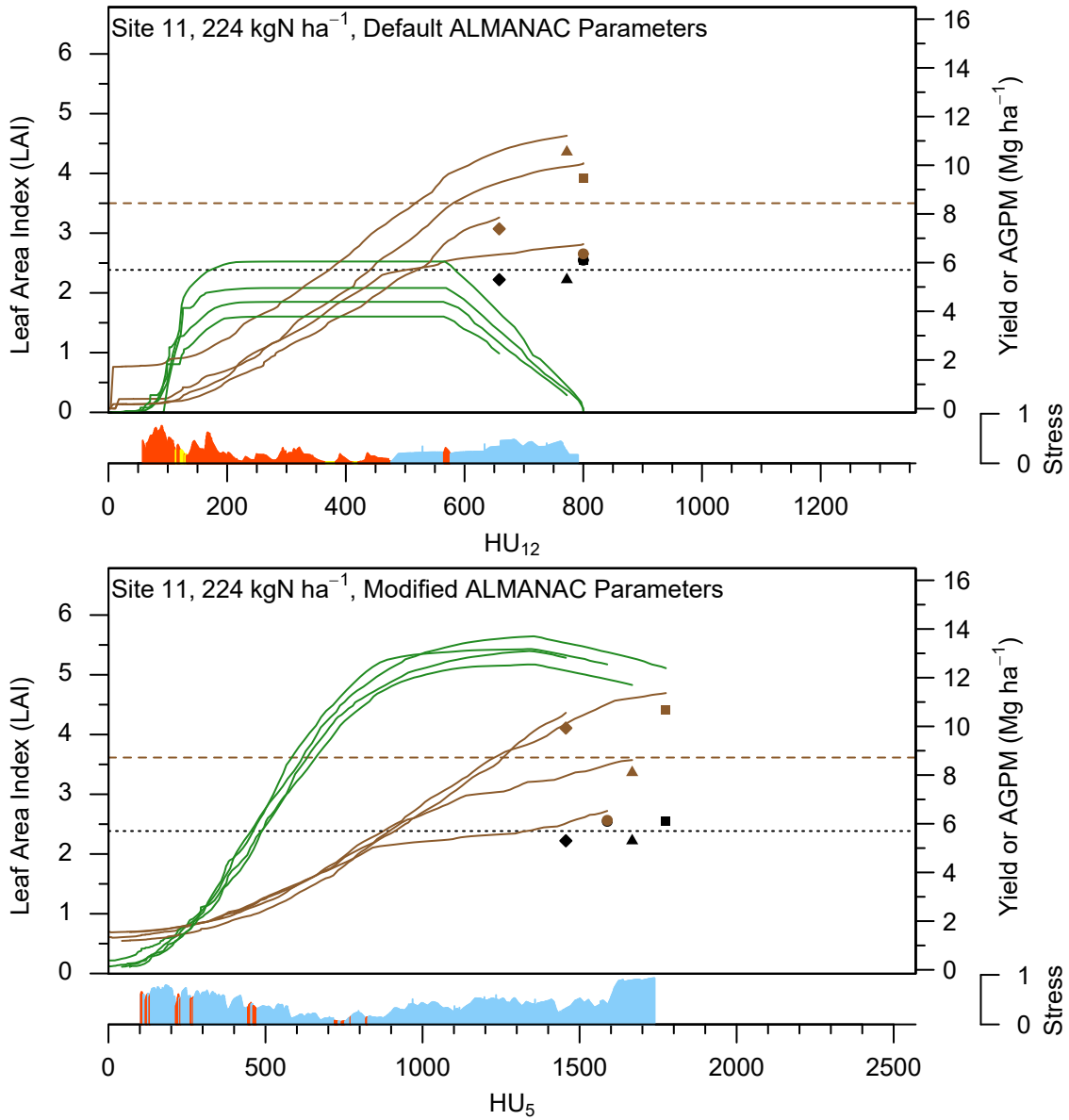


Figure 67. For Site 11 with 224 kgN ha⁻¹ fertilizer application (Table 2), comparison of daily simulated leaf area index (LAI), aboveground plant mass (AGPM), and dominant plant growth stress for the default ALMANAC parameters and the modified parameters presented herein. Water, nitrogen, and temperature stress values represent the average over all simulation years. Superimposed on the daily outputs are annual and multiyear average (MYA) simulated and field-measured yields.

ALMANAC stresses: ■ Water ■ Nitrogen ■ Temperature
 ALMANAC outputs: — LAI — AGPM
 ALMANAC yields: - - - MYA ■ 2002 ● 2003 ▲ 2004 ◆ 2005
 Field yields: - - - - MYA ■ 2002 ● 2003 ▲ 2004 ◆ 2005
 MYA Weather (Apr – Sep): 458 mm precipitation, 800 HU₁₂, 1926 HU₅

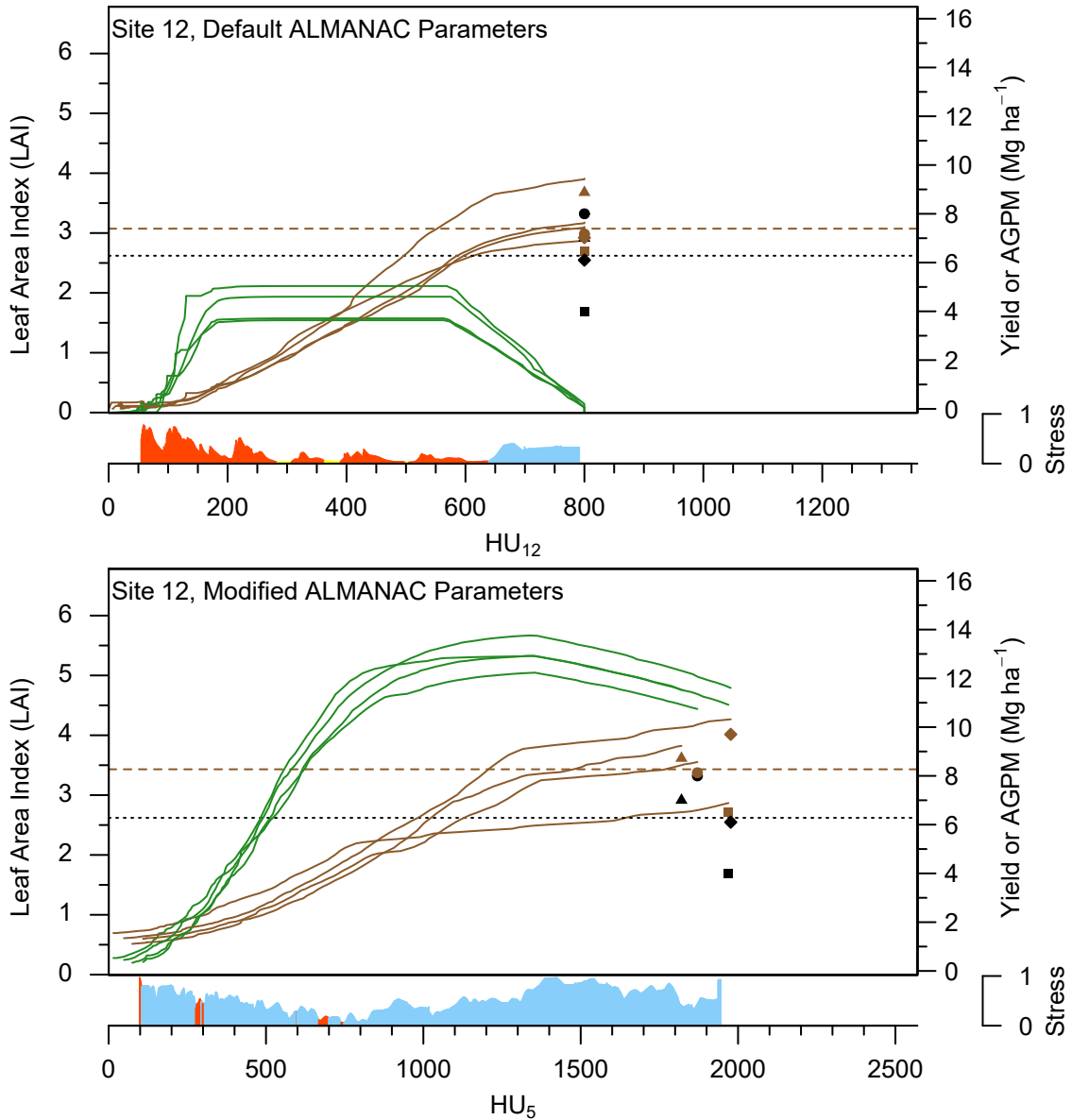


Figure 68. For Site 12 (Table 2), comparison of daily simulated leaf area index (LAI), aboveground plant mass (AGPM), and dominant plant growth stress for the default ALMANAC parameters and the modified parameters presented herein. Water, nitrogen, and temperature stress values represent the average over all simulation years. Superimposed on the daily outputs are annual and multiyear average (MYA) simulated and field-measured yields.

ALMANAC stresses: ■ Water ■ Nitrogen ■ Temperature
 ALMANAC outputs: — LAI — AGPM
 ALMANAC yields: - - - MYA ■ 1984 ● 1985 ▲ 1986 ◆ 1987 ▲ 1988
 Field yields: - - - MYA ■ 1984 ● 1985 ▲ 1986 ◆ 1987 ▲ 1988
 MYA Weather (Apr – Sep): 508 mm precipitation, 800 HU₁₂, 2485 HU₅

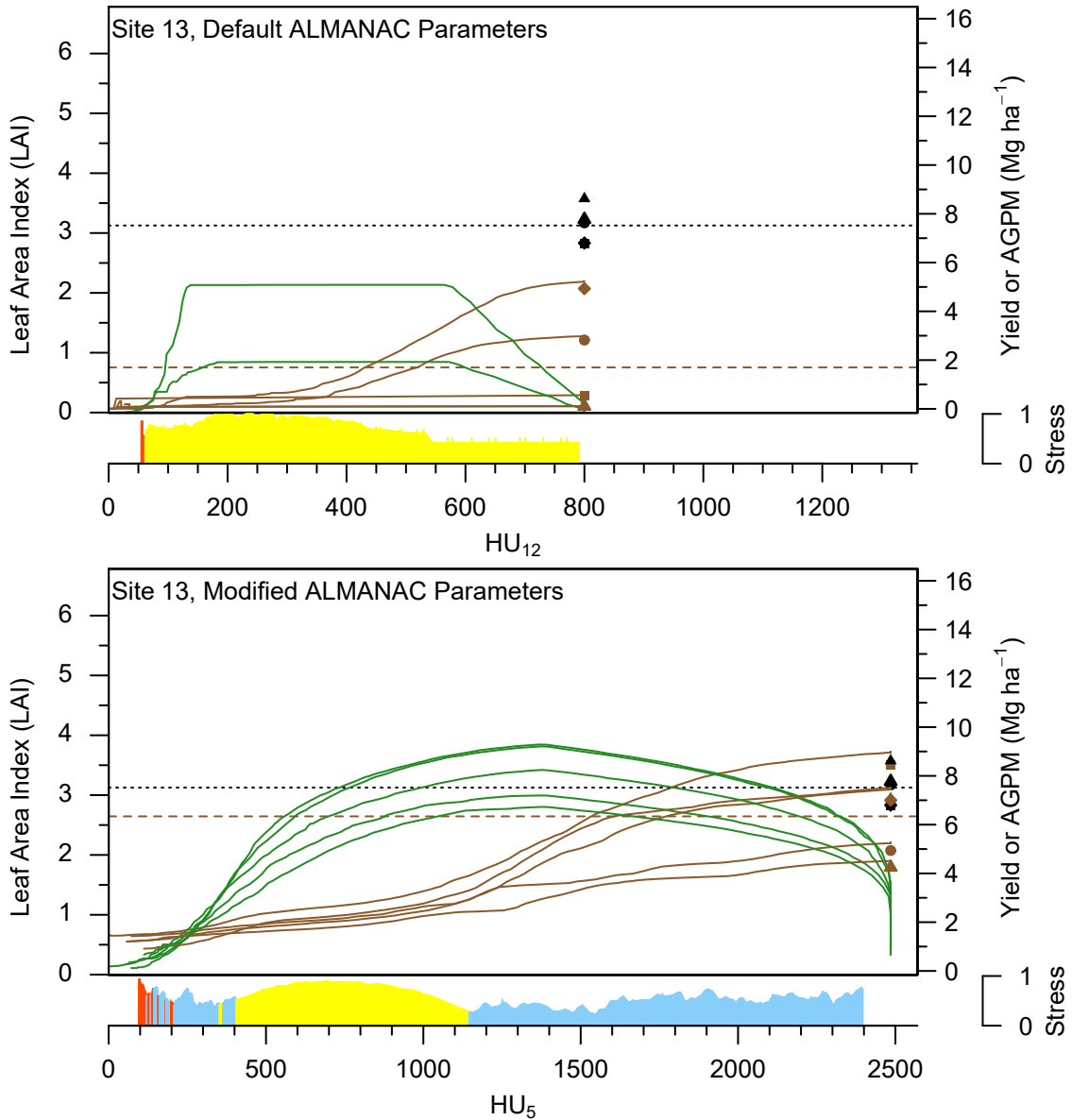


Figure 69. For Site 13 (Table 2), comparison of daily simulated leaf area index (LAI), aboveground plant mass (AGPM), and dominant plant growth stress for the default ALMANAC parameters and the modified parameters presented herein. Water, nitrogen, and temperature stress values represent the average over all simulation years. Superimposed on the daily outputs are annual and multiyear average (MYA) simulated and field-measured yields.

APPENDIX B
ALMANAC SUPPLEMENTAL METHODS

Table 17. Required ALMANAC soil parameters.

Source	SSURGO Table	Description	Notation		Unit	
			ALMANAC	SSURGO	ALMANAC	SSURGO
ALNC	—	maximum number of soil layers	TSLA	—	—	—
ALNC	—	minimum thickness of maximum soil layer	ZQT	—	m	—
ALNC	—	minimum soil profile thickness	ZF	—	m	—
ALNC	—	initial soil water content (fraction of field capacity)	FFC	—	—	—
ALNC	—	minimum depth to water table	WTMN	—	m	—
ALNC	—	maximum depth to water table	WTMX	—	m	—
ALNC	—	initial depth to water table	WTBL	—	m	—
ALNC	—	soil weathering code	XIDS	—	—	—
ALNC	—	sub-surface flow travel time	RFTT	—	d	—
ALNC	—	organic N concentration	WN	—	g Mg ⁻¹	—
ALNC	—	nitrate concentration	WNO3	—	g Mg ⁻¹	—
ALNC	—	labile P concentration	AP	—	g Mg ⁻¹	—
ALNC	—	crop residue	RSD	—	Mg ha ⁻¹	—

Table 17. cont.

Source	SSURGO Table	Description	Notation		Unit	
			ALMANAC	SSURGO	ALMANAC	SSURGO
ALNC	—	phosphorus sorption ratio	PSP	—	—	—
ALNC	—	subsurface flow travel time	RT	—	—	—
ALNC	—	organic P concentration	WP	—	g Mg^{-1}	—
SXRL	—	wilting point [‡]	U	—	m m^{-1}	—
SXRL	—	field capacity [‡]	FC	—	m m^{-1}	—
SRGO	component	hydrologic soil group	HSG	hydgrp	—	—
SRGO	component	soil albedo	SALB	albedodry_r	—	—
SRGO	component	elevation, representative	ELEV_R	elev_r	m	m
SRGO	component	slope, representative [‡]	SLOPE_R	slope_r	m m^{-1}	%
SRGO	component	slope length, representative	SLOPELG_R	slopelenusle_r	m	m
SRGO	chorizon	soil layer [‡]	LAYER	—	—	—
SRGO	chorizon	depth from surface to the bottom of the soil layer	Z	hzdepb_r	m	cm
SRGO	chorizon	bulk density of the soil layer	BD	dbthirdbar_r	Mg m^{-3}	g m^{-3}
SRGO	chorizon	sand content	SAN	sandtotal_r	%	%

Table 17. cont.

Source	SSURGO Table	Description	Notation		Unit	
			ALMANAC	SSURGO	ALMANAC	SSURGO
SRGO	horizon	silt content	SIL	silttotal_r	%	%
SRGO	horizon	soil pH	PH	ph1to1h2o_r	—	—
SRGO	horizon	sum of bases	SMB	sumbases_r	cmol _c kg ⁻¹	meq 100 g ⁻¹
SRGO	horizon	organic carbon [‡]	CBN	om_r	%	%
SRGO	horizon	calcium carbonate	CAC	caco3_r	%	%
SRGO	horizon	cation exchange capacity	CEC	cec7_r	cmol _c kg ⁻¹	meq 100 g ⁻¹
SRGO	horizon	coarse fragment content [‡]	ROK	fraggt10_r, frag3to10_r, sieveno10_r	% v/v	% w/w
SRGO	horizon	bulk density (oven dry)	BDD	dbovendry_r	Mg m ⁻³	g m ⁻³
SRGO	horizon	saturated conductivity	SC	ksat_r	mm h ⁻¹	μm s ⁻¹

[†] ALNC = ALMANAC default; SXRL = Saxton and Rawls (2006); SRGO = SSURGO soil survey database

[‡] See Section 3.3.2 for parameter details

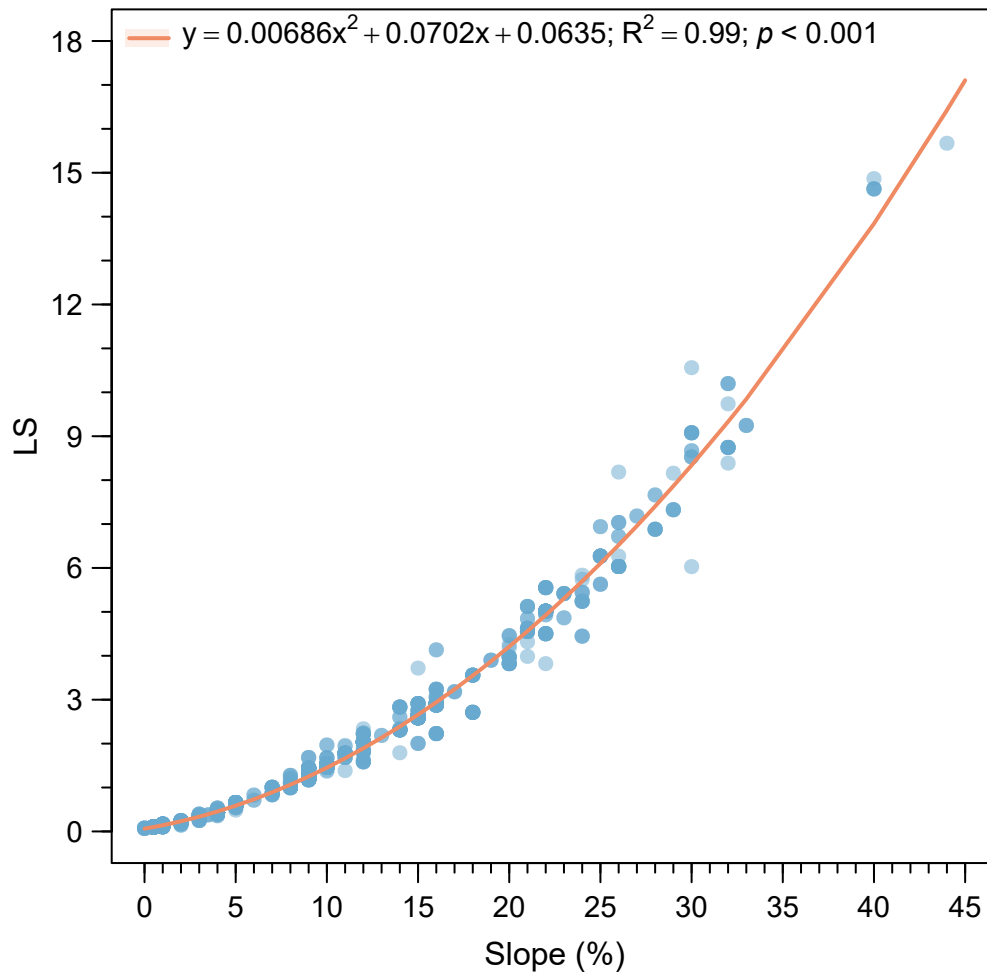


Figure 70. Relationship between slope and the length-slope (LS) factor of the Universal Soil Loss Equation, for 3471 SSURGO soil components within the study region.

Table 18. Presence (+) or absence (–) of tillage, planting, harvest, and fertilizing operations for corn grown in conventional tillage (CT), reduced tillage (RT), and no-till (NT) management systems.

Crop	Operation			Management System		
	Type	Details	Timing [†]	CT	RT	NT
Soybean	Till	Field cultivator	5 DPP	+	+	–
Soybean	Plant	Planter (drill)	Varies	+	+	+
Soybean	Harvest	Harvest seed	Varies	+	+	+
Soybean	Fertilize	Spreader	5 DAH	+	+	+
Soybean	Fertilize	Anhydrous applicator	6 DAH	+	+	+
Soybean	Till	Chisel plow	10 DAH	+	–	–
Corn	Till	Field cultivator	5 DPP	+	+	–
Corn	Plant	Planter (row)	Varies	+	+	+
Corn	Fertilize	Sprayer	40 DAP	+	+	+
Corn	Harvest	Harvest seed	Varies	+	+	+
Corn	Harvest	Harvest crop residue	Varies	+	+	+
Corn	Till	Disk-chisel	5 DAH	+	–	–
Corn	Till	Chisel plow	10 DAH	+	+	–

[†] DPP = days prior to planting, DAH = days after harvest, DAP = days after planting

Table 19. Presence (+) or absence (–) of tillage, planting, harvest, and fertilizing operations for wheat grown in conventional tillage (CT), reduced tillage (RT), and no-till (NT) management systems.

Crop	Operation			Management System		
	Type	Details	Timing [†]	CT	RT	NT
Soybean	Till	Field cultivator	5 DPP	+	+	–
Soybean	Plant	Planter (drill)	Varies	+	+	+
Soybean	Harvest	Harvest seed	Varies	+	+	+
Soybean	Fertilize	Spreader	5 DAH	+	+	+
Soybean	Fertilize	Anhydrous applicator	6 DAH	+	+	+
Soybean	Till	Chisel plow	10 DAH	+	–	–
Wheat	Till	Field cultivator	5 DPP	+	+	–
Wheat	Plant	Planter (drill)	Varies	+	+	+
Wheat	Harvest	Harvest seed	Varies	+	+	+
Wheat	Harvest	Harvest crop residue	Varies	+	+	+
Wheat	Till	Chisel plow	5 DAH	+	+	–
Wheat	Till	Chisel plow	10 DAH	+	–	–

[†] DPP = days prior to planting, DAH = days after harvest

APPENDIX C
SUPPLEMENT TO CHAPTER IV

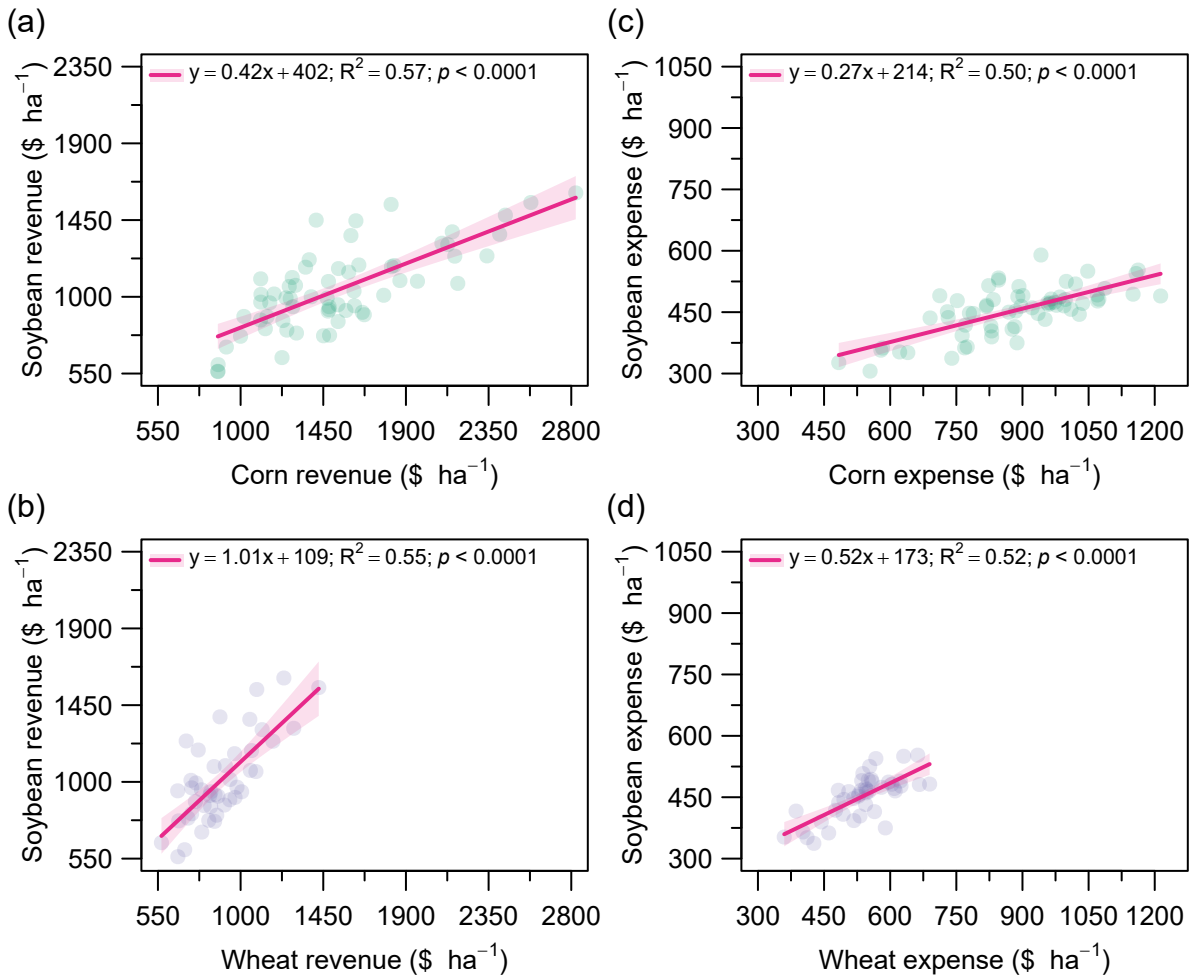


Figure 71. Using annual FINBIN data for 2010 to 2015, aggregated by USDA Agricultural District, the estimation of soybean revenue as a function of (a) corn revenue and (b) wheat revenue, and the estimation of soybean expense as a function of (c) corn expense and (d) wheat expense.

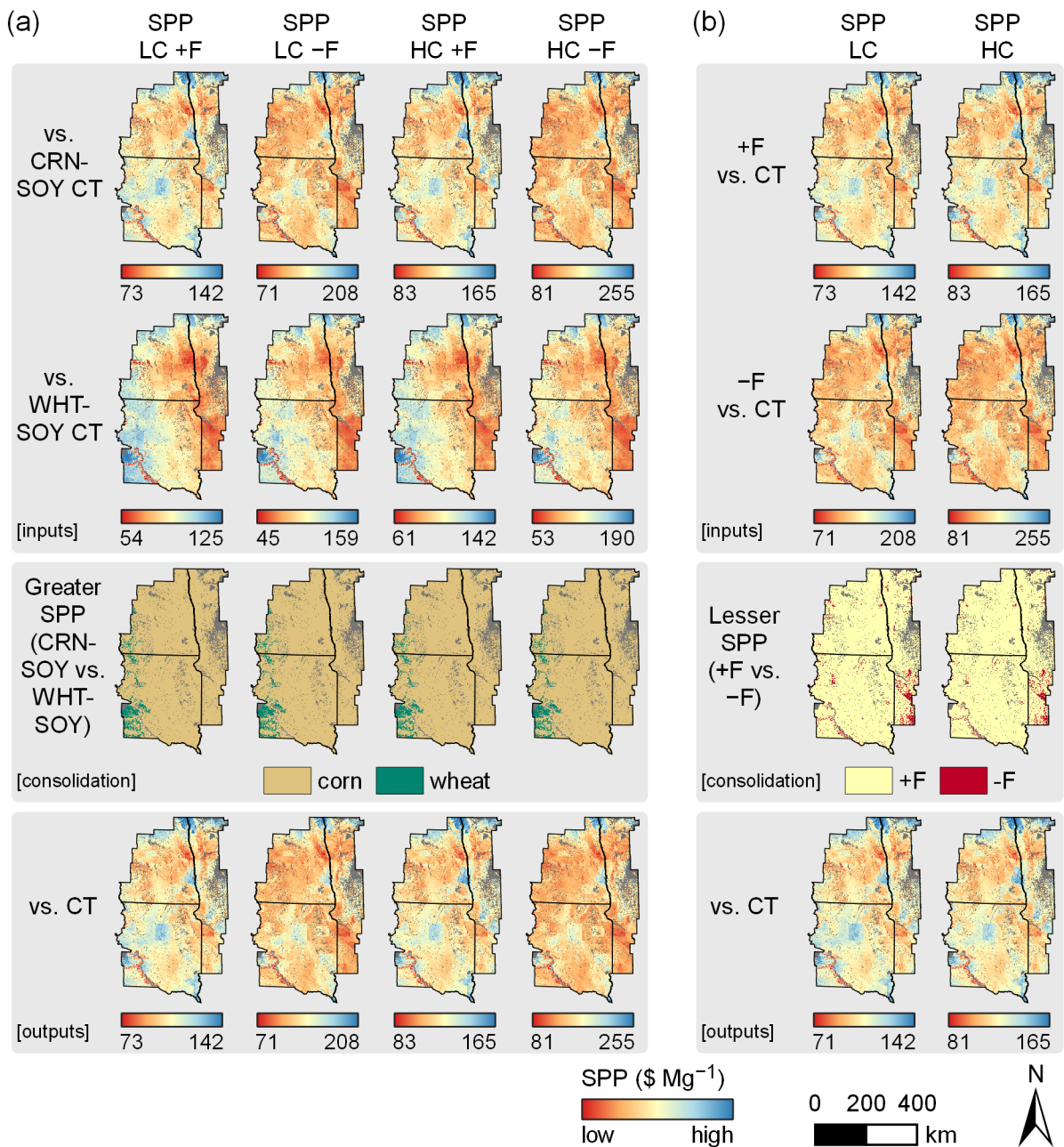


Figure 72. Consolidation of switchgrass parity price (SPP) estimates across (a) its competing cropping systems in a conventional tillage (CT) system and (b) management systems with (+F) or without (-F) fertilizer applications. In (a), SPP estimates for all combinations of establishment scenario (low-cost [LC] or high-cost [HC]) and fertilizer application are consolidated by keeping the competing cropping system requiring the greatest SPP (corn-soybean [CRN-SOY] or wheat-soybean [WHT-SOY]). In (b), the LC and HC outputs from (a) are consolidated to keep the lowest SPP across the +F and -F options.

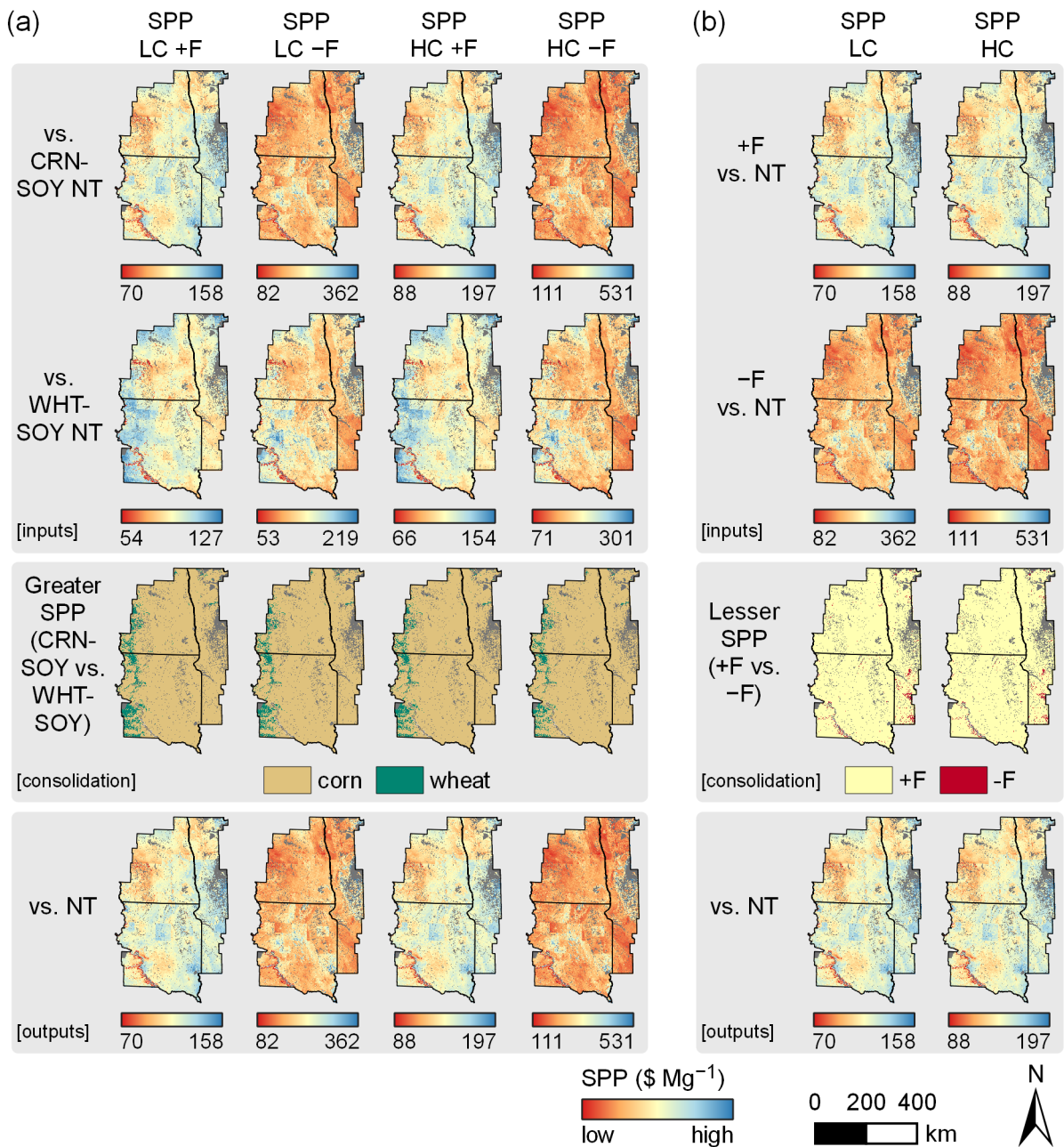


Figure 73. Consolidation of switchgrass parity price (SPP) estimates across (a) its competing cropping systems in a no-till (NT) system and (b) management systems with (+F) or without (-F) fertilizer applications. In (a), SPP estimates for all combinations of establishment scenario (low-cost [LC] or high-cost [HC]) and fertilizer application are consolidated by keeping the competing cropping system requiring the greatest SPP (corn-soybean [CRN-SOY] or wheat-soybean [WHT-SOY]). In (b), the LC and HC outputs from (a) are consolidated to keep the lowest SPP across the +F and -F options.

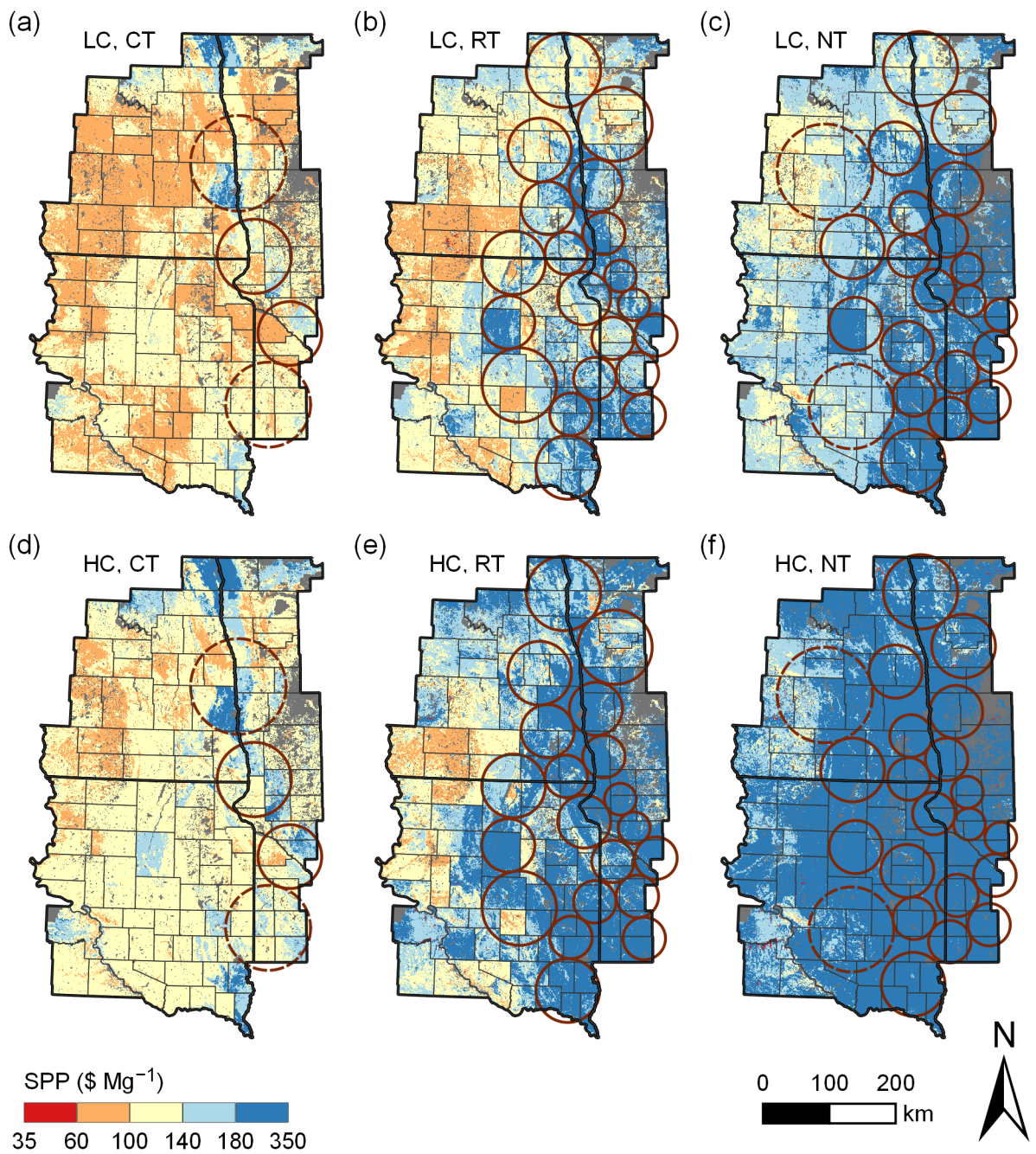


Figure 74. For the low-cost (LC) establishment scenario, the biomass price necessary for switchgrass to generate the same annualized net return as a single year of corn or wheat (SPP, switchgrass parity price) under (a) conventional tillage (CT), (b) reduced tillage (RT) or (c) no-till (NT). For the high-cost (HC) establishment scenario, (d – f) same as (a – c).

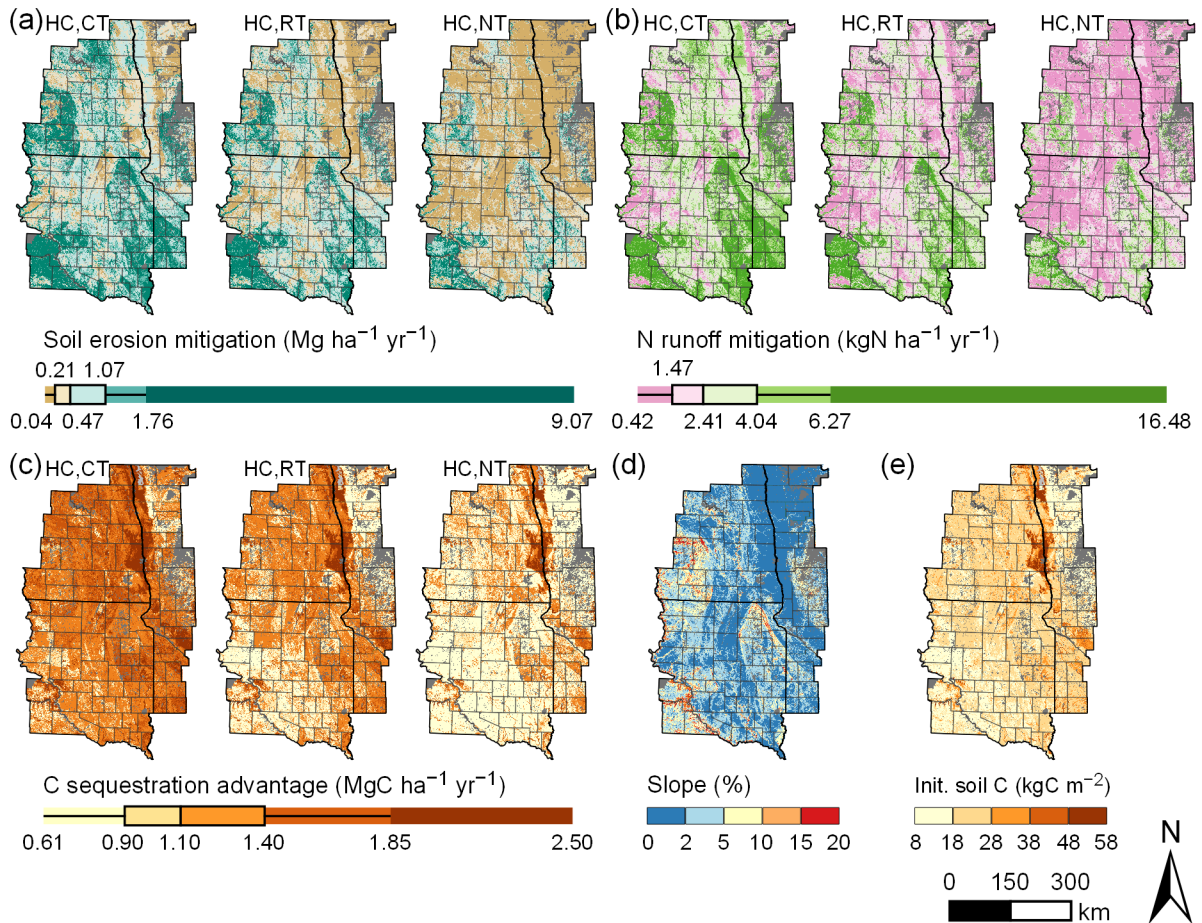


Figure 75. Environmental benefits of switchgrass production relative to corn or wheat and under the most profitable fertilization option (e.g. Figure 36) for the high-cost (HC) establishment scenario: (a) mitigation of soil erosion, (b) mitigation of nitrogen (N) runoff into surface water, and (c) carbon (C) sequestration. Maps of (d) slope and (e) initial soil C from SSURGO are provided to provide context to the spatial patterns of a – c.

REFERENCES

- Aakre, D. 2014. Custom farm work rates on North Dakota farms, 2013, by North Dakota farming regions. Tech. Rep. EC499, North Dakota State University Extension Service, Fargo, ND.
- Abadi Ghadim, A.K. and D.J. Pannell. 1999. A conceptual framework of adoption of an agricultural innovation. *Agr. Econ.* 21:145–154. doi:10.1016/S0169-5150(99)00023-7.
- Abatzoglou, J.T. 2013. Development of gridded surface meteorological data for ecological applications and modelling. *Int. J. Climatol.* 33:121–131. doi:10.1002/joc.3413.
- Abraha, M., S.K. Hamilton, J. Chen, and G.P. Robertson. 2018. Ecosystem carbon exchange on conversion of Conservation Reserve Program grasslands to annual and perennial cropping systems. *Agr. Forest Meteorol.* 253-254:151–160. doi:10.1016/j.agrformet.2018.02.016.
- Acharya, B.S. and H. Blanco-Canqui. 2018. Lignocellulosic-based bioenergy and water quality parameters: A review. *GCB Bioenergy.* 10:504–533. doi:10.1111/gcbb.12508, accessed 15 Feb. 2019.
- Adler, P.R., M.A. Sanderson, A.A. Boateng, P.J. Weimer, and H.J.G. Jung. 2006. Biomass yield and biofuel quality of switchgrass harvested in fall or spring. *Agron. J.* 98:1518–1525. doi:10.2134/agronj2005.0351.
- AgFunder. 2019. 2018 AgFunder agrifood tech investing report. AgFunder, San Francisco, CA. <https://agfunder.com/research/agrifood-tech-investing-report-2018>, accessed 22 Mar. 2019.
- Akyüz, F.A., H. Kandel, and D. Morlock. 2017. Developing a growing degree day model

- for North Dakota and northern Minnesota soybean. *Agr. Forest Meteorol.* 239:134–140. doi:10.1016/j.agrformet.2017.02.027.
- Al-Kaisi, M.M., X. Yin, and M.A. Licht. 2005. Soil carbon and nitrogen changes as influenced by tillage and cropping systems in some Iowa soils. *Agr. Ecosyst. Environ.* 105:635–647. doi:10.1016/j.agee.2004.08.002.
- Alderson, J. and W.C. Sharp. 1994. Grass varieties in the United States. Agricultural Handbook No. 170, USDA Soil Conservation Service, Washington, DC.
- Allen, R.G., L.S. Pereira, D. Raes, and M. Smith. 1998. Crop evapotranspiration: Guidelines for computing crop water requirements. FAO Irrigation and Drainage Paper 56, FAO, Rome.
- Analla, M. 1998. Model validation through the linear regression fit to actual versus predicted values. *Agr. Sys.* 57:115–119. doi:10.1016/S0308-521X(97)00073-5.
- Anderson, E.K., A.S. Parrish, T.B. Voigt, V.N. Owens, C.H. Hong, and D. Lee. 2013. Nitrogen fertility and harvest management of switchgrass for sustainable bioenergy feedstock production in Illinois. *Ind. Crop. Prod.* 48:19–27. doi:10.1016/j.indcrop.2013.03.029.
- Arnhold, E. 2017. *easynls*: Easy nonlinear model. R package version 5.0. R Foundation for Statistical Computing, Vienna, AT. <https://CRAN.R-project.org/package=easynls>, accessed 27 Mar. 2019.
- Arundale, R.A. 2012. The higher productivity of the bioenergy feedstock *Miscanthus x giganteus* relative to *Panicum virgatum* is seen both into the long term and beyond Illinois. Ph.D. dissertation, University of Illinois, Urbana-Champaign, IL.
- Arya, S., D. Mount, S.E. Kemp, and G. Jefferis. 2017. *RANN*: Fast nearest neighbour search (wraps ANN library) using L2 metric. R package version 2.5.1. R Foundation for Statistical Computing, Vienna, AT. <https://CRAN.R-project.org/package=RANN>, accessed 27 Mar. 2019.

- Aust, S. 2015. Stevens County official: Abengoa plant shut down, workers laid off. The Garden City Telegram. <http://www.gctelegram.com/ab45d454-9571-5461-befc-d264946fc9c0.html>, accessed 29 Jan. 2019.
- Awada, T., L.E. Moser, W.H. Schacht, and P.E. Reece. 2002. Stomatal variability of native warm-season grasses from the Nebraska Sandhills. *Can. J. Plant Sci.* 82:349–355. doi: 10.4141/P01-031.
- Baker, N.T. 2011. Tillage practices in the conterminous United States, 1989-2004—datasets aggregated by watershed. Data Series 573, US Department of the Interior, US Geological Survey, Reston, VA.
- Bangsund, D.A., E.A. DeVuyst, and F.L. Leistritz. 2008. Evaluation of breakeven farm-gate switchgrass prices in south central North Dakota. *Agribusiness and Applied Economics Report No. 632*, North Dakota State University, Department of Agribusiness and Applied Economics, Agricultural Experiment Station, Fargo, ND.
- Barney, J.N. and J.M. DiTomaso. 2010. Bioclimatic predictions of habitat suitability for the biofuel switchgrass in North America under current and future climate scenarios. *Biomass Bioenergy.* 34:124–133. doi:10.1016/j.biombioe.2009.10.009.
- Bates, D., M. Mächler, B. Bolker, and S. Walker. 2015. Fitting linear mixed-effects models using lme4. *J. Stat. Softw.* 67:1–48. doi:10.18637/jss.v067.i01.
- Bauer, A., A.B. Frank, and A.L. Black. 1992. A crop calendar for spring wheat and for spring barley. *North Dakota Farm Res.* 49:21–25.
- Behrman, K.D., J.R. Kiniry, M. Winchell, T.E. Juenger, and T.H. Keitt. 2013. Spatial forecasting of switchgrass productivity under current and future climate change scenarios. *Ecol. Appl.* 23:73–85. doi:10.1890/12-0436.1.

- Behrman, K.D., T.H. Keitt, and J.R. Kiniry. 2014. Modeling differential growth in switchgrass cultivars across the central and southern Great Plains. *BioEnergy Res.* 7:1165–1173. doi: 10.1007/s12155-014-9450-8.
- Bellocchi, G., M. Rivington, M. Donatelli, and K. Matthews. 2010. Validation of biophysical models: Issues and methodologies. A review. *Agron. Sustain. Dev.* 30:109–130. doi: 10.1051/agro/2009001.
- Bennett, A.B. and R. Isaacs. 2014. Landscape composition influences pollinators and pollination services in perennial biofuel plantings. *Agr. Ecosyst. Environ.* 193:1–8. doi: 10.1016/j.agee.2014.04.016.
- Bennett, N.D., B.F. Croke, G. Guariso, J.H. Guillaume, S.H. Hamilton, A.J. Jakeman, S. Marsili-Libelli, L.T. Newham, J.P. Norton, C. Perrin, S.A. Pierce, B. Robson, R. Seppelt, A.A. Voinov, B.D. Fath, and V. Andreassian. 2013. Characterising performance of environmental models. *Environ. Modell. Softw.* 40:1–20. doi:10.1016/j.envsoft.2012.09.011.
- Berdahl, J.D., A.B. Frank, J.M. Krupinsky, P.M. Carr, J.D. Hanson, and H.A. Johnson. 2005. Biomass yield, phenology, and survival of diverse switchgrass cultivars and experimental strains in western North Dakota. *Agron. J.* 97:549–555. doi:10.2134/agronj2005.0549.
- Blanco-Canqui, H. 2013. Crop residue removal for bioenergy reduces soil carbon pools: How can we offset carbon losses? *BioEnergy Res.* 6:358–371. doi:10.1007/s12155-012-9221-3.
- Blanco-Canqui, H. and R. Lal. 2009a. Corn stover removal for expanded uses reduces soil fertility and structural stability. *Soil Sci. Soc. Am. J.* 73:418–426. doi:10.2136/sssaj2008.0141.
- Blanco-Canqui, H. and R. Lal. 2009b. Crop residue removal impacts on soil productivity and environmental quality. *Crit. Rev. Plant Sci.* 28:139–163. doi:10.1080/07352680902776507.

- Blanco-Canqui, H., R.B. Mitchell, V.L. Jin, M.R. Schmer, and K.M. Eskridge. 2017. Perennial warm-season grasses for producing biofuel and enhancing soil properties: An alternative to corn residue removal. *GCB Bioenergy*. 9:1510–1521. doi:10.1111/gcbb.12436, accessed 15 Feb. 2019.
- Bock, M., P.Y. Gasser, W.W. Pettapiece, A.J. Brierley, A. Bootsma, P. Schut, D. Neilsen, and C.A.S. Smith. 2018. The Land Suitability Rating System is a spatial planning tool to assess crop suitability in Canada. *Front. Env. Sci*. 6:77. doi:10.3389/fenvs.2018.00077.
- Bonner, J.I., G.K. Cafferty, J.D. Muth, D.M. Tomer, E.D. James, A.S. Porter, and L.D. Karlen. 2014. Opportunities for energy crop production based on subfield scale distribution of profitability. *Energies*. 7:6509–6526. doi:10.3390/en7106509.
- Boote, K., J. Jones, G. Hoogenboom, and J. White. 2010. The role of crop systems simulation in agriculture and environment. *Int. J. Agr. Env. Inf. Sys*. 1:41–54. doi:10.4018/jaeis.2010101303.
- Boote, K.J., J.W. Jones, and N.B. Pickering. 1996. Potential uses and limitations of crop models. *Agron. J*. 88:704–716. doi:10.2134/agronj1996.00021962008800050005x.
- Boyer, C.N., D.D. Tyler, R.K. Roberts, B.C. English, and J.A. Larson. 2012. Switchgrass yield response functions and profit-maximizing nitrogen rates on four landscapes in Tennessee. *Agron. J*. 104:1579–1588. doi:10.2134/agronj2012.0179.
- Bracmort, K. 2019a. The Renewable Fuel Standard (RFS): An overview. Tech. Rep. R43325, Congressional Research Service, Washington, DC.
- Bracmort, K. 2019b. The Renewable Fuel Standard (RFS): Waiver authority and modification of volumes. Tech. Rep. R44045, Congressional Research Service, Washington, DC.
- Brady, S.J. 2000. Conservation Compliance and Wetlands Conservation Provisions of the Omnibus Farm Acts of 1985, 1990, and 1996. In: A comprehensive review of Farm Bill

- contributions to wildlife conservation, 1985-2000, editors W. Hohman and D. Halloum, USDA Natural Resources Conservation Service, Wildlife Habitat Management Institute, Technical Report, pp. 5–18.
- Brady, S.J. 2005. Highly Erodible Land and Swampbuster provisions of the 2002 Farm Act. In: Fish and wildlife benefits of Farm Bill conservation programs: 2000-2005 update, editor J.B. Haufler, The Wildlife Society, Bethesda, MD, Technical Review 05-2, pp. 5–16.
- Brandes, E., A. Plastina, and E.A. Heaton. 2018. Where can switchgrass production be more profitable than corn and soybean? An integrated subfield assessment in Iowa, USA. *GCB Bioenergy*. 10:473–488. doi:10.1111/gcbb.12516, accessed 22 Mar. 2019.
- Brennan, L.A. and W.P. Kuvlesky Jr. 2005. North American grassland birds: An unfolding conservation crisis? *J. Wildlife Manage.* 69:1–13. doi:10.2193/0022-541X(2005)069(0001:NAGBAU)2.0.CO;2, accessed 17 Feb. 2019.
- Brown, R., N. Rosenberg, C. Hays, W. Easterling, and L. Mearns. 2000. Potential production and environmental effects of switchgrass and traditional crops under current and greenhouse-altered climate in the central United States: A simulation study. *Agr. Ecosyst. Environ.* 78:31–47. doi:10.1016/S0167-8809(99)00115-2.
- Brown, T.R. and R.C. Brown. 2013. A review of cellulosic biofuel commercial-scale projects in the United States. *Biofuel. Bioprod. Bior.* 7:235–245. doi:10.1002/bbb.1387, accessed 15 Feb. 2019.
- Bughrara, S., R. Leep, D.H. Min, D. Hudson, and T. Dietz. 2007. Switchgrass as a biofuel for Michigan. Bulletin E-2987, Michigan State University Extension, East Lansing, MI.
- Burke, I.C., W.K. Lauenroth, and D.P. Coffin. 1995. Soil organic matter recovery in semiarid grasslands: Implications for the Conservation Reserve Program. *Ecol. Appl.* 5:793–801. doi:10.2307/1941987, accessed 17 Feb. 2019.

- Carriquiry, M.A., X. Du, and G.R. Timilsina. 2011. Second generation biofuels: Economics and policies. *Energy Policy*. 39:4222–4234. doi:10.1016/j.enpol.2011.04.036.
- Casler, M., K. Vogel, C. Taliaferro, and R. Wynia. 2004. Latitudinal adaptation of switchgrass populations. *Crop Sci*. 44:293–303. doi:10.2135/cropsci2004.2930.
- Casler, M., K. Vogel, C. Taliaferro, N. Ehlke, J. Berdahl, E. Brummer, R. Kallenbach, C. West, and R. Mitchell. 2007. Latitudinal and longitudinal adaptation of switchgrass populations. *Crop Sci*. 47:2249–2260. doi:10.2135/cropsci2006.12.0780.
- Casler, M.D. 2012. Switchgrass breeding, genetics, and genomics. In: *Switchgrass: A valuable biomass crop for energy*, editor A. Monti, Springer, London, UK, pp. 29–53.
- Casler, M.D. and A.R. Boe. 2003. Cultivar × environment interactions in switchgrass. *Crop Sci*. 43:2226–2233. doi:10.2135/cropsci2003.2226.
- Casler, M.D., C.M. Tobias, S.M. Kaeppler, C.R. Buell, Z.Y. Wang, P. Cao, J. Schmutz, and P. Ronald. 2011. The switchgrass genome: Tools and strategies. *Plant Genome*. 4:273–282. doi:10.3835/plantgenome2011.10.0026.
- Chakrabarti, S., T. Bongiovanni, J. Judge, L. Zotarelli, and C. Bayer. 2014. Assimilation of SMOS soil moisture for quantifying drought impacts on crop yield in agricultural regions. *IEEE J-STARS*. 7:3867–3879. doi:10.1109/JSTARS.2014.2315999.
- Chen, M. and P.M. Smith. 2017. The U.S. cellulosic biofuels industry: Expert views on commercialization drivers and barriers. *Biomass Bioenergy*. 102:52–61. doi:10.1016/j.biombioe.2017.05.002.
- Chen, M. and P.M. Smith. 2018. Mixed methods research of integrated cellulosic biorefinery (ICBR) scale-up barriers in the United States: A case study. *Bioprod. Bus*. 3:51–62.
- CIMMYT. 1988. From agronomic data to farmer recommendations: An economics training

- manual. CIMMYT, Mexico. <https://ispc.cgiar.org/sites/default/files/pdf/120.pdf>, accessed 17 Feb. 2019.
- Claassen, R., T. Wade, V. Breneman, R. Williams, and C. Loesch. 2018. Preserving native grassland: Can Sodsaver reduce cropland conversion? *J. Soil Water Conserv.* 73:67A–73A. doi:10.2489/jswc.73.3.67A.
- Coffin, A.W., T.C. Strickland, W.F. Anderson, M.C. Lamb, R.R. Lowrance, and C.M. Smith. 2016. Potential for production of perennial biofuel feedstocks in conservation buffers on the Coastal Plain of Georgia, USA. *BioEnergy Res.* 9:587–600. doi:10.1007/s12155-015-9700-4.
- Cooperative Extension System. 2008. Corn, water requirements. Extension Publications. <http://articles.extension.org/pages/14080/corn-water-requirements>, accessed 27 Jun. 2018.
- Coulter, J. 2009. Optimum plant population for corn in Minnesota. Tech. Rep. M 1244, University of Minnesota Extension Service, St. Paul, MN.
- Coulter, J. 2012. Planting date considerations for corn. University of Minnesota Extension Service, St. Paul, MN. <http://blog-crop-news.extension.umn.edu/2012/03/planting-date-considerations-for-corn.html>, accessed 8 May 2015.
- Coulter, J. 2015. Agronomic responses of corn to planting date and plant density. University of Minnesota Extension Service, St. Paul, MN. <http://www.extension.umn.edu/agriculture/corn/planting/corn-planting-date-and-plant-density/>, accessed 8 May 2015.
- Cronshey, R., R.H. McCuen, N. Miller, W. Rawls, S. Robbins, and D. Woodward. 1986. Urban hydrology for small watersheds. Tech. Rep. TR-55, USDA Natural Resources Conservation Service, Conservation Engineering Division, Washington, DC.
- Crooks, E. 2018. Ethanol hopes rise as crude oil prices surge. *Financial Times*. <https://www.ft.com/content/4f1164fc-589c-11e8-bdb7-f6677d2e1ce8>, accessed 29 Jan. 2019.

- Dale, B.E., J.E. Anderson, R.C. Brown, S. Csonka, V.H. Dale, G. Herwick, R.D. Jackson, N. Jordan, S. Kaffka, K.L. Kline, L.R. Lynd, C. Malmstrom, R.G. Ong, T.L. Richard, C. Taylor, and M.Q. Wang. 2014. Take a closer look: Biofuels can support environmental, economic and social goals. *Environ. Sci. Technol.* 48:7200–7203. doi:10.1021/es5025433.
- Dale, V.H., K.L. Kline, J. Wiens, and J. Fargione. 2010. Biofuels: Implications for land use and biodiversity. *Biofuels and Sustainability Reports*. Ecological Society of America, Washington, DC.
- Davis, S.C., W.J. Parton, F.G. Dohleman, C.M. Smith, S.D. Grosso, A.D. Kent, and E.H. DeLucia. 2010. Comparative biogeochemical cycles of bioenergy crops reveal nitrogen-fixation and low greenhouse gas emissions in a *Miscanthus* × *giganteus* agro-ecosystem. *Ecosystems*. 13:144–156. doi:10.1007/s10021-009-9306-9.
- Davis, S.C., W.J. Parton, S.J.D. Grosso, C. Keough, E. Marx, P.R. Adler, and E.H. DeLucia. 2012. Impact of second-generation biofuel agriculture on greenhouse-gas emissions in the corn-growing regions of the US. *Front. Ecol. Environ.* 10:69–74. doi:10.1890/110003, accessed 22 Mar. 2019.
- De La Torre Ugarte, D.G. and D.E. Ray. 2000. Biomass and bioenergy applications of the POLYSYS modeling framework. *Biomass Bioenergy*. 18:291–308. doi:10.1016/S0961-9534(99)00095-1.
- de Wit, A. and C. van Diepen. 2007. Crop model data assimilation with the Ensemble Kalman filter for improving regional crop yield forecasts. *Agr. Forest Meteorol.* 146:38–56. doi: 10.1016/j.agrformet.2007.05.004.
- DeJong, J. 2017. Getting to root of problem. <https://www.wallacesfarmer.com/corn/getting-root-problem>, accessed 8 Aug. 2018.
- Di Paola, A., R. Valentini, and M. Santini. 2016. An overview of available crop growth and

- yield models for studies and assessments in agriculture. *J. Sci. Food Agr.* 96:709–714. doi:10.1002/jsfa.7359, accessed 8 Aug. 2018.
- Doraiswamy, P.C., S. Moulin, P.W. Cook, and A. Stern. 2003. Crop yield assessment from remote sensing. *Photogramm. Eng. Rem. S.* 69:665–674. doi:doi:10.14358/PERS.69.6.665.
- Dorigo, W., R. Zurita-Milla, A. de Wit, J. Brazile, R. Singh, and M. Schaepman. 2007. A review on reflective remote sensing and data assimilation techniques for enhanced agroecosystem modeling. *Int. J. Appl. Earth Obs.* 9:165–193. doi:10.1016/j.jag.2006.05.003.
- Drinnon, D., H. McCord, K. Goddard, and J. Walton. 2015. Guidebook for the sustainable production practices of switchgrass in the Southeastern U.S. Tech. Rep. 14-0058, University of Tennessee Institute of Agriculture, Knoxville, TN.
- DTN. 2018. DTN fertilizer index. DTN, Burnsville, MN. <https://www.dtnpf.com>, accessed 4 May 2017.
- Dunn, C.P., F. Stearns, G.R. Guntenspergen, and D.M. Sharpe. 1993. Ecological benefits of the Conservation Reserve Program. *Conserv. Biol.* 7:132–139. doi:10.1046/j.1523-1739.1993.07010132.x, accessed 17 Feb. 2019.
- DuPont. 2015. DuPont celebrates the opening of the world’s largest cellulosic ethanol plant. Press Release. <http://www.dupont.com/corporate-functions/media-center/press-releases/dupont-celebrates-opening-of-worlds-largest-cellulosic-ethanol-plant.html>, accessed 29 Jan. 2019.
- DuPont Pioneer. 2015. Planting rate estimator. <https://www.pioneer.com/home/site/us/tools-apps/planting-tools/planting-rate-estimator/>, accessed 8 Aug. 2018.
- Edwards, W. 2014. Estimating a value for corn stover. *Ag Decision Maker A1-70*, Iowa State University Extension, Ames, IA.

- Edwards, W. and A. Johanns. 2010. 2010 Iowa farm custom rate survey. Ag Decision Maker A3-10, Iowa State University Extension, Ames, IA.
- Edwards, W., A. Johanns, and A. Chamra. 2013. 2013 Iowa farm custom rate survey. Ag Decision Maker A3-10, Iowa State University Extension, Ames, IA.
- EFC Systems. 2019. Agronomic planning and sustainability. <https://www.efcsystems.com/index.php/agronomicplanningandsustainability/>, accessed 23 Mar. 2019.
- Eichelmann, E., C. Wagner-Riddle, J. Warland, B. Deen, and P. Voroney. 2016. Comparison of carbon budget, evapotranspiration, and albedo effect between the biofuel crops switchgrass and corn. *Agr. Ecosyst. Environ.* 231:271–282. doi:10.1016/j.agee.2016.07.007.
- Eller, D. 2017. DowDuPont shuts Nevada cellulosic ethanol plant, looks for a buyer. *Des Moines Register*. <https://www.desmoinesregister.com/story/money/agriculture/2017/11/02/dowdupont-shutters-nevada-cellulosic-ethanol-plant-looks-buyer/824606001/>, accessed 29 Jan. 2019.
- Erickson, K.W., C.B. Moss, and A.K. Mishra. 2004. Rates of return in the farm and nonfarm sectors: How do they compare? *J. Agric. Appl. Econ.* 36:789–795. doi:10.1017/S1074070800027024.
- Euliss Jr., N.H., R.A. Gleason, A. Olness, R.L. McDougal, H.R. Murkin, R.D. Robarts, R.A. Bourbonniere, and B.G. Warner. 2006. North American prairie wetlands are important nonforested land-based carbon storage sites. *Sci. Total Environ.* 361:179–188. doi:10.1016/j.scitotenv.2005.06.007.
- Evans, J.M., R.J. Fletcher, and J. Alavalapati. 2010. Using species distribution models to identify suitable areas for biofuel feedstock production. *GCB Bioenergy.* 2:63–78. doi:10.1111/j.1757-1707.2010.01040.x, accessed 9 Jun. 2018.

- Faber, S., S. Rundquist, and T. Male. 2012. Plowed under: How crop subsidies contribute to massive habitat losses. Environmental Working Group, Washington, DC.
- Fang, H., S. Liang, G. Hoogenboom, J. Teasdale, and M. Cavigelli. 2008. Corn-yield estimation through assimilation of remotely sensed data into the CSM-CERES-Maize model. *Int. J. Remote Sens.* 29:3011–3032. doi:10.1080/01431160701408386.
- Fang, H., S. Liang, and G. Hoogenboom. 2011. Integration of MODIS LAI and vegetation index products with the CSM–CERES–Maize model for corn yield estimation. *Int. J. Remote Sens.* 32:1039–1065. doi:10.1080/01431160903505310.
- Fargione, J.E., T.R. Cooper, D.J. Flaspohler, J. Hill, C. Lehman, T. McCoy, S. McLeod, E.J. Nelson, K.S. Oberhauser, and D. Tilman. 2009. Bioenergy and wildlife: Threats and opportunities for grassland conservation. *BioScience.* 59:767–777. doi:10.1525/bio.2009.59.9.8, accessed 17 Feb. 2019.
- Fawcett, J. 2013. How deep can corn roots go? *Wallaces Farmer.* <http://magissues.farmprogress.com/wal/WF01Jan13/wal036.pdf>, accessed 22 Jun. 2015.
- Fehrenbacher, K. 2015. How tech billionaire Vinod Khosla’s biofuel dream went bad. *Fortune.* <http://fortune.com/kior-vinod-khosla-clean-tech/>, accessed 29 Jan. 2019.
- Feng, Q., I. Chaubey, B. Engel, R. Cibin, K. Sudheer, and J. Volenec. 2017. Marginal land suitability for switchgrass, *Miscanthus* and hybrid poplar in the Upper Mississippi River Basin (UMRB). *Environ. Modell. Softw.* 93:356–365. doi:10.1016/j.envsoft.2017.03.027.
- Fike, J.H., J.W. Pease, V.N. Owens, R.L. Farris, J.L. Hansen, E.A. Heaton, C.O. Hong, H.S. Mayton, R.B. Mitchell, and D.R. Viands. 2017. Switchgrass nitrogen response and estimated production costs on diverse sites. *GCB Bioenergy.* 9:1526–1542. doi:10.1111/gcbb.12444, accessed 17 Feb. 2019.

- FINBIN. 2019. The FINPACK farm financial database. University of Minnesota, Center for Farm Financial Management, St. Paul, MN. <https://finbin.umn.edu/>, accessed 17 Feb. 2019.
- Fischer, A., L. Kergoat, and G. Dedieu. 1997. Coupling satellite data with vegetation functional models: Review of different approaches and perspectives suggested by the assimilation strategy. *Remote Sens. Rev.* 15:283–303. doi:10.1080/02757259709532343.
- Flénet, F., J.R. Kiniry, J.E. Board, M.E. Westgate, and D.C. Reicosky. 1996. Row spacing effects on light extinction coefficients of corn, sorghum, soybean, and sunflower. *Agron. J.* 88:185–190.
- Fletcher Jr., R.J., B.A. Robertson, J. Evans, P.J. Doran, J.R. Alavalapati, and D.W. Schemske. 2011. Biodiversity conservation in the era of biofuels: Risks and opportunities. *Front. Ecol. Environ.* 9:161–168. doi:10.1890/090091, accessed 17 Feb. 2019.
- Follett, R.F., K.P. Vogel, G.E. Varvel, R.B. Mitchell, and J. Kimble. 2012. Soil carbon sequestration by switchgrass and no-till maize grown for bioenergy. *BioEnergy Res.* 5:866–875. doi:10.1007/s12155-012-9198-y.
- Foster, D., F. Swanson, J. Aber, I. Burke, N. Brokaw, D. Tilman, and A. Knapp. 2003. The importance of land-use legacies to ecology and conservation. *BioScience.* 53:77–88. doi:10.1641/0006-3568(2003)053[0077:TIOLUL]2.0.CO;2, accessed 17 Feb. 2019.
- Franzen, D.W. 2014a. Fertilizing hard red spring wheat and durum. Tech. Rep. SF712, NDSU Extension Service, Fargo, ND.
- Franzen, D.W. 2014b. Soil fertility recommendations for corn. Tech. Rep. SF722, NDSU Extension Service, Fargo, ND.
- Gallagher, P.W., M. Dikeman, J. Fritz, E.J. Wailes, W.M. Gauthier, and H. Shapouri. 2003. Biomass from crop residues: Cost and supply estimates. Tech. Rep. 819, USDA, Office of the Chief Economist, Washington, DC.

- Gamble, J.D., J.M. Jungers, D.L. Wyse, G.A. Johnson, J.A. Lamb, and C.C. Sheaffer. 2015. Harvest date effects on biomass yield, moisture content, mineral concentration, and mineral export in switchgrass and native polycultures managed for bioenergy. *BioEnergy Res.* 8:740–749. doi:10.1007/s12155-014-9555-0.
- Garland, C.D. 2008. Growing and harvesting switchgrass for ethanol production in Tennessee. Tech. Rep. SP701-A, University of Tennessee Extension, Knoxville, TN.
- Gelfand, I., T. Zenone, P. Jasrotia, J. Chen, S.K. Hamilton, and G.P. Robertson. 2011. Carbon debt of Conservation Reserve Program (CRP) grasslands converted to bioenergy production. *Proc. Natl. Acad. Sci. USA.* 108:13864–13869. doi:10.1073/pnas.1017277108.
- Gelfand, I., R. Sahajpal, X. Zhang, R.C. Izaurralde, K.L. Gross, and G.P. Robertson. 2013. Sustainable bioenergy production from marginal lands in the US Midwest. *Nature.* 493:514. doi:10.1038/nature11811.
- Gijsman, A., S. Jagtap, and J. Jones. 2002. Wading through a swamp of complete confusion: How to choose a method for estimating soil water retention parameters for crop models. *Eur. J. Agron.* 18:77–106. doi:10.1016/S1161-0301(02)00098-9.
- Gleason, R.A., N.H. Euliss Jr., B.A. Tangen, M.K. Laubhan, and B.A. Browne. 2011. USDA conservation program and practice effects on wetland ecosystem services in the Prairie Pothole Region. *Ecol. Appl.* 21:S65–S81. doi:10.1890/09-0216.1, accessed 17 Feb. 2019.
- Grassini, P., E. Hunt, R.B. Mitchell, and A. Weiss. 2009. Simulating switchgrass growth and development under potential and water-limiting conditions. *Agron. J.* 101:564–571. doi:10.2134/agronj2008.0200x.
- Haan, C.T., B.J. Barfield, and J.C. Hayes. 1994. Design hydrology and sedimentology for small catchments. Elsevier, San Diego, CA.

- Hall, R.G., K.D. Reitsma, and D.E. Clay. 2009. Corn planting guide. In: Best management practices for corn production in South Dakota, editors D.E. Clay, K.D. Reitsma, and S.A. Clay, South Dakota State University, South Dakota Cooperative Extension Service, Brookings, SD, pp. 13–16.
- Halvorson, A.D. and C.E. Stewart. 2015. Stover removal affects no-till irrigated corn yields, soil carbon, and nitrogen. *Agron. J.* 107:1504–1512. doi:10.2134/agronj15.0074.
- Hamdar, B. 1999. An efficiency approach to managing Mississippi's marginal land based on the Conservation Reserve Program (CRP). *Resour. Conserv. Recy.* 26:15–24. doi: 10.1016/S0921-3449(98)00067-6.
- Hammer, G.L., Z. Dong, G. McLean, A. Doherty, C. Messina, J. Schussler, C. Zinselmeier, S. Paszkiewicz, and M. Cooper. 2009. Can changes in canopy and/or root system architecture explain historical maize yield trends in the US Corn Belt? *Crop Sci.* 49:299–312. doi: 10.2135/cropsci2008.03.0152.
- Han, W., Z. Yang, L. Di, and R. Mueller. 2012. CropScape: A web service based application for exploring and disseminating US conterminous geospatial cropland data products for decision support. *Comput. Electron. Agr.* 84:111–123. doi:10.1016/j.compag.2012.03.005.
- Hancock, D.W. 2017. The management and use of switchgrass in Georgia. Bulletin 1358, University of Georgia Cooperative Extension, Athens, GA.
- Hansen, L. 2007. Conservation Reserve Program: Environmental benefits update. *Agr. Resour. Econ. Rev.* 36:267–280. doi:10.1017/S1068280500007085.
- Hansen, L. and M. Ribaud. 2008. Economic measures of soil conservation benefits: Regional values for policy assessment. Tech. Rep. 1922, USDA Economic Research Service, Washington, DC.

- Harl, N. 2014. The Agricultural Act of 2014. AgDM Newsletter. Iowa State University Extension and Outreach, Ames, IA. <https://www.extension.iastate.edu/agdm/articles/harl/HarlMar14.html>, accessed 13 Apr. 2019.
- Harris, W.L., B. Lubben, J.L. Novak, and L.D. Sanders. 2008. The Food, Conservation, and Energy Act of 2008 summary and possible consequences. Working Paper DAERS-WP-1-72008, University of Nebraska, Lincoln, NE.
- Harrison, S. 1990. Regression of a model on real-system output: An invalid test of model validity. *Agr. Sys.* 34:183–190. doi:10.1016/0308-521X(90)90083-3.
- Hartkamp, A.D., J.W. White, and G. Hoogenboom. 1999. Interfacing geographic information systems with agronomic modeling: A review. *Agron. J.* 91:761–772. doi:10.2134/agronj1999.915761x.
- Hartman, J.C., J.B. Nippert, R.A. Orozco, and C.J. Springer. 2011. Potential ecological impacts of switchgrass (*Panicum virgatum* L.) biofuel cultivation in the Central Great Plains, USA. *Biomass Bioenergy.* 35:3415–3421. doi:10.1016/j.biombioe.2011.04.055.
- Haufler, J.B., editor. 2005. Fish and wildlife benefits of Farm Bill conservation programs: 2000-2005 update. Technical Review 05-2. The Wildlife Society, Bethesda, MD.
- Heaton, E., T. Voigt, and S.P. Long. 2004. A quantitative review comparing the yields of two candidate C4 perennial biomass crops in relation to nitrogen, temperature and water. *Biomass Bioenergy.* 27:21–30. doi:10.1016/j.biombioe.2003.10.005.
- Heggenstaller, A.H., K.J. Moore, M. Liebman, and R.P. Anex. 2009. Nitrogen influences biomass and nutrient partitioning by perennial, warm-season grasses. *Agron. J.* 101:1363–1371. doi:10.2134/agronj2008.0225x.
- Hilker, J., J. Black, and O. Hesterman. 1987. Breakeven analysis for comparing alternative crops. Tech. Rep. E-2021, Michigan State University Extension, East Lansing, MI.

- Hohman, W. and D. Halloum, editors. 2000. A comprehensive review of Farm Bill contributions to wildlife conservation, 1985-2000. Technical Report. USDA Natural Resources Conservation Service, Wildlife Habitat Management Institute.
- Holman, J., R. Gillen, J.L. Moyer, T. Roberts, K. Harmony, P. Sloderbeck, T. Dumler, K. Martin, S. Staggenborg, W. Fick, S. Maxwell, and C. Thompson. 2011. Kansas switchgrass production handbook. Tech. Rep. MF3018, Kansas State University Agricultural Experiment Station and Cooperative Extension Service.
- Homer, C.H., J.A. Fry, and C.A. Barnes. 2012. The National Land Cover Database. U.S. Geological Survey, Washington, DC. <https://doi.org/10.3133/fs20123020>, accessed 27 Mar. 2019.
- Hoque, M., G. Artz, and C. Hart. 2015. Estimated cost of establishment and production of 'Liberty' switchgrass. Ag Decision Maker A1-29, Iowa State University Extension, Ames, IA.
- Hurvich, C., J. Simonoff, and C. Tsai. 1998. Smoothing parameter selection in nonparametric regression using an improved Akaike information criterion. *J. Roy. Stat. Soc. B.* 60:271–293. doi:10.1111/1467-9868.00125, accessed 8 Jun. 2018.
- IMPACT Model Team. 2015. The International Model for Policy Analysis of Agricultural Commodities and Trade (IMPACT). International Food Policy Research Institute, Washington, DC. <https://www.ifpri.org/program/impact-model>, accessed 8 Aug. 2018.
- Ines, A.V., N.N. Das, J.W. Hansen, and E.G. Njoku. 2013. Assimilation of remotely sensed soil moisture and vegetation with a crop simulation model for maize yield prediction. *Remote Sens. Environ.* 138:149–164. doi:10.1016/j.rse.2013.07.018.
- Jager, H.I., L.M. Baskaran, C.C. Brandt, E.B. Davis, C.A. Gunderson, and S.D. Wullschleger. 2010. Empirical geographic modeling of switchgrass yields in the United States. *GCB Bioenergy.* 2:248–257. doi:10.1111/j.1757-1707.2010.01059.x, accessed 9 Jun. 2018.

- Jain, A. 2019. Integrated Science Assessment Model – ISAM. University of Illinois Department of Atmospheric Sciences, Urbana-Champaign, IL. <http://climate.atmos.uiuc.edu/isam2/>, accessed 23 Mar. 2019.
- Jain, A.K., M. Khanna, M. Erickson, and H. Huang. 2010. An integrated biogeochemical and economic analysis of bioenergy crops in the midwestern United States. *GCB Bioenergy*. 2:217–234. doi:10.1111/j.1757-1707.2010.01041.x, accessed 16 Feb. 2019.
- James, L.K., S.M. Swinton, and K.D. Thelen. 2010. Profitability analysis of cellulosic energy crops compared with corn. *Agron. J.* 102:675–687. doi:10.2134/agronj2009.0289.
- Jin, V.L., M.R. Schmer, B.J. Wienhold, C.E. Stewart, G.E. Varvel, A.J. Sindelar, R.F. Follett, R.B. Mitchell, and K.P. Vogel. 2015. Twelve years of stover removal increases soil erosion potential without impacting yield. *Soil Sci. Soc. Am. J.* 79:1169–1178. doi:10.2136/sssaj2015.02.0053.
- Jin, X., L. Kumar, Z. Li, H. Feng, X. Xu, G. Yang, and J. Wang. 2018. A review of data assimilation of remote sensing and crop models. *Eur. J. Agron.* 92:141–152. doi:10.1016/j.eja.2017.11.002.
- Jobbágy, E.G. and R.B. Jackson. 2000. The vertical distribution of soil organic carbon and its relation to climate and vegetation. *Ecol. Appl.* 10:423–436. doi:10.1890/1051-0761(2000)010[0423:TVDOSO]2.0.CO;2, accessed 17 Feb. 2019.
- Johnson, J.M.F., R.R. Allmaras, and D.C. Reicosky. 2006. Estimating source carbon from crop residues, roots and rhizodeposits using the national grain-yield database. *Agron. J.* 98:622–636. doi:10.2134/agronj2005.0179.
- Johnson, W.C., B. Werner, G.R. Guntenspergen, R.A. Voldseth, B. Millett, D.E. Naugle, M. Tulbure, R.W.H. Carroll, J. Tracy, and C. Olawsky. 2010. Prairie wetland complexes as landscape functional units in a changing climate. *BioScience*. 60:128–140. doi: 10.1525/bio.2010.60.2.7, accessed 17 Feb. 2019.

- Johnston, C.A. 2014. Agricultural expansion: Land use shell game in the U.S. Northern Plains. *Landscape Ecol.* 29:81–95. doi:10.1007/s10980-013-9947-0.
- Jones, C.D., X. Zhang, A.D. Reddy, G.P. Robertson, and R.C. Izaurralde. 2017a. The greenhouse gas intensity and potential biofuel production capacity of maize stover harvest in the US Midwest. *GCB Bioenergy.* 9:1543–1554. doi:10.1111/gcbb.12473, accessed 22 Mar. 2019.
- Jones, J.W., J.M. Antle, B. Basso, K.J. Boote, R.T. Conant, I. Foster, H.C.J. Godfray, M. Herrero, R.E. Howitt, S. Janssen, B.A. Keating, R. Munoz-Carpena, C.H. Porter, C. Rosenzweig, and T.R. Wheeler. 2016. Brief history of agricultural systems modeling. *Agr. Sys.* 155:240–254. doi:10.1016/j.agry.2016.05.014.
- Jones, J.W., J.M. Antle, B. Basso, K.J. Boote, R.T. Conant, I. Foster, H.C.J. Godfray, M. Herrero, R.E. Howitt, S. Janssen, B.A. Keating, R. Munoz-Carpena, C.H. Porter, C. Rosenzweig, and T.R. Wheeler. 2017b. Toward a new generation of agricultural system data, models, and knowledge products: State of agricultural systems science. *Agr. Sys.* 155:269–288. doi:10.1016/j.agry.2016.09.021.
- Jungers, J.M., J.E. Fargione, C.C. Sheaffer, D.L. Wyse, and C. Lehman. 2013. Energy potential of biomass from conservation grasslands in Minnesota, USA. *PloS ONE.* 8:e61209. doi:10.1371/journal.pone.0061209.
- Jungers, J.M., T.W. Arnold, and C. Lehman. 2015. Effects of grassland biomass harvest on nesting pheasants and ducks. *Am. Midl. Nat.* 173:122–132. doi:10.1674/0003-0031-173.1.122, accessed 8 Jun. 2018.
- Jungers, J.M., L.H. DeHaan, D.J. Mulla, C.C. Sheaffer, and D.L. Wyse. 2019. Reduced nitrate leaching in a perennial grain crop compared to maize in the Upper Midwest, USA. *Agr. Ecosyst. Environ.* 272:63–73. doi:10.1016/j.agee.2018.11.007.

- Kaiser, D., F. Fernandez, and J. Coulter. 2018. Fertilizing corn in Minnesota. University of Minnesota Extension Service, St. Paul, MN. <https://extension.umn.edu/crop-specific-needs/fertilizing-corn-minnesota>, accessed 27 Mar. 2019.
- Kaiser, D.E. and J.A. Lamb. 2012. Fertilizing soybean in Minnesota. Tech. Rep. AG-FO-03813-C, University of Minnesota Extension Service, St. Paul, MN.
- Kaiser, D.E., J.A. Lamb, J.J. Wiersma, and A. Sims. 2013. Fertilizing wheat in Minnesota. Tech. Rep. AG-FO-3814-C, University of Minnesota Extension Service, St. Paul, MN.
- Kandel, H. 2014. Soybean production field guide for North Dakota and northwestern Minnesota. Tech. Rep. A1172B, NDSU Extension Service, Fargo, ND.
- Kang, S., W. Post, D. Wang, J. Nichols, V. Bandaru, and T. West. 2013a. Hierarchical marginal land assessment for land use planning. *Land Use Policy*. 30:106–113. doi:10.1016/j.landuspol.2012.03.002.
- Kang, S., W.M. Post, J.A. Nichols, D. Wang, T.O. West, V. Bandaru, and R.C. Izaurrealde. 2013b. Marginal lands: Concept, assessment and management. *J. Agric. Sci.* 5:129.
- Kang, S., S.S. Nair, K.L. Kline, J.A. Nichols, D. Wang, W.M. Post, C.C. Brandt, S.D. Wullschleger, N. Singh, and Y. Wei. 2014. Global simulation of bioenergy crop productivity: Analytical framework and case study for switchgrass. *GCB Bioenergy*. 6:14–25. doi:10.1111/gcbb.12047, accessed 16 Mar. 2019.
- Karlen, D.L., S.J. Birrell, J.M.F. Johnson, S.L. Osborne, T.E. Schumacher, G.E. Varvel, R.B. Ferguson, J.M. Novak, J.R. Fredrick, J.M. Baker, J.A. Lamb, P.R. Adler, G.W. Roth, and E.D. Nafziger. 2014. Multilocation corn stover harvest effects on crop yields and nutrient removal. *BioEnergy Res.* 7:528–539. doi:10.1007/s12155-014-9419-7.
- Keeler, B.L., B.J. Krohn, T.A. Nickerson, and J.D. Hill. 2013. U.S. federal agency models offer

- different visions for achieving Renewable Fuel Standard (RFS2) biofuel volumes. *Environ. Sci. Technol.* 47:10095–10101. doi:10.1021/es402181y.
- Kenney, I., H. Blanco-Canqui, D.R. Presley, C.W. Rice, K. Janssen, and B. Olson. 2015. Soil and crop response to stover removal from rainfed and irrigated corn. *GCB Bioenergy*. 7:219–230. doi:10.1111/gcbb.12128, accessed 15 Feb. 2019.
- Kiniry, J. 1999. Response to questions raised by Sinclair and Muchow. *Field Crop. Res.* 62:245–247. doi:10.1016/S0378-4290(99)00012-X.
- Kiniry, J., J. Landivar, M. Witt, T. Gerik, J. Cavero, and L. Wade. 1998. Radiation-use efficiency response to vapor pressure deficit for maize and sorghum. *Field Crop. Res.* 56:265–270. doi:10.1016/S0378-4290(97)00092-0.
- Kiniry, J., C. Tischler, and G. Van Esbroeck. 1999. Radiation use efficiency and leaf CO₂ exchange for diverse C₄ grasses. *Biomass Bioenergy*. 17:95–112. doi:10.1016/S0961-9534(99)00036-7.
- Kiniry, J., K. Cassida, M. Hussey, J. Muir, W. Ocumpaugh, J. Read, R. Reed, M. Sanderson, B. Venuto, and J. Williams. 2005. Switchgrass simulation by the ALMANAC model at diverse sites in the southern US. *Biomass Bioenergy*. 29:419–425. doi:10.1016/j.biombioe.2005.06.003.
- Kiniry, J., L. Lynd, N. Greene, M.V.V. Johnson, M. Casler, and M.S. Laser. 2008a. Biofuels and water use: Comparison of maize and switchgrass and general perspectives. In: *New research on biofuels*, editors J. Wright and D. Evans, Nova Science Publishers, Inc., pp. 1–14.
- Kiniry, J., M.V. Johnson, R. Mitchell, K. Vogel, J. Kaiser, S. Bruckerhoff, and R. Cordsiemon. 2011. Switchgrass leaf area index and light extinction coefficients. *Agron. J.* 103:119–122. doi:10.2134/agronj2010.0280.

- Kiniry, J.R. and A.J. Bockholt. 1998. Maize and sorghum simulation in diverse Texas environments. *Agron. J.* 90:682–687.
- Kiniry, J.R., J.R. Williams, P.W. Gassman, and P. Debaeke. 1992. A general, process-oriented model for two competing plant species. *Trans. ASAE.* 35:801–810.
- Kiniry, J.R., J.R. Williams, D.J. Major, R.C. Izaurralde, P.W. Gassman, M. Morrison, R. Bergentine, and R.P. Zentner. 1995. EPIC model parameters for cereal, oilseed, and forage crops in the northern Great Plains region. *Can. J. Plant Sci.* 75:679–688.
- Kiniry, J.R., M.A. Sanderson, J.R. Williams, C.R. Tischler, M.A. Hussey, W.R. Ocumpaugh, J.C. Read, G. Van Esbroeck, and R.L. Reed. 1996. Simulating Alamo switchgrass with the ALMANAC model. *Agron. J.* 88:602–606. doi:10.2134/agronj1996.00021962008800040018x.
- Kiniry, J.R., J.R. Williams, R.L. Vanderlip, J.D. Atwood, D.C. Reicosky, J. Mulliken, W.J. Cox, H.J. Mascagni, S.E. Hollinger, and W.J. Wiebold. 1997. Evaluation of two maize models for nine U.S. locations. *Agron. J.* 89:421–426.
- Kiniry, J.R., J.G. Arnold, and Y. Xie. 2002. Applications of models with different spatial scales. In: *Agricultural system models in field research and technology transfer*, editors L.R. Ahuja, L. Ma, and T.A. Howell, CRC Press, Boca Raton, FL, pp. 207–227.
- Kiniry, J.R., B. Bean, Y. Xie, and P.y. Chen. 2004. Maize yield potential: Critical processes and simulation modeling in a high-yielding environment. *Agr. Sys.* 82:45–56. doi:10.1016/j.agsy.2003.11.006.
- Kiniry, J.R., M.R. Schmer, K.P. Vogel, and R.B. Mitchell. 2008b. Switchgrass biomass simulation at diverse sites in the northern Great Plains of the U.S. *BioEnergy Res.* 1:259–264. doi:10.1007/s12155-008-9024-8.

- Kleijnen, J.P.C., B. Bettonvil, and W. Van Groenendaal. 1998. Validation of trace-driven simulation models: A novel regression test. *Manage. Sci.* 44:812–819. doi:10.1287/mnsc.44.6.812, accessed 11 Jun. 2018.
- Kochsiek, A.E. and J.M.H. Knops. 2012. Maize cellulosic biofuels: Soil carbon loss can be a hidden cost of residue removal. *GCB Bioenergy.* 4:229–233. doi:10.1111/j.1757-1707.2011.01123.x, accessed 15 Feb. 2019.
- Koller, M. and W.A. Stahel. 2011. Sharpening Wald-type inference in robust regression for small samples. *Comput. Stat. Data. An.* 55:2504–2515. doi:https://doi.org/10.1016/j.csda.2011.02.014.
- Kort, J., M. Collins, and D. Ditsch. 1998. A review of soil erosion potential associated with biomass crops. *Biomass Bioenergy.* 14:351–359. doi:10.1016/S0961-9534(97)10071-X.
- Krohn, B. 2015. Switching to switchgrass: Pathways and consequences of bioenergy switchgrass entering the Midwestern landscape. Ph.D. dissertation, University of Minnesota, St. Paul, MN.
- Kuznetsova, A., P.B. Brockhoff, and R.H.B. Christensen. 2017. lmerTest package: Tests in linear mixed effects models. *J. Stat. Softw.* 82:1–26. doi:10.18637/jss.v082.i13.
- Lade, G.E., C.Y. Cynthia Lin Lawell, and A. Smith. 2018. Designing climate policy: Lessons from the Renewable Fuel Standard and the blend wall. *Am. J. Agr. Econ.* 100:585–599. doi:10.1093/ajae/aax092.
- Landis, D.A., C. Gratton, R.D. Jackson, K.L. Gross, D.S. Duncan, C. Liang, T.D. Meehan, B.A. Robertson, T.M. Schmidt, K.A. Stahlheber, J.M. Tiedje, and B.P. Werling. 2018. Biomass and biofuel crop effects on biodiversity and ecosystem services in the North Central US. *Biomass Bioenerg.* 114:18–29. doi:10.1016/j.biombioe.2017.02.003.

- Lane, D.M., D. Scott, M. Hebl, R. Guerra, D. Osherson, and H. Zimmer. 2019. Describing bivariate data. In: Introduction to statistics. Online edition., Rice University, University of Houston Clear Lake, Tufts University. <http://onlinestatbook.com/2/index.html>, accessed 16 Feb. 2019.
- Lane, J. 2017. Beta Renewables in cellulosic ethanol crisis, as Grupo M&G parent files for restructuring. Biofuels Digest. <https://www.biofuelsdigest.com/bdigest/2017/10/30/beta-renewables-in-cellulosic-ethanol-crisis-as-grupo-mg-parent-files-for-restructuring/>, accessed 29 Jan. 2019.
- Lark, T.J., M.J. Salmon, and H.K. Gibbs. 2015. Cropland expansion outpaces agricultural and biofuel policies in the United States. *Environ. Res. Lett.* 10:044003. doi:10.1088/1748-9326/10/4/044003.
- Lark, T.J., B. Larson, I. Schelly, S. Batish, and H.K. Gibbs. 2018. Accelerated conversion of native prairie to cropland in Minnesota. *Environ. Conserv.* pp. 1–8. doi:10.1017/S0376892918000437.
- Lazarus, W.F. 2011. Machinery cost estimates. University of Minnesota Extension Service, St. Paul, MN.
- Lazarus, W.F. 2012. Machinery cost estimates. University of Minnesota Extension Service, St. Paul, MN.
- Lazarus, W.F. 2013. Machinery cost estimates. University of Minnesota Extension Service, St. Paul, MN.
- Lazarus, W.F. 2014. Machinery cost estimates. University of Minnesota Extension Service, St. Paul, MN.
- Lazarus, W.F. 2015. Machinery cost estimates. University of Minnesota Extension Service, St. Paul, MN.

- Lazarus, W.F. and A. Smale. 2010. Machinery cost estimates. University of Minnesota Extension Service, St. Paul, MN.
- LeBauer, D., R. Kooper, P. Mulrooney, S. Rohde, D. Wang, S.P. Long, and M.C. Dietze. 2018. BETYdb: A yield, trait, and ecosystem service database applied to second-generation bioenergy feedstock production. *GCB Bioenergy*. 10:61–71. doi:10.1111/gcbb.12420, accessed 22 Mar. 2019.
- LeDuc, S.D., X. Zhang, C.M. Clark, and R.C. Izaurralde. 2017. Cellulosic feedstock production on Conservation Reserve Program land: Potential yields and environmental effects. *GCB Bioenergy*. 9:460–468. doi:10.1111/gcbb.12352, accessed 17 Feb. 2019.
- Lee, D.K. and A. Boe. 2005. Biomass production of switchgrass in central South Dakota. *Crop Sci*. 45:2583–2590. doi:10.2135/cropsci2005.04-0003.
- Lee, D.K., V.N. Owens, and J.J. Doolittle. 2007. Switchgrass and soil carbon sequestration response to ammonium nitrate, manure, and harvest frequency on Conservation Reserve Program land. *Agron. J.* 99:462–468. doi:10.2134/agronj2006.0152.
- Lefcheck, J.S. 2016. piecewiseSEM: Piecewise structural equation modeling in R for ecology, evolution, and systematics. *Methods Ecol. Evol.* 7:573–579. doi:10.1111/2041-210X.12512.
- Lemus, R., E. Charles Brummer, C. Lee Burras, K.J. Moore, M.F. Barker, and N.E. Molstad. 2008. Effects of nitrogen fertilization on biomass yield and quality in large fields of established switchgrass in southern Iowa, USA. *Biomass Bioenergy*. 32:1187–1194. doi:10.1016/j.biombioe.2008.02.016.
- Lewis, M.S. and M. Kelly. 2014. Mapping the potential for biofuel production on marginal lands: Differences in definitions, data and models across scales. *ISPRS Int. J. Geo-Inf.* 3:430–459. doi:10.3390/ijgi3020430.

- Liere, H., T.N. Kim, B.P. Werling, T.D. Meehan, D.A. Landis, and C. Gratton. 2015. Trophic cascades in agricultural landscapes: Indirect effects of landscape composition on crop yield. *Ecol. Appl.* 25:652–661. doi:10.1890/14-0570.1, accessed 17 Feb. 2019.
- Linden, D.R., C.E. Clapp, and R.H. Dowdy. 2000. Long-term corn grain and stover yields as a function of tillage and residue removal in east central Minnesota. *Soil Tillage Res.* 56:167–174.
- Lutt, N., M. Jeschke, and S.D. Strachan. 2016. High night temperature effects on corn yield. *Crop Insights* Vol. 26, No. 16, DuPont Pioneer Agronomy Sciences, Johnston, IA.
- Ma, Z., C. Wood, and D. Bransby. 2001. Impact of row spacing, nitrogen rate, and time on carbon partitioning of switchgrass. *Biomass Bioenergy.* 20:413–419. doi:10.1016/S0961-9534(01)00008-3.
- Mabee, W., P. McFarlane, and J. Saddler. 2011. Biomass availability for lignocellulosic ethanol production. *Biomass Bioenerg.* 35:4519–4529. doi:10.1016/j.biombioe.2011.06.026.
- Madakadze, I.C., B.E. Coulman, P. Peterson, K.A. Stewart, R. Samson, and D.L. Smith. 1998a. Leaf area development, light interception, and yield among switchgrass populations in a short-season area. *Crop Sci.* 38:827–834. doi:10.2135/cropsci1998.0011183X003800030035x.
- Madakadze, I.C., K. Stewart, P.R. Peterson, B.E. Coulman, R. Samson, and D.L. Smith. 1998b. Light interception, use-efficiency and energy yield of switchgrass (*Panicum virgatum* L.) grown in a short season area. *Biomass Bioenergy.* 15:475–482. doi:10.1016/S0961-9534(98)00060-9.
- Madakadze, I.C., K. Stewart, P.R. Peterson, B.E. Coulman, and D.L. Smith. 1999a. Switchgrass biomass and chemical composition for biofuel in eastern Canada. *Agron. J.* 91:696–701. doi:10.2134/agronj1999.914696x.

- Madakadze, I.C., K.A. Stewart, P.R. Peterson, B.E. Coulman, and D.L. Smith. 1999b. Cutting frequency and nitrogen fertilization effects on yield and nitrogen concentration of switchgrass in a short season area. *Crop Sci.* 39:552–557. doi:10.2135/cropsci1999.0011183X003900020041x.
- Madakadze, I.C., K.A. Stewart, R.M. Madakadze, and D.L. Smith. 2003. Base temperatures for seedling growth and their correlation with chilling sensitivity for warm-season grasses. *Crop Sci.* 43:874–878. doi:10.2135/cropsci2003.8740.
- Maechler, M., P. Rousseeuw, C. Croux, V. Todorov, A. Ruckstuhl, M. Salibian-Barrera, T. Verbeke, M. Koller, E.L.T. Conceicao, and M.A. di Palma. 2018. *robustbase: Basic robust statistics*. R package version 0.93-0. R Foundation for Statistical Computing, Vienna, AT. <http://robustbase.r-forge.r-project.org/>, accessed 27 Mar. 2019.
- Maniatis, K., I. Landälv, L. Waldheim, E. van den Heuvel, and S. Kalligeros. 2017. Building up the future: Technology status and reliability of the value chains. European Commission, Sub Group on Advanced Biofuels, Brussels, BE. <https://publications.europa.eu/en/publication-detail/-/publication/f1c977d1-67a4-11e8-ab9c-01aa75ed71a1/language-en/format-PDF>, accessed 27 Mar. 2019.
- Maughan, M.W. 2011. Evaluation of switchgrass, *M. x giganteus*, and sorghum as biomass crops: Effects of environment and field management practices. Ph.D. dissertation, University of Illinois, Urbana-Champaign.
- Maung, T.A. and C.R. Gustafson. 2013. Economic impact of harvesting corn stover under time constraint: The case of North Dakota. *Econ. Res. Intl.* 2013:321051. doi:10.1155/2013/321051.
- Maung, T.A., C.R. Gustafson, D.M. Saxowsky, T. Miljkovic, and J.F. Nowatzki. 2012. Market information on sourcing cellulosic feedstock for biofuel production in Northern Plains region of the United States. *J. Agric. Sci. Technol.* 2:10.

- McGranahan, A.D. 2014. Ecologies of scale: Multifunctionality connects conservation and agriculture across fields, farms, and landscapes. *Land*. 3:739–769. doi:10.3390/land3030739.
- McGuire, B. and S. Rupp. 2013. Perennial herbaceous biomass production and harvest in the Prairie Pothole Region of the northern Great Plains: Best management guidelines to achieve sustainability of wildlife resources. National Wildlife Federation, Washington, DC. <https://www.nwf.org/~media/PDFs/Wildlife/BiomassBMGPPR.pdf>, accessed 27 Mar. 2019.
- McIntyre, N.E. and T.R. Thompson. 2003. A comparison of Conservation Reserve Program habitat plantings with respect to arthropod prey for grassland birds. *Am. Midl. Nat.* 150:291–302. doi:10.1674/0003-0031(2003)150[0291:ACOCR2.0.CO;2.
- McIsaac, G.F., M.B. David, and C.A. Mitchell. 2010. Miscanthus and switchgrass production in central Illinois: Impacts on hydrology and inorganic nitrogen leaching. *J. Environ. Qual.* 39:1790–1799. doi:10.2134/jeq2009.0497.
- McLaughlin, S.B., J.R. Kiniry, C.M. Taliaferro, and D. De La Torre Ugarte. 2006. Projecting yield and utilization potential of switchgrass as an energy crop. *Adv. Agron.* 90:267–297. doi:10.1016/S0065-2113(06)90007-8.
- McMinimy, M.A. 2015. Biomass Crop Assistance Program (BCAP): Status and issues. Tech. Rep. R41296, Congressional Research Service, Washington, DC.
- Meehan, T.D., A.H. Hurlbert, and C. Gratton. 2010. Bird communities in future bioenergy landscapes of the Upper Midwest. *Proc. Natl. Acad. Sci. USA.* 107:18533. doi:10.1073/pnas.1008475107.
- Meehan, T.D., B.P. Werling, D.A. Landis, and C. Gratton. 2011. Agricultural landscape simplification and insecticide use in the midwestern United States. *Proc. Natl. Acad. Sci. USA.* 108:11500. doi:10.1073/pnas.1100751108.

- Miao, R., D.A. Hennessy, and H. Feng. 2016. The effects of crop insurance subsidies and Sodsaver on land use change. *J. Agr. Resour. Econ.* 41:247–265.
- Miesel, J.R., L.C. Jach-Smith, M.J. Renz, and R.D. Jackson. 2017. Distribution of switchgrass (*Panicum virgatum* L.) aboveground biomass in response to nitrogen addition and across harvest dates. *Biomass Bioenergy.* 100:74–83. doi:10.1016/j.biombioe.2017.03.012.
- Miguez, F.E., X. Zhu, S. Humphries, G.A. Bollero, and S.P. Long. 2009. A semimechanistic model predicting the growth and production of the bioenergy crop *Miscanthus × giganteus*: description, parameterization and validation. *GCB Bioenergy.* 1:282–296. doi:10.1111/j.1757-1707.2009.01019.x, accessed 23 Mar. 2019.
- Miguez, F.E., M. Maughan, G.A. Bollero, and S.P. Long. 2012. Modeling spatial and dynamic variation in growth, yield, and yield stability of the bioenergy crops *Miscanthus × giganteus* and *Panicum virgatum* across the conterminous United States. *GCB Bioenergy.* 4:509–520. doi:10.1111/j.1757-1707.2011.01150.x, accessed 22 Mar. 2019.
- Mitchell, R., K.P. Vogel, and D.R. Uden. 2012. The feasibility of switchgrass for biofuel production. *Biofuels.* 3:47–59. doi:10.4155/bfs.11.153.
- Mitchell, R., D. Lee, and M. Casler. 2014. Switchgrass. In: *Cellulosic energy cropping systems*, Wiley-Blackwell, pp. 75–89. doi:10.1002/9781118676332.ch5. <https://onlinelibrary.wiley.com/doi/abs/10.1002/9781118676332.ch5>.
- Mitchell, R., K. Vogel, and M. Schmer. 2015. Switchgrass (*Panicum virgatum*) for biofuel production. *Extension Publications.* <http://www.extension.org/pages/26635/switchgrass-panicum-virgatum-for-biofuel-production>, accessed 9 Jun. 2018.
- Mitchell, R.B., M.R. Schmer, W.F. Anderson, V. Jin, K.S. Balkcom, J. Kiniry, A. Coffin, and P. White. 2016. Dedicated energy crops and crop residues for bioenergy feedstocks in the central and eastern USA. *BioEnergy Res.* 9:384–398. doi:10.1007/s12155-016-9734-2.

- MN Interagency Work Group. 2014. The Minnesota Nutrient Reduction Strategy. Minnesota Interagency Work Group, St. Paul, MN. <https://www.pca.state.mn.us/sites/default/files/wq-s1-80.pdf>, accessed 17 Feb. 2019.
- Monsi, M. and T. Saeki. 1953. On the factor light in plant communities and its importance for matter production. (In German). *Japan J. Bot.* 14:22–52.
- Mooney, D.F., B.L. Barham, and C. Lian. 2015. Inelastic and fragmented farm supply response for second-generation bioenergy feedstocks: *Ex ante* survey evidence from Wisconsin. *Appl. Econ. Perspect.* P. 37:287–310. doi:10.1093/aapp/ppu033, accessed 22 Mar. 2019.
- Moore, K.J., S. Birrell, R.C. Brown, M.D. Casler, J.E. Euken, H.M. Hanna, D.J. Hayes, J.D. Hill, K.L. Jacobs, C.L. Kling, D. Laird, R.B. Mitchell, P.T. Murphy, D.R. Raman, C.V. Schwab, K.J. Shinnars, K.P. Vogel, and J.J. Volenec. 2014. Midwest vision for sustainable fuel production. *Biofuels.* 5:687–702. doi:10.1080/17597269.2015.1015312.
- Morefield, P.E., S.D. LeDuc, C.M. Clark, and R. Iovanna. 2016. Grasslands, wetlands, and agriculture: The fate of land expiring from the Conservation Reserve Program in the midwestern United States. *Environ. Res. Lett.* 11:094005. doi:10.1088/1748-9326/11/9/094005.
- Moriasi, D., J. Arnold, M. Van Liew, R. Bingner, R. Harmel, and T. Veith. 2007. Model evaluation guidelines for systematic quantification of accuracy in watershed simulations. *T. ASABE.* 50:885. doi:10.13031/2013.23153.
- Moulin, A.P. and H.J. Beckie. 1993. Evaluation of the CERES and EPIC models for predicting spring wheat grain yield over time. *Can. J. Plant Sci.* 73:713–719. doi:10.4141/cjps93-093, accessed 8 Aug. 2018.
- Moulin, S., A. Bondeau, and R. Delecolle. 1998. Combining agricultural crop models and satellite observations: From field to regional scales. *Int. J. Remote Sens.* 19:1021–1036. doi:10.1080/014311698215586.

- Muir, J.P., M.A. Sanderson, W.R. Ocumpaugh, R.M. Jones, and R.L. Reed. 2001. Biomass production of 'Alamo' switchgrass in response to nitrogen, phosphorus, and row spacing. *Agron. J.* 93:896–901. doi:10.2134/agronj2001.934896x.
- Mukhala, E. and P. Hoefsloot. 2004. AgroMetShell. Agrometeorology Group, Environment and Natural Resources Service, Food and Agricultural Organization of the United Nations, Rome, Italy. http://www.fao.org/nr/climpag/aw_6.en.asp, accessed 8 Aug. 2018.
- Mulkey, V.R., V.N. Owens, and D.K. Lee. 2006. Management of switchgrass-dominated Conservation Reserve Program lands for biomass production in South Dakota. *Crop Sci.* 46:712–720. doi:10.2135/cropsci2005.04-0007.
- Muth, D. and K. Bryden. 2013. An integrated model for assessment of sustainable agricultural residue removal limits for bioenergy systems. *Environ. Modell. Softw.* 39:50–69. doi:10.1016/j.envsoft.2012.04.006.
- Muth, D.J., D.S. McCorkle, J.B. Koch, and K.M. Bryden. 2012. Modeling sustainable agricultural residue removal at the subfield scale. *Agron. J.* 104:970–981. doi:10.2134/agronj2012.0024.
- Muth, D.J., K.M. Bryden, and R.G. Nelson. 2013. Sustainable agricultural residue removal for bioenergy: A spatially comprehensive US national assessment. *Appl. Energy.* 102:403–417.
- Naeve, S.L. 2009. Soybean seeding rates in Minnesota. University of Minnesota Extension Service, St. Paul, MN. <https://extension.umn.edu/soybean-planting/soybean-seeding-rates-minnesota>, accessed 27 Mar. 2019.
- NCDC. 2005. Probability levels for 1971-2000 freeze dates and growing season lengths. Data Set 9641C, National Climatic Data Center, Asheville, NC.
- NDSU. 2016. 2016 North Dakota custom rates part II – late season operations. North Dakota State University Experiment Station and Extension Service, Fargo, ND. <https://www.ag>

- .ndsu.edu/logancountyextension/quick-references/custom-rates-late-season-2016, accessed 27 Mar. 2019.
- Neild, R.E. and J.E. Newman. 1990. Growing season characteristics and requirements in the Corn Belt. Tech. Rep. NCH-40, University of Nebraska and Purdue University, Lincoln, NE and West Lafayette, IN.
- Newman, Y., M.J. Williams, Z. Hessel, and J. Vendramini. 2014. Production of biofuel crops in Florida: Switchgrass. Tech. Rep. SS AGR 291, University of Florida Institute of Food and Agricultural Sciences and Extension, Gainesville, FL.
- Norton, J. 2015. An introduction to sensitivity assessment of simulation models. *Environ. Modell. Softw.* 69:166–174. doi:10.1016/j.envsoft.2015.03.020.
- Norwood, C.A. 2001. Planting date, hybrid maturity, and plant population effects on soil water depletion, water use, and yield of dryland corn. *Agron. J.* 93:1034–1042.
- Nyakatawa, E., D. Mays, V. Tolbert, T. Green, and L. Bingham. 2006. Runoff, sediment, nitrogen, and phosphorus losses from agricultural land converted to sweetgum and switchgrass bioenergy feedstock production in north Alabama. *Biomass Bioenergy.* 30:655–664. doi:10.1016/j.biombioe.2006.01.008.
- Omonode, R.A. and T.J. Vyn. 2006. Vertical distribution of soil organic carbon and nitrogen under warm-season native grasses relative to croplands in west-central Indiana, USA. *Agr. Ecosyst. Environ.* 117:159–170. doi:10.1016/j.agee.2006.03.031.
- Ou, L., T.R. Brown, R. Thilakaratne, G. Hu, and R.C. Brown. 2014. Techno-economic analysis of co-located corn grain and corn stover ethanol plants. *Biofuel. Bioprod. Bior.* 8:412–422. doi:10.1002/bbb.1475, accessed 21 Mar. 2019.
- Parrish, D.J. and J.H. Fike. 2005. The biology and agronomy of switchgrass for biofuels. *Crit. Rev. Plant Sci.* 24:423–459. doi:10.1080/07352680500316433.

- Parton, W.J., M. Hartman, D. Ojima, and D. Schimel. 1998. DAYCENT and its land surface submodel: Description and testing. *Global Planet. Change.* 19:35–48. doi:10.1016/S0921-8181(98)00040-X.
- Perlack, R.D., L.L. Wright, A.F. Turhollow, R.L. Graham, B.J. Stokes, and D.C. Erbach. 2005. Biomass as feedstock for a bioenergy and bioproducts industry: The technical feasibility of a billion-ton annual supply. Tech. Rep. ORNL/TM-2005/66, Oak Ridge National Laboratory, Oak Ridge, TN.
- Perrin, R., K. Vogel, M. Schmer, and R. Mitchell. 2008. Farm-scale production cost of switchgrass for biomass. *BioEnergy Res.* 1:91–97. doi:10.1007/s12155-008-9005-y.
- Petrolia, D.R. 2006. Ethanol from biomass: Economic and environmental potential of converting corn stover and hardwood forest residue in Minnesota. Paper presented at: American Agricultural Economics Association Annual Meeting. Long Beach, CA. 23–26 Jul.
- Petrolia, D.R. 2008. The economics of harvesting and transporting corn stover for conversion to fuel ethanol: A case study for Minnesota. *Biomass Bioenergy.* 32:603–612. doi:10.1016/j.biombioe.2007.12.012.
- Pham, X. and M. Stack. 2018. How data analytics is transforming agriculture. *Bus. Horizons.* 61:125–133. doi:10.1016/j.bushor.2017.09.011.
- Pianosi, F., K. Beven, J. Freer, J.W. Hall, J. Rougier, D.B. Stephenson, and T. Wagener. 2016. Sensitivity analysis of environmental models: A systematic review with practical workflow. *Environ. Modell. Softw.* 79:214–232. doi:10.1016/j.envsoft.2016.02.008.
- Plastina, A., A. Johanns, and S. Weets. 2015. 2015 Iowa farm custom rate survey. Ag Decision Maker A3-10, Iowa State University Extension, Ames, IA.

- POET-DSM. 2014. POET-DSM to hold Project LIBERTY grand opening celebration. Press Release. <http://poet-dsm.com/pr/poet-dsm-to-hold-project-liberty-grand-opening>, accessed 29 Jan. 2019.
- POET-DSM. 2015. Seeing the world differently. Sioux Falls, SD. <http://poetdsm.com/resources/docs/POET-DSM-Brochure.pdf>, accessed 16 Feb. 2019.
- POET-DSM. 2017. POET-DSM achieves cellulosic ethanol breakthrough. Press Release. <http://poetdsm.com/pr/poet-dsm-achieves-cellulosic-biofuel-breakthrough>, accessed 29 Jan. 2019.
- POET-DSM. 2018. POET Biorefining Emmetsburg, Iowa Tier 2 application corn kernel fiber to cellulosic ethanol pathway (FPC Code: ETHCF204). Tech. Rep. T2N-1266, California Air Resources Board, Sacramento, CA.
- Powers, S.E., J.C. Ascough II, R.G. Nelson, and G.R. Larocque. 2011. Modeling water and soil quality environmental impacts associated with bioenergy crop production and biomass removal in the Midwest USA. *Ecol. Model.* 222:2430–2447. doi:10.1016/j.ecolmodel.2011.02.024.
- Powlson, D.S., M.J. Glendining, K. Coleman, and A.P. Whitmore. 2011. Implications for soil properties of removing cereal straw: Results from long-term studies. *Agron. J.* 103:279–287. doi:10.2134/agronj2010.0146s.
- PRISM Climate Group. 2019. 30-year normals. Oregon State University, Northwest Alliance for Computational Science and Engineering, Corvallis, OR. <http://prism.oregonstate.edu/normals/>, accessed 17 Feb. 2019.
- QGIS Development Team. 2018. QGIS geographic information system. Open Source Geospatial Foundation Project, Beaverton, OR. <http://qgis.osgeo.org/>, accessed 8 Aug. 2018.

- Qian, L., Z. Luo, Y. Du, and L. Guo. 2009. Cloud computing: An overview. In: Cloud computing. CloudCom 2009. Lecture notes in computer science, vol 5931, editors M. Jaatun, G. Zhao, and C. Rong, Springer, Berlin, Heidelberg, pp. 626–631.
- Qin, Z., Q. Zhuang, and X. Cai. 2015. Bioenergy crop productivity and potential climate change mitigation from marginal lands in the United States: An ecosystem modeling perspective. *GCB Bioenergy*. 7:1211–1221. doi:10.1111/gcbb.12212, accessed 22 Mar. 2019.
- Qin, Z., J.B. Dunn, H. Kwon, S. Mueller, and M.M. Wander. 2016a. Influence of spatially dependent, modeled soil carbon emission factors on life-cycle greenhouse gas emissions of corn and cellulosic ethanol. *GCB Bioenergy*. 8:1136–1149. doi:10.1111/gcbb.12333, accessed 22 Mar. 2019.
- Qin, Z., J.B. Dunn, H. Kwon, S. Mueller, and M.M. Wander. 2016b. Soil carbon sequestration and land use change associated with biofuel production: Empirical evidence. *GCB Bioenergy*. 8:66–80. doi:10.1111/gcbb.12237, accessed 22 Mar. 2019.
- R Core Team. 2018. R: A language and environment for statistical computing. R Foundation for Statistical Computing, Vienna, AT. <https://www.R-project.org/>, accessed 8 Aug. 2018.
- Ransom, J.K., D.W. Franzen, P. Glogoza, K. Hellevang, V. Hofman, M. McMullen, and R. Zollinger. 2004. Basics of corn production in North Dakota. Tech. Rep. A834, NDSU Extension Service, Fargo, ND.
- Rehm, G., G. Randall, J. Lamb, and R. Eliason. 2006. Fertilizing corn in Minnesota. Tech. Rep. FO-3790-C, University of Minnesota Extension Service, St. Paul, MN.
- Reitsma, K.D., T.E. Schumacher, V.N. Owens, D.E. Clay, A. Boe, and P.J. Johnson. 2011. Switchgrass management & production in South Dakota. Tech. Rep. 03-2006-2011, South Dakota State University Extension, Brookings, SD.

- Retka Schill, S. 2018. Zero to 10 million in 5 years. *Ethanol Producer Magazine*. <http://www.ethanolproducer.com/articles/15344/zero-to-10-million-in-5-years>, accessed 29 Jan. 2019.
- Reynolds, R.E., T.L. Shaffer, C.R. Loesch, and R.R. Cox Jr. 2006. The Farm Bill and duck production in the Prairie Pothole Region: Increasing the benefits. *Wildlife Soc. B.* 34:963–974. doi:10.2193/0091-7648(2006)34[963:TFBADP]2.0.CO;2, accessed 17 Feb. 2019.
- Reynolds, R.E., C.R. Loesch, B. Wangler, and T.L. Shaffer. 2007. Waterfowl response to the Conservation Reserve Program and Swampbuster Provision in the Prairie Pothole Region, 1992–2004. Reimbursable Funds Agreement 05-IA-04000000-N34, US Fish and Wildlife Service, US Geological Survey, Bismarck, ND, Jamestown, ND.
- Richards, B.K., C.R. Stoof, I.J. Cary, and P.B. Woodbury. 2014. Reporting on marginal lands for bioenergy feedstock production: A modest proposal. *BioEnergy Res.* 7:1060–1062. doi:10.1007/s12155-014-9408-x.
- Robertson, B.A., P.J. Doran, E.R. Loomis, J.R. Robertson, and D.W. Schemske. 2011a. Avian use of perennial biomass feedstocks as post-breeding and migratory stopover habitat. *PloS ONE.* 6:e16941. doi:10.1371/journal.pone.0016941.
- Robertson, B.A., P.J. Doran, L.R. Loomis, J.R. Robertson, and D.W. Schemske. 2011b. Perennial biomass feedstocks enhance avian diversity. *GCB Bioenergy.* 3:235–246. doi:10.1111/j.1757-1707.2010.01080.x.
- Robertson, G.P., S.K. Hamilton, B.L. Barham, B.E. Dale, R.C. Izaurralde, R.D. Jackson, D.A. Landis, S.M. Swinton, K.D. Thelen, and J.M. Tiedje. 2017. Cellulosic biofuel contributions to a sustainable energy future: Choices and outcomes. *Science.* 356:eaal2324. doi:10.1126/science.aal2324.
- Robertson, P.G., S.K. Hamilton, S.J. Del Grosso, and W.J. Parton. 2011c. The biogeochemistry of bioenergy landscapes: Carbon, nitrogen, and water considerations. *Ecol. Appl.* 21:1055–1067. doi:10.1890/09-0456.1, accessed 8 Jun. 2018.

- Samson, F.B., F.L. Knopf, and W.R. Ostlie. 1998. Grasslands. In: Status and trends of the nation's biological resources, vol. 2, editors M.J. Mac, P.A. Opler, C.E. Haecker, and P.D. Doran, USGS Northern Prairie Wildlife Research Center, Jamestown, ND, pp. 437–472.
- Samson, F.B., F.L. Knopf, and W.R. Ostlie. 2004. Great Plains ecosystems: Past, present, and future. *Wildlife Soc. B.* 32:6–15. doi:10.2193/0091-7648(2004)32[6:GPEPPA]2.0.CO;2, accessed 17 Feb. 2019.
- Sanderson, M., R. Reed, S. McLaughlin, S. Wullschleger, B. Conger, D. Parrish, D. Wolf, C. Taliaferro, A. Hopkins, W. Ocumpaugh, M. Hussey, J. Read, and C. Tischler. 1996. Switchgrass as a sustainable bioenergy crop. *Bioresour. Technol.* 56:83–93. doi:10.1016/0960-8524(95)00176-X.
- Sanderson, M., R. Reed, W. Ocumpaugh, M. Hussey, G. Van Esbroeck, J. Read, C. Tischler, and F. Hons. 1999. Switchgrass cultivars and germplasm for biomass feedstock production in Texas. *Bioresour. Technol.* 67:209–219. doi:10.1016/S0960-8524(98)00132-1.
- Sapp, M. 2017. POET-DSM's Project Liberty reaching production goals. *Biofuels Digest*. <http://www.biofuelsdigest.com/bdigest/2017/04/12/poet-dsms-project-liberty-reaching-production-goals/>, accessed 10 Jan. 2019.
- Sawyer, J., E. Nafziger, G. Randall, L. Bundy, G. Rehm, and B. Joern. 2006. Concepts and rationale for regional nitrogen rate guidelines for corn. Tech. Rep. PM 2015, Iowa State University Extension, Ames, IA.
- Saxton, K. and W. Rawls. 2006. Soil water characteristic estimates by texture and organic matter for hydrologic solutions. *Soil Sci. Soc. Am. J.* 70:1569–1578. doi:10.2136/sssaj2005.0117.
- Saxton, K.E., W.J. Rawls, J.S. Romberger, and R.I. Papendick. 1986. Estimating generalized soil-water characteristics from texture. *Soil Sci. Soc. Am. J.* 50:1031–1036. doi:10.2136/sssaj1986.03615995005000040039x.

- Schmer, M.R., K.P. Vogel, R.B. Mitchell, L.E. Moser, K.M. Eskridge, and R.K. Perrin. 2006. Establishment stand thresholds for switchgrass grown as a bioenergy crop. *Crop Sci.* 46:157–161. doi:10.2135/cropsci2005.0264.
- Schmer, M.R., K.P. Vogel, R.B. Mitchell, and R.K. Perrin. 2008. Net energy of cellulosic ethanol from switchgrass. *Proc. Natl. Acad. Sci. USA.* 105:464. doi:10.1073/pnas.0704767105.
- Sentinel Hub. 2019. NDVI (Normalized Difference Vegetation Index). <https://www.sentinel-hub.com/eoproducts/ndvi-normalized-difference-vegetation-index>, accessed 8 Mar. 2019.
- Shankle, M.W. and T.F. Garrett. 2014. Switchgrass production as a bioenergy crop in Mississippi. Bulletin 1210, Mississippi State University Agricultural and Forestry Experiment Station.
- Sharpley, A.N. and J.R. Williams. 1990. EPIC-Erosion/Productivity Impact Calculator: 1. Model documentation. Technical Bulletin Number 1768, United States Department of Agriculture, Washington, DC.
- Sharpley, A.N., C.A. Jones, C. Gray, and C.V. Cole. 1984. A simplified soil and plant phosphorus model: II. Prediction of labile, organic, and sorbed phosphorus. *Soil Sci. Soc. Am. J.* 48:805–809.
- Shortall, O. 2013. “Marginal land” for energy crops: Exploring definitions and embedded assumptions. *Energy Policy.* 62:19–27. doi:10.1016/j.enpol.2013.07.048.
- Sinclair, T. and R. Muchow. 1999a. Occam’s Razor, radiation-use efficiency, and vapor pressure deficit. *Field Crop. Res.* 62:239–243. doi:10.1016/S0378-4290(99)00011-8.
- Sinclair, T.R. and R.C. Muchow. 1999b. Radiation use efficiency. *Adv. Agron.* 65:215–265. doi:10.1016/S0065-2113(08)60914-1.

- Skevas, T., N.J. Hayden, S.M. Swinton, and F. Lupi. 2016. Landowner willingness to supply marginal land for bioenergy production. *Land Use Policy*. 50:507–517. doi:10.1016/j.landusepol.2015.09.027.
- Skevas, T., I. Skevas, and S.M. Swinton. 2018. Does spatial dependence affect the intention to make land available for bioenergy crops? *J. Agr. Econ.* 69:393–412. doi:10.1111/1477-9552.12233, accessed 22 Mar. 2019.
- Sleeter, B.M., T.L. Sohl, T.R. Loveland, R.F. Auch, W. Acevedo, M.A. Drummond, K.L. Saylor, and S.V. Stehman. 2013. Land-cover change in the conterminous United States from 1973 to 2000. *Global Environ. Chang.* 23:733–748. doi:10.1016/j.gloenvcha.2013.03.006.
- Smith, C.M., M.B. David, C.A. Mitchell, M.D. Masters, K.J. Anderson-Teixeira, C.J. Bernacchi, and E.H. DeLucia. 2013. Reduced nitrogen losses after conversion of row crop agriculture to perennial biofuel crops. *J. Environ. Qual.* 42:219–228. doi:10.2134/jeq2012.0210.
- Smith, P. 2014. Do grasslands act as a perpetual sink for carbon? *Glob. Change Biol.* 20:2708–2711. doi:10.1111/gcb.12561, accessed 17 Feb. 2019.
- Sobota, D.J., J.E. Compton, M.L. McCrackin, and S. Singh. 2015. Cost of reactive nitrogen release from human activities to the environment in the United States. *Environ. Res. Lett.* 10:025006. doi:10.1088/1748-9326/10/2/025006.
- Soil Survey Staff. 2013. Soil Survey Geographic (SSURGO) Database. USDA Natural Resources Conservation Service, Washington, DC. <https://websoilsurvey.sc.egov.usda.gov/>, accessed 20 Mar. 2013.
- Soil Survey Staff. 2018. Web Soil Survey. USDA Natural Resources Conservation Service, Washington, DC. <https://websoilsurvey.sc.egov.usda.gov/>, accessed 8 Aug. 2018.

- Spatial Reference. 2018. ESRI projection 102003 - USA contiguous Albers equal area conic. <http://spatialreference.org/ref/esri/usa-contiguous-albers-equal-area-conic/>, accessed 8 Aug. 2018.
- Spiess, A.N. 2018. propagate: Propagation of Uncertainty. R package version 1.0-6. R Foundation for Statistical Computing, Vienna, AT. <https://CRAN.R-project.org/package=propagate>, accessed 27 Mar. 2019.
- St. Arnaud, R. and G. Sephton. 1972. Contribution of clay and organic matter to cation-exchange capacity of Chernozemic soils. *Can. J. Soil Sci.* 52:124–126.
- Stahl, L., J. Coulter, and D. Bau. 2009. Narrow-row corn production in Minnesota. University of Minnesota Extension Service, St. Paul, MN. <http://www.extension.umn.edu/agriculture/corn/planting/narrow-row-corn-production/>, accessed 8 May 2015.
- State of Minnesota. 2019. Minnesota Buffer Law. <https://mn.gov/portal/buffer-law/>, accessed 23 Mar. 2019.
- Stine Seed Company. 2015. Corn maturity zones. <http://www.stinseed.com/>, accessed 11 Jun. 2018.
- Stockle, C.O. and J.R. Kiniry. 1990. Variability in crop radiation-use efficiency associated with vapor-pressure deficit. *Field Crop. Res.* 25:171–181. doi:10.1016/0378-4290(90)90001-R.
- Stokes, L.C. and H.L. Breetz. 2018. Politics in the U.S. energy transition: Case studies of solar, wind, biofuels and electric vehicles policy. *Energy Policy.* 113:76–86. doi:10.1016/j.enpol.2017.10.057.
- Stoll, M. and I. Saab. 2016. Soil temperature and corn emergence. *Crop Insights* Vol. 23, No. 1, DuPont Pioneer Agronomy Sciences, Johnston, IA.
- Stone, R.P. and D. Hilborn. 2012. Universal Soil Loss Equation (USLE). Tech. Rep. 12-051, Ontario Ministry of Agriculture, Food and Rural Affairs, Guelph, ON.

- Swinton, S.M., S. Tanner, B.L. Barham, D.F. Mooney, and T. Skevas. 2017. How willing are landowners to supply land for bioenergy crops in the northern Great Lakes region? *GCB Bioenergy*. 9:414–428. doi:10.1111/gcbb.12336, accessed 22 Mar. 2019.
- Tan, Z., S. Liu, N. Bliss, and L.L. Tieszen. 2012. Current and potential sustainable corn stover feedstock for biofuel production in the United States. *Biomass Bioenergy*. 47:372–386. doi:10.1016/j.biombioe.2012.09.022.
- Tapco Inc. 2019. Bulk material density table. https://www.tapcoinc.com/images/uploads/Tapco_Catalog_09_p88-94.pdf, accessed 17 Feb. 2019.
- Tarkalson, D.D., B. Brown, H. Kok, and D.L. Bjorneberg. 2011. Small grain residue management effects on soil organic carbon: A literature review. *Agron. J.* 103:247–252. doi:10.2134/agronj2010.0147s.
- Teel, A., S. Barnhart, and G. Miller. 2003. Management guide for the production of switchgrass for biomass fuel in southern Iowa. Tech. Rep. PM 1710, Iowa State University Extension, Ames, IA.
- Thomson, A.M., R.C. Izaurralde, T.O. West, D.J. Parrish, D.D. Tyler, and J.R. Williams. 2009. Simulating potential switchgrass production in the United States. Tech. Rep. PNNL-19072, United States Department of Energy Pacific Northwest National Laboratory, Richland, WA.
- Thornton, P., J. Dent, and Z. Bacsı. 1991. A framework for crop growth simulation model applications. *Agr. Sys.* 37:327–340. doi:10.1016/0308-521X(91)90056-G.
- Tilman, D., R. Socolow, J.A. Foley, J. Hill, E. Larson, L. Lynd, S. Pacala, J. Reilly, T. Searchinger, C. Somerville, and R. Williams. 2009. Beneficial biofuels—the food, energy, and environment trilemma. *Science*. 325:270. doi:10.1126/science.1177970.
- Timmons, D.S. 2012. Estimating a technically feasible switchgrass supply function: A western Massachusetts example. *BioEnergy Res.* 5:236–246. doi:10.1007/s12155-011-9136-4.

- Tober, D., W. Duckwitz, N. Jensen, and M. Knudson. 2007. Switchgrass biomass trials in North Dakota, South Dakota, and Minnesota. United States Department of Agriculture Natural Resources Conservation Service, Bismarck, ND. https://www.nrcs.usda.gov/Internet/FSE_PLANTMATERIALS/publications/ndpmcpu7093.pdf, accessed 28 Mar. 2019.
- Tol, R.S. 2011. The social cost of carbon: Trends, outliers and catastrophes. Tech. Rep. 377, The Economic and Social Research Institute, Dublin, IE.
- Touré, A., D.J. Major, and C.W. Lindwall. 1995. Comparison of five wheat simulation models in southern Alberta. *Can. J. Plant Sci.* 75:61–68. doi:10.4141/cjps95-010, accessed 8 Aug. 2018.
- Tufte, E. 2001. Chapter 6: Data-ink maximization and graphical design. In: *The visual display of quantitative information*, Graphics Press, Cheshire, CT, pp. 123–137. 2nd ed.
- Tyndall, J.C., E.J. Berg, and J.P. Colletti. 2011. Corn stover as a biofuel feedstock in Iowa's bio-economy: An Iowa farmer survey. *Biomass Bioenergy*. 35:1485–1495. doi:10.1016/j.biombioe.2010.08.049.
- Tyner, W.E. 2008. The US ethanol and biofuels boom: Its origins, current status, and future prospects. *BioScience*. 58:646–653. doi:10.1641/B580718, accessed 15 Feb. 2019.
- Uden, D.R., R.B. Mitchell, C.R. Allen, Q. Guan, and T.D. McCoy. 2013. The feasibility of producing adequate feedstock for year-round cellulosic ethanol production in an intensive agricultural fuelshed. *BioEnergy Res.* 6:930–938. doi:10.1007/s12155-013-9311-x.
- United States Interagency Working Group. 2016. Technical update of the social cost of carbon for regulatory impact analysis under Executive Order 12866. Interagency Working Group on Social Cost of Greenhouse Gases, United States Government, Washington, DC. https://www.epa.gov/sites/production/files/2016-12/documents/sc_co2_tsd_august_2016.pdf, accessed 17 Feb. 2019.

University of Idaho Climatology Lab. 2018. gridMET. <http://www.climatologylab.org/gridmet.html>, accessed 8 Aug. 2018.

University of Missouri. 2015. MU soybean gene zoo. <http://genezoo.missouri.edu/soybean.cfm>, accessed 8 Aug. 2018.

University of Nebraska-Lincoln NDMC, USDA, and NOAA. 2018. U.S. Drought Monitor. National Drought Mitigation Center, U.S. Department of Agriculture, National Oceanic and Atmospheric Association. <http://droughtmonitor.unl.edu/>, accessed 8 Aug. 2018.

U.S. Bureau of Economic Analysis. 2019. Gross Domestic Product: Chain-type Price Index [GDPCTPI]. FRED, Federal Reserve Bank of St. Louis, St. Louis, MO. <https://fred.stlouisfed.org/series/GDPCTPI>, accessed 17 Feb. 2019.

U.S. Department of Energy. 2011. US billion-ton update: Biomass supply for a bioenergy and bioproducts industry. Tech. Rep. ORNL/TM-2011/224, Oak Ridge National Laboratory, Oak Ridge, TN.

U.S. Department of Energy. 2016. 2016 Billion-ton report: Advancing domestic resources for a thriving bioeconomy, volume 1: Economic availability of feedstocks. Tech. Rep. ORNL/TM-2016/160, Oak Ridge National Lab (ORNL), Oak Ridge, TN.

U.S. Department of Energy. 2017. 2016 Billion-ton report: Advancing domestic resources for a thriving bioeconomy, volume 2: Environmental sustainability effects of select scenarios from volume 1. Tech. Rep. ORNL/TM-2016/72, Oak Ridge National Lab (ORNL), Oak Ridge, TN.

US DOE. 2014. Grand opening of Abengoa's biorefinery: Nation's third commercial-scale facility. US Department of Energy, Office of Energy Efficiency and Renewable Energy. <https://www.energy.gov/eere/bioenergy/articles/grand-opening-abengoa-s-biorefinery-nation-s-third-commercial-scale-facility>, accessed 29 Jan. 2019.

- US DOE. 2019. Fuel conversion factors to gasoline gallon equivalents. <https://epact.energy.gov/fuel-conversion-factors>, accessed 17 Feb. 2019.
- US EIA. 2019. State Energy Data System (SEDS): 1960-2016 (complete). US Energy Information Administration, Washington, DC. <https://www.eia.gov/state/seds/seds-data-complete.php>, accessed 17 Feb. 2019.
- US EPA. 2019. Public data for the Renewable Fuel Standard. US Environmental Protection Agency, Washington, DC. <https://www.epa.gov/fuels-registration-reporting-and-compliance-help/public-data-renewable-fuel-standard>, accessed 17 Feb. 2019.
- US NREL. 2019. The biofuels atlas. US National Renewable Energy Laboratory, Washington, DC. <https://maps.nrel.gov/biofuels-atlas>, accessed 17 Feb. 2019.
- USDA. 2016. U.S. agriculture and forestry greenhouse gas inventory: 1990–2013. Technical Bulletin No. 1943, United States Department of Agriculture, Office of the Chief Economist, Climate Change Program Office.
- USDA. 2018. Summary report: 2015 national resources inventory. Natural Resources Conservation Service and Center for Survey Statistics and Methodology, Washington, DC and Ames, IA. <http://www.nrcs.usda.gov/technical/nri/15summary>, accessed 17 Feb. 2019.
- USDA ARS. 2019a. NLET - National Load Estimating Tool. USDA Agricultural Research Service Grassland, Soil and Water Research Laboratory, Temple, TX. <https://nlet.brc.tamus.edu/>, accessed 17 Feb. 2019.
- USDA ARS. 2019b. SWIFT - Small Watershed Nutrient Forecasting Tool. USDA Agricultural Research Service Grassland, Soil and Water Research Laboratory, Temple, TX. <https://swift.brc.tamus.edu/Home/Index>, accessed 17 Feb. 2019.
- USDA ERS. 2000. Farm resource regions. Agricultural Information Bulletin 760, USDA Economic Research Service, Washington, DC.

- USDA ERS. 2009. Agriculture Resource Management Survey (ARMS). USDA Economic Research Service, Washington, DC. <https://www.ers.usda.gov/data-products/arms-farm-financial-and-crop-production-practices/arms-data/>, accessed 8 Aug. 2018.
- USDA ERS. 2010. Agriculture Resource Management Survey (ARMS). USDA Economic Research Service, Washington, DC. <https://www.ers.usda.gov/data-products/arms-farm-financial-and-crop-production-practices/arms-data/>, accessed 8 Aug. 2018.
- USDA ERS. 2015a. Commodity costs and returns. USDA Economic Research Service, Washington, D.C. <https://www.ers.usda.gov/data-products/commodity-costs-and-returns/>, accessed 8 Aug. 2018.
- USDA ERS. 2015b. Fertilizer use and price. USDA Economic Research Service, Washington, D.C. <https://www.ers.usda.gov/data-products/fertilizer-use-and-price.aspx>, accessed 8 Aug. 2018.
- USDA FSA. 2018. CRP enrollment and rental payments by state, 1986-2017. USDA Farm Service Agency, Washington, DC. <https://www.fsa.usda.gov/programs-and-services/conservation-programs/reports-and-statistics/conservation-reserve-program-statistics/index>, accessed 17 Feb. 2019.
- USDA NASS. 2006. Cropland Data Layer: Published crop-specific data layer. USDA National Agricultural Statistics Service, Washington, DC. <http://nassgeodata.gmu.edu/CropScape/>, accessed 8 Aug. 2018.
- USDA NASS. 2007. Cropland Data Layer: Published crop-specific data layer. USDA National Agricultural Statistics Service, Washington, DC. <http://nassgeodata.gmu.edu/CropScape/>, accessed 8 Aug. 2018.
- USDA NASS. 2008. Cropland Data Layer: Published crop-specific data layer. USDA National Agricultural Statistics Service, Washington, DC. <http://nassgeodata.gmu.edu/CropScape/>, accessed 8 Aug. 2018.

- USDA NASS. 2009. Cropland Data Layer: Published crop-specific data layer. USDA National Agricultural Statistics Service, Washington, DC. <http://nassgeodata.gmu.edu/CropScape/>, accessed 8 Aug. 2018.
- USDA NASS. 2010a. 2010 North Dakota custom rates part II – late season operations. USDA National Agricultural Statistics Service, North Dakota Field Office, Fargo, ND. https://www.nass.usda.gov/Statistics_by_State/North_Dakota/Publications/Cooperative_Projects/Custom_Rates/cuslate10.pdf, accessed 28 Mar. 2019.
- USDA NASS. 2010b. Cropland Data Layer: Published crop-specific data layer. USDA National Agricultural Statistics Service, Washington, DC. <http://nassgeodata.gmu.edu/CropScape/>, accessed 8 Aug. 2018.
- USDA NASS. 2012a. Census of agriculture. <https://quickstats.nass.usda.gov/>, accessed 8 Aug. 2018.
- USDA NASS. 2012b. Cropland Data Layer: Published crop-specific data layer. USDA National Agricultural Statistics Service, Washington, DC. <http://nassgeodata.gmu.edu/CropScape/>, accessed 8 Aug. 2018.
- USDA NASS. 2013. Cropland Data Layer: Published crop-specific data layer. USDA National Agricultural Statistics Service, Washington, DC. <http://nassgeodata.gmu.edu/CropScape/>, accessed 8 Aug. 2018.
- USDA NASS. 2014. Cropland Data Layer: Published crop-specific data layer. USDA National Agricultural Statistics Service, Washington, DC. <http://nassgeodata.gmu.edu/CropScape/>, accessed 8 Aug. 2018.
- USDA NASS. 2015a. Cropland Data Layer: Published crop-specific data layer. USDA National Agricultural Statistics Service, Washington, DC. <http://nassgeodata.gmu.edu/CropScape/>, accessed 8 Aug. 2018.

- USDA NASS. 2015b. Vegetation Condition Explorer: Published NDVI data layer. USDA National Agricultural Statistics Service, Washington, DC. <http://dss.csiss.gmu.edu/VegScale/>, accessed 8 Aug. 2018.
- USDA NASS. 2018. Quick Stats 2.0. <https://quickstats.nass.usda.gov/>, accessed 8 Aug. 2018.
- USDA NASS. 2019. District and county boundary maps by state. USDA National Agricultural Statistics Service, Washington, DC. https://www.nass.usda.gov/Charts_and_Maps/Crops_County/boundary_maps/indexgif.php, accessed 17 Feb. 2019.
- USDA NRCS. 2004. Revised Universal Soil Loss Equation. USDA NRCS, Washington, D.C. <https://www.ars.usda.gov/southeast-area/oxford-ms/national-sedimentation-laboratory/watershed-physical-processes-research/docs/revised-universal-soil-loss-equation-rusle-welcome-to-rusle-1-and-rusle-2/>, accessed 27 Mar. 2019.
- USDA NRCS. 2009. Soil quality indicators: Total organic carbon. USDA Natural Resources Conservation Service, Washington, DC. https://www.nrcs.usda.gov/wps/PA_NRCSConservation/download?cid=nrcs142p2_051877&ext=pdf, accessed 28 Mar. 2019.
- USDA NRCS. 2010. Aerial seeding of cover crops. Technical Note Agronomy # 36, USDA Natural Resources Conservation Service, Iowa State Office, Des Moines, IA.
- USDA NRCS. 2012. Release brochure for 'Alamo' switchgrass (*Panicum virgatum*). USDA Natural Resources Conservation Service James E. "Bud" Smith Plant Materials Center, Knox City, TX. https://www.nrcs.usda.gov/Internet/FSE_PLANTMATERIALS/publications/txpmcrb11189.pdf, accessed 28 Mar. 2019.
- USDA NRCS. 2014a. Section IV. Conservation practices. Residue and tillage management, no till. Code 329. In: Field office technical guide, USDA NRCS, North Dakota, pp. 1–4.
- USDA NRCS. 2014b. Section IV. Conservation practices. Residue and tillage management,

- reduced till. Code 345. In: Field office technical guide, USDA NRCS, North Dakota, pp. 1–4.
- USGS. 2019. Watershed Boundary Dataset. United States Geological Survey, Reston, VA. https://www.usgs.gov/core-science-systems/ngp/national-hydrography/watershed-boundary-dataset?qt-science_support_page_related_con=4#qt-science_support_page_related_con, accessed 17 Feb. 2019.
- VERBIO. 2018. VERBIO North America to purchase Nevada, Iowa cellulosic ethanol facility from DuPont Industrial Biosciences. Press Release. <https://www.verbio.de/en/press/news/press-releases/verbio-to-acquire-duponts-nevada-iowa-based-cellulosic-ethanol-plant/>, accessed 28 Jan. 2019.
- Vogel, K.P., J.J. Brejda, D.T. Walters, and D.R. Buxton. 2002. Switchgrass biomass production in the Midwest USA: Harvest and nitrogen management. *Agron. J.* 94:413–420. doi:10.2134/agronj2002.0413.
- Vogel, K.P., R.B. Mitchell, M.D. Casler, and G. Sarath. 2014. Registration of ‘Liberty’ switchgrass. *J. Plant Regist.* 8:242–247. doi:10.3198/jpr2013.12.0076crc.
- Voorhis, D. 2016. Hugoton cellulosic ethanol plant sold out of bankruptcy. *The Wichita Eagle*. <https://www.kansas.com/news/business/article119902263.html>, accessed 29 Jan. 2019.
- Wang, G., M. Danzl, P. Nyren, E. Aberle, E. Eriksmoen, T. Tjelde, J. Hendrickson, R. Warhurst, and A. Nyren. 2013. Establishment, persistence, yield and harvest regime of perennial forage species for bioenergy production across central and western North Dakota. North Dakota State University Extension, Fargo, ND. <https://www.ag.ndsu.edu/CentralGrasslandsREC/cgrec-annual-reports-1/2013-annual-report/CGREC10WangBioenergy.pdf>, accessed 28 Mar. 2019.
- Wang, X.F. 2010. fANCOVA: Nonparametric analysis of covariance. R package version 0.5-1. <https://CRAN.R-project.org/package=fANCOVA>, accessed 27 Mar. 2019.

- Ward, S.E., S.M. Smart, H. Quirk, J.R.B. Tallwin, S.R. Mortimer, R.S. Shiel, A. Wilby, and R.D. Bardgett. 2016. Legacy effects of grassland management on soil carbon to depth. *Glob. Change Biol.* 22:2929–2938. doi:10.1111/gcb.13246, accessed 17 Feb. 2019.
- Wayman, S., R.D. Bowden, and R.B. Mitchell. 2014. Seasonal changes in shoot and root nitrogen distribution in switchgrass (*Panicum virgatum*). *BioEnergy Res.* 7:243–252. doi: 10.1007/s12155-013-9365-9.
- Weaver, J. 1926. Root development of field crops. McGraw-Hill, New York, NY.
- Webb, E., M. Hilliard, C. Brandt, S. Sokhansanj, L. Eaton, and M. Martinez Gonzalez. 2014. Spatial analysis of depots for advanced biomass processing. Tech Rep ORNL/TM-2014/463, Oak Ridge National Laboratory, Oak Ridge, TN.
- Wentworth, C.K. 1922. A scale of grade and class terms for clastic sediments. *J. Geol.* 30:377–392.
- Werling, B.P., T.D. Meehan, B.A. Robertson, C. Gratton, and D.A. Landis. 2011. Biocontrol potential varies with changes in biofuel–crop plant communities and landscape perenniality. *GCB Bioenergy.* 3:347–359. doi:10.1111/j.1757-1707.2011.01092.x, accessed 17 Feb. 2019.
- Werling, B.P., T.L. Dickson, R. Isaacs, H. Gaines, C. Gratton, K.L. Gross, H. Liere, C.M. Malmstrom, T.D. Meehan, L. Ruan, B.A. Robertson, G.P. Robertson, T.M. Schmidt, A.C. Schrotenboer, T.K. Teal, J.K. Wilson, and D.A. Landis. 2014. Perennial grasslands enhance biodiversity and multiple ecosystem services in bioenergy landscapes. *Proc. Natl. Acad. Sci. USA.* 111:1652–1657. doi:10.1073/pnas.1309492111.
- West, T.O., C.C. Brandt, B.S. Wilson, C.M. Hellwinckel, D.D. Tyler, G. Marland, D.G. De La Torre Ugarte, J.A. Larson, and R.G. Nelson. 2008. Estimating regional changes in soil carbon with high spatial resolution. *Soil Sci. Soc. Am. J.* 72:285–294. doi:10.2136/sssaj2007.0113.

- Whitehead, R.L. 1996. Montana, North Dakota, South Dakota, Wyoming. In: Groundwater atlas of the United States, vol. HA 730-I, U.S. Geological Survey, pp. I1–I24.
- Wickham, H. 2009. *ggplot2: Elegant graphics for data analysis*. Springer-Verlag New York, New York, NY. <http://ggplot2.org>.
- Wiens, J., J.M. DiTomaso, and J. Hill. 2011. Biofuels and biodiversity. *Ecol. Appl.* 21:1085–1095. doi:10.1890/09-0673.1, accessed 8 Jun. 2018.
- Wiersma, J.J. and J.K. Ransom. 2005. Section II: Crop growth and scouting, Chapter 1: Growth and development. In: *The small grains field guide*, editors J.J. Wiersma and J.K. Ransom, University of Minnesota Extension Service and NDSU Extension Service, St. Paul, MN and Fargo, ND, pp. 44–53. 2nd ed.
- Wiersma, J.J., J.K. Ransom, and V. Hofman. 2005. Section I: Agronomic management, Chapter 5: Planting. In: *The small grains field guide*, editors J.J. Wiersma and J.K. Ransom, University of Minnesota Extension Service and NDSU Extension Service, St. Paul, MN and Fargo, ND, pp. 27–33. 2nd ed.
- Williams, J.R., C.A. Jones, J.R. Kiniry, and D.A. Spanel. 1989. The EPIC crop growth model. *Trans. ASAE.* 32:497–511.
- Willmott, C.J. 1981. On the validation of models. *Phys. Geogr.* 2:184–194. doi:10.1080/02723646.1981.10642213.
- Willmott, C.J. 1984. On the evaluation of model performance in physical geography. In: *Spatial statistics and models*, editors G.L. Gaile and C.J. Willmott, Springer Netherlands, Dordrecht, pp. 443–460. doi:10.1007/978-94-017-3048-8_23. https://doi.org/10.1007/978-94-017-3048-8_23.
- Wilson, D.M., E.A. Heaton, L.A. Schulte, T.P. Gunther, M.E. Shea, R.B. Hall, W.L. Headlee, K.J. Moore, and N.N. Boersma. 2014. Establishment and short-term productivity of annual

- and perennial bioenergy crops across a landscape gradient. *BioEnergy Res.* 7:885–898. doi:10.1007/s12155-014-9409-9.
- Wirt, A. 2014. Biomass program overview. POET-DSM, Sioux Falls, SD. <http://poet-dsm.com/resources/docs/POET-DSM%20Biomass%20Program%20Overview.pdf>, accessed 28 Mar. 2019.
- Woli, P., J.L. Paz, D.J. Lang, B.S. Baldwin, and J.R. Kiniry. 2012. Soil and variety effects on the energy and carbon balances of switchgrass-derived ethanol. *J. Sustain. Bioerng. Sys.* 2:65–74. doi:10.4236/jsbs.2012.24010.
- Wright, C.K. and M.C. Wimberly. 2013. Recent land use change in the western Corn Belt threatens grasslands and wetlands. *Proc. Natl. Acad. Sci. USA.* 110:4134. doi:10.1073/pnas.1215404110.
- Wright, C.K., B. Larson, T.J. Lark, and H.K. Gibbs. 2017. Recent grassland losses are concentrated around U.S. ethanol refineries. *Environ. Res. Lett.* 12:044001. doi:10.1088/1748-9326/aa6446.
- Wright, J., T. Scherer, and G. Sands. 2005. Section I: Agronomic management, Chapter 1: Water management. In: *The small grains field guide*, editors J.J. Wiersma and J.K. Ransom, University of Minnesota Extension Service and NDSU Extension Service, St. Paul, MN and Fargo, ND, pp. 7–10. 2nd ed.
- Wright, L. and A. Turhollow. 2010. Switchgrass selection as a “model” bioenergy crop: A history of the process. *Biomass Bioenergy.* 34:851–868. doi:10.1016/j.biombioe.2010.01.030.
- Wu, J. and B. Weber. 2012. Implications of a reduced Conservation Reserve Program. The Council on Food, Agricultural, and Resource Economics, Washington, DC. https://ageconsearch.umn.edu/bitstream/156625/2/Wu-Weber_Final.pdf, accessed 28 Mar. 2019.

- Wullschleger, S.D., E.B. Davis, M.E. Borsuk, C.A. Gunderson, and L.R. Lynd. 2010. Biomass production in switchgrass across the United States: Database description and determinants of yield. *Agron. J.* 102:1158–1168. doi:10.2134/agronj2010.0087.
- Xie, Y., J.R. Kiniry, V. Nedbalek, and W.D. Rosenthal. 2001. Maize and sorghum simulations with CERES-Maize, SORKAM, and ALMANAC under water-limiting conditions. *Agron. J.* 93:1148–1155.
- Xie, Y., J.R. Kiniry, and J.R. Williams. 2003. The ALMANAC model's sensitivity to input variables. *Agr. Sys.* 78:1–16. doi:10.1016/S0308-521X(03)00002-7.
- Yohai, V.J. 1987. High breakdown-point and high efficiency robust estimates for regression. *Ann. Stat.* 15:642–656. <http://www.jstor.org/stable/2241331>.
- Zambrano-Bigiarini, M. 2017. hydroGOF: Goodness-of-fit functions for comparison of simulated and observed hydrological time series. R package version 0.3-10. R Foundation for Statistical Computing, Vienna, AT. <http://hzambran.github.io/hydroGOF/>, accessed 27 Mar. 2019.
- Zhang, X., R. Izaurralde, D. Manowitz, T.O. West, W.M. Post, A.M. Thomson, V.P. Bandaru, J. Nichols, and J.R. Williams. 2010. An integrative modeling framework to evaluate the productivity and sustainability of biofuel crop production systems. *GCB Bioenergy.* 2:258–277. doi:10.1111/j.1757-1707.2010.01046.x, accessed 22 Mar. 2019.
- Zhang, X., R.C. Izaurralde, D.H. Manowitz, R. Sahajpal, T.O. West, A.M. Thomson, M. Xu, K. Zhao, S.D. LeDuc, and J.R. Williams. 2015. Regional scale cropland carbon budgets: Evaluating a geospatial agricultural modeling system using inventory data. *Environ. Modell. Softw.* 63:199–216. doi:10.1016/j.envsoft.2014.10.005.
- Zilverberg, C.J., K. Heimerl, T.E. Schumacher, D.D. Malo, J.A. Schumacher, and W.C. Johnson. 2018. Landscape dependent changes in soil properties due to long-term cultivation

and subsequent conversion to native grass agriculture. *Catena*. 160:282–297. doi: 10.1016/j.catena.2017.09.020.

Zollinger, R. 2010. 2010 North Dakota weed control guide. Tech. Rep. W-253, North Dakota State University Extension, Fargo, ND.

Zollinger, R. 2011. 2011 North Dakota weed control guide. Tech. Rep. W-253, North Dakota State University Extension, Fargo, ND.

Zollinger, R. 2012. 2012 North Dakota weed control guide. Tech. Rep. W-253, North Dakota State University Extension, Fargo, ND.

Zollinger, R. 2013. 2013 North Dakota weed control guide. Tech. Rep. W-253, North Dakota State University Extension, Fargo, ND.

Zollinger, R. 2014. 2014 North Dakota weed control guide. Tech. Rep. W-253, North Dakota State University Extension, Fargo, ND.

Zollinger, R. 2015. 2015 North Dakota weed control guide. Tech. Rep. W-253, North Dakota State University Extension, Fargo, ND.